AUSTRALIA

BMR JOURNAL

OF AUSTRALIAN GEOLOGY & GEOPHYSICS

VOLUME 10 NUMBER 3

BMR JOURNAL
OF AUSTRALIAN GEOLOGY & GEOPHYSICS

VOLUME 10 NUMBER 3

CONTENTS

Front cover: Tectonostratigraphic terranes of western Irian Jaya. A terrane analysis of the accretion history of the New Guinea orogen is presented in this issue, in a paper by C.J. Pigram & H.L. Davies.
Cover design by Mary Silver.

AUSTRALIAN GOVERNMENT PUBLISHING SERVICE CANBERRA 1987

Department of Primary Industries and Energy

Minister: The Hon. John Kerin, M.P.

Secretary: G. C. Evans

Bureau of Mineral Resources, Geology and Geophysics

Director: R. W. R. Rutland

Editor, BMR Journal: I. M. Hodgson

The BMR Journal of Australian Geology & Geophysics is a quarterly journal of research. It contains papers and shorter notes by scientists of the BMR or others who are collaborating with BMR. Discussion of papers is invited from anyone.

Subscriptions to the BMR Journal are managed by the Australian Government Publishing Service (Mail Order Sales, GPO Box 84, Canberra, ACT 2601; telephone (062) 95 4485), to which enquiries should be directed.

Other matters concerning the Journal should be sent to the Director, marked for the attention of the Editor, BMR Journal.

Month of issue: August

ISSN 0312-9608

Printed by Graphic Services Pty Ltd, 516-518 Grand Junction Road, Northfield, South Australia 5085

BMR Journal of Australian Geology & Geophysics, 10, 193-211

Terranes and the accretion history of the New Guinea orogen

C.J. Pigram[1] & H.L. Davies[1]

The New Guinea orogen consists of a southern part that was formerly the northern edge of the Australia craton and a northern part that consists of at least thirty-two tectonostratigraphic terranes, many of them composite in nature. Many of these terranes are of oceanic affinity, but the western part of the orogen is dominated by terranes of continental affinity. An analysis of the accretion history of the orogen shows that the orogen was initiated in middle to late Oligocene time. Older Palaeogene deformation events, previously thought to mark the initial stages of orogenesis, occurred as amalgamation formed composite terranes at sites in ocean basins far removed from the edge of the Australian craton. The accretion that led to formation of the orogen took place because the northward-moving Australian craton entered subduction zones at which composite terranes had been assembled.

Introduction

The concept that the western part of the Cordillera of western North America constitutes a vast tectonic collage of tectonostratigraphic terranes (Coney & others, 1980) has greatly influenced recent thinking about the evolution of orogenic belts, particularly those of the circum-Pacific region.

Tectonostratigraphic terranes are internally homogeneous geological provinces, the stratigraphy, fauna, tectonic style, palaeomagnetic signature and history of which contrast with those of adjoining provinces. Boundaries between terranes are sharp structural junctions, which cannot be easily explained by normal changes in facies, gradation in structural style or unconformities. Individual terranes vary from small allochtons to major geological provinces. Most are of unknown palaeogeography with respect to the nearby craton margin, and it was for this reason that Coney & others (1980) referred to them as suspect terranes.

Once the craton margin within an orogen has been identified, the remainder of the orogen comprises terranes. By identifying the terranes and using the techniques of terrane analysis (Jones & others, 1983) it may be possible to establish a time frame for the juxtaposing of the terranes with the craton and each other.

In this paper we apply the terrane concept to the island of New Guinea (Fig. 1), drawing on the results of recently completed reconnaissance geological mapping in western Irian Jaya, and a comprehensive program of regional geological mapping in Papua New Guinea (PNG). We identify the Mesozoic margin of the Australian craton in New Guinea (Thompson, 1962; Pigram & Panggabean, 1984) (Fig. 2) and 32 tectonostratigraphic terranes that lie outboard of the craton margin.

The New Guinea orogen has long been recognised as a product of collisional processes along the northern edge of the Australian craton. Wegener (1920), who postulated that the Australian continent had forced its way between the island chain of southeast Indonesia and the Bismarck Archipelago, thought that the mountain building preceded this collision rather than being caused by it. Later workers, particularly those working in Papua New Guinea (PNG) who reviewed the over-all development of the orogen, recognised that the Australian craton formed the southern part of the orogen and that the northernmost part consisted of one or more island-arc complexes (Thompson & Fisher, 1967; Thompson, 1967, 1972; Dewey & Bird, 1970; Page 1971; Davies & Smith, 1971; Davies, 1977; Dow, 1977; Jaques & Robinson, 1977; Hamilton, 1979; Kroenke, 1984). It was argued that the collision of the craton with the island-arc complex or complexes led to the formation of the orogen by telescoping of the craton margin, the emplacement of forearc material (ophiolite, metamorphics) over it, and the accretion of the island arc or arcs. The collision generally was seen as a synchronous event along that part of the craton margin east of Sarera Bay, although Davies (1982b) and Kroenke (1984) have argued for multiple collisions. Evidence indicated that the timing of the collision ranged from Eocene in east PNG to late Oligocene — early Miocene in western PNG, and many other details of the history of the orogen were not easily reconciled with the model of a simple continent/island arc collision.

Two of the earlier workers, in particular, anticipated the terrane concept. They were J.J. Hermes and J.E. Thompson. Hermes postulated that western Irian Jaya consisted of a number of unrelated fragments that were not juxtaposed until the mid-Tertiary (Visser & Hermes, 1962, p. 206, figure IV-2). Similarly, Thompson (1967, Thompson & Fisher, 1967) suggested that much of the orogen north of the craton margin was made up of 'sialic segments that moved independently within the oceanic crust' (Thompson & Fisher, 1967, p. 144).

Former craton margin in New Guinea

The New Guinea orogen occupies a large part of the island of New Guinea and adjacent small islands. That part of the orogen occupied by the deformed craton margin is shown in Figure 2. The craton consists of a southern autochthonous portion and a northern para-autochthonous portion, which forms the southern part of the orogen. Studies of the para-autochthonous portion by Hobson (1986) suggest that parts of the craton have been thrust southward by as much as 100 km.

This former margin developed in the early Mesozoic (Pigram & Panggabean, 1984) and, during Jurassic to Palaeogene time, was a passive margin across which miogeoclinal sediments were draped (Thompson & Fisher, 1967; Dow, 1977; Brown & others, 1980). The correct eastern limits of the craton were not recognised until Symonds & others (1984) pointed out that the Coral Sea was surrounded by passive continental margins. Before the initiation of the orogen and after the opening of the Coral Sea the northern margin of the Australian craton probably had the configuration shown in Figure 4A.

Western Irian Jaya has also been regarded as part of the craton (see Hamilton, 1979; Dow & Sukamto, 1984) that has always occupied its present-day position relative to the craton. However, Pigram & others (1982) and Pigram & Panggabean (1984) have argued that it is allochthonous, and palaeomagnetic data (Giddings & others, 1985) support this suggestion. In this paper, western Irian Jaya is shown to consist of a number of terranes and its accretion history is examined.

[1]Division of Marine Geoscience and Petroleum Geology, Bureau of Mineral Resources, GPO Box 378 Canberra, ACT 2601.

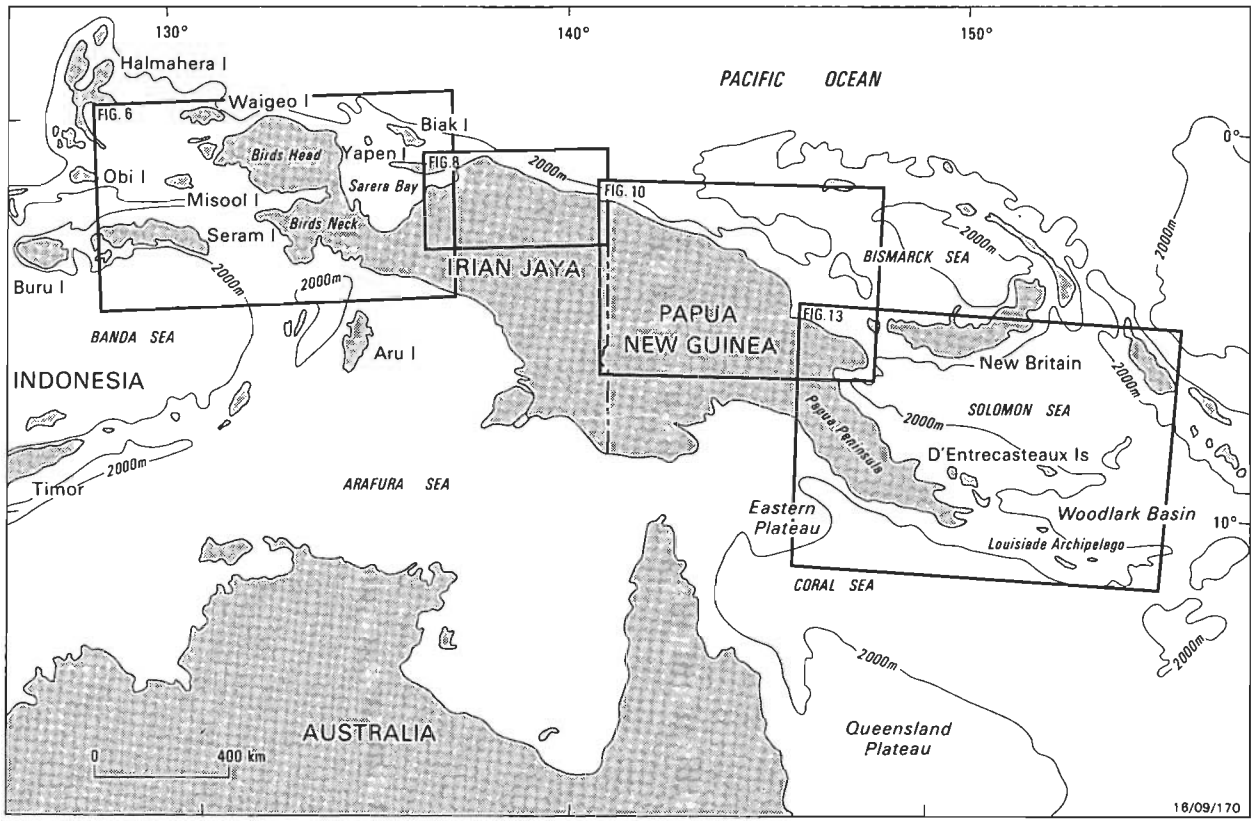

Figure 1. Locality map of New Guinea.
Boxes show the location of Figures 3, 5, 7, 10.

Terranes of the New Guinea orogen

Using comparative stratigraphy, we have identified thirty-two terranes in the New Guinea orogen (Figs 2, 6–14). Descriptions of each terrane are contained in Appendix 1. Below, we summarise the affinities of each terrane, discuss briefly the successor basins, and establish the accretion history of the orogen from a terrane analysis. The time frame developed for the evolution of the orogen reconciles many of the conflicts in previous interpretations.

Terrane affinities

The terranes of New Guinea each record unique stratigraphic histories, which reflect widely varying depositional environments, ranging from terranes with continental basement and well-layered inner shelf sedimentary strata, such as the Kemum terrane, to deep-water chert and carbonate-dominated terranes, formed far from sources of terrigenous detritus (Port Moresby terrane), to island-arc terranes with ophiolite basement such as the Waigeo terrane. The interpreted orgin of each terrane in terms of a continental or oceanic setting is shown in Table 1.

The Jimi, Bena Bena, and Lengguru terranes are considered to be part of the collision-deformed continental margin of the Australian craton. The Kemum and, possibly, the Misool terranes are former microcontinents rifted from Gondwana in the early Mesozoic (Pigram & Panggabean, 1984; J.W. Giddings, personal communication, 1984) and reunited by accretion in the late Tertiary. Ophiolitic and island-arc complexes such as the Bowutu and Finisterre terranes form a major part of the orogen, particularly along its northern or outer part.

The terranes typically are separated by faults or sedimentary basins. The nature of the faults is usually not clear. Some, such as the Sorong Fault Zone, are transcurrent; others, such as the Owen Stanley Fault, are thought to be thrusts. Many of the long linear faults that separate terranes have long been suspected of transcurrent movement (Thompson & Fisher, 1967; Bain, 1973), but unequivocal evidence is lacking. In the North American Cordillera many of the faults are thought to have caused displacements that led to dismembering and reorganisation of terranes after accretion (Coney & others, 1980). Such processes have probably occurred in New Guinea also, but have not been proven. The eastern end of the orogen is now being dismembered by the opening of the Woodlark Basin by seafloor spreading.

A feature of the New Guinea orogen is the large number of post-accretion basins that have formed across terrane boundaries, particularly those separating composite terranes. These include the Salawati, Bintuni, and North New Guinea Basins of Irian Jaya, and the Lumi, Aitape, Wewak, and Aure Troughs of Papua New Guinea. All these basins are of Miocene and younger age; they formed rapidly and typically contain 3–7 km of turbiditic sediments (Visser & Hermes, 1962; Brown & others, 1975; Pieters & others, 1983; Williams & Amiruddin, 1983; Hutchison & Norvick, 1980). Some of the basins were short lived: for example, the North New Guinea Basin of northern Irian Jaya formed in late Miocene or early Pliocene times, but has been deformed. The sequence has been faulted, folded, in part overturned, and intruded by extensive shale diapirs (Williams & Amiruddin, 1983; Williams & others, 1984). The basin existed for less than 10 Ma. The manner in which these basins formed and their relation to terrane accretion lies beyond the scope of this paper. However, some of the basins may be pull-apart

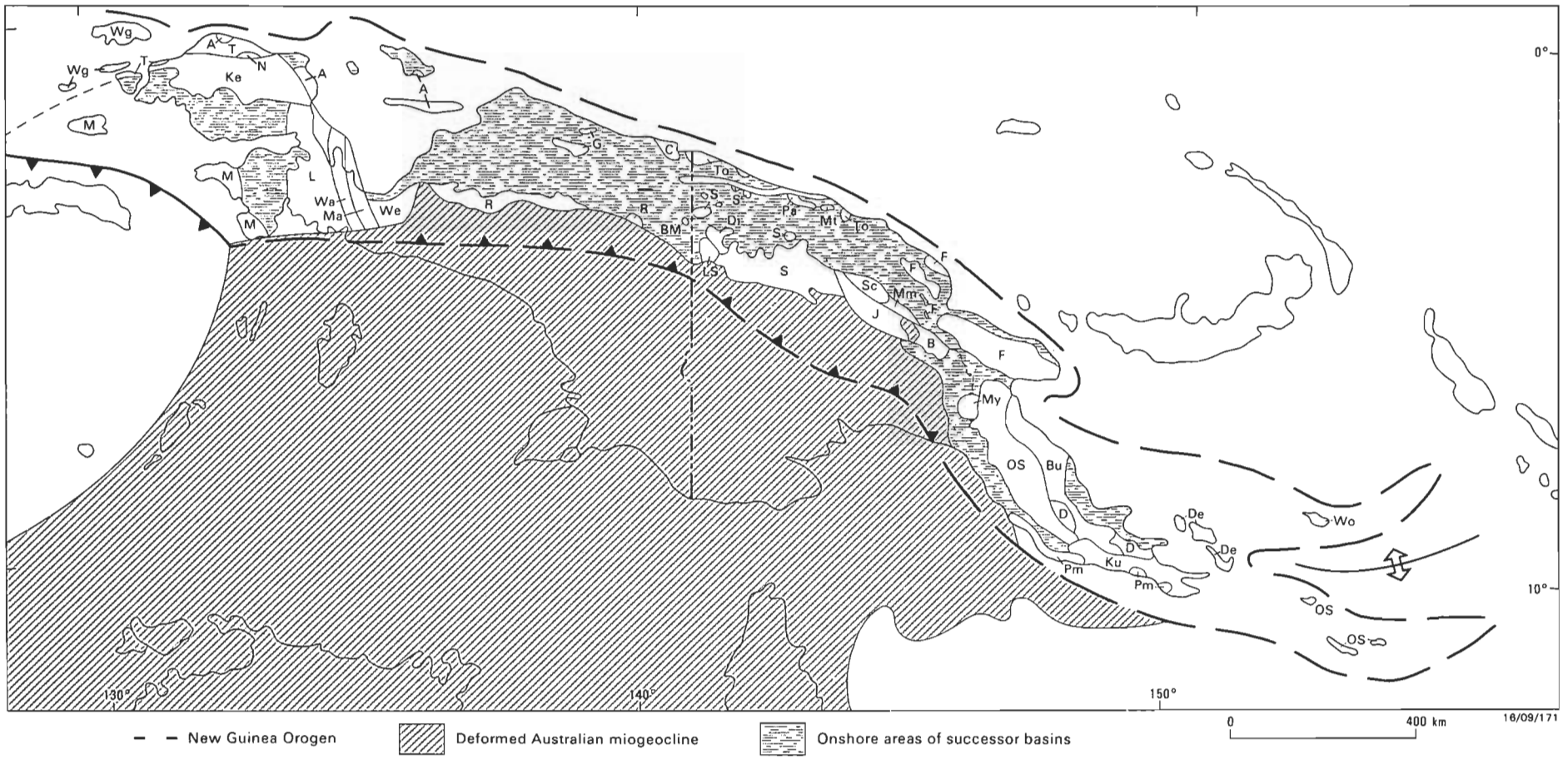

Figure 2. The New Guinea orogen and terranes described in this paper.

That part of the Australian craton which forms the southern part of the orogen is indicated. Only the onshore parts of various successor basins are shown. Wg, Waigeo; M, Misool; T, Tamrau; A, Arfak; Ke, Kemum; L, Lengguru; Wa, Wandamen; Ma, Maransabadi; We, Weyland; R, Rouffaer; G, Gauttier; C, Cyclops; BM, Border Mountains; To, Torricelli; S, Sepik; LS, Landslip; Di, Dimaie; Pa, Prince Alexander; Tu, Mount Turu; J, Jimi; Sc, Schrader; Mm, Marum; Bb, Bena Bena; F, Finisterre; My, Menyamya; OS, Owen Stanley; B, Bowutu; D, Dayman; PM, Port Moresby; Ku, Kutu; De, D'Entrecasteaux; Wo, Woodlark. Descriptions of each terrane are contained in Appendix I.

Table 1. Affinities of the tectonostratigraphic terranes in the New Guinea orogen.

Ocean floor (Seamounts, Plateaus)	Volcanic arc	Margin (slope rise)	Platform
Bowutu	Finisterre	Tamrau	Prince Alexander
Marum	Torricelli		Bena Bena
Mt. Turu	Arfak		Jimi
Rouffaer	Dimaie		Netoni
Menyamya	Woodlark		Mangguar
Cyclops			Border Mountains
?Dayman			Wandamen
Kutu			Schrader
Port Moresby			Kemum
..... Waigeo.....			Landslip
.....?Gauttier.....			Misool
		Weyland	
		Owen Stanley	
		Lengguru	
		?D'Entrecasteaux	
.....Sepik.....			

structures (e.g. Waipoga Basin). Others, such as the Pliocene Aure Trough may be more akin to molasse basins formed by downwarp caused by loading due to the overthrust of terranes. Davies (1977) and Davies & others (1984) have suggested that the small basins at the eastern end of the Papuan Peninsula are related to the formation of the Woodlark spreading centre.

The great variety of basin-forming mechanisms in the New Guinea orogen shows the complexities of modern analogs for the basins in which the thick, now highly deformed Mesozoic flysch that separates some of the terranes in the North American Cordillera were deposited (Coney & others, 1980; Jones & others, 1982).

Accretion history

The accretion history of an orogen can be gleaned from the ages of cover sequences (successor basins or overlap assemblages of Jones & others, 1983), the depositional age of detritus shed from one terrane to another (provenance linking of Jones & others, 1983), the age of intrusive rocks that were emplaced across terrane boundaries (stitching plutons of Jones & others, 1983), and metamorphic, structural, palaeontological, and palaeomagnetic histories (Jones & others, 1983; Williams & Hatcher, 1982). Further indications for the timing of accretion events can be obtained from the time of and stages in the development of the foreland basin. Beaumont (1981) and Jordon (1981) have shown that foreland basins develop as a consequence of loading the craton and, as terrane accretion is a loading event on the craton margin, it will initiate the development of a foreland basin. In the absence of other constraints on the timing of accretion events, the history of the foreland may provide useful clues. An outline of the accretion history of the New Guinea orogen is presented below.

Western Irian Jaya

Western Irian Jaya is unique in the New Guinea orogen in that its accretion history involves mainly continental terranes, with only two of its ten terranes (Waigeo and Arfak terranes) being of oceanic origin. It was probably this preponderance of continental terranes that led many people to view western Irian Jaya as an integral part of the Australian craton that had always occupied its present-day position (Dow & Sukamto, 1984; Norvick, 1979) or had been rotated or faulted into its present position in the Neogene (Visser & Hermes, 1962; Hermes, 1968; Thompson, 1972; Audley-Charles & others, 1972; Carter & others 1976; Hamilton, 1979).

However, palaeomagnetic data from the Kemum terrane (Giddings & others, 1985; personal communication, 1984) show that western Irian Jaya has not always occupied its present-day position relative to the Australian craton. The data show that the Kemum terrane and the Australian craton have the same polar wander path from the Late Carboniferous to Triassic, confirming the palaeontological evidence from the *Glossopteris* flora (Visser & Hermes, 1962; Pigram & Sukanta, 1982) and Permian brachiopods (Archbold & others, 1982) that the Kemum terrane originated as part of Gondwana. The Cretaceous and early Tertiary poles are off the main path, suggesting that some relative motion has occurred between the Kemum terrane and Australia. The data also show that no large-scale clockwise rotation of the Kemum terrane has taken place in the Neogene.

These data are important because they show that, although the Kemum terrane originated as part of Gondwana, it was detached by the Early Cretaceous and then had a history of movement independent of the Australian craton until at least the Miocene. The data have the further implication that, as the Kemum terrane forms the nucleus around which the other terranes of western Irian Jaya are clustered, these too may be allochthonous or, in the terminology of Coney & others (1980), suspect.

The development of western Irian Jaya was initiated by the amalgamation of the Kemum and Misool terranes in the latest Oligocene (by N4 time). The terranes are linked by an overlap assemblage of N4 and younger age (Salawati Basin) and a common deformation event (Pigram & others, 1982; N.R. Cameron, personal communication, 1983) that folded the Oligocene and other sediments before deposition of the overlap sequence. This composite Misool-Kemum terrane then amalgamated with the Lengguru terrane by late Miocene times, when all three terranes were contributing detritus to the overlapping Bintuni Basin. The amalgamation of the Misool-Kemum composite terrane with the Lengguru terrane may have involved the docking of the Misool-Kemum terrane with the Australian craton, as the Lengguru terrane is an Australian craton margin assemblage. However, it is not clear what the Lengguru terrane's relation to the craton was, and, if it is displaced, whether that displacement was a consequence of the docking of the Misool-Kemum composite terrane, or predated or postdated it.

To the north, the Tamrau terrane is linked to the Kemum terrane by an overlap assemblage of Pliocene sediments (Visser & Hermes, 1962; Pieters & others, 1983). Amalgamation of these two terranes may have occurred earlier, if the uplift of the northern edge of the Kemum terrane in the late Miocene was related to this event. The Tamrau and western Arfak terranes are linked by a Pliocene overlap assemblage (the Opmarai Formation of Pieters & others, 1983), while the Tamrau and Waigeo terranes are linked by the late Miocene and younger sediments of the Batanta Basin.

Eastern Irian Jaya

Too little is known of the geology of eastern Irian Jaya to document all the terranes and their accretion history. The Gauttier and Rouffaer terranes are linked by a middle Miocene and younger overlap sequence. A late Oligocene age for the oldest accretion event (perhaps the docking of the Rouffaer terrane) is indicated by initiation of sedimentation in the foreland Akimeugah Basin during the earliest Miocene.

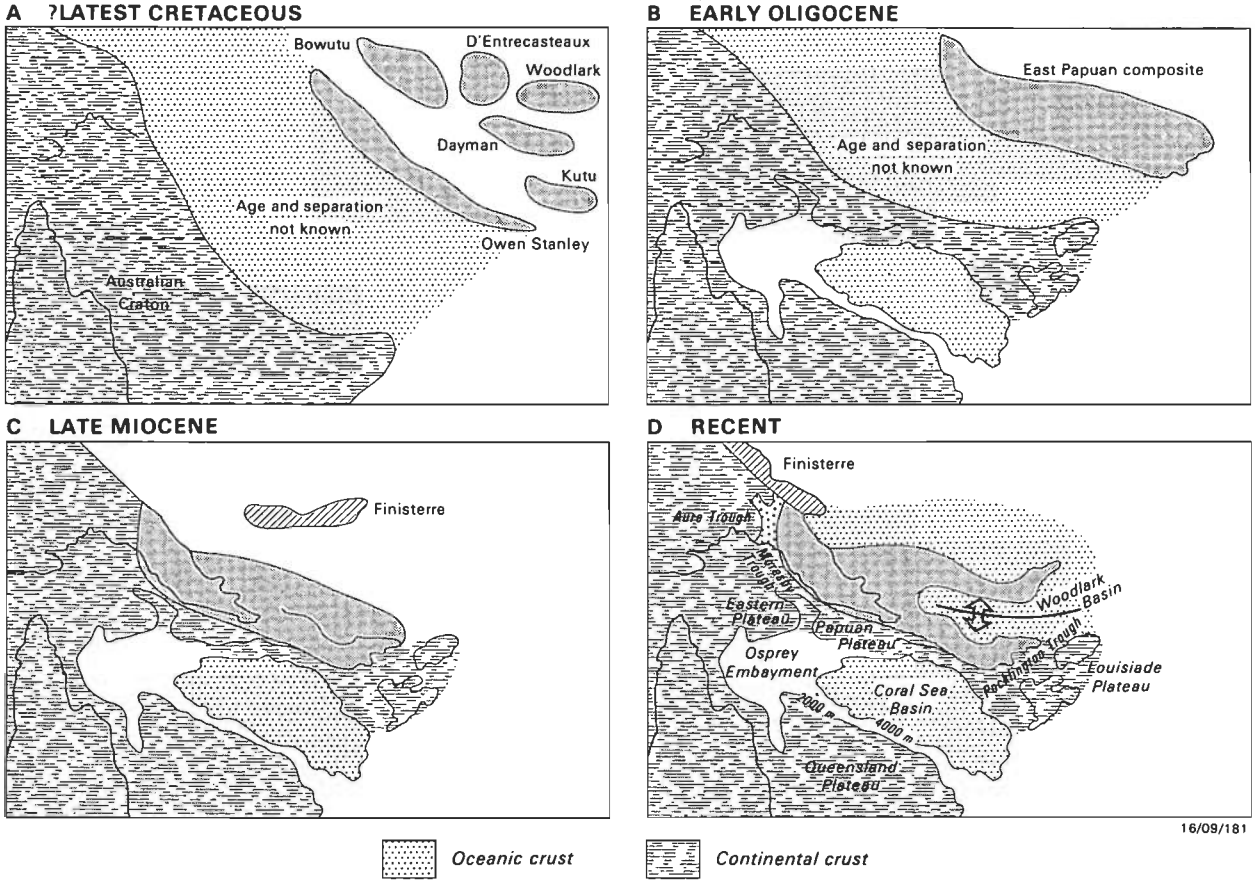

Figure 3. Schematic evolution of eastern Papua New Guinea, showing the formation of the east Papuan composite terrane by early Miocene time and its subsequent docking with a salient of the Australian craton by late Miocene time.

During the late Cretaceous the northeast edge of the Australian craton had the configuration shown in A. Outboard of it was an ocean basin of unknown age and dimension that contained or later developed features that were to become the terranes that amalgamated to form the East Papua composite terrane (EPCT). The shape of the terranes shown here has no significance. They are shown to indicate which terranes formed the EPCT by Oligocene time (B). By this time the Coral Sea Basin had opened and the Australian craton had the configuration shown in B. The EPCT had docked by late Miocene time (C), but was enlarged by the addition of the Port Moresby and Menyamya terranes during the Oligocene and early Miocene prior to dockings. The position of the Finisterre terrane in C has no palaeogeographic significance. It is shown as it is to indicate that the eastern part (at least) of the terrane must have docked after the EPCT. The western part of the Finisterre terrane may have docked just before or at about the same time as the EPCT. D shows the current position with the EPCT being dismembered by the opening of the Woodlark Basin. Diagrams not to scale.

Western Papua New Guinea

In the past, the development of the western PNG portion of the New Guinea orogen has been attributed to interaction between the Pacific and Australian plates, which culminated in a major orogeny in the Oligocene (Dow, 1977), and to continent and island arc collision (Davies, 1982a, b; Davies & Hutchison, 1982). The timing of the collision was thought to be late Eocene or early Oligocene by Davies & Hutchison (1982), latest Oligocene or end of early Miocene by Davies (1982a), while Davies (1982b) suggested that two arcs had collided, the first in the Oligocene and the second in the earliest Miocene.

Terrane analysis shows that the Sepik terrane is linked to the Australian craton by an overlap assemblage of late Oligocene to early Miocene (N3–N6) age (Kera Formation, Davies, 1983) and to the Landslip and Dimaie terranes by the middle Miocene and younger sediments of the Wogamush embayment. The northern terranes of Torricelli, Prince Alexander and Mount Turu are linked by an early Miocene overlap sequence. These early Miocene sediments, found along the north side of the Lumi Trough — the Puwani Limestone, Amogu conglomerate, and basal Senu Beds of Hutchison & Norvick (1980) — do not have equivalents on the south side of the basin. The overlap sequence that links the northern and southern terranes is the middle Miocene and younger strata of the Lumi Trough. This implies that the Sepik terrane docked with the Australian craton before the northern terranes docked with the Sepik terrane.

Further east, the Jimi terrane is stitched to the Sepik terrane by the late middle Miocene South Yuat Batholith (11.2–12.5 Ma; Page, 1976) and to the Bena Bena terrane by the middle Miocene Bismarck Intrusive Complex. The Schrader and Marum terranes amalgamated after the middle Eocene, and are linked to the western end of the Finisterre terrane by the Miocene and younger overlap assemblage of the Ramu Basin. The eastern part of the Finisterre terrane did not dock until after the middle Miocene (see discussion below on eastern PNG). This is in agreement with Jaques & Robinson (1977), who suggested that the western end of the Finisterre terrane docked before the eastern end, and with Johnson & Jaques (1980) and Falvey & Pritchard (1984), who suggested that the Finisterre terrane docked in the last 4 Ma. The relationship between the Sepik and Jimi terranes suggests they were juxtaposed by left-lateral movements on the Bismarck Fault Zone before emplacement of the South Yuat Batholith in the late middle Miocene. Also, parts of the Schrader terrane strongly resemble the northern part of the Owen Stanley terrane (Pigram, 1978). If the Schrader terrane should prove to be a dismembered portion of the Owen Stanley terrane it would imply a left-lateral offset of approximately 300 km along the Ramu–Markham and Bundi Fault Zones.

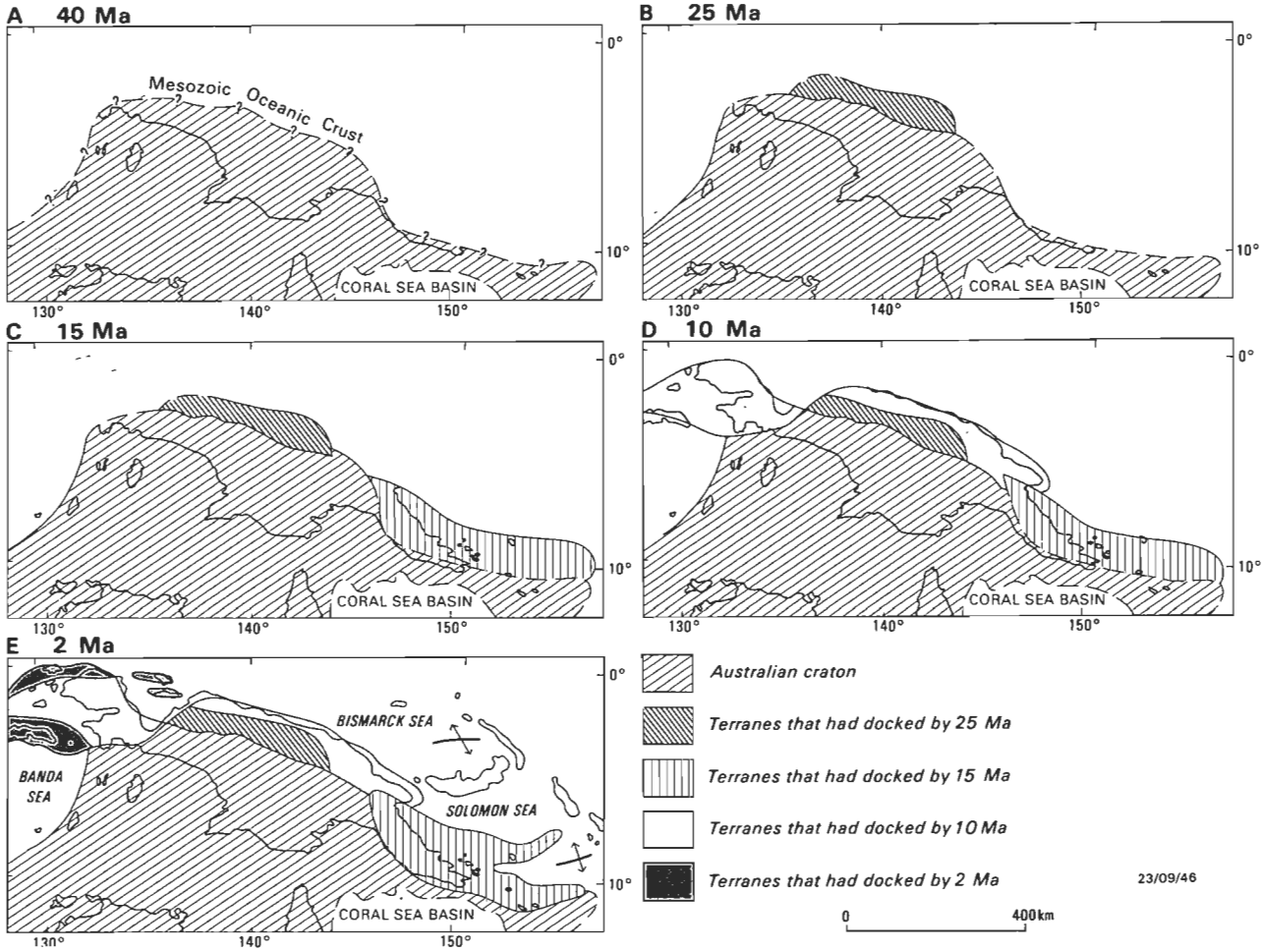

Figure 4. Simplified schematic accretion history of the New Guinea orogen.
The terranes are shaded according to their docking time. Successor basin sequences are not shown. The coastlines of southern New Guinea and northern Australia are shown in parts A-D for reference only. A: 40 Ma — Before the first docking event the northern edge of the Australian continent faced an ocean basin that had developed in Mesozoic time (Pigram & Panggabean, 1984). The Coral Sea Basin had formed in the Paleocene (Weissel & Watts, 1979) and was separated from the ocean basin to the north by a salient of continental crust. The Australian continent was moving northward. B: 25 Ma — by latest Oligocene the first composite terrane (the Sepik terrane) had docked. The Rouffaer terrane of eastern Irian Jaya is shown as having docked by this time also, but there is no age control for this assumption. C: 14 Ma — by latest middle Miocene, the northern part of the East Papua composite terrane had docked, but the eastern part of the terrane may not have docked with the Papuan and Louisade Plateau until a little later. D: 10 Ma — by early late Miocene time the Western Irian Jaya composite terrane and the northern island-arc terranes of central New Guinea had docked. The Jimi, Bena Bena, and Schrader terranes had reached their present-day position relative to the Sepik and Finisterre terrane. E: 2 Ma — by the Pliocene the northern terranes of western Irian Jaya (Tamrau, Arfak, and Waigeo terranes) had docked, while the Seram composite terrane docked about 2 Ma and completed what remains the present-day configuration of the orogen. No docking event has taken place along the orogen to the east of the Sarera Bay since the Pliocene, which is consistent with the establishment of a divergent regime leading to the opening of small ocean basins in the region. The opening of the Woodlark Basin is currently dismembering the eastern end of the East Papua composite terrane.

Eastern Papua New Guinea

The evolution of eastern PNG has been seen as the consequence of continent or microcontinent–island arc collision related to the opening of the Coral Sea. Davies & Smith (1971) suggested that the Australian craton collided with an island arc in the Eocene, causing obduction of the Papuan ultramafic belt and deformation of the leading edge of the craton. This deformed edge was subsequently detached and rotated away from the craton to form the Papuan Peninsula by the opening of the Coral Sea in the Eocene.

Pieters (1978) suggested a variation on this concept by proposing that a sliver of continent was rifted away from the craton by the opening of the Coral Sea and collided with the arc to produce the Papuan Peninsula. Hamilton (1979) suggested that eastern PNG was simply the eastern continuation of a continent–island arc collision that affected the entire margin of the Australian craton east of Sarera Bay.

Analysis of the accretion history of eastern PNG shows that it involves the amalgamation of several terranes of diverse origin in the Palaeogene to form a large composite terrane somewhere to the north or east of the Australian craton. This composite terrane then docked with the Australian craton in late Miocene times. A schematic history of the amalgamation and docking events of eastern PNG is shown in Figure 3.

The amalgamation of the Owen Stanley, Dayman, and Bowutu terranes may have begun as early as 52 Ma (early Eocene), if the metamorphism of the proto-Owen Stanley terrane was a consequence of this event. By late Oligocene time, the Menyamya terrane had amalgamated with this composite microcontinent (Fig. 3B).

By the end of the Oligocene, the Owen Stanley, Kutu, Dayman, Bowutu, and part of Port Moresby terranes had amalgamated to form a large composite terrane (East Papua

composite terrane) that was separated from the Australian craton by an oceanic basin (Fig. 3B). The evidence for this basin is found in the deep-water sediments of the Port Moresby terrane and the Paleocene ophiolite complex of the Menyamya terrane. The submarine tholeiitic basalts of the Kutu terrane may also have floored the basin. The presence of an ocean basin separating the Owen Stanley terrane from the Australian craton was recognised by Thompson & Fisher (1965) and implied by Hamilton (1979). This basin was separated from the Coral Sea basin, which had opened in the Paleocene (Weissel & Watts, 1979) by a long salient of the Australian craton made up of the Eastern, Papuan and, possibly, the Louisiade Plateaus (Symonds & others, 1984) (Fig. 3B).

Docking of the East Papua composite terrane with this salient of the Australian craton occurred in the middle or late Miocene. The western end of the composite terrane is linked to the craton by Pliocene sediments of the Aure Trough. Further evidence comes from the time of deformation of sediments in the Aure Trough, Port Moresby, and east Papuan regions. Aure Trough sediments were deformed in early middle Miocene and early upper Miocene times (Dow & others, 1974; Brown & others, 1975; Tingey & Grainger, 1976). In the Port Moresby area deformation postdates N6/N7 (late early Miocene) bathyal sediments of the Fairfax Formation (Rogerson & others, 1981; G. Francis, personal communication, 1986), and in east Papua upper Te (early Miocene)

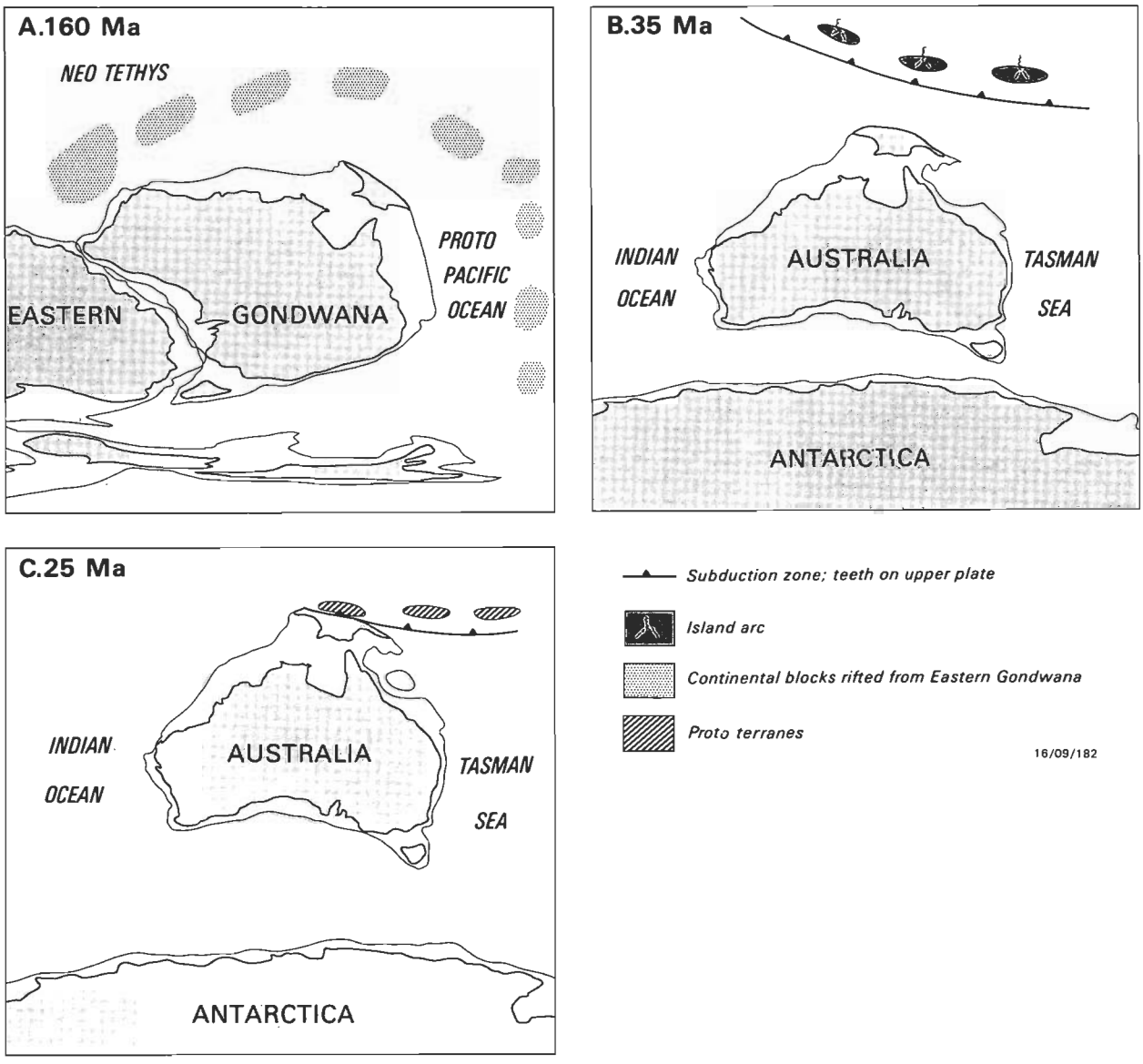

Figure 5. Schematic diagram of events that led to the formation of the northern margin of the Australian craton, its subsequent northward movement, and collision of the craton with a subduction zone (or zones), which led to the development of the New Guinea orogen.
A. 160 Ma, Late Jurassic — Rifting of eastern Gondwana during the Late Triassic to Middle Jurassic formed what became the northern edge of the Australian craton (Pigram & Panggabean, 1984), and across which Jurassic to mid-Tertiary miogeoclinal sediments were draped. B. 35 Ma, Early Oligocene — The Australian continent had detached from Gondwana in the late Cretaceous and started travelling rapidly northward during the Eocene (Cande & Mutter, 1982). We speculate that this northward flight of Australia was accommodated by the development of a subduction zone or zones, over which island arcs developed, somewhere to the north of the continent. The island-arc complex is shown schematically because its configuration and location in relation to the Australian craton at this time is now known. C. 25 Ma, Latest Oligocene. The ocean basin that lay to the north of the Australian craton was consumed and, by 25 Ma, the leading edge of the craton entered a subduction zone, causing the accretion of the Sepik composite terrane and the initiation of the development of the New Guinea orogen. The subsequent evolution of the orogen probably involved the development of short-lived microplates with complex boundaries. Sorting out their complexities remains one of the long-term objectives of studies of the New Guinea orogen. Base maps are from Smith, Hurley & Briden (1981).

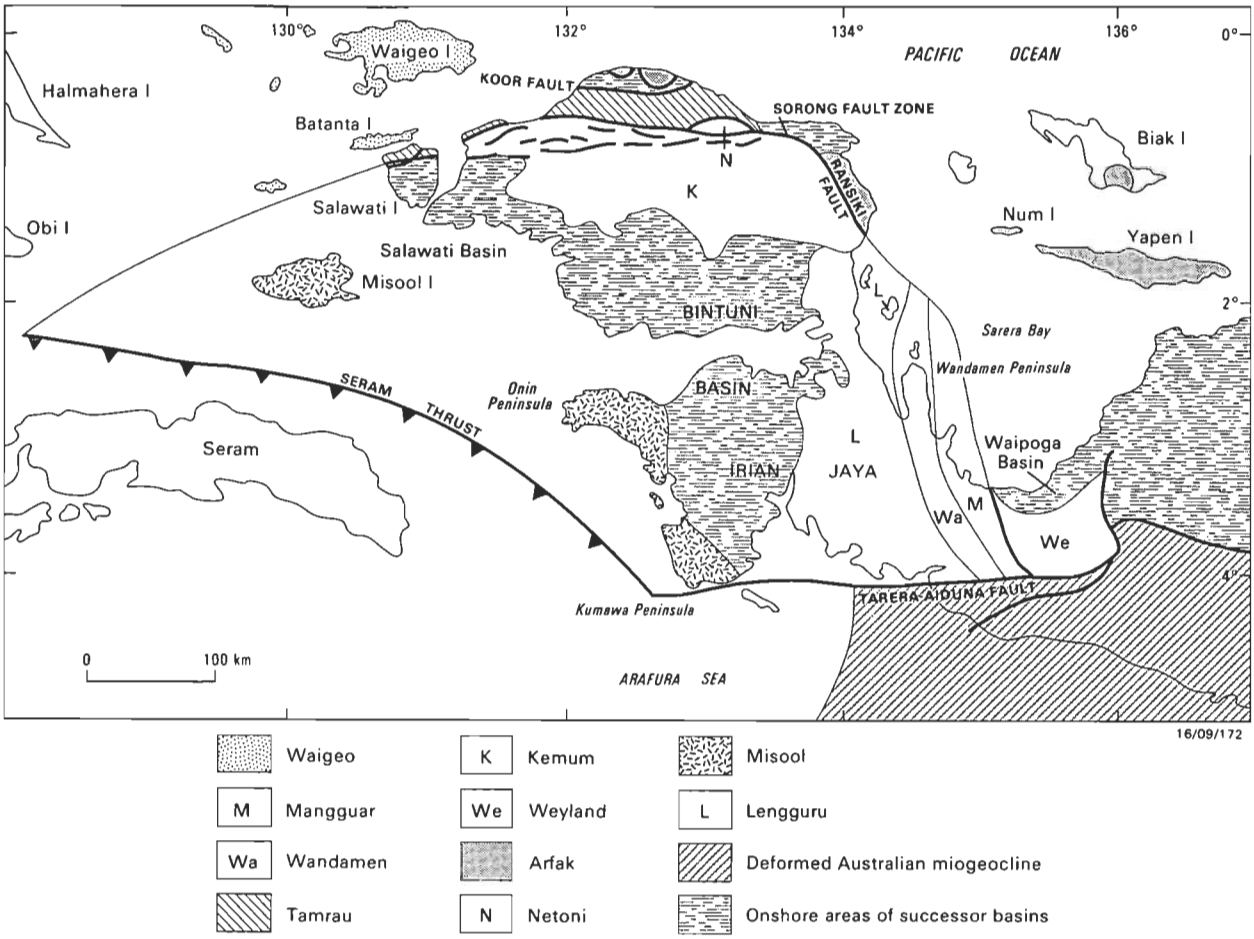

Figure 6. Map of the terranes of Western Irian Jaya.
Only the onshore areas of the successor basins are shown. Terranes on Seram Island that docked with the Misool terrane in late Pliocene to Pleistocene (Audley-Charles & others, 1979) are not discussed.

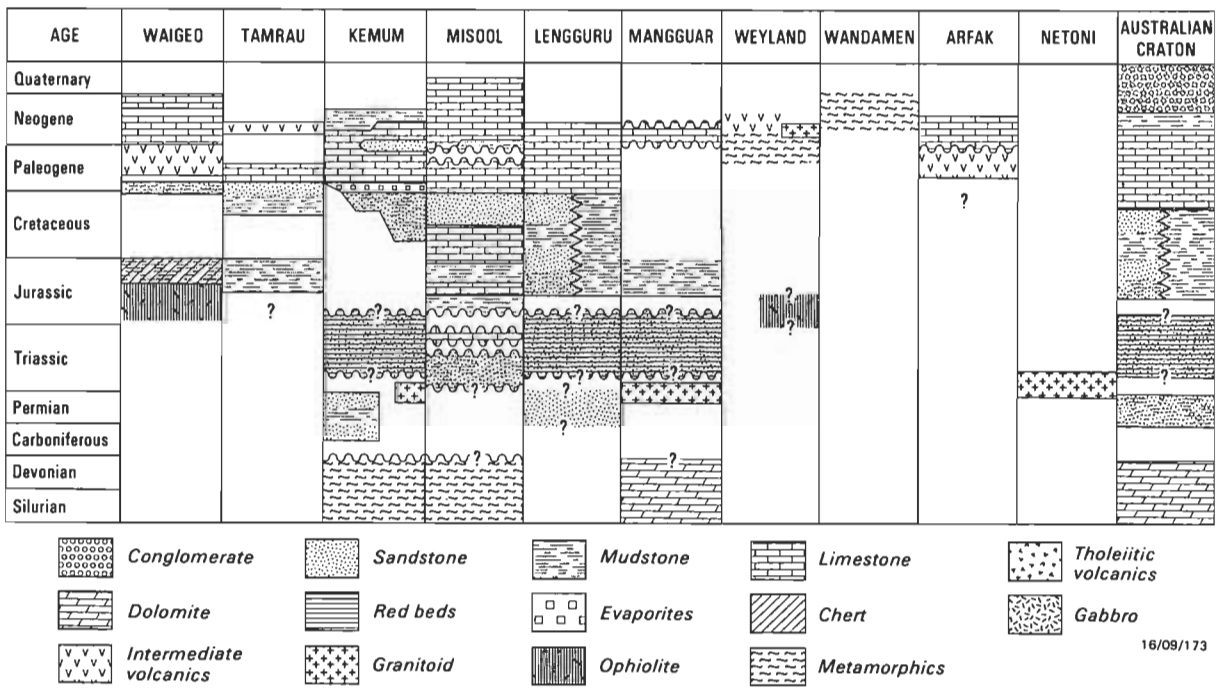

Figure 7. Stratigraphic columns for terranes of Western Irian Jaya.
See Figure 6 for location of terranes.

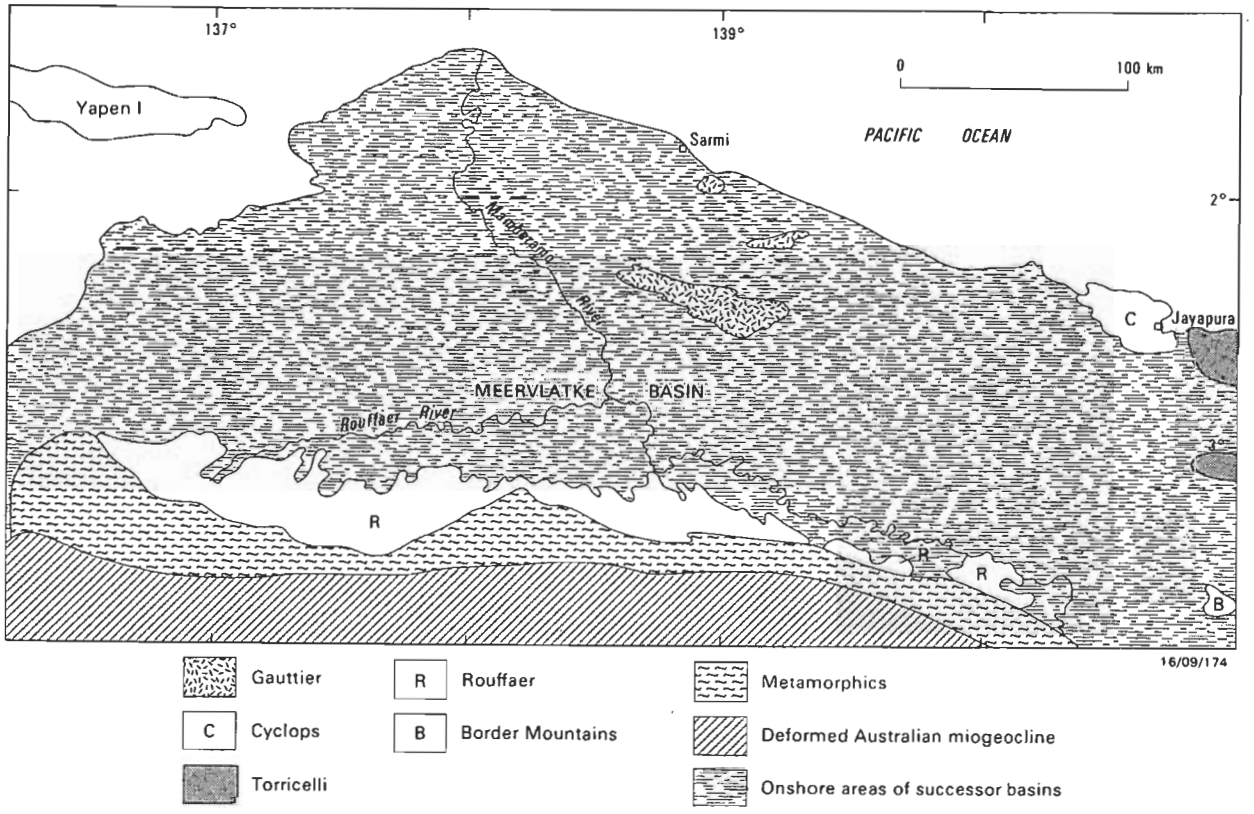

Figure 8. Map of terranes of eastern Irian Jaya.
The location of Rouffaer terrane is based on Landsat and airphoto interpretation. The narrow belt of metamorphics between the Rouffaer terrane and the Australian craton maybe a composite terrane.

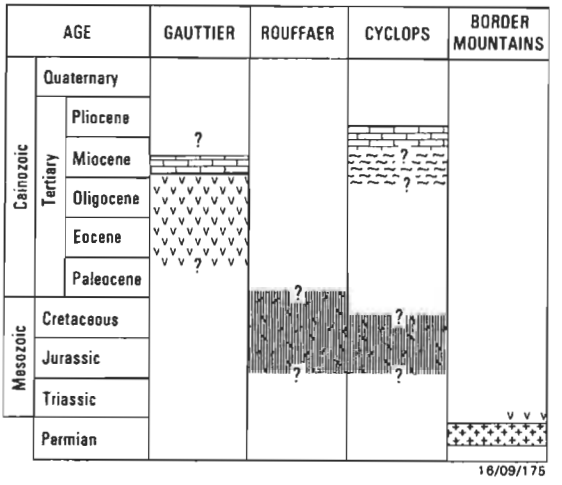

Figure 9. Stratigraphic columns for the terranes of eastern Irian Jaya.
See Figure 8 for terrane location.

sediments are the youngest involved in the deformation of the southern margin of the terrane. A mid-Miocene time for docking is also consistent with the uplift of the Papuan Ultramafic Belt (Smith & Davies, 1976) and the first appearance of siliciclastic turbidites in the Coral Sea Basin (Andrews & others, 1975).

The latest event in the accretion history of eastern PNG was the docking of the Finisterre terrane after the East Papua composite terrane had docked with the Australian craton, i.e. post middle Miocene. Rapid rates of uplift in the eastern Finisterre terrane (Chappell, 1974) may indicate that it is still being thrust southward over the Australian craton (Johnson & Jaques, 1980).

Post-docking lateral translation of terranes in the order of hundreds of kilometres would not affect the arguments presented above. Post docking translation of terranes by thousands of kilometres clearly would, but movements of that order seem unlikely.

Several implications for the palaeogeography of the east Papuan region arise out of the accretion history discussed above. The Menyamya, Port Moresby, and Kutu terranes are interpreted as remnants of an ocean basin that existed northeast of the Eastern and Papuan Plateaus (Fig. 3) before the opening of the Coral Sea. The pre-middle Miocene sediments of the Aure Trough may have been deposited in widely separated locations, the western assemblage (Darai Limestone) being deposited on the eastern edge of the Australian craton, and the eastern assemblage (Aure beds), on the western edge of the East Papuan composite terrane, while they were separated by an ocean basin. It follows that the Aure Trough may have an oceanic basement in part, a suggestion supported by anomalously high gravity values across the Aure Trough (St. John, 1967).

Overview of terrane accretion

The New Guinea orogen developed as the consequence of the docking of several terranes (many of which were large composite terranes) since the late Oligocene (Fig. 4). Eocene

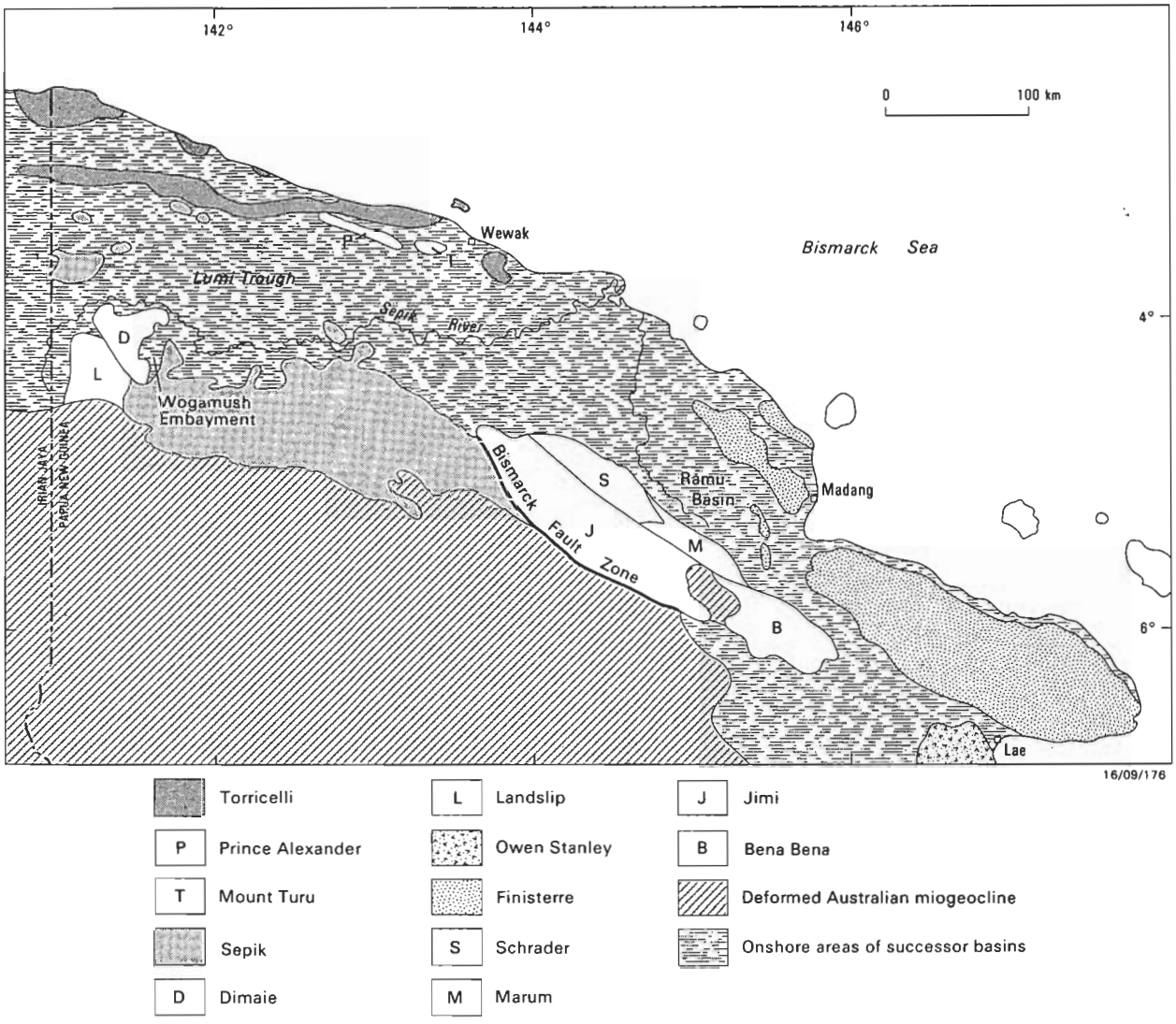

Figure 10. Map of the terranes of western Papua New Guinea.
Some of these terranes (e.g. Sepik terrane) are composite.

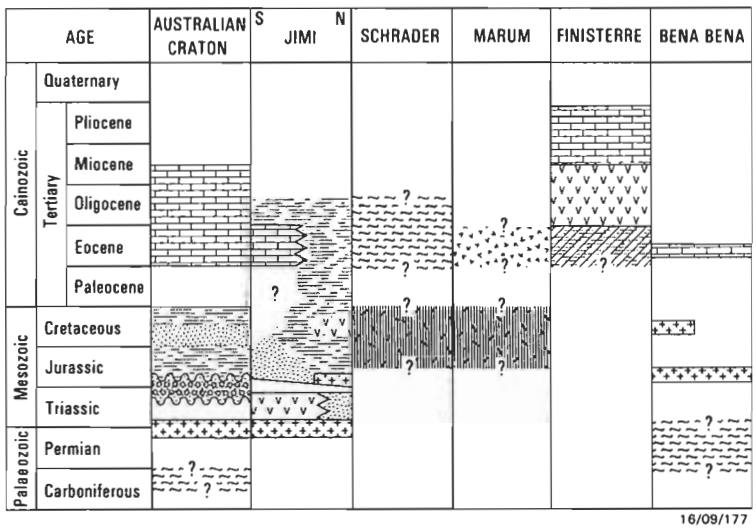

Figure 11. Stratigraphic columns for the terranes of the eastern part of western Papua New Guinea.
See Figure 10 for terrane location.

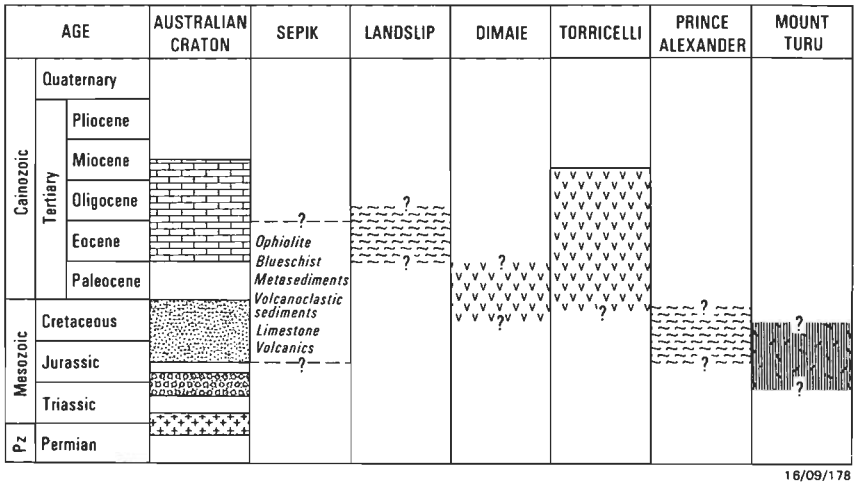

Figure 12. Stratigraphic columns for the terranes of the western part of western Papua New Guinea.
See Figure 10 for terrane location.

deformation events that had previously been thought to mark the initial stages of orogenesis, took place as composite terranes were assembled at sites in ocean basins far removed from the craton edge. The first terrane to dock against the Australian craton was the Sepik composite terrane in the late Oligocene (prior to N3 time) (Fig. 4B). We have extended this docking event into Irian Jaya, based on the time of development of the foreland basin. This event was followed by the docking of the East Papua composite terrane along the eastern edge of the craton by middle Miocene time (Fig. 4C). By late Miocene time the Misool-Kemum composite terrane, the Torricelli-Prince Alexander-Mt Turu terranes, and the western end of the Finisterre terrane had all docked (Fig. 4D). By 2 Ma the eastern part of the Finisterre terrane had docked, as had several small terranes in western Irian Jaya and the terranes of Seram (Fig. 4E).

The apparent absence of docking events in eastern New Guinea since the Pliocene is consistent with the establishment of a number of young ocean basins (e.g. Woodlark and Bismark Basins) and, hence, the lack of a convergent regime along the northern edge of the orogen (see Johnson, 1979). The opening of the Woodlark Basin is currently dismembering the eastern end of the East Papua composite terrane.

Seafloor spreading is thought to be the major process by which terranes are transported across an ocean basin to a continental margin. In New Guinea, unlike North America, subduction beneath the craton was not taking place during the docking of terranes. There is no magmatic evidence for subduction beneath the craton during the Paleogene and early Miocene. Rather, docking occurred because the Australian continent, which was moving northward, entered a subduction zone at which the terranes had assembled during the Palaeogene. The northern edge of the craton had entered the subduction zone by late Oligocene time (Fig. 5).

Conclusions

The New Guinea orogen north of the collision-deformed Australian craton margin is made up of at least thirty-two tectonostratigraphic terranes of varying affinities. Unlike other orogens of the circum-Pacific region, where terranes are predominantly of oceanic affinity, the New Guinea orogen contains a large proportion (about 45%) of terranes with continental affinities. Many of these such as the Jimi and Bena Bena terranes, are probably displaced portions of the northern edge of craton. Others, however, such as the Kemum terrane, were formerly parts of Gondwana that were detached in early Mesozoic times and experienced a history independent of the craton before docking in the Miocene.

Many of the terranes now have their boundaries covered by successor or post-docking basins. These basins typically are Miocene and younger in age and contain from 3-7 km of turbidite fill. Some of these basins are probably pull-apart basins, while others may be molasse basins formed by loading due to the overthrust of terranes. These basins may be modern analogs of depositional environments of the now highly deformed Mesozoic flysch that separates some of the terranes in the North American Cordillera (Coney & others, 1980; Jones & others, 1982).

The analysis of the accretion history of the New Guinea Orogen shows that its development was initiated in the middle-late Oligocene. The Eocene deformation events that had previously been thought to mark the initial phase of development of the orogen are here related to amalgamation of terranes to form composite terranes at sites in ocean basins far removed from the craton. We suggest that the initial docking and accretion of the terranes took place without subduction beneath the craton, because the northward moving Australian continent began to enter, by late Oligocene time, a subduction zone at which composite terranes had been assembled during the Palaeogene.

Acknowledgements

This paper evolved over a considerable time, and aspects of its were discussed with colleagues in Indonesia, Papua New Guinea, and BMR. They are too numerous to mention individually, but we thank them for their help along the way. D.S. Trail read an early draft of the section on Irian Jaya. G. Francis and R. Rogerson read an early draft and drew our attention to new data. Two anonymous referees are thanked for their constructive suggestions. Figures were drawn by L. Hollands and T. Kimber.

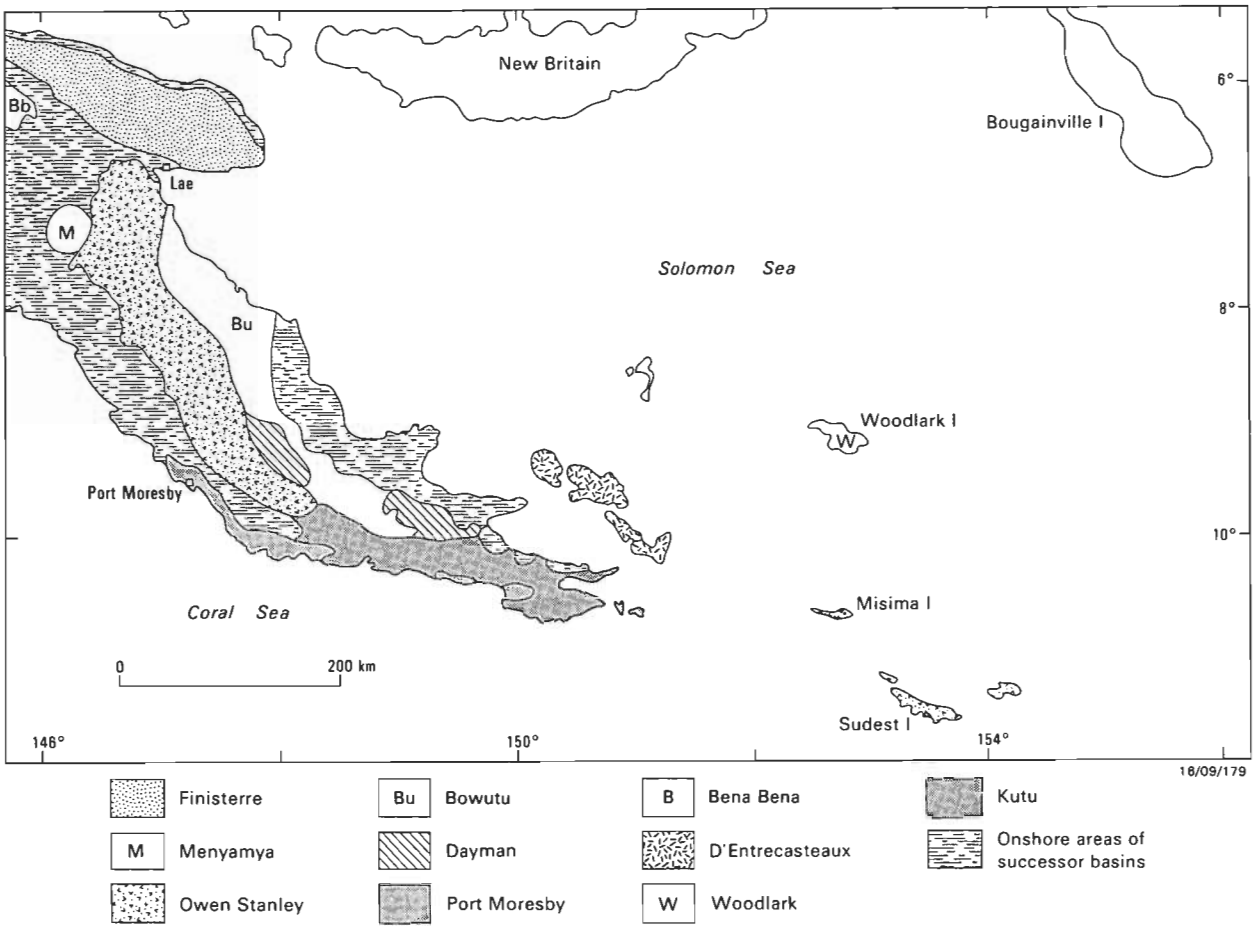

Figure 13. Map of the terranes of eastern Papua New Guinea.

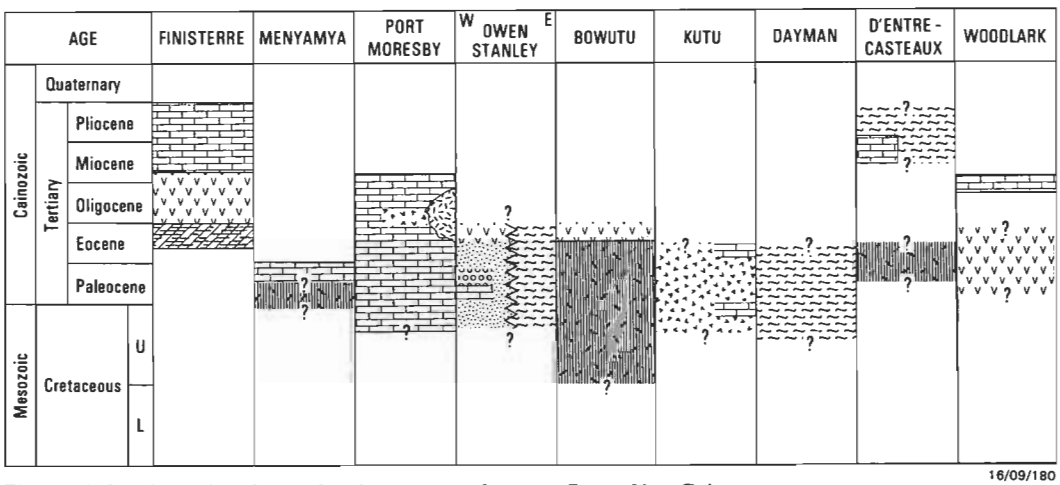

Figure 14. Stratigraphic columns for the terranes of eastern Papua New Guinea.
See Figure 13 for terrane location.

References

Andrews, J.E., Packham G., & Herring, J. 1975—*Initial Reports of the Deep Sea Drilling Project*, 30.

Archbold, N.W., Pigram, C.J. Ratman, N. & Hakim, S., 1982—Permian brachiopod fauna from Irian Jaya. Indonesia: significance for Gondwana—Southeast Asia relationships. *Nature*, 296, 556-558.

Ashley, P.M., & Flood, R.H., 1981—Low-K tholeiites and high-K igneous rocks from Woodlark Island, Papua New Guinea. *Journal of the Geological Society of Australia*, 28, 227-240.

Audley-Charles, M.G., Carter, D.J., & Milson, J.S., 1972—Tectonic development of Eastern Indonesia in relation to Gondwanaland dispersal. *Nature*, 239, 35-39.

Audley-Charles, M.G., Carter, D.J., Barber, A.J., Norvick, M.S., & Tjokrosapoetro, S., 1979—Reinterpretation of the geology of Seram: implication for the Banda Arcs and northern Australia. *Journal of the Geological Society, London,* 136, 547-568.

Bain, J.H.C., 1973—A summary of the main structural elements of Papua New Guinea. *In* Coleman, P.J., (editor), The Western Pacific, island arcs, marginal seas, geochemistry. *University of Western Australia Press, Perth*. 147-161.

Bain, J.H.C. & Mackenzie, D.E., 1975—Ramu — 1:250 000 Geological Series. *Bureau of Mineral Resources, Australia, Explanatory Notes*, SB/55-5.

Bain, J.H.C., Mackenzie, D.E., & Ryburn, R.J., 1975—Geology of the Kubor Anticline, central highlands of Papua New Guinea. *Bureau of Mineral Resources, Australia, Bulletin* 155

Beaumont, C., 1981—Foreland basins. *Geophysical Journal of the Royal Astronomical Society*, 65, 291-329.

Brown, C.M., 1977—Yule, Papua New Guinea — 1:250 000 Geological Series. *Bureau of Mineral Resources, Australia, Explanatory Notes*, SC/55-2.

Brown, C.M., Pieters, P.E., & Robinson, G.P., 1975—Stratigraphic and structural development of the Aure Trough and adjacent shelf and slope areas. *The APEA Journal*, 15, 61-71.

Brown, C.M., Pigram, C.J., & Skwarko, S.K., 1980—Mesozoic stratigraphy and geological history of Papua New Guinea. *Palaeogeography, Palaeoclimatology, Palaeoecology*, 29, 301-322.

Cande, S.C., & Mutter, J.C., 1982—A revised identification of the oldest seafloor spreading anomaly between Australia and Antarctica. *Earth and Planetary Science Letters*, 58, 151-160.

Carter, D.J., Audley-Charles, M.G., & Barber, A.J., 1976—Stratigraphical analysis of island arc — continental margin collision in Eastern Indonesia. *Journal of the Geological Society, London*, 132 179-198.

Chappell, J., 1974—Geology of coral terraces on Huon Peninsula, New Guinea: A study of Quaternary tectonic movements and sea level changes. *Bulletin of the Geological Society of America*, 85, 553-570.

Coney, P.J., Jones, D.L., & Monger, J.W.H. 1980—Cordilleran suspect terranes. *Nature*, 228, 329.

Davies, H.L., 1971—Peridotite-gabbro-basalt complex in eastern Papua: an overthrust plate of oceanic mantle and crust. *Bureau of Mineral Resources, Australia, Bulletin* 128.

Davies, H.L., 1973—Fergusson Island, Papua New Guinea — 1:250 000 Geological Series. *Bureau of Mineral Resources, Australia, Explanatory Notes*, SC/56- 5.

Davies, H.L., 1977—Crustal structure and emplacement of ophiolite in southeastern Papua New Guinea. *Geological Survey of Papua New Guinea, Report* 77/15.

Davies, H.L., 1978—Geology and mineral resources of Papua New Guinea. *Proceedings, Third Regional Conference on Geology and Mineral Resources of Southeast Asia, Bangkok, Thailand*, 685-699.

Davies, H.L., 1980a—Folded thrust fault and associated metamorphics in the Suckling-Dayman massif, Papua New Guinea. *American Journal of Science*, 280-A, 171-191.

Davies, H.L., 1980b—Crustal structure and emplacement of ophiolite in southeastern Papua New Guinea. *In* Allegre, C. & Aubouin, J. (compilers), Orogenic mafic ultramafic association. *Centre National de la Recherche Scientifique, Paris, Colloques Internationaux*, 272, 17-33.

Davies, H.L., 1982a—Mianmin — 1:250 000 Geological Series. *Papua New Guinea Geological Survey, Explanatory Notes* SB/54-3.

Davies, H.L., 1982b—The Papua New Guinea thrust belt, longitude 141-144 East *In* BMR Symposium 1982 Abstracts. *Bureau of Mineral Resources, Australia, Record*, 1982/3, 24.

Davies, H.L., 1983—Wabag — 1:250 000 Geological Series. *Papua New Guinea Geological Survey, Explanatory Notes*, SB/54-8.

Davies, H.L. & Hutchison, D.S., 1982—Ambunti — 1:250 000 Geological Series. *Papua New Guinea Geological Survey, Explanatory Notes*, SB/54-4.

Davies, H.L. & Ives, D.J., 1965—The geology of Fergusson and Goodenough Islands, Papua. *Bureau of Mineral Resources, Australia, Report* 82.

Davies, H.L., & Smith, I.E., 1971—Geology of eastern Papua. *Geological Society of America Bulletin*, 82, 3299-3312.

Davies, H.L. & Smith, I.E., 1974—Tufi-Cape Nelson — *Bureau of Mineral Resources, Australia, Explanatory Notes* SC/55-8,4.

Davies, H.L., Symonds, P.A., & Ripper, I.D., 1984—Structure and evolution of the southern Solomon Sea region. *BMR Journal of Australian Geology & Geophysics*, 9, 49-68.

Dewey, J.F., & Bird, J.M., 1970—Mountain belts and global tectonics, *Journal of Geophysical Research*, 75, 2625-2647.

Doutch, H.F., 1981—Plate tectonic map of the Circum-Pacific region — Southwest Quadrant. *American Association of Petroleum Geologists, Tulsa.*

Dow, D.B., 1977—A geological synthesis of Papua New Guinea. *Bureau of Mineral Resources, Australia, Bulletin* 201.

Dow, D.B., & Hamonangan, B., 1981—Systematic geological map Indonesia— Enarotali 1:250 000 sheet. Preliminary edition. *Indonesian Geological Research and Development Centre, Bandung.*

Dow, D.B., & Plane, M.D., 1965—The geology of the Bena Bena goldfields. *Bureau of Mineral Resources, Australia, Report* 79.

Dow, D.B., & Sukamto, R., 1984 — Western Irian Jaya: the end product of oblique plate convergence in the Late Tertiary. *Tectonophysics*, 106, 109-140.

Dow, D.B., Smit, J.A.J., Bain, J.H.C., & Ryburn, R.J., 1972—Geology of the South Sepik Region, New Guinea. *Bureau of Mineral Resouces, Australia, Bulletin*, 133.

Dow, D.B., Smit, J.A.J., & Page, R.W., 1974—Wau, Papua New Guinea—1:250 000 Geological Series. *Bureau of Mineral Resources, Australia, Explanatory Notes* SB/55-14.

Dow, D.B., Trail, D.S., Ratman, Nana & Hamonangan, Bhakti, 1985—Geological data record: Enarotali 1:250 000 sheet area, Irian Jaya. *Indonesian Geological Research and Development Centre, Open File Report.*

Falvey, D.A., & Pritchard, T., 1984—Preliminary palaeomagnetic results from northern Papua New Guinea: evidence for large microplate rotations. *Transactions of the Third Circum-Pacific Energy and Mineral Resources Conference, Honolulu, 1982*, 593-599.

Giddings, J., Klootwijk, C., Sunata, W., Loxton, C., Pigram, C., & Davies, H., 1985—Palaeomagnetism of Australia's active northern margin in New Guinea. *Abstracts, Third Circum-Pacific Terranes Conference, Sydney.*

Glaessner, M.F., 1949—Mesozoic fossils from the Snake River, Central New Guinea. *Memoir of the Queensland Museum*, 12(4), 165-180.

Haig, D.W., 1982—Deep-sea foraminifera from Paleocene sediments, Port Moresby, Papua New Guinea. *Journal of Foraminiferal Research*, 12(4), 287-297.

Hamilton, W., 1979—Tectonics of the Indonesian Region. *United States Geological Survey, Professional Paper* 1078.

Hermes, J.J., 1968—The Papuan geosyncline and the concept of geosynclines. *Geologie en Mijnbouw*, 47(2), 81-97.

Hobson, P.M., 1986—A thin skinned model for the Papuan Thrust Belt and some implications for hydrocarbon exploration. *The APEA Journal*, 26, 214-224.

Hutchison, D.S., & Norvick, M.S., 1980—Geology of the north Sepik Region, Papua New Guinea. *Bureau of Mineral Resources, Australia, Record* 1980/24.

Jaques, A.L., 1976—High potash island arc volcanics from the Finisterre and Adelbert Ranges, northern Papua New Guinea. *Geological Society of America Bulletin*, 87, 861-867.

Jaques, A.L., 1981—Petrology and petrogenesis of cumulate periodotites and gabbros from the Marum ophiolite complex, northern Papua New Guinea. *Journal of Petrology*, 22, 1-40.

Jaques, A.L., & Robinson, G.P., 1977—The continent/island arc collision in northern Papua New Guinea. *BMR Journal of Australian Geology & Geophysics*, 2, 289-303.

Jaques, A.L., & Robinson, G.P., 1980—Bogia, Papua New Guinea 1:250 000 geological series. *Geological Survey of Papua New Guinea, Explanatory Notes* SB/55-1.

Jaques, A.L., Chappell, B.W., & Taylor, S.R., 1978—Geochemistry of LIL-element enriched tholeiites from the Marum ophiolite complex, northern Papua New Guinea. *BMR Journal of Australian Geology & Geophysics*, 3, 297-310.

Johnson, R.W., 1979—Geotectonics and volcanism in Papua New Guinea: a review of the late Cainozoic. *BMR Journal of Australian Geology & Geophysics*, 4, 181-207.

Johnson, R.W., & Jaques, A.L., 1980—Continent-arc collision and reversal of arc polarity: new interpretation from a critical area. *Tectonophysics*, 63, 111-124.

Jones, D.L., Howell, D.G., Coney, P.J., & Monger, J.W.H., 1983—Recognition character, and analysis of tectonostratigraphic terranes in western North America. *In* Hashimoto, M., & Uyeda, S. (editors), Accretion tectonics in the circum-Pacific region. *Terra Scientific Publishing Company, Tokyo.* 21-35.

Jordon, T.E., 1981—Thrust loads and foreland basin evolution, Cretaceous, western United States. *AAPG Bulletin*, 65, 2506-2520.

Kroenke, L.W., 1984—Cenozoic tectonic development of the southwest Pacific. ESCAP, *CCOP/SOPAC Technical Bulletin* 6.

McMillan, N.J., & Malone, E.J., 1960—The geology of the eastern Central Highlands of New Guinea. *Bureau of Mineral Resources, Australia, Report* 48.

Norvick, M.S., 1979—The tectonic history of the Banda arcs, eastern Indonesia: a review. *Journal of the Geological Society, London*, 136, 519-525.

Norvick, M., & Hutchison, D.S., 1980—Aitape-Vanimo — 1:250 000 geological series. *Geological Survey of Papua New Guinea, Explanatory Notes*, SA/54-15, SA/54-11.

Page, R.W., 1971—Geochronology of igneous rocks in the Papua New Guinea region. *PhD thesis, Australian National University, Canberra.*

Page, R.W., 1976—Geochronology of igenous rocks in the Papua New Guinea region. *Bureau of Mineral Resources, Australia, Bulletin* 162.

Pieters, P.E., 1978—Port Moresby-Kalo-Aroa, Papua New Guinea — 1:250 000 Geological Series. *Bureau of Mineral Resources, Australia, Explanatory Notes,* SC/55-6, 7, 11.

Pieters, P.E., Ryburn, R.J., & Trail, D.S., 1979—Geological reconnaissance in Irian Jaya 1976 and 1977. *Bureau of Mineral Resources, Australia, Record* 1979/19.

Pieters, P.E., Hartono, U., & Amri, Chairul, 1982—Geological data record: Mar 1:250 000 sheet area, Irian Jaya. *Indonesian Geological Research and Development Centre, Open File Report.*

Pieters, P.E., Pigram, C.J., Trail, D.S., Dow, D.B., Ratman, N., & Sukamto, R., 1983—The stratigraphy of western Irian Jaya. *Indonesian Geological Research and Development Centre, Bulletin* 8, 14-48.

Pieters, P.E., Hakim, S., & Atmawinata, S., 1985—Geological data record — Ransiki 1:250 000 sheet area, Irian Jaya. *Indonesian Geological Research and Development Centre, Open File Report.*

Pigram, C.J., 1978—Geology of the Schrader Range. *Geological Survey of Papua New Guinea, Report* 76/4.

Pigram, C.J., & Sukanta, U., 1982—Geological data record — Taminabuan 1:250 000 sheet area, Irian Jaya. *Indonesian Geological Research and Development Centre, Open File Report.*

Pigram, C.J., & Panggabean, H., 1984—Rifting of the northern margin of the Australian continent and the origin of some microcontinents in eastern Indonesia. *Tectonophysics*, 107, 331-353.

Pigram, C.J., Challinor, A.B., Hasibuan, F., Rusmana, E., & Hartono, U., 1982—Lithostratigraphy of the Misool Archipelago, Irian Jaya. *Geologie en Mijnbouw*, 61, 245-279.

Pigram, C.J., Robinson, G.P., & Lumban Tobing, S., 1982—Late Cainozoic origin of the Bintuni Basin and adjacent Lengguru Fold Belt, Irian Jaya. *Proceedings of the Eleventh Annual Convention, Indonesian Petroleum Association*, 109-126.

Pigram, C.J., Arnold, G.A., & Griffin, T.J., in prep.—Geology of the Minj 1:100 000 Sheet area. *Geological Survey of Papua New Guinea, Report.*

Robinson, G.P., 1974—Huon-Sag Sag — 1:250 000 Geological Series. *Bureau of Mineral Resources, Australia, Explanatory Notes* SB/55-11.

Robinson, G.P., Jaques, A.L., & Brown, C.M., 1976—Madang — 1:250 000 Geological Series. *Bureau of Mineral Resources, Australia, Explanatory Notes* SB/55-6.

Rogerson, R., Haig, D.W., & Nion, S.T.S., 1981—Geology of Port Moresby. *Geological Survey of Papua New Guinea Report* 81/16.

Rogerson, R., Williamson, A., Francis, G., & Sandy, M.J., 1982—Geology and mineralization of the Kainantu area. *Geological Survey of Papua New Guinea, Report* 82/23.

Smith, A.G., Hurley, A.M., & Briden, J.C. IV, 1981—Phanerozoic paleocontinental world maps. *Cambridge University Press.*

Smith, I.E., & Davies, H.L., 1973a—Abau, Papua New Guinea — 1:250 000 geological series. *Bureau of Mineral Resources, Australia, Explanatory Notes* SC/55-12.

Smith, I.E., & Davies, H.L., 1973b—Samarai, Papua New Guinea — 1:250 000 geological series. *Bureau of Mineral Resources, Australia, Explanatory Notes* SC/56-9.

Smith, I.E., & Davies, H.L., 1976—Geology of southeast Papuan mainland. *Bureau of Mineral Resources, Australia, Bulletin* 165.

St. John, V.P., 1967—The gravity field of New Guinea. *University of Tasmania, Ph.D. thesis*

Supriatna, S., Apandi, T., & Simandjuntak, T., in press—Geology of Waigeo Island, Irian Jaya. *Indonesian Geological Research and Development Centre, Report.*

Symonds, P.A., Fritsch, J., & Schluter, H.U., 1984—Continental margin around the western Coral Sea Basin: structural elements, seismic sequences and petroleum geological aspects. *In* Watson, S.T. (editor), *Transactions of Third Circum-Pacific Energy and Mineral Resources Conference, Hawaii*, 143-152.

Thompson, J.E., 1967—A geological history of eastern New Guinea. *The APEA Journal*, 83-93.

Thompson, J.E., 1972—Continental drift and the geological history of Papua New Guinea. *The APEA Journal*, 12, 64-69.

Thompson, J.E., & Fisher, N.H., 1967—Mineral deposits of New Guinea and Papua and their tectonic setting. *Proceedings, 8th Commonwealth Mining and Metallurgical Congress*, 6, 115-148.

Tingey, R.J., & Grainger, D.J., 1976—Markham, Papua New Guinea — 1:250 000 geological series. *Bureau of Mineral Resources, Australia, Explanatory Notes* SB/55-14.

Trail, D.S., 1967—Geology of Woodlark Island, Papua. *Bureau of Mineral Resources, Australia, Report* 115.

Visser, W.A., & Hermes, J.J., 1962—Geological results of the exploration for oil in Netherlands New Guinea. *Government Printing Office, The Hague*, 20, p.265.

Wegener, A., 1929—Die Entstehung der Kontinente und Ozeane. 4th edition. *Vieweg, Braunschweig.* (1966 English translation by Dover Publication, New York).

Weissel, J.K., & Watts, A.B., 1979—Tectonic evolution of the Coral Sea Basin. *Journal of Geophysical Research*, 84, 4572-4582.

Williams, H., & Hatcher, R.D. Jr., 1982—Suspect terranes and accretionary history of the Appalachian orogen. *Geology*, 10, 530-536.

Williams, P.R., & Amiruddin, 1983—Diapirism and deformation east of the Mamberambo River, northern Irian Jaya. *Proceedings, Indonesian Petroleum Association, 12th Annual Conference.*

Williams, P.R., Pigram C.J., Dow, D.B., & Amiruddin, 1984—Melange production and the importance of shale diapirism in accretionary terrains. *Nature*, 309, 145-146.

Williamson, A., 1984—Gold mineralisation on Woodlark Island, Milne Bay Province. *Geological Survey of Papua New Guinea Report* 84/10.

Appendix 1. Terrane descriptions

The terranes described below occupy part of the orogen to the north of the craton margin. Only those terranes that occur on the island of New Guinea and adjacent small islands are described. We do not discuss terranes occuring on islands, such as Seram and Halmahera, that may form a western extension of the orogen. To simplify the description and discussion of the terranes, the New Guinea orogen has been divided into 4 regions; from west to east these are Western and Eastern Irian Jaya and Western and Eastern Papua New Guinea (Fig. 1).

Western Irian Jaya

A map of the ten terranes identified in western Irian Jaya is presented in Figure 6 and stratigraphic colums for each of the terranes along with that for the Australian craton are shown in Figure 7.

Kemum terrane

The Kemum terrane is a large continental terrane that occupies most of the Birds Head south of the Sorong Fault Zone. It is separated from the Arfak terrane to the east by the Ransiki Fault Zone. It is partly overthrust by the Lengguru terrane along its southeastern margin, and its southern margin is covered by Miocene sediments of the successor Bintuni and Salawati Basins. The Kemum terrane is the northern part of the western Irian Jaya microcontinent of Pigram & others (1982) and Pigram & Panggabean (1984).

The terrane consists of Siluro-Devonian turbidites, which were isoclinally folded and metamorphosed in the Late Devonian or Early Carboniferous and intruded by Early Carboniferous and Permo-Triassic granitoids. This basement is overlain by Middle Carboniferous to Late Permian shallow marine to paralic siliciclastic sediments. The Mesozoic section is thin, incomplete and locally absent. Jurassic to Triassic red beds overlie the Palaeozoic rocks and are in turn overlain by Cretaceous shallow marine sediments. The latest Cretaceous to early Eocene was marked by the local development of evaporitic sediment, and the Eocene section consists mainly of limestone (Visser & Hermes, 1962; Pigram & Sukanta, 1982; Pieters & others, 1983, 1985). This sequence was folded in the latest Oligocene, before N4 (N.R. Cameron, personal communication, 1984).

Misool terrane

The Misool terrane is a continental terrane that is largely submerged, but crops out on Misool Archipelago and the Kumawa and Onin Peninsulas of western Irian Jaya. The terrane is bounded to the southwest by the Seram Trough. The boundaries between the Misool

and Kemum, and Misool and Lengguru terranes are covered by Miocene and younger sediments of the Salawati and Bintuni Basins. The Misool terrane is the southwesterly part of the western Irian Jaya microcontinent of Pigram & others (1982) and Pigram & Panggabean, (1984).

The Misool terrane consists of a Palaeozoic basement of an isoclinally folded and metamorphosed turbidite sequence overlain unconformably by an almost complete sequence of Mesozoic sediments. The sequence consists of Triassic turbidites, Late Triassic shallow-water limestone, Early Jurassic to early Late Cretaceous bathyal mudstone and limestone, which is tuffaceous near the top, and Late Cretaceous fluvio-deltaic clastics and nodular limestone. The Palaeogene section is dominated by shallow-water carbonates. The pre-Miocene section was folded in late Oligocene to early Miocene time (Pigram & others, 1982). The post-Palaeozoic section is highly fossiliferous and consequently well dated.

Tamrau terrane

The Tamrau terrane, named for the Tamrau Mountains, is found in the northern Birds Head and northern Salawati Island of Irian Jaya. In the northern Birds Head the terrane is separated from the Arfak terrane by the Koor Fault Zone, and from the Kemum terrane by the Sorong Fault Zone. The Tamrau terrane on Salawati Island is separated from the Waigeo terrane on Batanta Island by a narrow strait, which probably contains a strand of the Sorong Fault Zone. The Tamrau terrane partly corresponds to Pieters & others' (1982) Tamrau Block.

The terrane consists of Middle to Late Jurassic and (?)Late Cretaceous bathyal shale and minor quartz sandstone, (?)Late Cretaceous quartz sandstone, (?)Palaeogene calcilutite and middle Miocene intermediate volcanics and epiclastic sediments. The Jurassic and Neogene rocks are well dated, but there is no age control for the other sediments.

The Tamrau terrane is unlike any other of the terranes in western Irian Jaya. Similar associations of Mesozoic bathyal shale and mid-Miocene intermediate volcanics are known from the northern flank of the central ranges in east Irian Jaya and Papua New Guinea (Visser & Hermes, 1962; Dow, 1977).

Waigeo terrane

The Waigeo terrane is named after Waigeo Island in northwest Irian Jaya. The rocks of this terrane are exposed on Waigeo Island and on numerous small islands to the west, including Batanta and Kofiau. A small elongate sliver of the terrane occurs along the northern edge of the Birds Head east of Sorong. Waigeo Island is separated from the Birds Head by a shallow strait, which may coincide with a strand of the Sorong Fault Zone.

The terrane consists of an ophiolite complex overlain by Late Jurassic bathyal sediments. Both these units supplied detritus to the overlying Palaeocene to Eocene turbidites, which are overlain by late Eocene to Miocene basaltic to andesitic pillow lavas, lava breccia with intercalations of tuffaceous sandstone, mudstone, tuff, and minor conglomerate. The volcanic sequence is overlain by Miocene limestone (Supriatna & others, in press). The terrane is interpreted as a late Eocene to Miocene island-arc complex built on an oceanic basement. The pre-Late Jurassic age for the ophiolite makes it one of the oldest in the region and also suggests it is allochthonous, as the oceanic crust of the Philippine Plate to the north and the Caroline Basin to the west are both Paleogene or younger (Doutch, 1981).

Arfak terrane

The Arfak terrane is named for the Arfak Mountains in the northeastern Birds Head of Irian Jaya. The terrane has been dismembered and forms several subterranes, which are found on Biak, Yapen, and Num Islands at the head of Sarera Bay, and in the Arfak and Tosem Mountains of the northern Birds Head, The Arfak Mountains subterrane is separated from the Kemum terrane on its southwest side by the Ransiki Fault. The terrane extends offshore to the east and is covered by Late Cainozoic sediments. In the northern Birds Head, the terrane is separated from the Tamrau terrane to the south by the Koor Fault and Neogene sediments.

The terrane consists of upper Eocene to middle Miocene basaltic to andesitic lava, breccia, and tuff, and is intruded by dykes and stocks of dolerite and gabbro. They are overlain by early to middle Miocene limestone (Pieters & others, 1982, 1983, 1985). Foraminifera are common in limestone lenses in the volcanics and four K-Ar isotope ages give a range of 10.5 Ma to 33.1 Ma. The terrane is interpreted as an island-arc complex.

Netoni terrane

The Netoni terrane, named for Mount Netoni, is a small terrane (60 km × 18 km) in the northwestern Birds Head, adjacent to the Sorong Fault Zone. It is faulted against the Tamrau terrane on the northern side, and the Kemum terrane on its southern side. The terrane consists of Late Permian to Early Triassic (245–225 Ma) granitoids, ranging in composition from quartz syenite to diorite and adamellite (Pieters & others, 1982).

Lengguru terrane

The Lengguru terrane occupies the eastern half of the Birds Neck in western Irian Jaya. It is named after, and largely corresponds to, the Lengguru fold belt of Visser & Hermes (1962). The Lengguru terrane is in fault contact with the Wandamen terrane to the east, forms part of the west side of Sarera Bay in the northeast, and is covered by sediments of the post middle Miocene Bintuni Basin along its western margin. Its southern margin is formed by the Tarera-Aiduna fault zone. The style of the contact between the Lengguru and Kemum terranes is not clear; possibly, the Lengguru terrane is thrust over the Kemum terrane. The terrane consists of middle Jurassic to Cretaceous siliciclastic littoral to bathyal sediments, overlain by Late Cretaceous to middle Miocene carbonates, which consist of a western shallow-water facies and an eastern deep-water facies (Visser & Hermes, 1962; Pieters & others, 1983). The nature of the basement to the Lengguru terrane is not known. This entire sequence was folded and thrust to the west during the late Cainozoic. The terrane has contributed detritus to the Bintuni Basin since the late Miocene.

The Middle Jurassic to mid Miocene sequence of the Lengguru terrane is very similar to that of the Australian craton to the southeast. The present-day distribution of shallow and deep-water facies of the Middle Jurassic and Cretaceous clastic sediments suggests that they were derived from a quartz-rich source to the west, but this implied source area is now occupied by the Misool terrane, which was the site of bathyal sedimentation during the Mesozoic. Clearly, the Lengguru terrane is no longer linked to its Mesozoic source areas.

Wandamen terrane

The Wandamen terrane occurs along the southwestern side of Sarera Bay, where it crops out on Roon Island, the Wandamen Peninsula, and the Wondiwoi Range. The northern end of the terrane forms a dissected elongate dome, which is thought to be a metamorphic core complex. The terrane is in fault contact with the Lengguru and Mangguar terranes.

The Wandamen terrane consists of northern high-grade and southern low-grade metamorphic portions. The high-grade portion consists mainly of amphibolite-grade gneiss and amphibolite. The gneiss is quartzo-feldspathic, formed from a protolith of granite, granodiorite, and quartz-monzonite. Metabasic rocks are much less common and appear to be metamorphosed basalts or gabbros. Some are retrogressively metamorphosed eclogite (Pieters & others, 1979, 1983). Minor pelitic schists and carbonate-bearing metasediments also occur (Pieters & others, 1979). The southern low-grade terrane is mostly dark slate, phyllite, metawacke, and quartzite of greenschist facies, with rare marble, chlorite schist, and metachert. The protoliths appear to be mainly turbidites in which no fossils are preserved and, hence, their age is not known. K-Ar isotope ages on biotite and hornblende give late Miocene to late Pliocene ages for the high-grade rocks (Pieters & others, 1979, 1983).

Mangguar terrane

The Mangguar terrane named for the Mangguar Peninsula, is a long narrow terrane (225 × 30 km) that occurs along the southwest side of Sarera Bay and extends south to the Tarera-Aiduna Fault Zone in the Birds Neck. In the south it is in fault contact with the

Wandamen and Weyland terranes, and to the north it is largely submerged.

The terrane consists of (?)Palaeozoic siliciclastics and dolomite, Permian and Triassic granitoids, Triassic to Jurassic red beds, Jurassic to Cretaceous mudstone, and Miocene shallow-water limestone (Pieters & others, 1983; Dow & others, 1985). The Mangguar terrane may be a composite terrane, consisting of elements of both the Australian craton and the Kemum terrane. The Palaeozoic sediments resemble those of the Australian craton to the south, but the Permian and Triassic granitoids are only known from the Kemum terrane, Netoni terrane, Sorong Fault Zone, Border Mountains terrane, and the Australian craton in Papua New Guinea. However, the position of the Mangguar terrane north of the Australian craton between the Wandamen and Weyland terranes suggests that it is entirely allochthonous.

Weyland terrane

The Weyland terrane lies south of Sarera Bay and is named after the Weyland Mountains; it corresponds to the Weyland overthrust of Dow & Sukamto (1984). The terrane is bounded by faults: the southern margin is faulted against the Australian craton along the Tarera-Aiduna Fault, the eastern margin is bounded by the Siriwo Fault; and the western margin, by an unnamed fault that separates it from the Mangguar terrane.

The terrane consists of slate, phyllite, and minor metavolcanics, calcsilicates, peridotite, and amphibolite, intruded by a large Miocene diorite and granodiorite batholith, and overlain by coeval andesitic volcanics (Pieters & others, 1983).

Mini-terranes in the Sorong and Ransiki fault ones

The Sorong and Ransiki Fault Zones range in width from a few hundred metres to 10 km and contain a wide range of 'mini' terranes ranging in size from a few metres of several kilometres across. Many of these blocks may by derived from adjacent terranes (Pieters & others, 1982).

Eastern Irian Jaya

The geology of eastern Irian Jaya is poorly known and has never been systematically mapped. Only four terranes are described below, but doubtless more will be identified in future. A map of the terranes is presented in Figure 8 and stratigraphic columns in Figure 9.

Gauttier terrane

The Gauttier terrane is named for the Gauttier Ranges in northern Irian Jaya. It consists of one large (75 km × 25 km) and two smaller (30 km × 5 km and 5 km × 25 km) fault-bounded blocks, which are completely surrounded by middle Miocene (N12) and younger sediments and mud volcano fields (Williams & Amiruddin, 1983). The geology of the terrane is poorly known. It appears to consist mainly of basaltic lavas and breccia, overlain by purple, reddish to pink calcilutite and tuffs of unknown age (Visser & Hermes, 1962). The Gauttier terrane is possibly a dismembered portion of the Torricelli terrane to the east.

Cyclops terrane

The Cyclops terrane is named after the Cyclops Mountains west of Jayapura in northeastern Irian Jaya. The terrane, which is separated from the Torricelli terrane by Late Cainozoic sediments, consists of early Miocene acid to intermediate schist, amphibolite gneiss, and marble, faulted against peridotite, gabbro, dolerite, basalt, and serpentinite of unknown age (Pieters & others, 1979). The latter are overlain unconformably by Miocene and younger biomicrite and biocalcarenite. Two K-Ar ages (20.6 ± 0.4 Ma and 21.4 ± 0.4 Ma) have been reported for the metamorphic rocks (Pieters & others, 1979). Little is known of its structural and metamorphic history or the timing of the juxtaposing of the metamorphic and mafic and ultramafic rocks of this terrane.

Rouffaer terrane

The Rouffaer terrane, named for the Rouffaer River, extends along the northern flank of the central ranges of Irian Jaya from the Derewo River at 136°15'E in the west to approximately 140°E. The terrane consists of a poorly known ophiolite complex called the Irian Jaya Ophiolite by Dow & Sukamto (1984). Only the western end of the terrane has been mapped (Dow & Hamonangan, 1981), but it can be traced eastward on airphotos and satellite images. The principal rock types at the western end are periodite, pyroxenite, metagabbro, and serpentinite.

Border Mountains terrane

The Border Mountains terrane is named for the Border Mountains, which straddle the Indonesia-Papua New Guinea border at about 3°45'S. The terrane is thought to consist of mainly Permian granitoids (257–242 Ma) and dacitic volcanics, but the rock types are known only from float (Norvick & Hutchison, 1980). The boundaries shown in Figure 5 are interpreted from aerial photographs and satellite images. Similar rocks are known from the Australian craton to the southeast and from the Kemum, Netoni, and Mangguar terranes of western Irian Jaya.

Western Papua New Guinea

Twelve terranes have been identified in western Papua New Guinea. Stratigraphic columns for each terrane and the Australia craton are shown in Figure 11 and 12 and the location of each terrane in Figure 10.

Sepik composite terrane

The terrane is named after the Sepik River. It is a large composite terrane that crops out along the north side of the central ranges south of the Sepik River and between the May River in the west and the Maramuni River in the east. The same rock types are common along the north side of the Sepik valley as far north as the axis of the northern ranges, suggesting that this terrane may also underlie the Lumi Trough. The Sepik composite terrane is in fault contact with the Landslip terrane to the west and the Jimi terrane to the east. To the south it has been thrust over Mesozoic platform, slope, and rise sediments of the Australian craton.

The Sepik composite terrane consists of at least 6 subterranes that are intimately mixed by thrusting and faulting. The terrane includes rocks of oceanic, island-arc, and continental origin. The predominant rock types are peridotite, blueschist, slate, phyllite, garnet—mica schist, quartzofeldspathic and calcic gneiss, volcanics, tuffaceous and volcaniclastic sediments, quartzose sediment, and limestone (Dow & others, 1972; Davies, 1982a, 1983; Davies & Hutchison, 1982).

The **April subterrane** consists of dismembered, thrust-bound sheets of peridotite with minor gabbro and pyroxenite, which are commonly serpentinised around their margins (Davies, 1982a, 1983; Davies & Hutchison, 1982;). The sheets are numerous and range in size from 25 × 8 km to blocks measured in tens of metres. They occur throughout the terrane and, in the northern Lagaip valley, directly overlie deformed Jurassic sediments (Davies, 1983) of the Australian craton margin.

The **Tau subterrane** consists of glaucophane—epidote and glaucophane— lawsonite mafic schist with chlorite, albite, white mica and quartz; some calcareous pelitic schist, rare ultramafic schist, and minor eclogite. This subterrane forms an overthrust sheet 55 km long with a maximum width of 12 km on the north side of the Schatteburg Mountains. It has overridden the Salumei and Sau subterranes. The age of the protolith is not known, but K-Ar glaucophane mineral ages of 38.7 Ma and 43.6 Ma suggest a late Eocene metamorphic event, while K-Ar ages on phengite (23–27 Ma) suggest a late Oligocene uplift age for this terrane (Davies, 1982a).

The **Ambunti subterrane** consists of garnet-mica schist, quartzofeldspathic, mafic and calcic gneiss with minor sericite schist, and phyllite. Protolith ages are not known, but five K-Ar and one Rb-Sr age determination suggest a late Oligocene (23–27 Ma) uplift age for this subterrane (Page, 1976; Davies, 1982a).

The **Salumei subterrane** consists of slate, phyllite, and sericitic schist derived from pelitic protoliths containing quartzose and lithic sandstones. A Cretaceous to early Tertiary age for these rocks is suggested by the presence of a Neocomian ammonite (Dow & others, 1972), Late Cretaceous-Tertiary bivalves and Cenomanian—Maastrichtian planktic foraminifera (Davies & Hutchison, 1982).

Blocks of Eocene shallow-water limestone (Davies, 1982a; Davies & Hutchison 1982) occur throughout this terrane. They may be either olistoliths, or dismembered parts of another terrane or the Australian craton.

The **Sau subterrane** consists of basalt and andesitic volcanics, red and green volcaniclastic sediment and limestone. Eocene planktic forams have been found in limestone and calcareous siltstone that form the matrix to volcanic breccia and agglomerate (Davies, 1983).

The **Sitipa subterrane** is confined to the Sitipa River area. It consists of dark-grey calcareous siltstone and shale with thin interbeds of fine quartz sandstone, and contains a characteristic Late Jurassic fauna (consisting of *Malayomaorica malayomaorica* and *Inoceramus* cf. *Haasti*) (Dow & others, 1972; Davies & Hutchison, 1982). This subterrane is identical to the Late Jurassic rocks of the Australian craton to the south and southeast. However, it is surrounded by other subterranes of the Sepik composite terrane, suggesting that it is either a window through the Sepik terrane or a displaced part of the Australian craton.

All the subterranes, except the Tau subterrane are intruded by Miocene granitoids and overlain by an overlap assemblage of middle Miocene and younger sediments and volcanics.

Landslip terrane

The Landslip terrane is named after the Landslip Ranges of western Papua New Guinea. The terrane occurs in the Landslip and West Ranges south of the Sepik River adjacent to the Irian Jaya border. The terrane is faulted against Middle and Late Jurassic black shale to the south (Trangiso Fault), the Sepik terrane to the southeast (Abi fault), and the Dimaie terrane to the northeast (Idam Fault). The western side of the terrane is buried beneath Late Cainozoic sediments of the upper Sepik Valley.

The Landslip terrane consists of mica schist, hornblende gneiss, minor marble, phyllite, and minor green mafic schist. The metamorphics are predominantly of amphibolite facies with some greenschist facies rocks. The protolith was pelitic sediment and mafic and minor calcareous rocks of unknown age. Limited isotope age dating of the metamorphism suggests that the most recent metamorphic event was completed by the late Oligocene (Davies, 1982a). It is possible that the Landslip terrane was formerly part of the Australian craton (like the Bena Bena terrane) that has been displaced and affected by a younger metamorphic overprint.

Dimaie terrane

The Dimaie terrane is named after the Dimaie River, a tributary of the Sepik River, and is located between the Sepik and May Rivers in western Papua New Guinea near the Irian Jaya border. The terrane is faulted against the Landslip terrane (Idam Fault), and surrounded on all other sides by Late Cainozoic sediments of the Lumi Trough. It consists of chloritised amygdaloidal and vesicular glassy basalt and andesite submarine lava, lava breccia, agglomerate and tuff, intruded by probably contemporaneous gabbro. There is little age control on these rocks. They are intruded by Eocene and Miocene stocks and overlain by late early Miocene sediments. They are regarded as Late Cretaceous to Eocene in age by Davies (1982a). The Sau subterrane of the Sepik composite terrane resembles the Dimaie terrane and may be dismembered parts of it.

Torricelli terrane

The Torricelli terrane is named for the Torricelli Mountains, which form part of the north coast ranges of Papua New Guinea. The terrane forms a linear east-west belt about 275 km long, extending from near Wewak to southeast of Jayapura in Irian Jaya. It is separated from the Prince Alexander and Mount Turu terranes by Late Cainozoic sediments, and, along its southern margin, is faulted against small outliers of metamorphic rock, which are referred to the Sepik terrane, but might belong to the Landslip terrane.

The Torricelli terrane consists of a basic to intermediate volcanic complex (Bliri Volcanics) and a coeval intrusive complex (Torricelli Intrusive Complex) (Hutchison & Norvick, 1980). The Bliri Volcanics are a mixed sequence of mainly basaltic and andesitic lavas and associated volcaniclastic rocks with minor argillite, small limestone lenses and, locally, thinly bedded radiolarian chert and tuffaceous limestone. Pillow lavas and pillow breccias are common. Foraminifera from calcareous rocks distributed throughout the section give ages ranging from Palaeocene to early Miocene. Possible Late Cretaceous faunas in volcanics, and reworked Late Cretaceous faunas in cover sediments suggest that the base of the sequence may be older (Hutchison & Norvick, 1980).

The intrusive rocks consist of medium-grained, non-porphyritic gabbro and diorite, dolerite, subordinate monzonite and granodiorite, and rare adamellite, harzburgite, and pyroxenite. The rocks are commonly highly deformed by fracturing, shearing, and brecciation. Twenty-one K-Ar isotopic age determinations indicate that the complex is partly Late Cretaceous (73.2–68.0 Ma), and partly late Eocene to early Miocene (41.3–17.3 Ma) (Hutchison & Norvick, 1980).

Prince Alexander terrane

The Prince Alexander terrane is named after the Prince Alexander Ranges of northern Papua New Guinea. It is a narrow southeasterly trending terrane separated from the Torricelli terrane by a complex fault system that is largely covered by Neogene sediments. The Mount Turu terrane occurs along strike from the Prince Alexander terrane, but the two are separated by Neogene sediments.

The terrane consists of deformed plutonic and metamorphic rocks, including granodiorite, diorite, dolerite, amphibolite, orthogneiss and quartz-mica- epidote schist, which are intruded by undeformed biotite adamellite stocks and andesite porphyry dykes. Shearing of the deformed rocks is accompanied by intense fracturing and mylonitisation; cataclastic rocks are common (Hutchison & Norvick, 1980). K-Ar isotope ages indicate that the high-grade metamorphic rocks are Early Cretaceous and the undeformed stocks and dykes are late Oligocene to early Miocene. A single K-Ar isotope age on a boulder of weathered granite indicates that part of the complex may be as old as Middle Jurassic (Hutchison & Norvick, 1980).

Mount Turu terrane

The Mount Turu terrane is a small terrane (27 km × 5 km) southwest of Wewak and centred on Mount Turu, a part of the north coast ranges of Papua New Guinea. It is separated from the Prince Alexander and Torricelli terranes by Late Cainozoic sediments. Its southern margin is faulted against low to medium-grade metamorphic rocks that are referred to the Sepik terrane. It consists of highly faulted and sheared ultramafic and basic rocks of unknown age and is intruded by Miocene adamellite and granodiorite. The terrane has a low gravity expression, suggesting that it is thin and possibly thrust over the Sepik composite terrane (Hutchison & Norvick, 1980).

Jimi terrane

The Jimi terrane is a large terrane (200 km long and 50 km wide) along the north side of the central ranges. It is named after the Jimi River, which drains a large part of the terrane. The terrane is separated from the Marum and Schrader terranes by the Bundi fault zone, and from the Sepik terrane by the Maramuni Fault. It is stitched to the Sepik terrane by the middle Miocene South Yuat batholith. The Bismarck Fault Zone separates the terrane from the Australian craton, and the large batholith of the middle Miocene Bismarck Intrusive Complex separates it from, and stitches it to, the Bena Bena terrane. The terrane consists of Permian to Triassic granitoids overlain by Middle Triassic black shale and a Middle to Late Triassic bimodal volcanic complex. The complex consists of acid and basic lavas, breccia tuffs, and basic dykes with an extensive non-marine and marine epiclastic apron. This complex is intruded by Early to Middle Jurassic granitoids and is overlain by a Jurassic sequence consisting of basal volcaniclastic sands which pass up into shaly facies. In the south of the terrane, the Jurassic shale gives way to Cretaceous shale with minor sandstone; to the northwest, the Jurassic shale passes up into Cretaceous basaltic and andesitic volcanics overlain by Late Cretaceous to Eocene shale (Bain & others, 1975; Pigram, 1978; Pigram & others, in press; Davies & Hutchison, 1982).

This sequence may have been part of the northern edge of the Australian continent (Brown & others, 1980; Pigram & Panggabean, 1984), but its present position, partly adjacent to the eastern end of the Sepik terrane, suggests that it has been displaced in a northwesterly direction. It should be considered a terrane, until the amount of movement between it and the Australian craton has been determined.

Schrader terrane

The Schrader terrane is named for the Schrader Range, which occurs between the Yuat and Ramu Rivers. It is separated from the Jimi terrane by the Bundi Fault Zone, and is overthrust by the Marum terrane. To the east and north it is covered by sediments of the late Cainozoic Sepik-Ramu Basin.

The Schrader terrane is a composite terrane consisting of a series of probable thrust slices made up to greenschist facies slate, phyllite, meta-volcanics, metasandstone and metaconglomerate, marble, marl, and a small ultramafic and mafic complex. The relationship between each slice unit is not known, but all exhibit the same structural history (Pigram, 1978). Rocks of the terrane are poorly dated. Deformed pelecypods of Late Cretaceous age have been collected from metasandstone, and Eocene foraminifera occur in float samples that may have been shed from the marble within the terrane. The terrane is intruded by middle Miocene granitoids. The southwestern edge of the terrane consists entirely of Late Cretaceous black calcareous slate with Late Cretaceous to Eocene limestone blocks scattered through it (Pigram, 1978).

Marum terrane

The Marum terrane is named after the Marum River, which cuts the terrane. It lies on the northern flank of the Bismarck Mountains, and is separated from the Bena Bena and Jimi terranes by the Bundi Fault Zone. The terrane is probably in thrust contact with the Schrader terrane; to the northeast, its contact with the Finisterre terrane is obscured by the Late Cainozoic Ramu Basin.

The Marum terrane consists of two allochthons; a large periodotite-gabbro massif and a smaller spilitic pillow basalt and argillite sheet that lies to the south and partly beneath the large massif. The peridotite-gabbro massif consists of a basal tectonite peridotite overlain by cumulate peridotite and gabbro. The two allochthons form northeasterly dipping thrust sheets. Windows through the peridotite-gabbro sheet and gravity data suggest that the terrane is thrust over the Schrader terrane (Jaques, 1981; Jaques & others, 1978). The age of formation of this ophiolite complex is uncertain. K-Ar isotope dating of cumulate gabbros indicates a maximum age of 173 Ma (Early Jurassic), but a granophyric diorite gave a much younger Paleocene date (59 ± 2.5 Ma). Probable Eocene fauna (radiolaria) occur in the argillite that overlies the pillow basalt (Jaques, 1981). The age of emplacement of the complex is not well constrained. It post-dates late Cretaceous to Eocene shales of the Schrader terrane found beneath the complex, and predates Quaternary alluvial deposits of the Ramu Valley.

Bena Bena terrane

The Bena Bena terrane, named after the Bena Bena River, is located in the eastern highlands of Papua New Guinea. It is separated from the Finisterre terrane by the Ramu-Markham Fault Zone and from the Marum terrane by the Bundi Fault Zone. The terrane is stitched to the Jimi terrane to the northwest by the large batholith of the middle Miocene Bismarck Intrusive Complex, and its southern boundary is covered by late Oligocene and younger sediments.

The Bena Bena terrane consists of slate, phyllite, and greenschist facies schists with minor amphibolite and marble intruded by Early Jurassic and early Late Cretaceous granitoids (McMillan & Malone, 1960; Dow & Plane, 1965; Tingey & Grainger, 1976; Page, 1976; Rogerson & others, 1982). The metamorphic rocks are unconformably overlain by Eocene limestone which contains schist clasts (Robinson & others, 1976). The metamorphics were formed from quartz-rich greywacke and sandstone, siltstone, and shale, the ages of which are unknown. Metamorphism occurred before the Jurassic.

Rogerson & others (1982) and Pigram & Panggabean (1984) considered the Bena Bena terrane to be part of the northern edge of the Australian craton. It is treated here as a distinct terrane because that relationship has not been proved.

Finisterre terrane

The Finisterre terrane is named after the Finisterre Range, which forms part of the north coast ranges of Papua New Guinea. It occurs in a discontinuous southeasterly trending belt, about 300 km long; that extends from south of Bogia to the Huon Peninsula and includes rocks of the Adelbert, Finisterre, and Saruwaged Ranges. The terrane is separated from the Owen Stanley and Bena Bena terranes by the Ramu-Markham Fault Zone and from the Marum, Schrader, and Torricelli terranes by the Late Cainozoic Sepik and Ramu Basins.

The terrane is an island-arc complex that consists of a thick sequence of middle and upper Eocene hemipelagic and pelagic sediments overlain by an Oligocene to early Miocene basaltic to andesitic volcanic complex with high-potash, high-alumina basaltic and shoshonitic affinities (Jaques, 1976). The volcanic complex is overlain by thick shallow-water limestone of middle Miocene to Pliocene age (Robinson, 1974; Robinson & others, 1976; Jaques & Robinson, 1980).

Preliminary palaeomagnetic data for the eastern end of the Finisterre terrane (Falvey & Pritchard, 1984) suggest that, during the Palaeogene, it was part of an extensive linear island arc formed by New Britain, New Ireland, Manus, and the Solomon Islands. This arc was subsequently broken up and Falvey & Pritchard (1984) suggested that the Finisterre terrane docked with the Australian craton some time after the early Pliocene.

Eastern Papua New Guinea

Eight terranes have been identified in eastern Papua New Guinea, and are described below. A map of the distribution of the terranes is shown in Figure 13 and stratigraphic columns for each terrane in Figure 14.

Owen Stanley terrane

The Owen Stanley terrane crops out over a large part of the East Papuan mainland and in the Louisiade Archipelago. It is named after the Owen Stanley Ranges, and in east Papua it forms a southeasterly trending terrane, 375 km long and up to 80 km wide, which extends from near Lae in the north to approximately 148°10′E. This part of the terrane is in fault contact with the Bowutu terrane for much of its eastern boundary. In the southeast it may be faulted against the Dayman terrane. The northwestern end of the terrane is separated from the Finisterre terrane by the Ramu-Markham Fault Zone. To the west, the Owen Stanley terrane is separated from the Menyamya terrane by an overlap assemblage of late Oligocene to early Miocene shallow marine sediments. Along its southern margin it is stitched to the Port Moresby terrane by the Oligocene Sadowa Gabbro.

The Owen Stanley terrane is made up of two belts. The eastern belt comprises low-grade greenschist facies metasediments of pelitic and psammitic derivation with subordinate metavolcanics, minor blueschists, and granulites adjacent to the Bowutu terrane. The western belt consists of argillite, shale, lithic and feldspathic sandstone, greywacke, minor limestone, pebble conglomerate, and spilitic volcanics (Dow & others, 1974; Davies & Smith, 1971; Brown, 1977; Pieters, 1978). The relationship between the belts is not clear. Davies & Smith (1971) suggested that the sediments rested unconformably on the metamorphics, but Brown (1977) and Pieters (1978) suggested the belts are lateral equivalents, and separated them at a chlorite isograd.

The age of the protoliths for the metamorphic rocks of the terrane is poorly known. Middle Cretaceous (Aptian-Cenomanian) molluscs (Glaessner, 1949) have been found in the northern part of the terrane, but, elsewhere, little control exists. Similarly, the age of the metamorphism is not well known. Eocene limestone containing schist clasts and strained quartz has been reported from near Tapini (Davies & Smith, 1971; Brown, 1977). A K-Ar age of 52 Ma for a hornblende granulite from near the Owen Stanley Fault is reported by Davies & Smith (1971) and Rb-Sr isotope age data (Page, 1976) on metasediments near Wau give an early Miocene age (21 Ma).

The belt of sediments is also largely unfossiliferous, but Late Cretaceous to Paleocene, early Eocene, and late Oligocene to early Miocene foraminifera are found in limestone lenses (Brown, 1977; Pieters, 1978; G. Francis, personal communication, February, 1986), which are generally sheared and may be fault bounded. The terrane is overlain by late Oligocene and younger sediments and volcanics, and intruded by Oligocene gabbro and Miocene granitoids.

Bowutu terrane

The Bowutu terrane forms an arcuate terrane, 400 km long and 25-40 km wide, along the northern side of the Owen Stanley Range in East Papua. Smaller areas of peridotite on Fergusson and Normanby Islands are also included in this terrane. It is separated from the Owen Stanley, Dayman, and Kutu terranes by the Owen Stanley fault zone (Davies, 1971; Smith & Davies, 1976; Davies, 1980b). The terrane on Fergusson and Normanby Islands is in fault contact with the D'Entrecastreaux terrane.

The Bowutu terrane consists of the Papuan Ultramafic Belt (PUB) (Davies, 1971), which is intruded by Eocene tonalite and unconformably overlain by middle Eocene andesitic volcanics (Davies, 1971, 1977). The PUB consists of 4-8 km of ultramafic rock overlain by about 4 km of gabbroic rocks, which are overlain by about 4 km of basaltic volcanics. The complex appears to be Cretaceous in age, based on several K-Ar isotope ages on rocks from the gabbroic and basaltic layers, and the occurrence of a poorly preserved foraminifera in sediments associated with the basalts (Davies, 1977).

Kutu terrane

The Kutu terrane, named after the Kutu River in east Papua, crops out over an extensive area of the southeast Papuan mainland and on Sideia and Basilaki Islands. It is in fault contact with the Dayman, Owen Stanley, and Bowutu terranes.

The Kutu terrane consists of submarine tholeiitic basalt with minor dolerite, gabbro, and rare ultramafic rocks, interbedded volcanolithic sandstone, argillite, and calcilutite. The calcilutite lenses contain Maastrichtian and middle Eocene planktic foraminifera (Smith & Davies, 1973 a,b, 1976). The terrane is intruded by minor middle and late Miocene monzonite and syenite stocks and dykes.

Dayman terrane

The Dayman terrane is named for Mount Dayman in east Papua. Parts of the dismembered terrane occur in the Owen Stanley Ranges east of Port Moresby, around Mt Dayman and on Normanby Island. The terrane is thought to be thrust over the Owen Stanley terrane and is, in turn, overthrust by the Bowutu terrane. Near Mt Dayman, the southern margin of the terrane is in presumed fault contact with the Kutu terrane, and is covered along its northern edge by middle Miocene to Quaternary sediments of the Cape Vogel Basin. On Normanby Island, the terrane is in fault contact with the D'Entrecasteaux terrane.

The Dayman terrane consists of green mafic schist, with minor pelitic schist and marble. Metamorphic grade ranges from prehnite-pumpellyite to lawsonite—glaucophane and greenschist facies (Pieters, 1978; Davies, 1980a). The protolith was predominantly mafic volcanics with minor sediments. The age of the volcanic protoliths is not known, but the calcareous sedimentary protoliths of the Bonenau schist member in the Mt Dayman region contain late Cretaceous and Eocene faunas (Davies & Smith, 1974). A single K-Ar age on metamorphic amphibole from the western part of the terrane gives an Eocene age (42 ± 4 Ma) for the metamorphism (Davies, 1980b). The Dayman Dome has features in common with the metamorphic core complexes of western North America.

Woodlark terrane

The Woodlark terrane forms a largely submerged ridge that extends eastward from the Trobriand Islands. Woodlark Island, the only emergent part of the ridge, has a basement of lava, pillow lava, pyroclastics, and sediments of Eocene age (Williamson, 1984). These rocks are overlain by late Oligocene limestone, which contains reworked, probably Eocene, large benthonic foraminifera (Davies & others, 1984; Trail, 1967; Ashley & Flood, 1981).

The ridge was formerly next to that part of the Owen Stanley terrane found in the Louisiade Archipelago, but has been rifted from it by the formation of the Woodlark Basin by sea-floor spreading during Pliocene to Holocene time.

D'Entrecasteaux terrane

The D'Entrecasteaux terrane crops out on Fergusson, Goodenough, and Normanby Islands of the D'Entrecasteaux Islands in eastern Papua New Guinea. These islands form the southern part of a large shallow platform that extends to just north of the Trobriand Islands. The terrane consists of quartzo-feldspathic gneiss and layered amphibolite intruded by Pliocene granodiorite batholiths. The metamorphics are of amphibolite and pyroxene granulite and eclogite facies, and form domes with granodiorite cores, (Davies & Ives 1965; Davies & Smith, 1971; Davies, 1973). The age of the metamorphics is not known. The protoliths appear to have been predominantly of granodiorite composition with minor basic volcanics. This terrane may be an eastern extension of the Owen Stanley terrane.

Port Moresby terrane

The Port Moresby terrane is named for and occurs in the vicinity of Port Moresby and along the southern part of the Papuan peninsula to the east. The western part of the terrane is in fault contact with the Owen Stanley terrane. The nature of the contact of the eastern part of the terrane with the Kutu terrane is not known.

The Port Moresby terrane consists of ?Oligocene gabbroic rocks and a highly faulted and repeated sequence that contains a mixture of deep and shallow-water sediments. Neritic Campanian arenaceous limestone is juxatoposed with deep-water sediments, which include Maastrichtian-Paleocene middle to lower bathyal and Eocene abyssopelagic carbonate and siliceous rocks, as well as terrigenous turbidites. No upper Eocene or lower Oligocene units are known. Late Oligocene tuff and tuffaceous sediments, and bathyal turbidites and carbonates of late Oligocene to early Miocene and latest Miocene to earliest Pliocene age also occur (Pieters, 1978; Rogerson & others, 1981; Smith & Davies 1973a, b; Haig, 1982; D.W. Haig, personal communication, July 1985). The sediments generally contain abundant planktic foraminifera and are well dated.

Deformation of this terrane in the Port Moresby area occurred during the Oligocene to middle or late Miocene and, possibly, in the earliest Pliocene (Rogerson & others, 1981; D.W. Haig, personal communication, July, 1985).

Menyamya terrane

The Menyamya terrane, which is located west of Wau, is named after the town of Menyamya. It is a small elliptical terrane, measuring approximately 35 km × 25 km. The western edge of the terrane is in thrust fault contact with early middle Miocene sediments, which contain detritus derived from the terrane. To the east, its contact with the Owen Stanley terrane is covered by an overlap assemblage of late Oligocene to early Miocene marine sediments.

The terrane consists of sheared mafic and ultramafic rocks, basic volcanics, grey and red siltstone, chert and bathyal limestone (Uyaknji Complex) of probably Paleocene to Eocene age (T.J. Griffin, personal communication, December 1984). The terrane is interpreted as oceanic crust that formed close to an exposed landmass (T.J. Griffin, personal communication, December 1984) and was thrust westward in middle to late Miocene time.

BMR Journal of Australian Geology & Geophysics, 10, 213-224

Hydrocarbon generation potential in the Otway Basin, Australia

E. Anne Felton[1] & K.S. Jackson[2]

The Otway Basin is a rifted margin basin containing a sequence of Mesozoic to Tertiary sediments up to 7500 m thick, resting on a Palaeozoic metasedimentary and granitic basement. Hydrocarbon shows are common throughout the basin, the most significant occurrences being small gas fields in basal upper Cretaceous sandstone in the eastern part of the basin, one of which is in commercial production, and a 3 m oil column in Lindon 1 in basal Tertiary sandstone in the central basin area. A lack of commercial oil discoveries in twenty-five years of active exploration and the small size of the known gas fields, together with uncertainty about source rock quality and maturation levels, have tended to downgrade the petroleum potential of the Otway Basin. Geochemical data, mainly from the Cretaceous sequence, indicate that both Upper and Lower Cretaceous rocks have fair quality gas source potential. Some thin beds of oil-prone source rocks may be present, mainly in the Lower Cretaceous and lower Tertiary sequences. Cretaceous structural development appears to have exerted a strong control on maturation throughout the basin. Hydrocarbons formed early in the basin's history are unlikely to have been preserved.

Introduction

This study was undertaken as part of BMR's continuing assessment of Australia's petroleum resources, and aimed to give an indication of petroleum source-rock quality and establish an organic maturity profile for the Otway Basin, particularly in the Cretaceous section. Source potential of the Torquay Basin, regarded by some as part of the Otway Basin (Robertson & others, 1978), was discussed by Nicholas & others (1981) and is not further considered here.

Some maturation studies in the Otway Basin have been carried out using geohistory analysis of wells (Middleton & Falvey, 1983) and fission track analysis of detrital minerals (Duddy & others, 1985). Maturation and source potential for certain areas of the basin were discussed by Tabassi & Davey (1985), Holdgate (1981), Holdgate & others (1985), and Struckmeyer & Cook (in press). Our data are complementary to these investigations.

Sixty-three core samples from 10 exploration wells (Table 3) were analysed by the Australian Mineral Development Laboratories (AMDEL) for total organic carbon (TOC), extractable organic matter (EOM), and composition of extract. Gas chromatograms of the saturates fraction of the extract were obtained. Vitrinite reflectance and maceral abundancies in the dispersed organic matter also were determined by AMDEL from polished sections of the cores, using standard organic petrological techniques.

Unpublished open-file source-rock analyses and vitrinite reflectance data, also obtained from core sampling (Jackson & others, 1983), were integrated with the data obtained from BMR sampling. Core samples, while more accurately located in a well, have the disadvantage of not providing continuous downhole coverage. Hence canned cuttings, provided by Beach Petroleum from North Paaratte 1 and 3 wells (30 m sample interval) were subjected to head-space gas analysis at BMR, for better source-rock assessment of the Otway Basin sequence in the Port Campbell area. Shell pyrolysis sniff analyses of cuttings from Caroline 1, Flaxmans 1, and Nautilus 1A are also incorporated into this study.

Geological setting

The Otway Basin extends west-northwest for some 500 km along the southern Australian coast (Fig. 1), and contains up to 7500 m of Mesozoic to Tertiary sediments on a Palaeozoic metasedimentary and granitic basement.

The sedimentary sequence comprises four major lithogenetic units (Table 1): the Upper Jurassic to Lower Cretaceous Otway Group, consisting of up to 4500 m of continental lithic sandstone, siltstone and shale, and minor coal; up to 5000 m of Upper Cretaceous marine mudstone and sandstone (Sherbrook Group); lower Tertiary marine to fluvial sandstone and mudstone (Wangerrip and Nirranda Groups), and upper Tertiary calcareous mudstone and limestone (Heytesbury Group). These units are separated by major regional unconformities. Other unconformities exist within the Tertiary sequence and, possibly, also in the Otway Group (Esso, 1974) and Sherbrook Group.

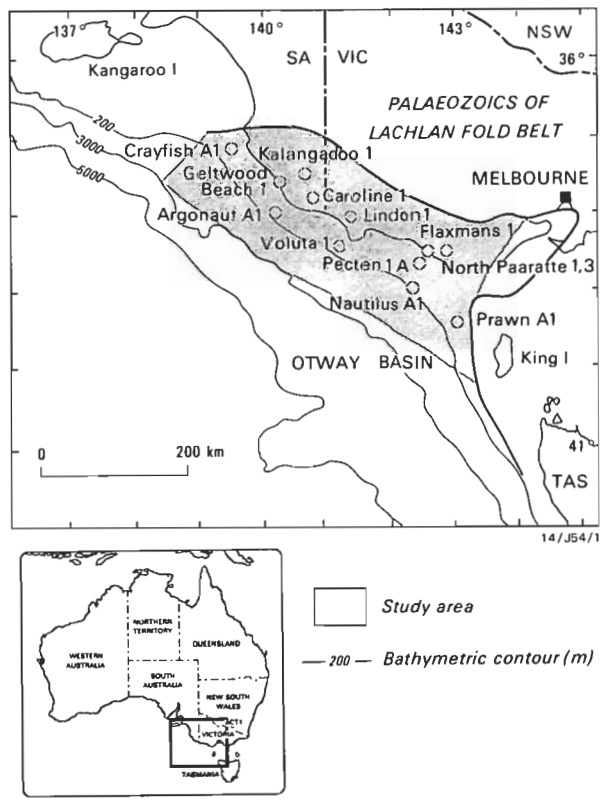

Figure 1. Otway Basin, with locations of wells used in geochemical study.

The Otway Basin is a rifted-margin basin formed during the separation of Australia from Antarctica. The structural style of the basin is dominated by west-northwest-trending down-to-basin normal faults. This faulting was probably initiated as the basin began to subside in the Early Cretaceous, when the crust thinned before continental break-up, reaching a maximum during mid-Cretaceous to early Tertiary time as seafloor spreading commenced (Weissel & Hayes, 1972; Cande & Mutter, 1982; Mutter & others, 1985). A north-

[1]Resource Assessment Division, Bureau of Mineral Resources, GPO Box 378, Canberra, ACT 2601
[2]Shell Development (Australia) Pty Ltd.

northeast-trending system of horsts and grabens onshore developed during the Late Cretaceous. The Voluta Trough subsided relative to the Mussel Platform during this time: Upper Cretaceous sediments are up to 5000 m thick in the western Voluta Trough, and only 1000 m thick over much of the Mussel Platform (estimated from data in Robertson & others, 1978). The southwestern offshore margin of the basin is a basement high on the mid-continental slope, over which Cretaceous sediments thin (Denham & Brown, 1976). Onshore, the basin edge is defined by outcrop limits of Cretaceous and Tertiary rocks.

Petroleum potential

The petroleum geology of the Otway Basin has been discussed in a number of publications (BMR, 1966; Leslie, 1966; Weeks & Hopkins, 1967; Wopfner & Douglas, 1971; Denham & Brown, 1976), and reviewed by Ellenor (1976), Robertson & others (1978), McPhee (1980), Tallis (1980), Laws (1985), and Felton & Jackson (1985).

Principal exploration objectives are porous and permeable sandstones overlying unconformities at or near the base of both Upper and Lower Cretaceous sedimentary sequences (Waarre Sandstone and Pretty Hill Sandstone, respectively) (Table 1). Seals are provided by overlying and adjacent fine-grained or otherwise impermeable sediments.

A commercial gas discovery has been made in the eastern part of the basin, where gas occurs in reservoir sands of the Waarre Sandstone (McPhee & others, 1980). Oil and gas shows in the Cretaceous sequence are widely distributed in the basin (Robertson & others, 1978; Wopfner & others, 1971).

Table 1. Stratigraphy of the Otway Basin

Age	Group	Formation
Pliocene to Oligocene	Heytesbury Group	Port Campbell Limestone Gellibrand Marl Clifton Formation
Eocene	Nirranda Group	Narrawaturk Marl Mepunga Sandstone
Paleocene	Wangerrip Group	Dilwyn Formation Pember Mudstone Pebble Point Formation
Late Cretaceous	Sherbrook Group	Curdies Formation Paaratte Formation Nullawarre Greensand Belfast Mudstone Flaxman Formation Waarre Sandstone
Early Cretaceous (Late Jurassic?)	Otway Group	Eumeralla Formation Pretty Hill Sandstone

Table 2. Ranges and average values of total organic carbon by stratigraphic formation

Formation	TOC%		Number of samples
	Range	Average	
Gellibrand Marl	0.15–0.43	0.26	7
Dilwyn Formation	1.87–3.00	2.23	4
Pebble Point Formation	1.65–2.13	1.89	2
Curdies Formation	1.37–8.01	1.53*	3
Paaratte Formation	1.49–3.10	2.26	
Belfast Mudstone (incl. Flaxman Formation)	0.86–2.59	1.50	13
Waarre Sandstone	1.14		1
Eumeralla Formation	0.25–7.75	0.62*	10
Pretty Hill Sandstone	0.26–15.9	0.82*	7

* Highest value in range removed for calculation of average

Lindon 1 well, drilled in December 1983, intersected 3.0 m of oil-saturated sandstone in the basal Tertiary Pebble Point Formation overlying the Cretaceous–Tertiary unconformity (Tabassi & Davey, 1985). Drilling offshore has been disappointing, and only 2 of the 16 wells drilled have recorded hydrocarbon shows. Pecten 1A tested gas at the rate of 2500–4100 m^3/d(max) from the Waarre Sandstone. Crayfish A1 recovered a small amount of gas from a formation interval test in the Pretty Hill Sandstone, and fluorescence and reservoir bitumen were observed deeper in the same formation (Esso, 1968).

Most of the potential hydrocarbon traps tested by drilling are associated with syndepositional down-to-basin normal faulting. These include simple fault traps (reservoir rock faulted against cap rock or sealed by impervious fault zones) and anticlinal (roll over) traps, which developed concomitantly with faulting. Most wells in the basin have tested structural traps, although stratigraphic traps (both unconformity and facies pinchout traps) next to basement highs represent potential plays throughout the basin.

Fault-related traps formed mainly during mid-Cretaceous to early Tertiary time (100–55 Ma), after which major faulting ceased (Robertson & others, 1978). Minor movement on pre-existing faults probably continued, particularly offshore, as the basin stabilised into its present structural configuration with blocks of continental crust subsiding to abyssal depths after continental breakup about 45 Ma ago (Robertson & others, 1978). Such movement may have breached hydrocarbon reservoirs and may account in part for the observed strandings of inspissated oil along the southern coast of Australia (McKirdy & Horvath, 1976; McKirdy, 1985; McKirdy & others, 1986).

The absence of commercial oil discoveries and the small size of the discovered gas fields, together with uncertainty about source-rock quality and maturation levels, have downgraded the prospectivity of the Otway Basin.

Source-rock evaluation

Core data

Source-rock richness. For each formation sampled, the range and average value of total organic carbon, a measure of source-rock richness, are given in Table 2. A value of 0.5 per cent total organic carbon is widely accepted as a minimum for adequate source potential (Dickey & Hunt, 1972). On that basis, the Gellibrand Marl has no source potential. All other formations contain adequate organic matter, the Dilwyn and Paaratte Formations being the richest. The Lower Cretaceous Eumeralla Formation and Pretty Hill Sandstone, although relatively lean over-all, contain some rich intervals in Crayfish A1 well.

Further organic geochemical data for the core samples are presented in Table 3. The interpreted ratings included in Table 3 have been obtained from a cross plot of total hydrocarbons — saturated hydrocarbons (SATS) plus aromatic hydrocarbons (AROM) — against total organic carbon (TOC) (Fig. 2). For immature source rocks, *ultimate* hydrocarbon source potential can be estimated by evaluating the amounts of extractable organic matter (EOM) relative to TOC.

The Dilwyn Formation rates as a fair to very good source of both oil and gas, although it is immature where sampled for this study, and both Upper and Lower Cretaceous formations rate as fair hydrocarbon sources, predominantly for gas.

Maturation. Vitrinite reflectance data (Table 3) indicate that the Upper and Lower Cretaceous formations are largely immature and rarely reach the vitrinite reflectance range of 0.7 to 1.2 per cent widely accepted as the interval within which most hydrocarbons, particularly oil, are generated (the 'oil window'). Graphical presentation of the vitrinite reflectance data by well (Fig. 3) clearly illustrates this point, and only deeper samples from Crayfish A1, Prawn A1 and Voluta 1 reach the oil window.

Normal and isoprenoid alkane profiles for selected cores from Voluta 1 provide further evidence of the largely immature

Table 3. Organic geochemical data

Index no.	Well name	Core no.	Depth (m)	Lithology	TOC (%)	EOM (ppm)	SATS (ppm)	AROM (ppm)	POLAR (ppm)	ASPH (ppm)	Ro Mean Max	Source rating
Gellibrand Marl												
1	Nautilus-A1		844.9	Lst	0.16	57	2	1	40			Lean-barren
2	Nautilus-A1		847.3	Lst	0.15	31	1	1	14			Lean-barren
3	Nautilus-A1		951.5	Calc. shale	0.18	42	1	1	20			Lean-barren
4	Nautilus-A1		114.3	Calc. shale	0.25	90	2	2	40			Lean-barren
5	Nautilus-A1		1259.7	Shaly Lst	0.21	108	5	25	46			Lean-barren
6	Nautilus-A1		1414.2	Calc. shale	0.43	186	9	4	99			Lean-barren
7	Nautilus-A1		1577.3	Calc. shale	0.42	106	5	2				Lean-barren
Dilwyn Formation												
8	Caroline-1		213.1		3.00	5500	587	1430	198		0.40	Very good
9	Caroline-1		748.0		2.05	877	121	246	81		0.44	Fair
10	Voluta-1	2	909.2	Siltstone	1.98	2564	92	13	215	1541	(0.34)[1]	Gas source
11	Prawn-A1		1201.2	Sandy siltstone	1.87	654	62	13	78	252		Gas source
Pebble Point Formation												
12	Nautilus-A1		1729.4	Siltstone	1.65	1661	42	74	150	676		Fair
13	Nautilus-A1		1733.9		2.13	2611	84	68	339	1554	(0.47)	Fair
Curdies Formation												
14	Argonaut-A1	3	981.5	Silty sandstone	8.01	5490	55	5	840	3997	0.39	Gas source
15	Prawn-A1	3	1299.2	Shale	1.37	887	61	27	138	349	(0.40)	Gas source
16	Voluta-1	5	1413.9	Silty claystone	1.70	1402	102	28	243	411	0.63	Fair
Paaratte Formation												
17	Caroline-1		1250.9		1.80	339	71	55	149		0.56	Fair
18	Argonaut-A1	5	1310.6	Silty sandstone							0.47	Fair
19	Argonaut-A1	6	1472.9	Silty mudstone	3.10	595	65	8	139	147	(0.46)	Gas source
20	Argonaut-A1	8	1808.0	Sandstone							0.46	Gas source
21	Argonaut-A1	11	2734.2	Silty mudstone	2.06	1645	115	49	446	849	0.49	Fair
22	Voluta-1	8	1796.2	Siltstone	1.98	796	92	22	320	219	(0.51)	Gas source
23	Voluta-1	9	1917.3	Siltstone	2.94	803	96	26	202	248	(0.55)	Gas source
24	Voluta-1	10	2039.3	Siltstone	1.49	517	67	11	95	327	0.59	Gas source
25	Prawn-A1	8	2027.3	Shale	2.43	946	93	19	201	473	(0.51)	Gas source
Belfast Mudstone (including Flaxman Formation)												
26	Pecten-1A	3	1741.2	Sandstone							0.46	—
27	Nautilus-A1		1859.8	Shale	1.30	461	57	33	162	169		Gas source
28	Nautilus-A1	9	1860.4	Shale	1.56	1265	89	39	343	612	(0.49)	Fair
29	Nautilus-A1		2003.1	Shale	1.32	373	20	21	94	142		Gas source
30	Nautilus-A1	10	2008.5	Shale	2.59	1148	83	45	303	576	0.53	Gas source
31	Prawn-1	9	2184.5	Siltstone	1.10	420	58	4	117	131	0.55	Gas source
32	Prawn-1	10	2398.5	Coaly sandstone							0.54	Gas source
33	Prawn-1	12	2655.2	Shale	2.39	1859	138	87	530	829	0.54	Fair
34	Prawn-1	13	2832.5	Shale	2.26	2950	159	112	322	1387	0.61	Fair
35	Voluta-1	13	2460.0	Siltstone	1.37	450	78	14	123	156	0.62	Gas source
36	Voluta-1	15	2672.4	Siltstone	1.40	513	28	22	200	166	(0.50)	Gas source
37	Voluta-1	16	3036.3	Siltstone	1.23	784	29	21	234	260	(0.61)	Gas source
38	Voluta-1	18	3323.9	Siltstone	0.86	479	31	22	128	223	0.93	Gas source
39	Voluta-1	21	3654.3	Siltstone	0.98	752	103	44	205	223	(0.80)	Fair
40	Argonaut-A1	12	3039.7	Sandstone							0.52	—
41	Argonaut-A1	14	3448.9	Shale	1.09	792	52	28	145	450	(0.57)	Gas source
Waarre Sandstone												
42	Argonaut-A1	15	3559.2	Sandstone	1.14	1422	111	74	378	737	0.60	Fair
43	Flaxmans-1		2194.5								0.89	—
Eumeralla Formation												
44	Prawn-1	14	3008.0	Sandstone							0.86	—
45	Kalangadoo-1		764.7	NS	1.80	1310	227	200	217		0.42	Fair
46	Crayfish-A1	11	1467.9	Mudstone	7.75	8329	1103	408	2166	2432	0.39	Fair
47	Pecten-1A	4	1803.8	Sandstone							(0.55)	—
48	Prawn-A1	15	3099.3	Sandstone	0.26	212	71	10	71	40	0.63	Lean-barren
49	Prawn-A1	16	3190.3	Sandstone	1.42	1440	92	42	236	782	0.68	Fair
50	Kalangadoo-1		1717.2	NS	0.75	274	103	62	113		0.40	Fair
51	Kalangadoo-1		1866.6	NS	0.75	288	58	58	87		0.47	Fair
52	Kalangadoo-1		2154.3	NS	0.25	67	31	7	18		0.38	Lean-barren
53	Geltwood Beach-1	10	1342.6	NS	0.75	118	21	14	39		0.50	Gas source
54	Geltwood Beach-1	18	2144.3	NS	0.50	100	0	14	44		0.78	Lean-barren
55	Geltwood Beach-1	22	2725.5	NS	0.55	201	33	35	144		0.71	Lean-barren
56	Geltwood Beach-1	23	2855.7	NS	0.40	87	12	26	46		0.96	Lean-barren
Pretty Hill Sandstone												
57	Crayfish-A1	15	1662.9	Mudstone	0.26	245	60	11	46	98	(0.42)	Lean-barren
58	Crayfish-A1	18	1857.8	Shale	0.44	413	24	7	67	198	0.51	Lean-barren
59	Crayfish-A1	22	2470.3	Mudstone	15.9	21560	1229	1078	5261	11017	0.58	Fair
60	Crayfish-A1	26	2909.5	Sandstone	1.07	728	65	50	227	325	0.59	Fair
61	Crayfish-A1	27	3035.6	Mudstone	1.00	965	57	40	215	531	(0.74)	Fair
62	Crayfish-A1	28	3195.3	Mudstone	1.60	800	84	80	353	218		Fair
63	Geltwood Beach-1	29	3725.6	NS	0.55	302	25	118	95		1.26	Fair

[1]Values in brackets signify insufficient determinations for an accurate mean.

nature of the Upper Cretaceous sediments at this location (Fig. 4). The profiles show a gradual loss of bimodality, diminishing odd-over-even predominance between n.C_{25} and n.C_{31}, and decreasing pristane n.C_{17} and phytane n.C_{18} ratios with depth. These parameters indicate an increasingly mature sequence (Tissot & Welte, 1978). Adequate maturity for oil generation appears to have been attained only in the deepest sample, in the Belfast Mudstone. Variation of these profiles between wells is not great, because we have observed little difference in organic matter type within each Upper Cretaceous formation throughout the basin.

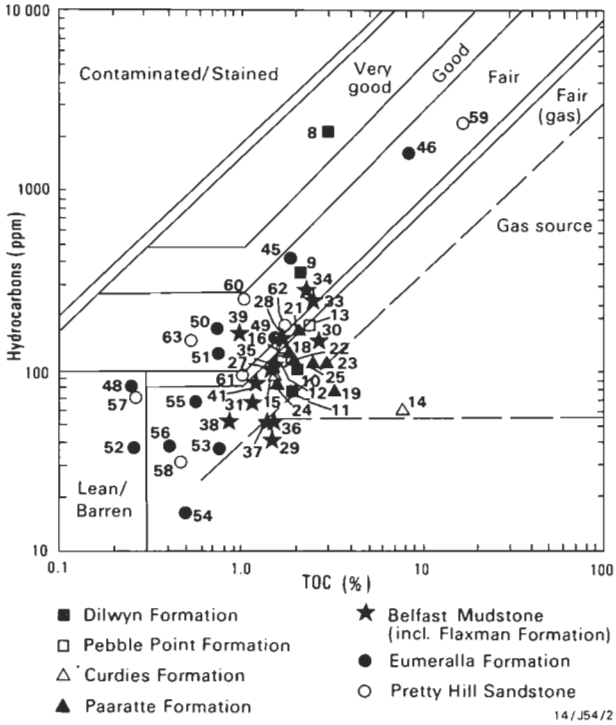

Figure 2. Total hydrocarbons versus total organic carbon, with petroleum source ratings.

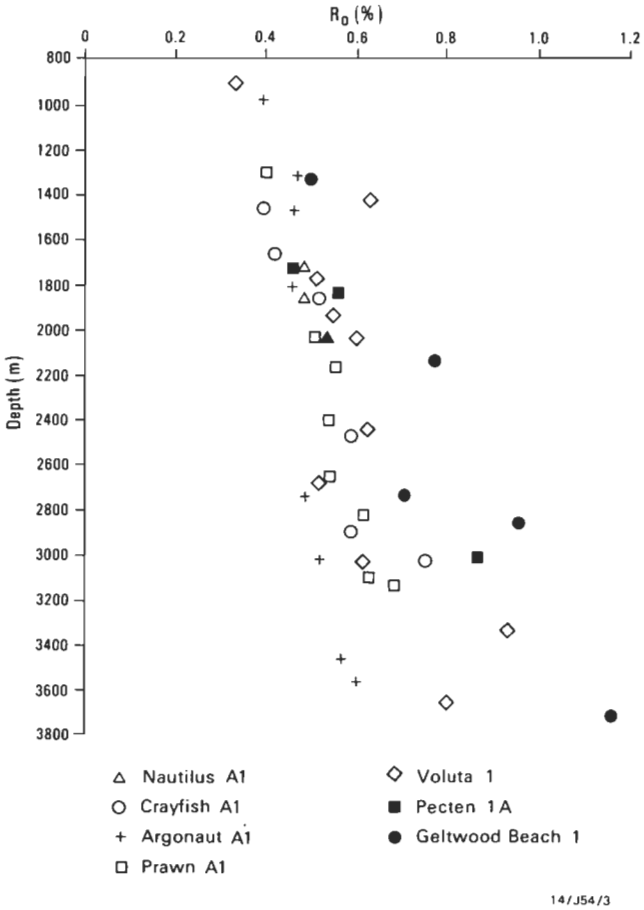

Figure 3. Vitrinite reflectance data plotted by well.

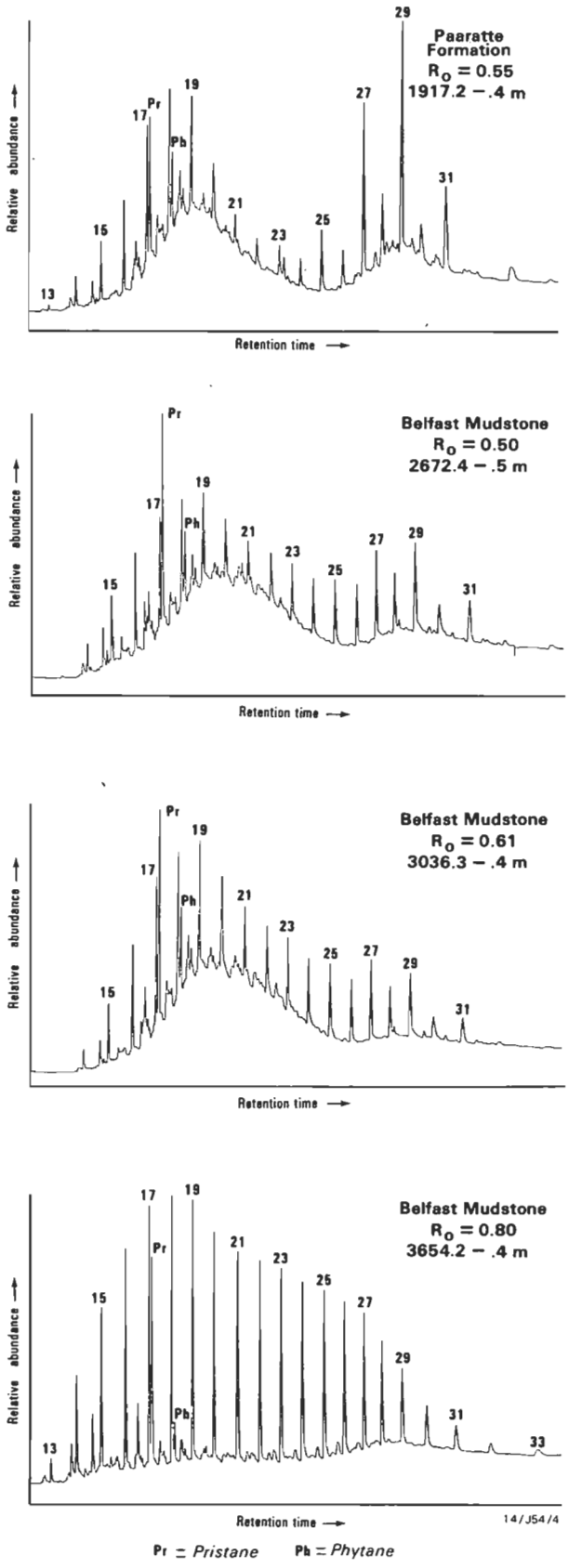

Figure 4. Gas chromatograms, Voluta 1.

Composition of organic matter. The ability of source beds to generate petroleum liquids or gases, assuming adequate maturation levels, depends on the types of organic matter present. Kerogen types I-IV of Tissot (1984) correspond to the four organic maceral groups, alginite, exinite, vitrinite, and inertinite, respectively (Waples, 1982). The petrographic determinations by AMDEL did not distinguish alginite, which may have been included in the exinite group.

For an appropriate set of geological factors, including adequate maturation level, kerogen types I-II (albinite/exinite) will yield predominantly oil, whereas kerogen type III (vitrinite) will yield predominantly gas (Waples, 1982). The potential of vitrinite to yield significant amounts of petroleum liquids has been suggested as a result of both petrographic and geological studies (Smith & Cook, 1984) and pyrolysis studies (Rouzaud & Oberlin, 1983). Inertinite has no hydrocarbon generation potential (Tissot, 1984).

Both late Upper and early Lower Cretaceous sediments contain, predominantly, vitrinite and inertinite (Table 4). The commonly high inertinite content downgrades over-all source potential. The Eumeralla Formation averages significantly more vitrinite relative to exinite than any other formation.

Exinite contents in the Cretaceous section are generally low, averaging 3 per cent (all samples). The most exinite is found in the Paaratte Formation in Voluta 1 and Argonaut 1. Exinites in the Late Cretaceous Curdies and Paaratte Formations and in the Early Cretaceous Eumeralla Formation are dominated by resinite, whereas the Belfast Mudstone exinites are more mixed in composition.

The gas-prone nature of the Cretaceous section, indicated by the source- potential plots (Fig. 2), may be due to maturity or type of organic matter, or a combination of both. Immature source rocks, unless extremely rich, are generally considered as gas generative and hence will plot as 'gas source' or 'fair' at best. However, Snowdon & Powell (1982) provided evidence for condensate and, possibly, oil generation at low maturity levels (as low as 0.45 per cent vitrinite reflectance), provided that the organic source is rich in resinite.

Summary. The core data indicate the presence of late Upper and early Lower Cretaceous source rocks that are immature and, hence, largely gas generative. An indication of their potential source quality, assuming they do reach oil maturity elsewhere in the basin, is given by the TOC and EOM values. The Paaratte Formation and Belfast Mudstone consistently have the highest EOM and TOC values and, hence, the best source potential (Table 2), but this is still largely for gas, owing to their vitrinite-dominated organic matter.

Head-space gas analysis — North Paaratte 1 and 3

The downhole analysis of head-space gas from canned cuttings for North Paaratte 1 and 3 (Figs. 5 & 6) enables an evaluation of source potential and organic maturity in the North Paaratte gas field, near Port Campbell. Methods of interpreting such data have been discussed by Jackson (1982) and are not further described here.

Data from both wells clearly indicate the immature nature of the section, as it is only within the bottom 90 m of North Paaratte 3, in the Otway Group, that wet gas content is higher than 50 per cent. Fair source quality (occasionally good in North Paaratte 3) is recognised in the Paaratte Formation, lower Belfast Mudstone, Waarre Sandstone, and Eumeralla Formation.

Table 4. Organic maceral data.

Rock unit	Well	Depth (m)	% Organic material	Relative proportions (%)[1]			Comments on exinite[2]
				Vitrinite	Inertinite	Exinite	
Dilwyn Fm	Voluta-1	909.2	1		Not counted		?A (one fragment)
Dilwyn Fm	Prawn-A1	1201.2	1	18	81	1	R, LD
Curdies Fm	Argonaut-A1	981.4	50	19	78	3	R,A, (C,LD traces)
Curdies Fm	Prawn-A1	1299.2	2	39	60	1	R,C, (v sparse sample)
Curdies Fm	Voluta-1	1413.9	1	30	70	1	R, LD
Paaratte Fm	Argonaut-A1	1472.9	15	8	85	7	R, S, LD
Paaratte Fm	Argonaut-A1	2734.2	7	19	76	5	R (LD, trace)
Paaratte Fm	Voluta-1	1796.2	5	18	74	8	R (LD,C, traces)
Paaratte Fm	Voluta-1	1917.3	3	12	83	5	R, C, ?A
Paaratte Fm	Voluta-1	2039.3	10	38	56	6	R, LD, ?A
Paaratte Fm	Prawn-A1	2027.3	7	33	65	2	R, S
Belfast Mdst	Nautilus-A1	1860.4	2	34	62	4	LD (?)
Belfast Mdst	Nautilus-A1	2008.5	3	23	73	4	?A, R
Belfast Mdst	Prawn-A1	2184.5	7	20	78	2	R, S
Belfast Mdst	Prawn-A1	2655.2	5	34	65	1	C, ?A
Belfast Mdst	Prawn-A1	2832.5	5	91	8	1	R, C
Belfast Mdst	Voluta-1	2460.0	10	20	78	2	A, R, LD
Belfast Mdst	Voluta-1	2674.4	15	15	80	5	R, LD, SE
Belfast Mdst	Voluta-1	3036.3	5	8	69	3	A, LD
Belfast Mdst	Voluta-1	3323.9	1	36	64	1	R, ?C (LD, trace only)
Belfast Mdst	Voluta-1	3654.3	1	29	70	1	BTM (?)
Belfast Mdst	Argonaut-A1	3448.9	2	13	83	4	R
Waarre Sst	Argonaut-A1	3559.2	25	30	68	2	R (LD, trace)
Eumeralla Fm	Crayfish-1	1467.9	20	85	12	2	R, S, LD
Eumeralla Fm	Prawn-A1	3099.3	3-5	61	38	1	R
Eumeralla Fm	Prawn-A1	3190.3	35	47	53	1	R
Pretty Hill Sst	Crayfish-1	1662.9	2	50	49	1	LD, S (rare)
Pretty Hill Sst	Crayfish-1	1857.8	2	69	27	4	S, LD (?)
Pretty Hill Sst	Crayfish-1	2470.3	10	63	36	1	S, R, LD
Pretty Hill Sst	Crayfish-1	2909.5	1-2	36	64	1	S, R
Pretty Hill Sst	Crayfish-1	3035.6	1	3	97	—	None
Pretty Hill Sst	Crayfish-1	3195.3	3	6	94	—	None

[1]Determined by point-counting polished sections

[2]Exinite minerals in decreasing order of abundance. Abbreviations: A, alginite; BMT, translucent matter; C, cutinite; LD, liptodetrinite; R, resinite; S, sporinite; SE, suberinite.

The Waarre Sandstone results are best ignored, as this formation is the reservoir for the field. Gas migration from the reservoir, particularly into overlying units, may also be possible, and would lead to increased total gas readings. The results from North Paaratte No. 3 are perhaps a better indication of maturity levels, as this was a dry hole.

The head-space gas data do not unambiguously resolve the question of the gas source for this field. Both the basal Belfast Mudstone and upper Otway Group are well placed to charge the Waarre Sandstone. Gas generation from either rock unit could have occurred during the early stage, or immature phase, of organic maturation. Also, the migration of thermally mature gas from deeper sources cannot be ruled out.

Pyrolysis sniff analyses — Flaxmans 1, Caroline 1, Nautilus 1A

Pyrolysis sniff analysis data (Konert & van der Veen, 1982a, 1982b, 1982c) enable continuous downhole assessment of source-rock potential. The Shell proprietary sniff analysis (not to be confused with Rock Eval) was conducted on 114 cuttings samples from the Upper and Lower Cretaceous sequence in Flaxmans 1 (Fig. 7), 118 cuttings samples from the Upper and Lower Cretaceous sequence in Caroline 1 (Fig. 8) and 85 cuttings samples from the Tertiary Gellibrand Marl and Upper Cretaceous Belfast Mudstone in Nautilus 1A (Fig. 9).

The results of the sniff analysis are expressed as 'source rock indication' (SRI) units. According to Konert & van der Veen (1982a), samples with SRI values of 30 or less do not represent source rocks. Values between 30 and 100 generally indicate marginal source rocks, while values above 100 commonly indicate good source rocks.

Organic matter type, determined microscopically, is used in addition to SRI to indicate relative potential for oil or gas generation. The humic organic matter reported by Konert & van der Veen (1982a, 1982b, 1982c) consists of vitrinite plus inertinite; their 'mixed' organic matter contains some material described as 'sapropelic' and/or 'liptinite' in addition to the humic fraction. Quantitative amounts are not given. The humic and sapropelic/liptinite fractions are regarded by Konert & van der Veen (1982a) as mainly gas generative and oil generative, respectively.

Most samples with marginal to good source rock indications, in Flaxmans 1, Caroline 1, and Nautilus A1, have gas generation potential, indicated by the humic organic matter. Oil generation potential is confined to a few intervals in Flaxmans 1: at 2197.6 m in the Waarre Sandstone, and at 2347 m and 2926 m in the Otway Group.

The 'very good' oil source in the Dilwyn Formation at 2131 m in Caroline 1 interpreted by BMR was not identified by the Shell sniff analysis, probably owing to sparse sampling in the upper part of that well. Other conclusions from the Shell data are in broad agreement with BMR data.

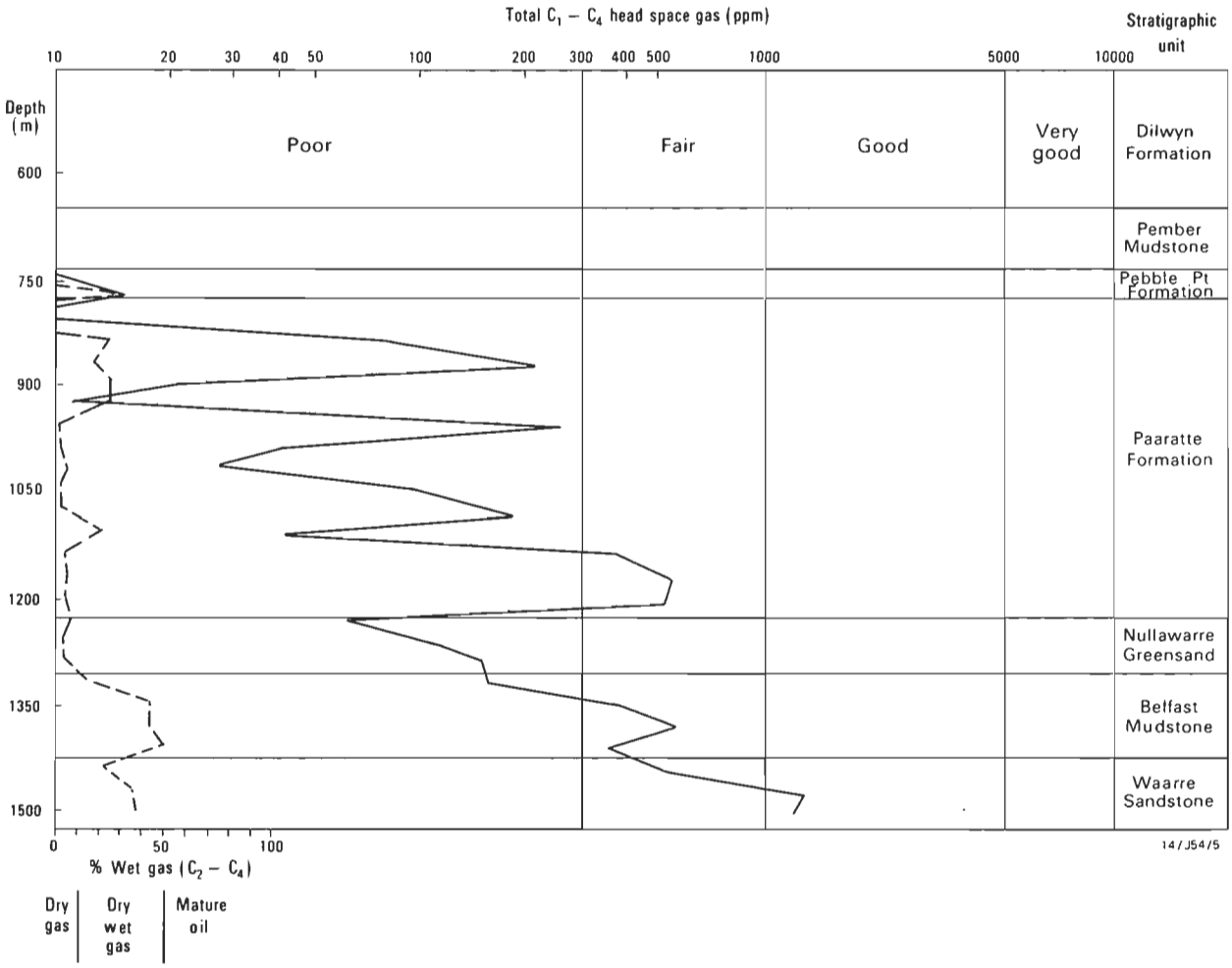

Figure 5. Head space cuttings gas analysis, North Paaratte 1.

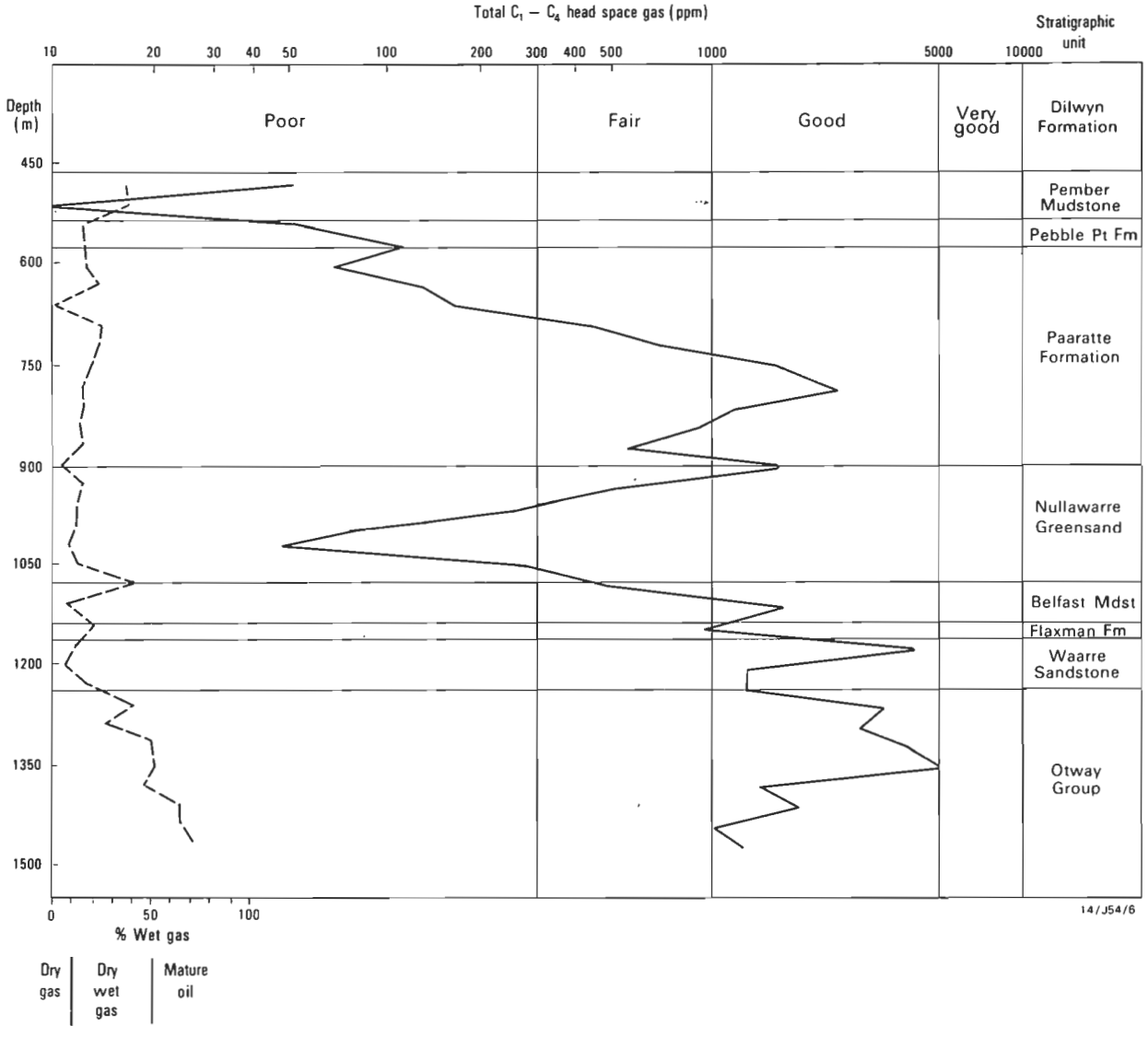

Figure 6. Head space cuttings gas analysis, North Paaratte 3.

Discussion

The mid-Cretaceous to early Tertiary (100–55 Ma) period of faulting associated with continental separation affected most of the basin and controlled fault-related trap development. Both structural and stratigraphic traps in the Cretaceous and early Tertiary can be considered to have been in a position to be charged by hydrocarbons generated after this time.

Mutter & others (1985) presented evidence of progressive younging of continental separation, from mid-Cretaceous in the western part of the Otway Basin to early Tertiary in the east. This model further constrains the critical relationship between structural trap formation and hydrocarbon generation in different parts of the basin.

Middleton & Falvey (1983) used vitrinite reflectance data to model maturation levels through time in the wells Pecten 1A and Voluta 1, in the Mussel Platform and Voluta Trough areas, respectively. They used the vitrinite reflectance interval 0.5–1.3 per cent as the oil generation window; we have modified their observations to accord with our usage of the interval 0.7–1.2 per cent as the oil window, and our limited data are in agreement with their reflectance data for Pecten 1A. Their modelling shows that the lower part of the Otway Group at this well locality lies almost entirely within the oil window at the present day, the depth to mature section being about 2600 m. Peak generation at the base of the Otway Group (Pecten 1A was terminated within the Otway Group.) is inferred to have been reached about 70 Ma ago, during fault-trap formation, and some hydrocarbons have been lost. However, the bulk of hydrocarbons from the Otway Group would appear, from their model, to have been generated less than 55 Ma ago, with generation continuing today. Gas flows were encountered in the Waarre Sandstone from above the oil window at 1770 m; this gas, consisting of methane and ethane, was probably generated in either the upper part of the Otway Group or the lower Belfast Mudstone/Flaxman Formation. The relatively organic-rich Upper Cretaceous and Tertiary sedimentary section is immature at the Pecten 1A location.

At Voluta 1, present-day depth to mature sediments was shown by Middleton & Falvey (1983) to be approximately the same as at Pecten 1A, that is about 1600 m. Our reflectance data, which are mean maxima and might be expected to be higher than the mean random reflectance values used by Middleton & Falvey, are consistently lower, even allowing for their reported standard deviations, particularly in the 2000–3000 m interval. This suggests that the depth to mature sediments could be as much as 1000 m greater than their estimate. This is supported by our saturated hydrocarbon

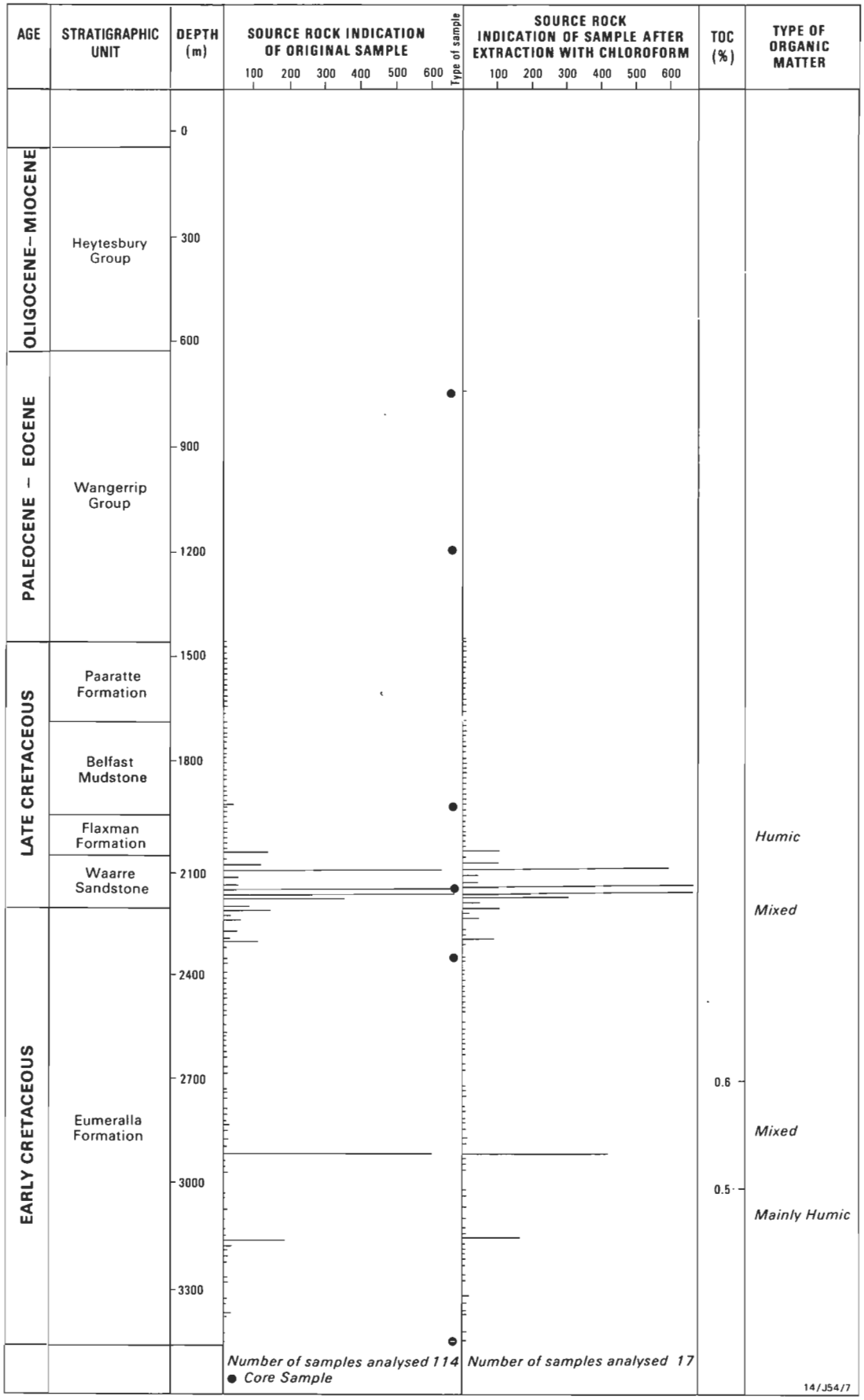

Figure 7. Sniff analysis data, Flaxmans 1.

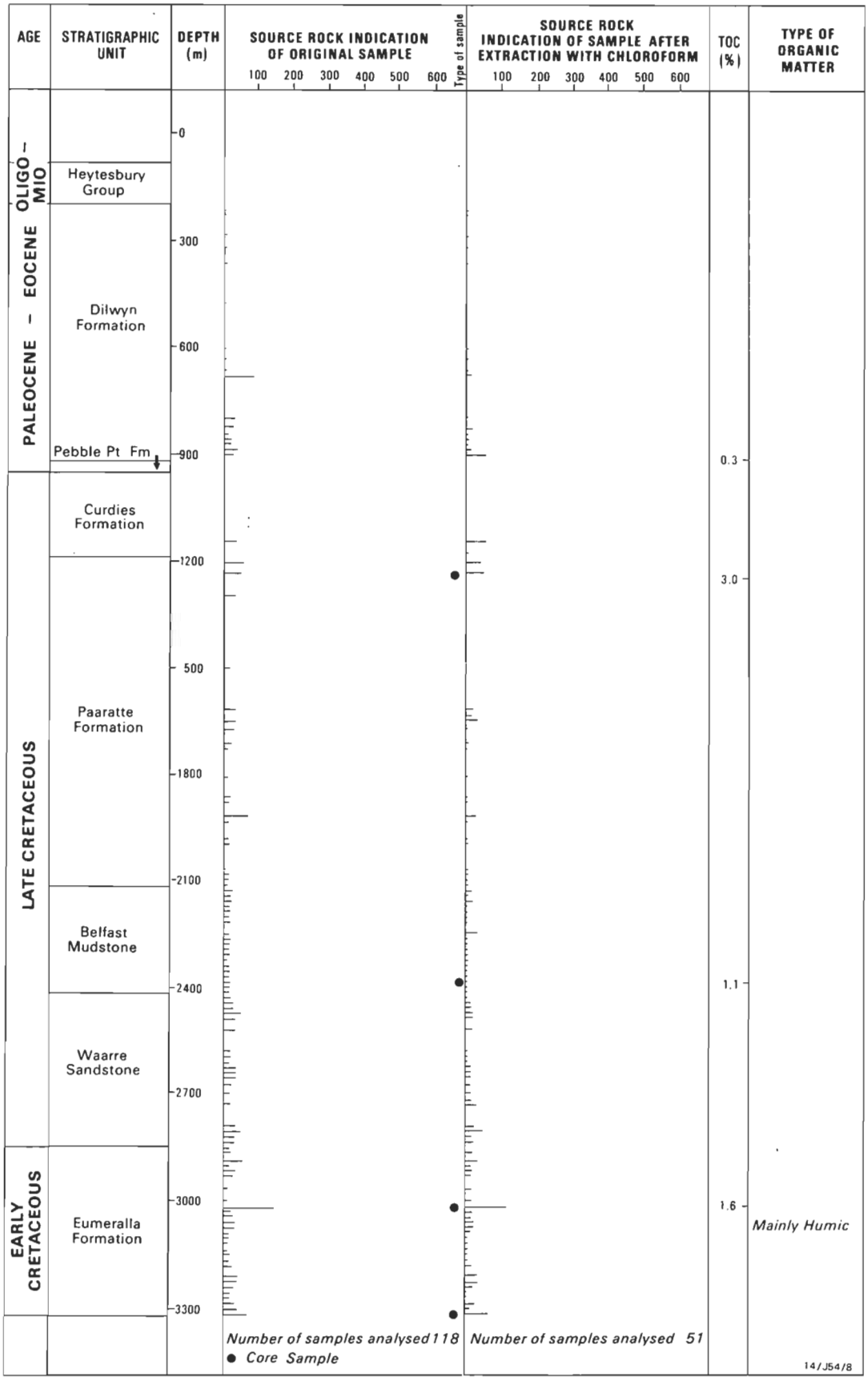

Figure 8. Sniff analysis data, Caroline 1.

distributions for Voluta 1 (Fig. 4). A depth of 3400 m to the oil window is estimated from our vitrinite reflectance data (Fig. 3).

Minor methane and traces of ethane and propane encountered in Voluta 1 at 3300 m (Shell, 1967) further suggest that the rocks are only marginally mature at this depth and that generation is occurring in the basal Upper Cretaceous and Lower Cretaceous rocks, below the sequence penetrated by the drill. As at Pecten 1A, the uppermost Cretaceous and lower Tertiary formations are immature, and the bulk of hydrocarbons from lower parts of the sequence can be inferred to have been generated subsequent to trap formation.

The considerable difference in depths to the top of the oil window between the Mussel Platform (2600 m in Pecten 1A, and about 2600 m at the Nautilus A1 locality, extrapolated from reflectance data in Figure 3) and the Voluta Trough implies that these two structurally distinct areas experienced very different maturation histories, a conclusion supported by the thermal modelling studies of Duddy & others (1985), using fission track analysis. Their study has shown that the rocks in the western part of the onshore basin are currently experiencing their maximum temperature. The potential for hydrocarbon generation is therefore quite recent, and suitable drilling targets are likely to be present at shallow depths. Fission track data from the eastern onshore part of the basin in the Otway Ranges area show that any hydrocarbon generation there took place in high heat-flow conditions shortly after Otway Group sedimentation commenced, and certainly prior to a major uplift in this area at about 95 Ma ago.

The few available maturation data from onshore wells suggest that depths to mature sequences are similar to or slightly less in most offshore wells. In Caroline 1 and Geltwood Beach 1, vitrinite reflectance values of 0.7 per cent are estimated from reflectance plots (Fig. 3) to occur at 1700 m and 2100 m, respectively. A single reflectance value of 0.89 per cent at 2193 m in Flaxmans 1 leads us to estimate a depth of about 1800 m to the oil window.

Conclusions

From our examination of the limited available data, it appears that both the Upper and Lower Cretaceous of the Otway

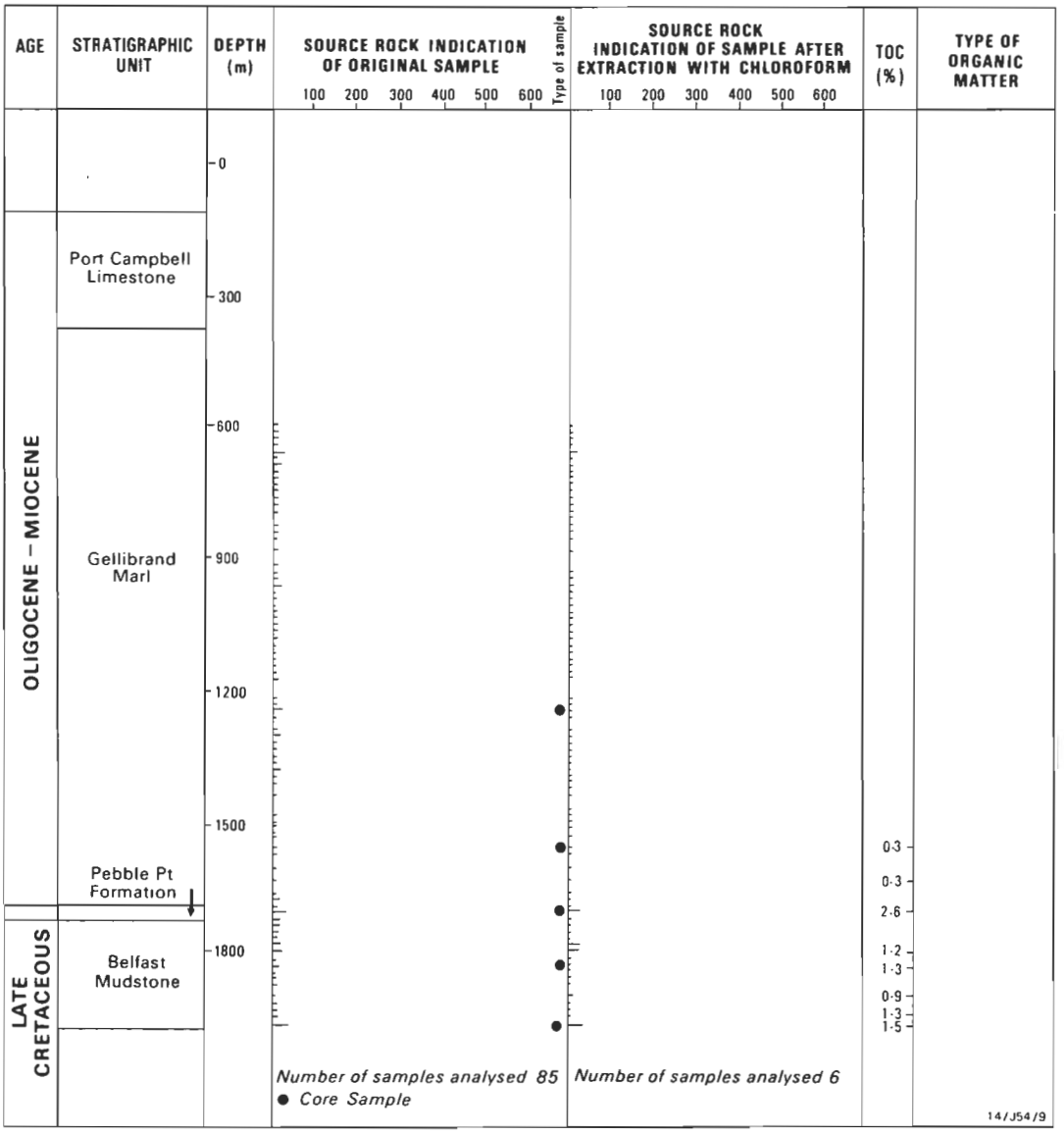

Figure 9. Sniff analysis data, Nautilus A1.

Basin contain fair quality source rocks for gas, particularly the Paaratte Formation, Belfast Mudstone, and Otway Group. Prospects of significant oil generation in the offshore Otway Basin are downgraded by the low levels of organic maturity and by the vitrinite-rich, exinite-poor nature of the source rocks. Some thin beds of oil-prone source rocks may be present, particularly in the Otway Group and Dilwyn Formation.

It is evident from data from the Voluta and Pecten wells and from the fission track studies of Duddy & others (1985) that there is a strong structural control on the maturation levels observed throughout the basin and that particular attention should be paid to the structural setting in which a well may be drilled. Hydrocarbons formed early in the basin's history are unlikely to have been preserved, owing to limited structural trap development and breaching of traps by later faulting.

The best prospects for hydrocarbon discoveries, particularly of oil, are in areas where the Upper Cretaceous and Tertiary have reached peak maturity since major structuring ceased about 55 Ma ago. This is most likely in areas where there is a thick Tertiary sequence and/or where high heat flow has been maintained during Tertiary and Quaternary time.

Acknowledgements

We thank Beach Petroleum NL for providing samples from North Paaratte 1 and 3, and for permission to publish the analytical results. The manuscript was critically reviewed by Evelyn Nicholas, Geoffrey O'Brien, David McKirdy, and an unknown reviewer, who suggested many improvements. The figures were drafted by R. Fabbo.

References

BMR 1966—A preliminary review of the Otway Basin. *Bureau of Mineral Resources, Australia, Record* 1966/170.

Cande, S.C., & Mutter, J.C., 1982—Revised identification of the oldest seafloor spreading anomalies between Australia and Antarctica. *Earth and Planetary Science Letters*, 58, 151-160.

Dickey, P.A. & Hunt, J.M., 1972—Geochemical and hydrologic methods of prospecting for stratigraphic traps. *American Association of Petroleum Geologists Memoir* 16, 136-67.

Denham, J.I. & Brown, B.R., 1976—A new look at the Otway Basin. *APEA Journal*, 16(1), 91-98.

Duddy, I.R., Gleadow, A.J.W., Green, P.F., & Lovering, J.F., 1985—Thermal history of the Otway Basin from fission track analysis of detrital apatites. *In* Otway 85 : Earth Resources of the Otway Basin. Summary papers and excursion guides, Mount Gambier, South Australia, 7-10 February, 1985. *Geological Society of Australia, South Australia and Victorian Divisions*, 3-4.

Ellenor, D.W., 1976—Otway Basin. *In* Leslie, R.B., Evans, H.J., & Knight, C.L., (editors), Economic geology of Australia and Papua New Guinea. Volume 3 — Petroleum. *Australasian Institute of Mining and Metallurgy, Monograph* 7, 82-91.

Esso, 1968—Crayfish A-1 well completion report. *Bureau of Mineral Resources, Australia, Petroleum Search Subsidy Acts File* 1967/4266 (unpublished).

Esso, 1974—Trumpet well completion report. *Bureau of Mineral Resources, Australia, Petroleum Search Subsidy Acts File* 1973/1013 (unpublished).

Felton, E.A., & Jackson, K.S., 1985—Otway Basin hydrocarbons - their source and generation. *In* Otway 85 : Earth Resources of the Otway Basin. Summary papers and excursion guides, Mount Gambier, South Australia, 7-10 February, 1985. *Geological Society of Australia, South Australian and Victorian Divisions*, 12.

Holdgate, G.R. 1981—Stratigraphy, sedimentology and hydrocarbon prospects of the Dilwyn Formation in the central Otway Basin of southeastern Australia. *Proceedings of the Royal Society of Victoria*, 93, 129-148.

Holdgate, G.R., Mackay, G.H. & Smith, G.C. 1985—The Portland Trough, Otway Basin - geology and petroleum potential. *In* Second South Eastern Australia Oil Exploration Symposium — programme and abstracts. *Petroleum Exploration Society of Australia, Victoria-Tasmania Branch, Melbourne*, 13.

Jackson, K.S., 1982—Geochemical evaluation of the petroleum potential of the Toko Syncline, Georgina Basin, Queensland. *BMR Journal of Australian Geology & Geophysics*, 7(1), 1-10.

Jackson, K.S., Forman, D.J., Felton, E.A., Nicholas, E., & Denardi, R.—1983 Geochemical and organic microscopy data from Australia's petroleum source rocks. *Bureau of Mineral Resources, Australia, Report* 240; *BMR Microform* MF180.

Konert, G., & van der Veen, F.M., 1982a—Source rock analysis of cuttings and cores from well Caroline-1, Australia. *Report* RKER 82.080 *for Shell Research B.V.* (unpublished).

Konert, G., & van der Veen, F.M., 1982b—Source rock analysis of cuttings and cores from well Flaxmans-1, Australia. *Report* RKER 82.110 *for Shell Research B.V.* (unpublished)

Konert, G., & van der Veen, F.M., 1982c—Source rock analysis of cuttings and cores from well Nautilus-1, Australia. *Report* RKER 82.154 *for Shell Research B.V.* (unpublished).

Laws, R., 1985—Petroleum exploration in the Otway Basin, South Australia. *In* Otway 85 : Earth Resources of the Otway Basin. Summary papers and excursion guides, Mount Gambier, South Australia, 7-10 February, 1985. *Geological Society of Australia, South Australian and Victorian Divisions*, 9-14.

Leslie, R.B., 1966—Petroleum exploration in the Otway Basin. *Eighth Commonwealth Mining and Metallurgy Congress, Australia and New Zealand 1965, Proceedings*, 5, 203-216.

McPhee, I., 1980—Review of the exploration history of the Otway Basin. *In* South eastern Australia oil exploration symposium — absracts. *Petroleum Exploration Society of Australia, Victoria-Tasmania Branch, Melbourne*, 12-13.

McPhee, I., McNicol, M., & Harrison, D., 1980—The North Paaratte Gasfield. *In* South eastern oil exploration symposium — abstracts. *Petroleum Exploration Society of Australia, Victoria-Tasmania Branch, Melbourne*, 14.

McKirdy, D.M., 1985—Coorongite, coastal bitumen, and their origins from the laustrine algae *Botryococcus* in the western Otway Basin. *In* Otway 85: Earth Resources of the Otway Basin. Summary papers and excursion guides, Mt. Gambier, South Australia, 7-10 February 1985. *Geological Society of Australia, South Australian and Victorian Divisions*, 34-49.

McKirdy, D.M. & Hovath, Z., 1976—Geochemistry and significance of coastal bitumen from southern and northern Australia. *APEA Journal*, 16(1), 123-135.

McKirdy, D.M., Cox, R.E., Volkman, J.K. & Howell, V.J., 1986—Botryococcane in a new class of Australian non-marine crude oils. *Nature*, 320, 57-59.

Middleton, M.F. & Falvey, D.A., 1938—Maturation modelling in Otway Basin, Australia. *AAPG Bulletin*, 67(2), 271-279.

Mutter, J.C., Hegarty, K.A., Cande, S.C. & Wiessel, J.K., 1985—Breakup between Australia and Antarctica: a brief review in the light of new data. *Tectonophysics*, 114, 225-279.

Nicholas, E., Lockwood, K.L., Martin, A.R. & Jackson, K.S., 1981—Petroleum potential of the Bass Basin. *BMR Journal of Australian Geology & Geophysics*, 6, 199-212.

Robertson, C.S., Cronk, D.K., Mayne, S.J. & Townsend, D.G., 1978—A review of petroleum exploration and prospects in the Otway Basin. *Bureau of Mineral Resources, Australia, Record* 1978/91.

Rouzaud, J.N., & Oberlin, A., 1983—Rôle des résines sur la comportement a la pyrolyse et les propriétés optiques des charbons. *Comptes Rendus Académie Sciences, Paris*, 296, 757-760.

Shell (Shell Development Australia Pty Ltd), 1967—Voluta-1 well completion report. *Bureau of Mineral Resources, Australia, Petroleum Search Subsidy Acts File* 1967/4239 (unpublished).

Snowdon, L.R. & Powell, T.G., 1982—Immature oil and condensate — modification of hydrocarbon generation potential for terrestrial organic matter. *AAPG Bulletin*, 66(6), 775-788.

Struckmeyer, H.I.M., & Cook, A.C. in press—Source rock and maturation characteristics of the sedimentary sequence in the Otway Basin. *In* The Otway Basin: regional geology and petroleum exploration. *Department of Fuel, Technology and Resources, Victoria.*

Tabassi, A. & Davey, L.K. 1985—Recovery of oil from the basal Tertiary Pebble Point Formation at Lindon No. 1 - summary, results and implications. *In* Second Southstern Australia oil exploration

symposium — programme and abstracts. *Petroleum Exploration Society of Australia, Victoria-Tasmania Branch, Melbourne*, 6.

Tallis, N., 1980—Introduction to the geology of the Otway Basin. *In* South eastern Australian oil exploration symposium — abstracts. *Petroleum Exploration Society of Australia, Victoria-Tasmania Branch, Melbourne*, 11-12.

Tissot, B.P. 1984—Recent advances in petroleum geochemistry applied to hydrocarbon exploration. *AAPG Bulletin*, 69 (5), 545-563.

Tissot, B. & Welte, D.H., 1978—Petroleum formation and occurrence. *Springer-Verlag, New York*.

Waples, D. 1982—Organic geochemistry for exploration geologists. *International Human Resources Development Corporation, Boston*.

Weeks, L.G. & Hopkins, B.M. 1967—Geology and exploration of three Bass Strait basins, Australia. *AAPG Bulletin*, 51(5), 742-760.

Weissel, J.K. & Hayes, D.E. 1972—Magnetic anomalies in the southest Indian Ocean. *In* Hayes, D.E. (editor), Antarctic Oceanology II: The Australian-New Zealand Sector. *American Geophysical Union, Antarctic Research Series*, 19, 165-196.

Wopfner, H. & Douglas, J.G., (editors), 1971—The Otway Basin of southeastern Australia. *Geological Surveys of South Australia and Victoria, Special Bulletin*.

Wopfner, H., Kenley, P.R., & Thornton, R.C.N. 1971—Hydrocarbon occurrences and potential of the Otway Basin. *In* Wopfner, H., & Douglas, J.G., (editors), The Otway Basin of southeastern Australia. *Geological Surveys of South Australia and Victoria, Special Bulletin*.

BMR Journal of Australian Geology & Geophysics, 10, 225-232

Southwest Seismic Zone of Western Australia: measurement of vertical ground movements by repeat levelling and gravity surveys

Peter Wellman[1] & Ray Tracey[1]

This paper presents results of repeat surveys of levelling and gravity, analysed to determine areas of vertical ground movement in the Southwest Seismic Zone, 75–200 km east of Perth. Levelling surveys over parts of the earthquake zone have been made during four periods, starting in 1958. Differences between repeat levelling surveys separated by 10 or more years show areas of vertical ground movement, the areas being 20–50 km across with relative height changes of 50–100 mm amplitude. Some of the vertical ground motion is movement at the time of earthquakes, some is later rebound in the same earthquake areas, and other movement does not appear to be associated with large or small earthquakes and could be due to either elastic strain, or non-seismic faulting. Precise gravity observations at 10 km spacing were made in 1980–81 and repeated in 1983. The differences between the surveys do not show any significant gravity changes. Future studies should be set up to monitor stress, strain and earthquakes in a group of small, diverse test areas, using the global positioning system.

Introduction

The Australian continent is totally within the Australian (Indian) lithospheric plate, so its seismic activity is relatively small by world standards. However, within Australia there are some zones where intra-plate earthquakes are of sufficient magnitude to cause significant property damage. The most economically destructive earthquakes in recent years have been within the Southwest Seismic Zone in Western Australia, 75–200 km east of Perth (Fig. 1). Earthquakes in this zone have caused damage not only in the vicinity of the earthquake but also in Perth, partly because Perth is built on sediments that are relatively unconsolidated and deep, and these amplify ground movement.

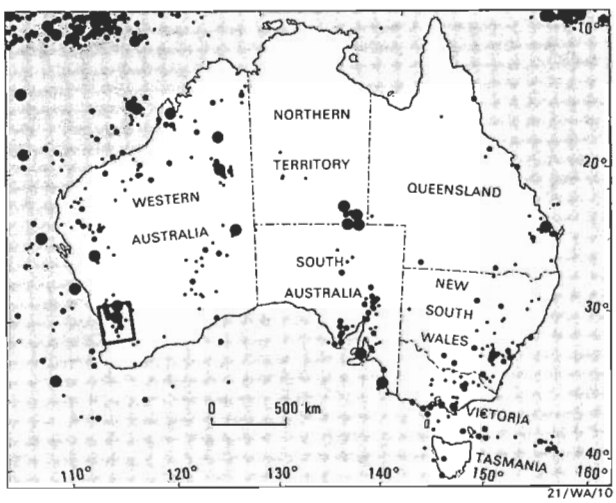

Figure 1. Australian seismicity (1873–1980).
Rectangle gives the location of the Southwest Seismic Zone and the location of subsequent figures.

So far this century the three largest earthquakes in the Southwest Seismic Zone have been the 14 October 1968 Meckering earthquake (ML 6.9), the 10 March 1970 Calingiri earthquake (ML 5.9), and the 2 June 1979 Cadoux earthquake (ML 6.2). Integrated descriptions of these earthquakes have been given by Gordon & Lewis (1980) and Lewis & others (1981).

Studies of the Southwest Seismic Zone as a whole include seismic monitoring of earthquakes, strong-motion monitoring, focal-plane solutions of major earthquakes (Denham & others, 1980), stress measurements (Denham & others, 1980; Denham & Alexander, 1981), studies of surface faulting and local displacements from surveying (Gordon & Lewis, 1980; Lewis & others, 1981), and very preliminary studies of strain from regional geodetic surveys (Wellman, 1981).

In 1980 the Geological Survey of Western Australia and the Bureau of Mineral Resources started an expanded program of repeat geodetic measurements to define horizontal and vertical ground movement within the Southwest Seismic Zone. There are three programs — optical levelling, repeat gravity measurements, and horizontal surveying, the aim of which is to investigate ground motions resulting from earthquakes in order to understand earthquakes more fully, and also to monitor ground motions through the region to define areas of anomalously high crustal strain that are areas of high earthquake risk. Results of the optical levelling and gravity programs, both of which measure vertical movements, are described in this paper.

Optical levelling

Optical levelling is the basic surveying method of finding elevation differences between permanent ground marks called bench marks. Measurements are made with an optical level and one or two graduated rods (staves). The elevation difference between two bench marks is measured by finding the sum of the elevation differences of numerous short setups between the two bench marks. Because the number of setups is large, the random errors in the measured elevation difference between two bench marks of distance *km* km apart result in an elevation difference with an error proportional to $km^{1/2}$. Levelling can be carried out to several accuracies (NMCA, 1976), the ratios between the accuracies being lst:2nd:3rd:4th::4:8.4:12:18. Roelse & others (1971) showed that the average accuracy for third-order levelling in Australia is 7.9 $mm.km^{-1/2}$.

Most bench marks are concrete blocks with a metal mark exposed on the top. Just prior to the 1981–1984 second-order levelling, deep bench marks (which should be more stable than normal benchmarks) were placed by the Australian Survey Office along the levelling traverses at approximately 10 km spacing.

Analysis of repeat levelling by least-squares adjustment

Division of levelling data into epochs

The levelling in the Southwest Seismic Zone is most conveniently divided into four periods.

[1]Division of Geophysics, Bureau of Mineral Resources, GPO Box 378, Canberra, ACT 2601.

1. 1960's levelling (Fig. 2) — observed between 1958 and the Meckering earthquake of October 1968. This consists of a framework of first-order levelling observed from 1959 to 1967, with intervening third-order levelling and minor fourth-order one-way and two-way levelling.

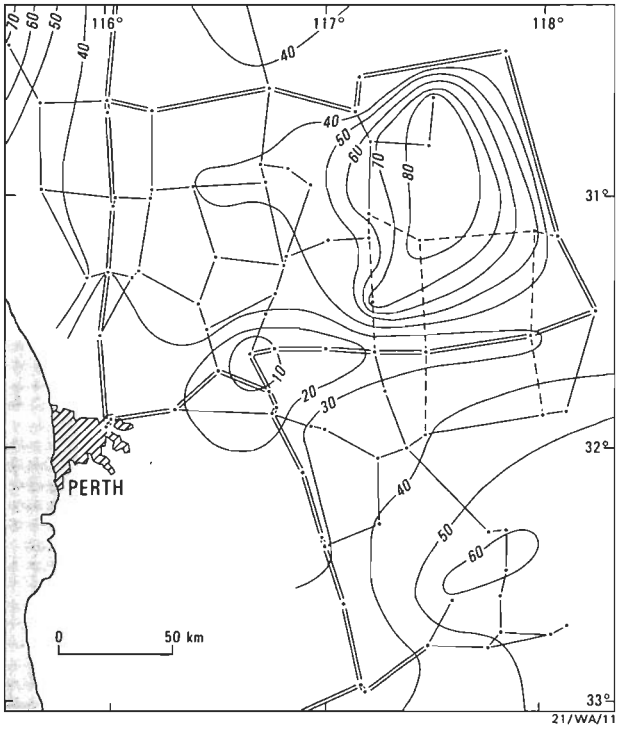

Figure 2. Distribution of 1960's levelling.
Accuracy of levelling varies with first order (double lines), third order (thin lines), fourth order and one way (dashed lines). Dots show junction points. Traverses between junction points shown as straight lines. Contours give calculated errors in mm relative to 0 at bench mark NM2.

2. 1970's levelling (Fig. 3) — mainly levelling of third-order standard observed in November and December 1968 immediately after the Meckering earthquake, in 1979 immediately after the Cadoux earthquake, and other traverses in the intervening period of third and fourth-order standard.

3. 1977 levelling — third-order levelling observed in 1977 that forms a small network 70 km across around Meckering.

4. 1980's levelling (Fig. 4) — a remeasurement of all the major level traverses in the Southwest Seismic Zone to second-order standard in the period 1981–1984.

The 1960's, 1970's, and 1977 periods of levelling were mainly observed by the Western Australian Lands and Survey Department, and the 1980's levelling was observed by the Australian Survey Office. Abstracts of all levelling are available from the Western Australian Lands and Survey Department, Perth, and computer-readable observed height differences can be obtained from the Division of National Mapping, Canberra.

Least squares adjustment of levelling

The levelling was reduced by J.B. Steed and G. Luton of the Division of National Mapping on computer programs MORTHO, LEVELONE, and LINEA (Roelse & others, 1971). The programs were modified to print out the whole variance-covariance matrix to give a better understanding of error propagation. The levelling network consists of

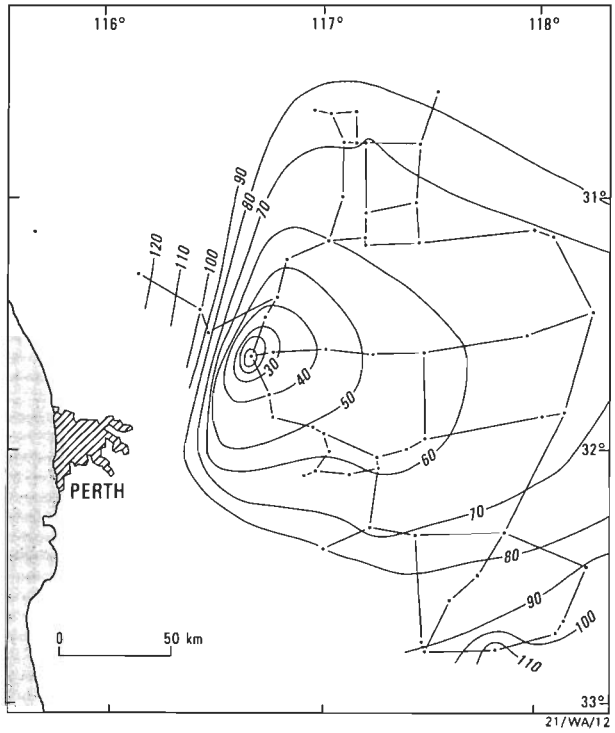

Figure 3. Distribution of 1970's third-order levelling.
Symbols as in Figure 2.

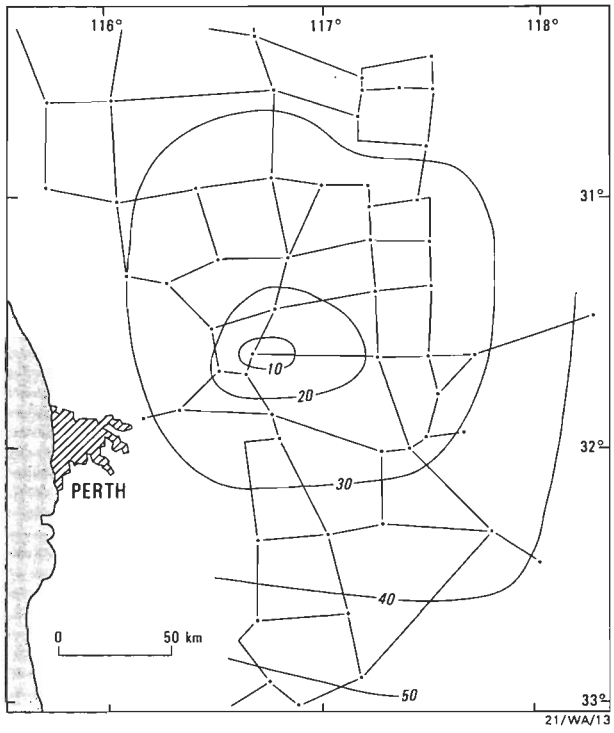

Figure 4. Distribution of 1980's second-order levelling.
Symbols as in Figure 2.

traverses, called levelling sections, with common bench marks at junction points. The least-squares program adjusts the total height differences of the levelling sections, the levelling sections being weighted on their relative strength. The height difference of a levelling section is the sum of the measured height differences between bench marks with the orthometric correction applied. The weight of each levelling section is the weight indicator divided by the distance in kilometres, where the weight indicator is proportional to the inverse of the

variance, and is 7 for first-order, 2 for second-order, 1 for third-order, 0.4 for fourth-order, and 0.2 for one-way levelling. For each epoch of levelling, a least-squares adjustment was made, using one fixed point. The fixed point for all epochs is bench mark NM2, at Australian Height Datum (AHD) (Roelse & others, 1971) junction point 172, with an AHD height of 149.224 m. This fixed point was chosen because it was one of the few that were part of each period of levelling and it was outside the area of ground movement near Meckering. The four periods of levelling had adjustments consistent with the modelled variance to within experimental error, according to the F test, with the exception of the 1960's levelling. The poor closure of the 1960's levelling network is thought to be due to (a) a combination of some levelling sections being of lower accuracy than the levelling order adopted, and (b) significant crustal movement during the 10-year period of levelling. The accuracy of the heights at the junction points relative to the fixed point is the basis of the contours shown in Figures 2 to 4. The adjusted height of each bench mark was calculated by adopting the adjusted heights of the junction points and linearly distributing a correction for each height difference.

Altitude changes and their significance

The mapped height change at a bench mark is the change in adopted height at the bench mark between the two epochs of levelling. The 1980's levelling is adopted as the second epoch in all comparisons, because it has the highest accuracy and good coverage of the earthquake zone. Where height changes vary slowly with distance, they are more likely to be due to random errors in levelling, and, where they vary rapidly with distance, they are more likely to be due to relative ground movement.

Figure 5 shows height changes between 1960's and 1980's levelling attributable to the Meckering, Calingiri, and Cadoux earthquakes (A, B, C in Fig. 5), height changes associated with the earthquake area near Quairading 50 km southeast of Meckering (D), and height changes not associated with seismicity (E-L).

Figure 6 shows height changes between the 1970's and 1980's levelling. Changes are attributable to (a) continued movement in the Meckering area (M of Fig. 6), and (b) continued movement in the earthquake area near Quairading (N) (see also Fig. 7) and in areas apparently not associated with seismicity (0-R).

The apparent changes in height between the 1977 and 1980's levelling reach only 34 mm. This is less than the expected errors at the 2 s.d. level, so the apparent regional changes in height are within the expected levelling standards and therefore not attributable to crustal movement.

Figure 8 shows the height changes along four traverses for the adjusted height differences 1980's-1960's, and 1980's-1970's. Also shown is the expected accumulation of error at the 1 s.d. level relative to one point on the traverse. Along some parts of the traverses the rate of change of height difference is over twice the rate of change of the 1 s.d. error. This is consistent with these height changes being due to crustal movement rather than measurement errors.

Analysis of repeat levelling by comparison of intervals

The levelling measurements can be independently analysed by comparison of the repeated measurements of height differences between adjacent bench marks. If h_1 and h_2 are the height differences between adjacent bench marks measured on two levelling surveys and d is the distance between the bench marks, then a measure of the significance of the change in height difference is s, where $s = (h_2 - h_1)/d^{1/2}$. The probability distribution of s, if it is due solely to random levelling errors, is for a zero mean and a standard deviation of $m = (p^2 + q^2)^{1/2}$, where p and q are

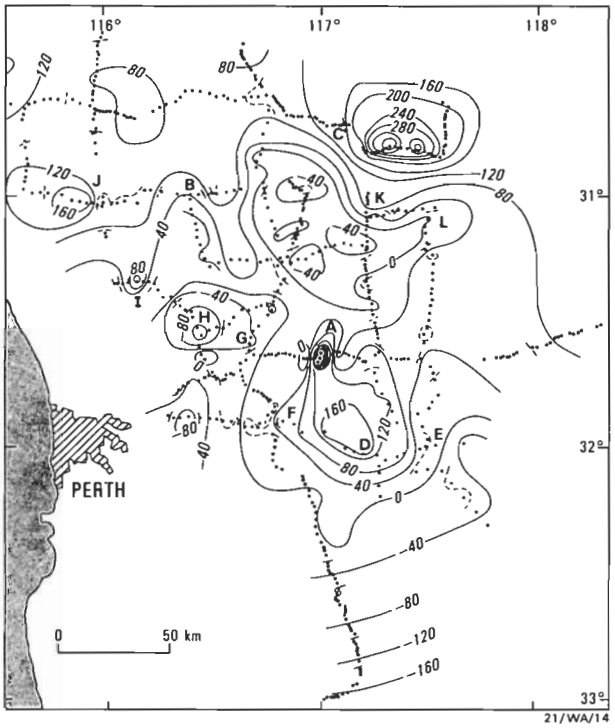

Figure 5. Differences between adjusted levelling networks.
1980's heights minus 1960's heights (mm) relative to bench mark NM2, which is assumed fixed. Dots show data points. Letters indicate locations of possible crustal movement.

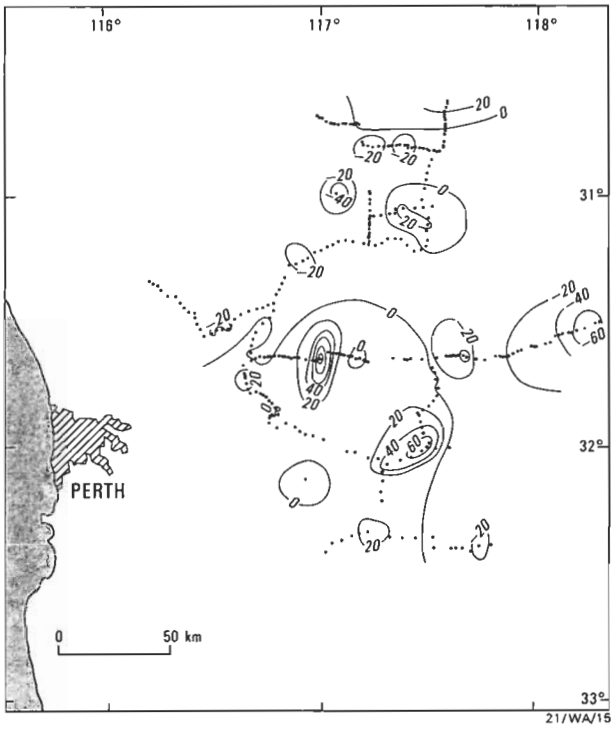

Figure 6. Differences between adjusted levelling networks.
1980's heights minus 1970's heights (mm). Letters indicate locations of possible crustal movement.

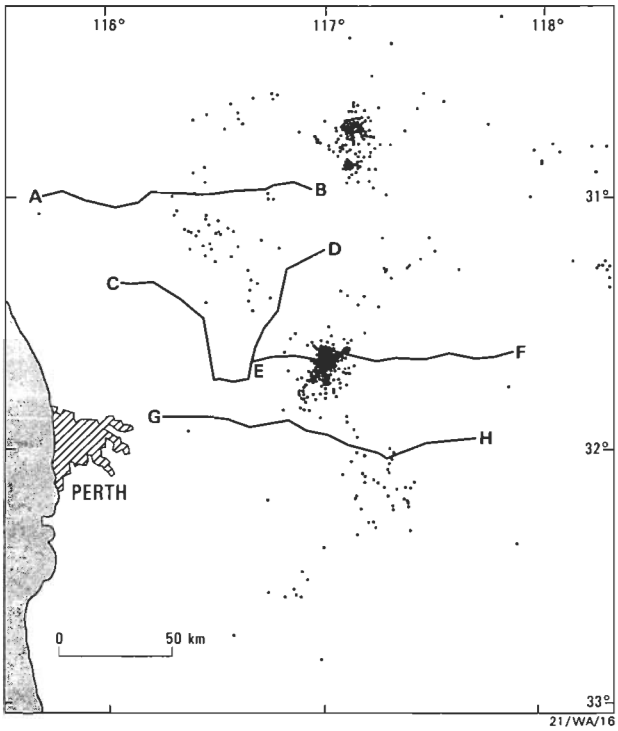

Figure 7. Distribution of earthquakes and location of Figure 8 traverses.

the expected accuracy of the two levelling surveys. If s is due to both random levelling errors and to ground movement (or movement of the bench mark relative to the ground), then the probability distribution of s for the affected bench marks should have a zero mean and a much larger standard deviation than m, the two normal distributions being superimposed and both having approximately zero mean.

Figure 9 shows histograms of s for when the surveys are first and second order, and third and second order. Note that for each distribution the tails are relatively large compared to the peak, confirming that the histogram is not a sample of a normal population. When plotted with a probability scale (Fig. 10), the data can be approximated by several straight line segments. The straight line near the centre of the distribution is interpreted as giving the distribution of random levelling errors, while the two parallel straight line segments at the extremes of the distribution are interpreted as giving the distribution due mainly to crustal movement and movement of bench marks. The standard deviations found for the central part of the distribution are 5.4 mm.km$^{-½}$ for first and second-order levelling, and 5.7 mm.km$^{-½}$ with a large uncertainty for third and second-order levelling. These accuracies are smaller than would be expected from the accuracies used by National Mapping of 3, 6, and 8 mm.km$^{-½}$ for first, second and third-order levelling. To be on the conservative side, the National Mapping accuracies have been adopted.

Levelling intervals with significant relative ground movement can be identified by standard deviations calculated for random levelling errors. Height differences were assumed to be significant at the 95% confidence level when they had values of s greater than ± 13 mm.km$^{-½}$ for first and second- order levelling, and greater than ± 20 mm.km$^{-½}$ for third and second-order levelling. The exact values are not critical, because many of the observed movements are much greater than 20 mm.km$^{-½}$. Table 1 lists pairs of bench marks that have moved relative to each other, and their distribution is shown in Figure 11. Table 2 lists those bench marks that have moved significantly relative to adjacent bench marks on both sides. The significance of these movements is discussed below.

Repeat gravity measurements

Surveys of acceleration due to gravity are another method of measuring Earth surface altitude changes and changes in the distribution of crustal masses. If crustal movement is caused by changes in crustal thickness, with no density changes, then the change in gravity at a site is at the rate of $+(3.085 - 0.419\ d)\ \mu m.s^{-2}.m^{-1}$. If density (d) is the average value of 2.67 $t.m^{-3}$, then the gravity change is 1.969 $\mu m.s^{-2}.m^{-1}$.

Two gravity surveys have been made over the Southwest Seismic Zone, one in two parts from 16 October 1980 to 19 November 1980 and 6 May 1981 to 5 August 1981, and the

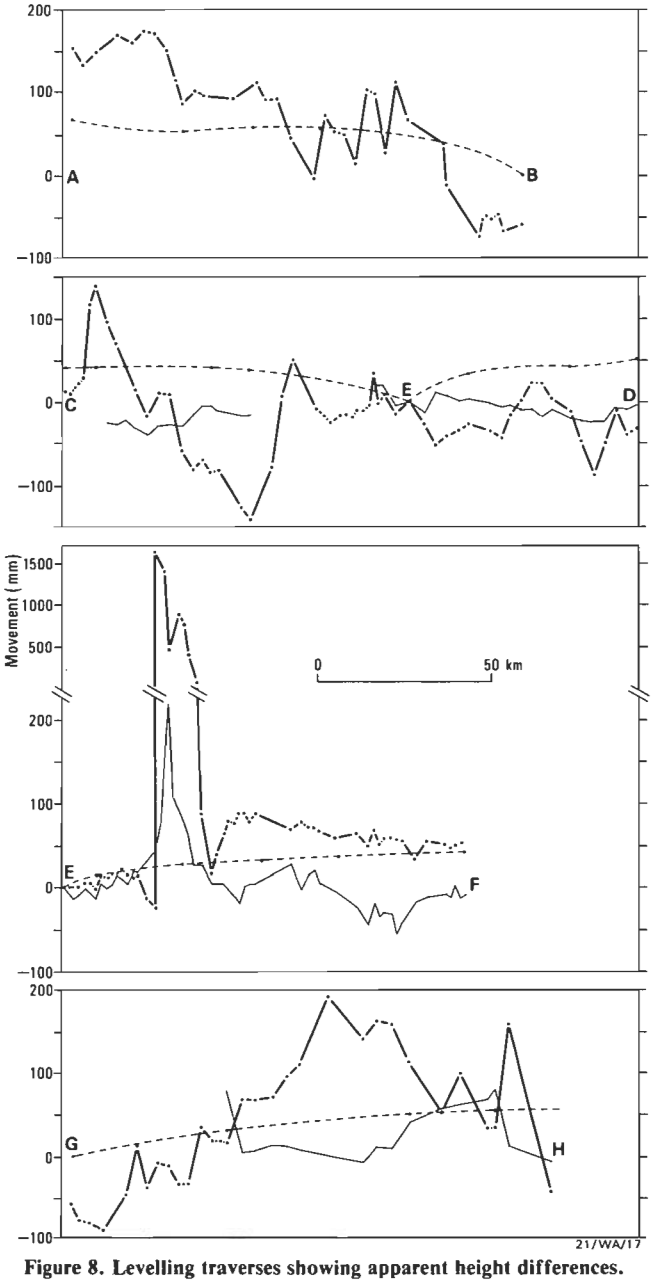

Figure 8. Levelling traverses showing apparent height differences. 1980's heights minus 1960's heights (thick lines) with predicted error (s.d.) in mm (dashed lines), 1980's heights minus 1970's heights (thin lines). Location of traverses shown on Figure 7.

other from 6 July 1983 to 23 November 1983. Gravity observations were made at intervals of approximately 10 km at the deep bench marks of the levelling network (Fig. 12). Unfortunately, the deep bench marks were not all in place in 1980–1981, thus many observations on the first survey were at proposed sites of the deep bench marks. Observations in 1983 were at the deep bench marks, and, if they were different, also at 1980–1981 observation sites. Observations were made in ladder sequence: if the stations on a levelling section are A,B,C..,Y,Z, measurements were made in the order A,B,C..,Y,Z, and, on another day, Z,Y..,C,B,A. Three LaCoste & Romberg gravity meters were used on each survey: G132, G460, and G518 in 1980–1981, and G20, G132 and G460 in 1983. Hence, at least six observations were made at each site during each survey. Meter G460 gave internally inconsistent results in 1983, so its 1983 measurements were not used in the final adjustments. Meters G460 and G518 had electronic output, and these meters were read using the manufacturer's galvanometer. All readings were corrected for Earth tides, and for the height of the gravity meter above the bench mark.

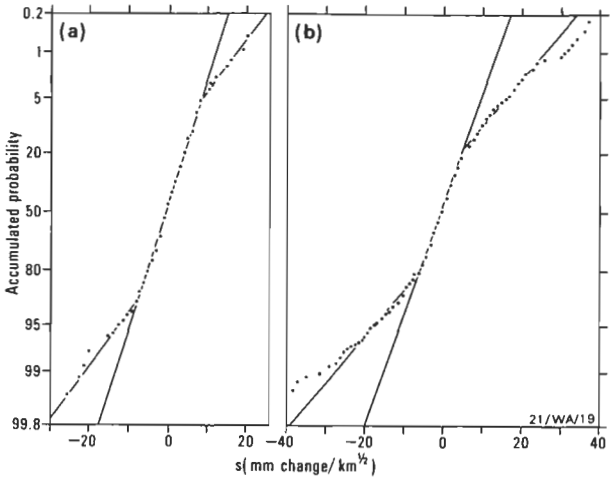

Figure 10. Probability plot of s for (a) first and second-order levelling, (b) second and third-order levelling.

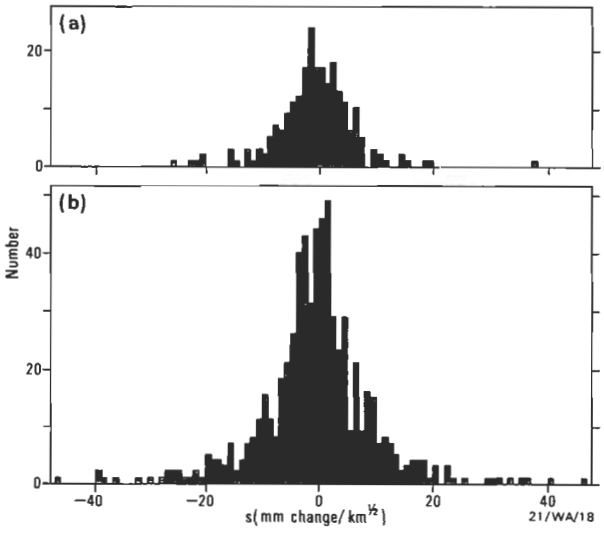

Figure 9. Histogram of significance of change of height difference (s in mm.km$^{-½}$).

(a) comparison of first and second-order levelling. (b) comparison of second and third-order levelling.

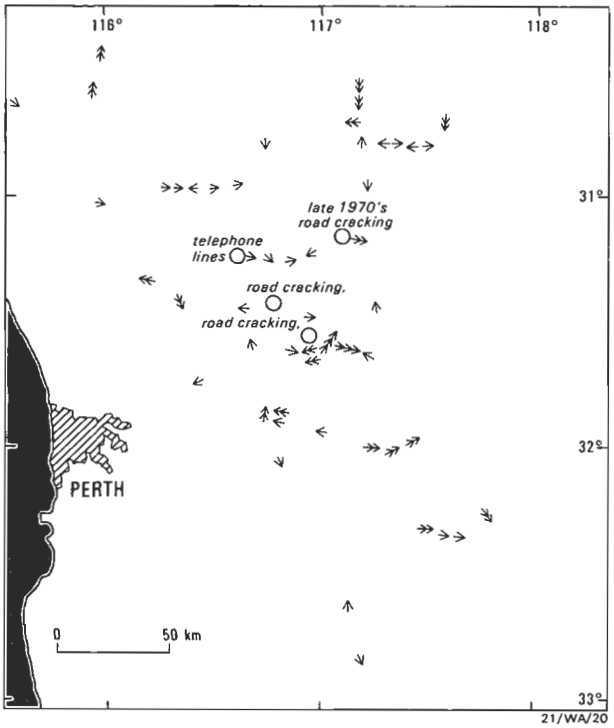

Figure 11. Location of ground movement between adjacent bench marks (mm).

Circled areas give location of cracked roads and slack telephone lines, from Gordon & Lewis (1980).

The gravity observations were reduced on a Hewlett Packard 1000 computer at BMR, using a computer program written in the New Zealand Department of Scientific and Industrial Research (Woodward & Carman, 1984; Paige & Saunders, 1978). The computer program reduces the gravity observations by least-squares adjustment. The main variables are the scale factors of the gravity meters, the drift rates of the gravity meters, and the gravity values of the observation sites. Errors are assumed to be associated with the gravity meter readings, not the gravity reading differences, as in McConnell & Ganter (1971). The error associated with the calculated gravity values is relative to the mean gravity value of that epoch of measurement. The expected error in the difference in the gravity values of the two surveys at 1 s.d. level is generally between 0.12 and 0.16 μm.s^{-2} (Fig. 12). At the 2 s.d. level this is equivalent to 0.12 to 0.16 m. Therefore, the uncertainty in the gravity changes over a three year period is similar to or greater than the height changes found in the levelling over a 10–30 year period (Figs. 5 & 6).

The gravity changes measured (Fig. 12) show a change from positive values in the south to negative in the north, with an abrupt boundary at about 31°S. These effects are interpreted as due to differences in the adopted scale of the two surveys and difficulties in integrating the two parts of the 1980–81 survey, which effectively joined at 31°S. If the areas north and south of 31°S are considered separately, the apparent gravity changes have an amplitude of about 30 μm.s^{-2} from the mean, which is consistent with all the apparent gravity changes being due to experimental error. Analysis of these two gravity surveys shows that errors in this technique are greater than the quantity to be measured.

There is a strong seasonal variation of rainfall in the surveyed area, resulting in a seasonal change in groundwater levels and minor changes in gravity acceleration, the amount of change depending on the change in water-table depth and the rock porosity over that depth interval. There seems no easy way to correct for this gravity change; its effects could be minimised by having the traverse ends on solid rock and carrying out surveys only at either high or low-water table.

Table 1. Ground movement (exclusive of bench marks near Meckering)

ASO run no.	AHD junction points	Order of levels	Years	BM no.	BM no.	Dist. (km)	Height change (mm)	s (mm.km$^{-½}$)
3	172–198	3,2	68–81	F366	F365	3.3	– 70.0	– 38.4
7	852–181	1,3	61–68	NM66A	NM67	0.9	– 30.9	– 32.0
30	172–2685	3,3	64–68	UA2	UA3	3.2	+ 50.9	+ 28.3
31	1029–1030	3,2	78–81	UB12	UB13	3.2	+ 49.4	+ 27.6
36	849–845	3,2	74–81	UB95	UB94	2.5	– 40.1	– 25.2
38	849–1025	3,2	63–81	UA97	UA98	3.2	+ 40.6	+ 22.6
38	849–1025	3,2	63–81	UB6	UB7	3.3	+ 54.3	+ 30.0
45	846–847	3,2	64–81	UB25	UB27	6.4	– 62.9	– 24.9
45	839–846	3,2	64–81	UB36	UB35	1.8	+ 90.1	+ 66.2
45	846–847	3,2	78–81	UB20	UB22	6.4	– 96.6	– 38.2
47	843–844	3,2	63–81	UA55	UA54	4.8	+ 48.4	+ 22.0
47	843–844	3,2	63–81	UA54	UA52	7.1	+ 55.9	+ 20.9
48	146–172	3,2	78–81	UA33	UA35	6.4	– 89.9	– 35.5
49	146–1027	1,2	63–81	KD70	KD71	1.6	+ 96.9	+ 76.4
49	146–1027	1,2	63–81	KD71	KD72	1.6	+ 24.6	+ 19.4
50	1027–1028	3,2	63–81	CK62	CK61	1.6	– 115.3	– 90.6
50	1027–1028	3,2	63–81	K4	K5	1.6	– 39.7	– 31.3
50	1027–1028	3,2	63–81	K5	K6	1.3	– 26.7	– 23.0
50	1027–1028	3,2	63–81	K9	K10	1.6	+ 71.4	+ 56.8
50	1027–1028	3,2	63–81	K12	K13	2.2	– 31.0	– 20.8
50	1027–1028	3,2	63–81	K13	K14	1.6	– 33.0	– 26.0
50	1027–1028	3,2	63–81	K16	K17	1.6	+ 46.7	+ 36.8
54	834–838	3,2	63–82	LM24	LM23	3.2	– 38.9	– 21.7
59	116–126	1,2	63–82	MG77	MG78	1.6	+ 19.8	+ 15.6
59	116–126	1,2	63–82	MG87	MG88	1.6	+ 18.3	+ 14.5
64	146–168	1,3	65–79	BM75	BM76	1.6	– 46.0	– 36.2
64	146–168	1,2	65–81	BM77	BM78	1.6	– 32.0	– 25.3
64	146–168	1,2	65–81	BM78	BM80	3.2	– 40.5	– 22.6
69	1028–1082	3,2	63–81	K19	K20	1.6	+ 39.6	+ 31.1
69	1028–1082	3,2	63–81	K20	K21	1.6	+ 50.9	+ 40.0
69	1028–1082	3,2	65–81	K21	UC64	0.7	– 20.1	– 23.2
69	1028–1082	3,2	65–81	UC64	UC65	1.6	– 47.7	– 37.7
69	1028–1082	3,2	65–81	UC66	UC67	1.6	+ 42.4	+ 33.5
69	1028–1082	3,2	65–81	UC71	UC72	1.6	– 37.4	– 29.3
88	844–848	3,2	74–81	UA51	UA50	3.2	– 44.2	– 24.7
88	844–848	3,2	74–81	UA48	UA47	3.2	– 93.6	– 52.3
88	844–848	3,2	74–81	UA44	UA43	3.2	+ 41.1	+ 23.0
93	859–2131	3,3	59–68	F365	YQ2	5.2	– 115.5	– 50.5
93	859–2131	3,3	59–68	YQ7	YQ8	4.4	– 51.2	– 24.3
93	859–2131	3,3	59–68	YQ12	YQ13	4.8	+ 82.9	+ 37.7
93	859–2131	3,3	59–68	YQ14	YQ15	6.0	+ 85.3	+ 34.7
98	852–1025	3,2	63–81	CK14	CK15	1.6	+ 37.1	+ 29.2
101	857–856	3,3	63–68	YQ16	QBR1	2.4	+ 75.9	+ 48.6
102	1003–1028	3,2	63–81	CK46	CK47	1.6	– 57.4	– 45.1
—	856–181	3,3	60–68	BRM6	BRM7	4.8	– 58.5	– 26.6

However, the calculated errors in gravity differences are so high relative to the small height changes found in levelling, that the ground- water effects between surveys seem minor. It is recommended that regular repeat gravity surveys not be continued, unless the accuracy of these surveys can be improved by an order of magnitude.

Discussion of results

1. Maps and profiles of apparent height changes derived from repeat levelling (Figs 5, 6, 8) show areas where the height changes are greater than the expected levelling errors. Some of these height changes are likely to be due to vertical crustal movements (Fig. 10). The vertical movement is manifest either as two-sided or one-sided anomalous areas. The two-sided anomalous areas (such as M and N of Fig. 6) have two zones of significant relative movement of opposite sign. The areas have an amplitude of 50–100 mm and an extent of 20–50 km. The areas are generally uplifted, not depressed, consistent with the Southwest Seismic Zone being in compression. The one-sided anomalous areas (such as J of Fig. 5) are isolated locations of significant movement. These areas have the same amplitude of relative movement (50–100 mm), but the extent of vertical movement is not known.

2. Much of the movement forming each uplift 20–50 km wide has occurred between only a few bench marks (Figs 5, 6, 8, & 11). This is consistent with the uplift being concentrated on one or a few faults or narrow zones, rather than being uniformly distributed. Monitoring of any uplift should be concentrated in those intervals of levelling traverse that have significant movement (Table 1). In most cases, more precise location of the zone of movement would be difficult with presently available data; however, reports of road cracking (e.g. Gordon & Lewis, 1980, p. 185) should in the future be fully documented, because they may indicate the exact position and type of deformation.

3. Numerous bench marks appear to have moved vertically relative to all surrounding bench marks (Table 2). Initially, the anomalous bench marks were thought to have moved relative to both the surrounding surface and the underlying rock. These apparently unstable bench marks and the occurrence of unstable valley fill were the main reason for placing the deep bench marks at 10 km intervals along the levelling traverses. However, during a field inspection by D. McKellar, R.P. Mather, and P. Wellman in April 1985, McKellar demonstrated that the anomalous bench marks were generally on thin sandy soil overlying rock (which should give relatively stable sites), and that the tops of the bench marks had not moved significantly relative to the original land surface, as marked by the present soil and fence level. These

Table 2. Bench marks that have moved relative to both adjacent bench marks

ASO run no.	AHD junction points	Order of levels	Years	BM no.	BM no.	Dist. (km)	Height change (mm)	s (mm.km$^{-½}$)
2	859–854	3,2	64–81	UB31	UB32	3.3	– 27.7	– 15.2
				UB32	UB33	3.2	35.5	+ 19.8
5	159–172	1,2	60–81	F384A	F383	1.6	– 25.2	– 19.6
				F383	F383A	1.6	+ 30.2	+ 23.7
6&3	172–198	1,2	59–81	SB2	SB1	1.7	– 36.3	– 27.9
				SB1	F373	2.3	+ 40.9	+ 27.0
11	172–181	1,2	61–81	NM57	NM58	1.6	– 19.2	– 15.2
				NM58	NM59	1.6	+ 14.9	+ 11.8
11	172–181	1,2	61–81	FBM5	NM66	3.5	+ 18.8	10.0
				NM66	NM66A	0.8	– 18.2	– 20.4
10	857–858	3,2	59–82	YQ15	YQ14	5.8	– 155.4	– 64.4
				YQ14	YQ13	3.9	+ 160.8	+ 81.4
13	857–863	3,2	59–82	BC12	KJ3	6.0	+ 89.3	+ 36.5
				KJ3	WG3	8.0	– 131.2	– 46.5
23	198–200	1,2	59–82	BM73	BM74	1.6	+ 131.2	+ 103.7
				BM74	BM75	1.6	– 120.3	– 95.1
31	1029–1030	3,2	80–81	UB10	UB11	2.3	– 53.6	– 35.2
				UB11	UB12	3.9	+ 41.3	21.0
38	849–1025	3,2	63–81	UB3	UB4	3.3	+ 86.3	+ 47.6
				UB4	UB6	6.5	– 82.9	– 32.5
45	846–847	3,2	64–81	UB28	MM37	3.2	– 48.1	– 26.9
				MM37	MM36	1.9	+ 28.6	+ 20.1
47	838–843	3,2	63–81	LM27	LM28	3.2	– 242.7	– 135.5
				LM28	LM30	6.3	+ 276.2	+ 109.9
50	1027–1028	3,2	63–81	CK61	CK60	1.6	+ 40.7	+ 32.1
				CK60	K1	2.2	– 52.3	– 35.4
52	126–146	1,2	63–82	MM96	MM97	1.6	– 32.0	– 25.3
				MM97	MM98	1.6	+ 36.8	+ 29.1
53	126–159	1,2	63–82	MG46A	MG47	3.6	+ 562.0	+ 296.2
				MG47	MG48	1.6	– 580.7	– 459.1
58	2259–2912	3,2	63–82	M8	M11	5.0	– 40.1	– 17.9
				M11	M12	1.8	+ 62.2	46.4
65	146–168	1,2	63–82	MK63	HV94	3.2	+ 28.6	+ 16.0
66	1082–3226	3,2	79–82	HV94	MK62	0.1	– 30.0	large
88	844–848	3,2	74–81	UA46	UA45	2.6	+ 67.9	+ 42.0
				UA45	UA44	3.2	– 88.8	– 49.6
97	852–1025	3,2	63–81	CK29	CK31	3.2	+ 113.1	+ 62.8
				CK31	CK32	1.6	– 82.7	– 65.2
98	852–1025	3,2	63–81	CK7	CK8	1.0	– 33.6	– 33.3
				CK8	CK9	2.2	+ 41.6	+ 27.9
99	857–2697	3,3	59–80	YQ16	QC1	3.5	+ 54.0	+ 28.7
				QC1	QC2	1.9	– 52.1	– 37.5
102	1003–1028	3,2	63–81	CK44	CK45	1.6	– 80.8	– 63.5
				CK45	CK46	1.6	+ 87.1	+ 68.4

bench marks are therefore not in the unstable valley fill, and it is now thought that the movement of the anomalous bench marks reflects movement of the underlying rock relative to that under the surrounding bench marks. The exact mechanism for this is not known, but the anomalous bench marks may be on fault wedges of crust. The relationship between the movement of these anomalous bench marks and the movement associated with faulting is not known; monitoring of these bench marks is thought to be less useful in earthquake prediction.

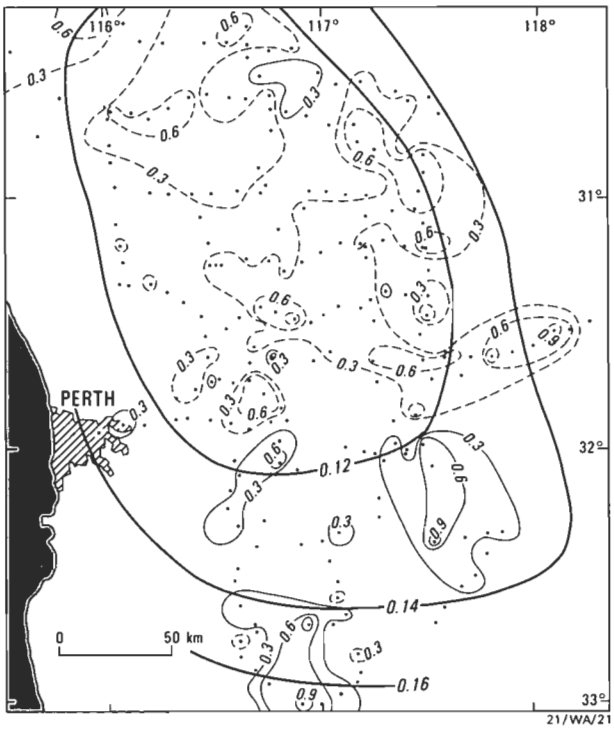

Figure 12. Calculated error in gravity differences (thick lines, s.d. in μm.s^{-2}).
Measured gravity differences (μm.s^{-2}) given by contours at −0.9, −0.6, −0.3, 0.3, 0.6, 0.9 (μm.s^{-2}), negative contours dashed.

4. In a study similar to the present one, Wellman (1981) analysed repeat distance measurements on traverses in the Southwest Seismic Zone. The traverses consist of a line of trigonometrical points 20–70 km apart. His results can be interpreted as indicating that horizontal crustal movement occurred between only a few trigonometrical stations and that the movement in 10 years was between 60 and 600 mm, with an average near 200 mm. Hence, both horizontal and vertical geodetic measurements are consistent with crustal movement being confined to narrow zones between rigid blocks. Between the blocks, vertical movement (50–100 mm) is smaller than horizontal movement (200 mm). Californian experience in crustal movement measurement is that, relative to vertical measurements, horizontal measurements are easier to make and more useful for prediction, because they directly reflect the causative horizontal stress and the elastic strain accumulation. Although the tectonic situations are different, this would also seem to apply in the Southwest Seismic Zone of Western Australia.

Future crustal movement monitoring

Before a mechanical model can be determined for the earthquakes of the Southwest Seismic Zone, two problems must be resolved:

1) how the high-amplitude east-west regional stress and its local variation are accommodated by crustal strain — the accommodation being localised displacements (seismic or aseismic) or elastic compression of large bodies of rock or both of these;

2) where are the areas of high elastic strain that have the highest earthquake risk as determined from the pattern of seismicity and crustal movement?

The above two problems are best solved by determination of the relation between stress, strain, and earthquakes in selected areas of different response.

The present paper and Wellman (1981) attempt to determine the position, magnitude, and time scale of vertical crustal movement. They therefore allow the identification of test areas for more intensive investigation, and show the magnitude of the crustal movements that occur.

Some possible future strategies for monitoring crustal movement in the Southwest Seismic Zone are as follows.

(a) Relevelling the whole second-order network (Fig. 4) after a period of 3–10 years. This option is relatively expensive and does not concentrate on areas of relatively greater interest. However, it may be desirable if several more large earthquakes occur in the earthquake zone.

(b) Relevelling short sections of the second-order network where (1) previous relevelling has shown that crustal movement has occurred in the past, (2) there have been earthquake swarms, or (3) there is reported road cracking. This option is relatively cheap and likely to give some indication of strain accumulation in areas of apparent higher risk. However, by itself it does not tackle the problem of the relation between stress, horizontal movement, vertical movement, elastic strain, and earthquakes.

(c) Identification of areas of relatively high seismic activity and/or crustal movement, and periodic remeasurement of horizontal and vertical positions of a compact geodetic network using GPS (Global Positioning System) receivers (Stolz & Lambeck, 1983), with periodic remeasurement of in-situ stress, and continued earthquake recording. This is the preferred option. The crustal movement part is relatively cheap, so measurements of position can be repeated at intervals of a few years. The crustal strain network geometry is not controlled by the distribution of major roads or hilltops, and the network geometry can be optimised and can cover all the area of interest. Both horizontal and vertical movements are simultaneously measured to an accuracy of 10–100 mm, and their interdependence can be determined. Studies of this type, determining the relationship between stress, strain, and earthquakes in a diverse set of areas, would greatly help in determining the mechanical model necessary for estimation of earthquake risk and future prediction of earthquakes.

Acknowledgements

We are grateful to the Australian Survey Office for carrying out the second order levelling surveys on which this study is primarily based, J.B. Steed and G. Luton of the Division of National Mapping, Canberra, for reducing and adjusting all the levelling surveys, and the Western Australian Lands and Survey Department for drawing BMR's attention to the changes in level and subsequently providing copies of old levelling measurements. We are also grateful to P. Morgan

of the Canberra College of Advanced Education who suggested the method of analysing levelling values using a probability scale, and D.J. Woodward and A.F. Carman of the Geophysics Division, DSIR, New Zealand, for many discussions and providing a copy of their computer program. Useful comments on the draft paper were received from B.C. Barlow, D. Denham, and H.A. Doyle. The figures were drafted by J. Convine.

References

Denham, D., & Alexander, L.G., 1981—Rock stress measurements, Cadoux to Wagin, WA. *CSIRO Australia, Division of Applied Mechanics Technical Report* 125.

Denham, D., Alexander, L.G., & Worotnicki, G., 1979—Stresses in the Australian crust: evidence from earthquake and in-situ stress measurements. *BMR Journal of Australian Geology & Geophysics*, 4, 289-295.

Denham, D., Alexander, L.G., & Worotnicki, G., 1980—The stress field near the sites of the Meckering (1968) and Calingiri (1970) earthquakes, Western Australia. *Tectonophysics*, 67, 283-317.

Gordon, F.R., & Lewis, J.D., 1980—The Meckering and Calingiri earthquakes, October 1968 and March 1980. *Geological Survey of Western Australia, Bulletin* 126.

Ishii, H., 1983—Southwestern Australia as an experimental site for earthquake prediction research. *Report to ad-hoc working group on international experimental sites for research on earthquake prediction, second meeting, Hamburg FRG, August 1983.*

Lewis, J.D., Daetwyler, N.D., Bunting, J.A., & Moncrieff, J.S., 1981—The Cadoux earthquake 2 June 1979. *Geological Survey of Western Australia, Report* 11.

McConnell, R.K., & Gantar, C., 1971—Adjustments and analyses of data for IGSN 71. *In* Morelli, C., Gantar, C., & others, The international gravity standardization net 1971 (I.G.S.N. 71). *International Association of Geodesy, Special Publication*, 4, 165-190.

NMCA, 1976—Standard specifications and recommended practices for horizontal and vertical control surveys. *National Mapping Council of Australia, Special Publication* 1, Second edition.

Paige, C.C. & Saunders, M.A., 1978—A bidiagonalization algorithm for sparse linear equations and least squares problems. *Applied Mathematics Division, Department of Scientific and Industrial Research, New Zealand, Technical Report* 80.

Roelse, A., Granger, H.W., & Graham, J.W., 1971—The adjustment of the Australian levelling survey 1970-1971. *Division of National Mapping, Australia, Technical Report* 12.

Stolz, A., & Lambeck, K., 1983—Geodetic monitoring of tectonic deformation in the Australian region. *Journal of the Geological Society of Australia*, 30, 411-422.

Tracey, R.M., 1982—Analysis of repeat levelling measurements to give ground deformation, southwest Australia. *Bureau of Mineral Resources, Australia, Record* 1982/30.

Wellman, P., 1981—Crustal movement determined from repeat surveying — results from southeastern and southwestern Australia. *Journal of the Geological Society of Australia*, 28, 311-321.

Williams, I.R., 1979—Recent fault scarps in the Mount Narryer area, Byro 1:250 000 sheet. *Geological Survey of Western Australia Annual Report*, 1978, 95-99.

Woodward, D.J., & Carman, A.F., 1984—Computer programs to reduce precise gravity observations. *Geophysics Division, Department of Scientific and Industrial Research, New Zealand, Technical Note* 93.

BMR Journal of Australian Geology & Geophysics, 10, 233-242

A new Devonian fish fauna, and revision of post-Ordovician stratigraphy in the Ross River Syncline, Amadeus Basin, central Australia.

G.C. Young[1], S. Turner[2], M. Owen[1], Robert S. Nicoll[1], J.R. Laurie[1], & J.D. Gorter[3].

A Devonian microvertebrate fauna from the N'Dahla Member, previously assigned to the Cambro-Ordovician Pacoota Sandstone, has led to a revision of the stratigraphy in the Ross River Syncline. The N'Dahla Member is included in the Devonian Pertnjara Group, and is correlated on faunal evidence with the Deering Siltstone Member of the Parke Siltstone in the central Amadeus Basin. The overlying sandstone, previously mapped as Mereenie Sandstone, is presumed to be equivalent to one of the overlying formations of the Pertnjara Group. The N'Dahla Member rests with angular unconformity on the underlying Pacoota Sandstone, this break possibly representing both the Rodingan and Pertnjara Movements of other authors. Evidence of the Devonian Pertnjara Movement in the Amadeus Basin is reviewed, and the possibility that the Mereenie Sandstone was never deposited in the Ross River sequence is discussed. The recognition of Mereenie Sandstone in other outcrops and wells in the eastern part of the Amadeus Basin requires re-examination.

Introduction

The N'Dahla Member of the Pacoota Sandstone (Cambro-Ordovician) was defined by Wells & others (1967, p.45) as a thin sequence of clayey and pebbly sandstone, with minor beds of conglomerate and thin beds of limestone, exposed in its type locality at the top of the Pacoota Sandstone at N'Dhala Gorge, in the Ross River Syncline, northeast Amadeus Basin (Fig. 1). Lithology was described as a 'dark red-brown to purple-brown medium to coarse-grained glauconitic poorly sorted friable porous and clayey sandstone'. Minor pebbles, conglomeratic beds of siltstone and limestone fragments, and thin beds of limestone were also recorded. Fossils listed from the N'Dahla Member included trilobites, gastropods, nautiloids, and worm tracks, indicating an Early Ordovician (late Tremadocian) age, and representing the middle of three informal time units designated for the Pacoota (Wells & others, 1970, p. 66). Some differences in outcrop and lithology were noted between the N'Dhala Gorge type locality, where the member 'weathers recessively and forms the waning slopes beneath a steep scarp of Mereenie Sandstone', and farther west on the northern limb of the Ross River Syncline where it was said to be more resistant, forming 'part of the ridge of Pacoota Sandstone' (Wells & others, 1967, p. 45). As mapped (BMR, 1983) this western part of the member was shown to be overlain by another sandstone of the Pacoota Sandstone, which was in turn overlain with a low-angle unconformity by the Mereenie Sandstone (?Siluro-Devonian). The unconformity was said to be clearly visible on air photos (Wells & others, 1967, p.48).

Fish scales suggesting a Devonian age were first noted in a sample submitted by Pancontinental Petroleum (J.D. Gorter) to R.S. Nicoll for conodont analysis. Further samples were collected by G.C. Young in the 1984 field season, and yielded an abundant microvertebrate fauna, together with reworked Early Palaeozoic microfossils, as summarised below. The vertebrate fauna is distinctively Devonian, and quite different

[1]Division of Continental Geology, Bureau of Mineral Resources, GPO Box 378, Canberra, ACT 2601.
[2]Queensland Museum, South Brisbane, Queensland.
[3]Pancontinental Petroleum Limited, Sydney, New South Wales. Present address: School of Applied Geology, University of New South Wales, Kensington, N.S.W.

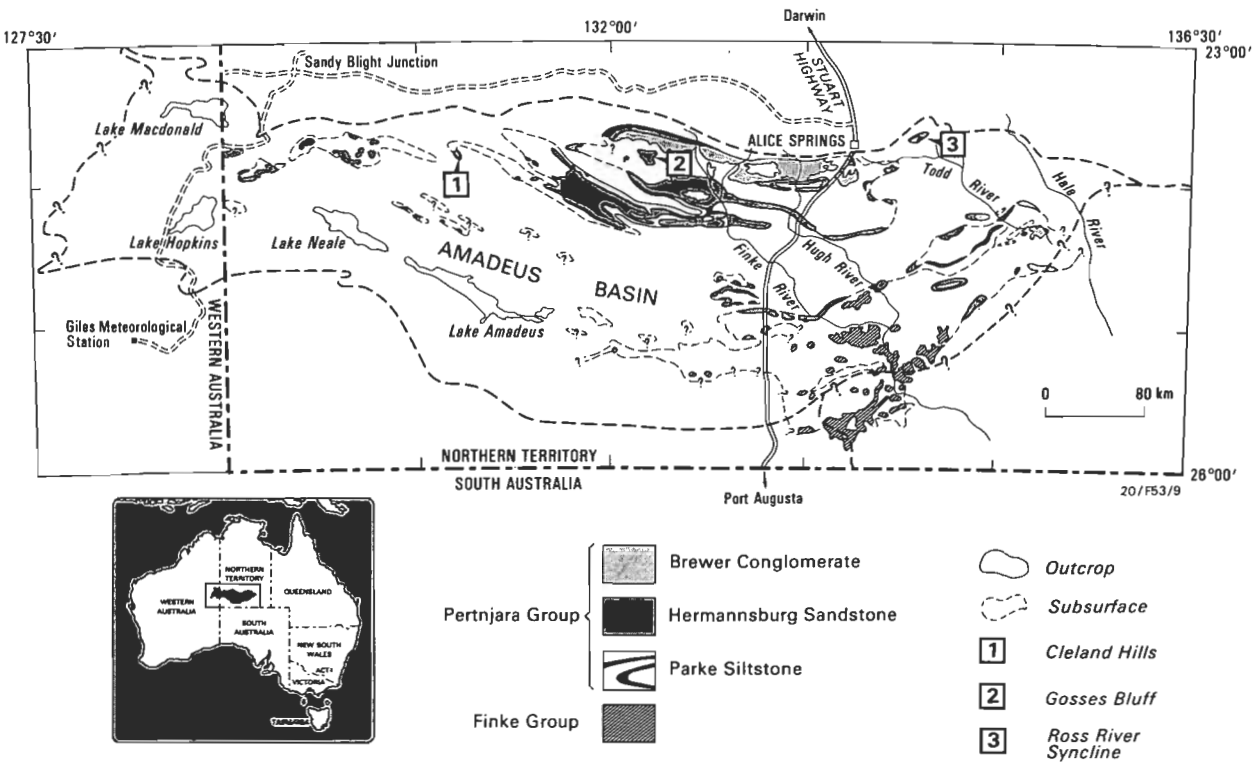

Figure 1. Amadeus Basin, central Australia, showing the distribution of Devonian rocks (Pertnjara and Finke Groups) and the three general localities discussed in this paper.

The new fish fauna reported here comes from the Ross River Syncline (locality 3).

from the vertebrate assemblage of Ordovician age known from elsewhere in the Amadeus Basin (e.g. Ritchie & Gilbert-Tomlinson, 1977). This new fauna has required a reinterpretation of the geology of the N'Dhala Gorge area and the stratigraphy of the sequence in the Ross River Syncline above the Pacoota Sandstone. The N'Dahla Member has been reassigned to the Devonian Pertnjara Group, as a member of its lowermost formation, the Parke Siltstone (Fig. 4).

Geology of the N'Dhala Gorge area

The first samples containing Devonian thelodont fish scales were collected (J.D.G.) adjacent to the car-park at N'Dhala Gorge (locality 1, Fig. 2), close to the site of earlier samples (AS257–259, collected in the 1960s) on which an Ordovician age for the N'Dahla Member was based. Much of the N'Dahla Member in this area is covered by scree, and a detailed re-assessment, assisted by the aerial photographs used in the original mapping, has led to a revision of the geology.

It is apparent that the contact between the N'Dahla Member and the underlying Pacoota Sandstone was placed too low in the sequence in the original mapping, and that samples AS257–259 were not collected from a horizon well within the N'Dahla Member, but came either from the basal part of the member or from the quartz arenite developed at the top of the underlying Pacoota Sandstone. This arenite forms a prominent dip slope around the closure of the Ross River Syncline, and is the highest horizon in the area in which macrofossils, apart from trace fossils, were observed during the 1984 field work. A re-examination of the original samples supports a mixed source. AS257 contains abundant fossil fragments, too incomplete for identification, but similar in appearance to those in the Pacoota, but which may have been reworked, since the lithology suggests that this specimen came from the N'Dahla Member. AS258 is of typical Pacoota lithology, with *Cruziana* and *Skolithos* type trace fossils. Its atypical red coloration could indicate derivation from the Palaeozoic weathered surface forming the top of the Pacoota Sandstone beneath the unconformity. Sample AS259 could not be located, but two further samples collected during the original mapping from near the westernmost exposure of the N'Dahla Member, about 3.5 km east of Williams Bore, were also examined. One of these (AS230) is of typical N'Dahla lithology, and contains abundant moulds of a small gastropod, which are too poorly preserved for identification. AS231 contains trilobite fragments and, together with

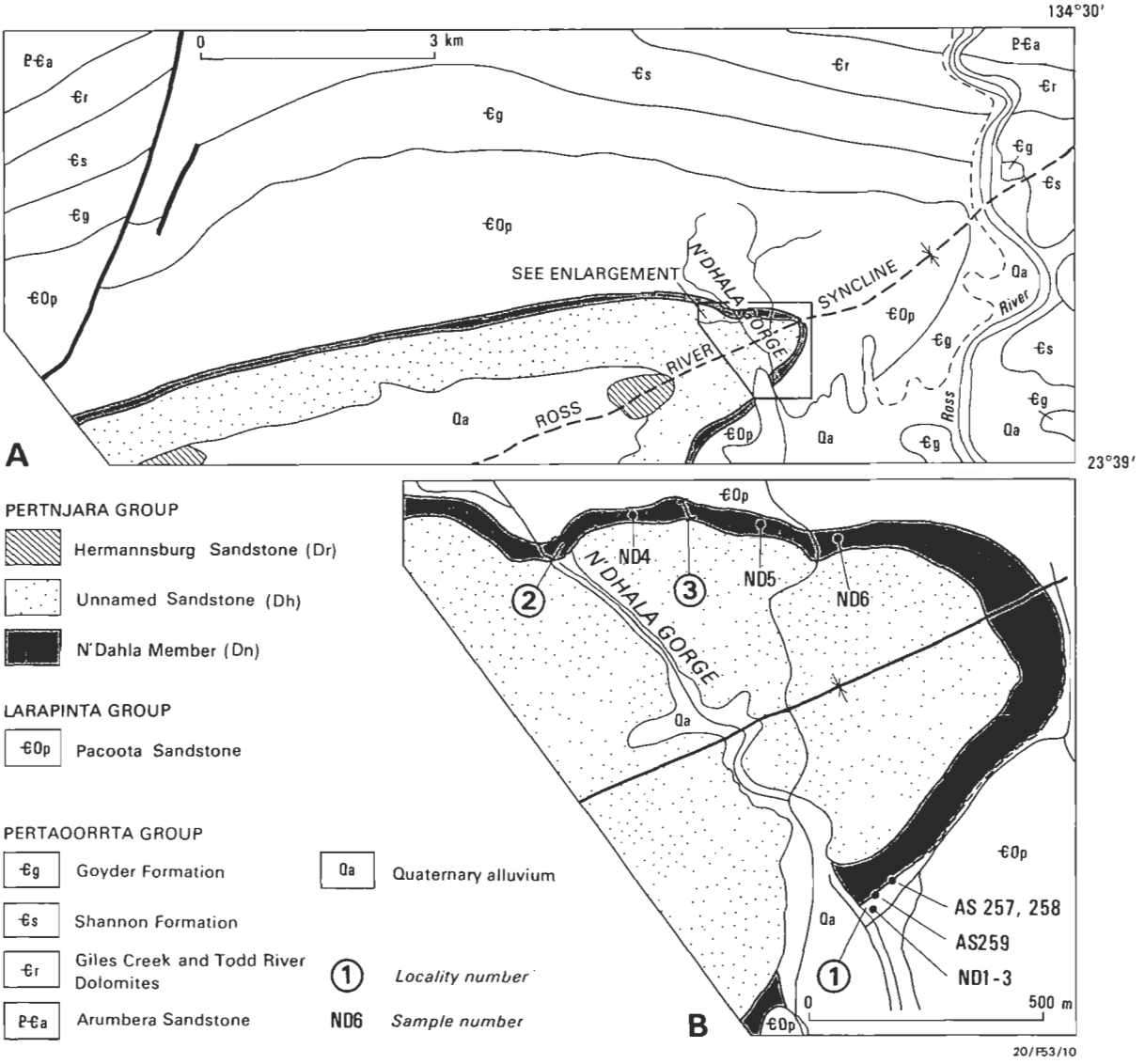

Figure 2. A — Geology of the Ross River–N'Dhala Gorge area. modified after the 1:100 000 Geological Special Sheet, Geology of the Alice Springs Region (BMR, 1983); B — N'Dhala Gorge area, showing field localities (1–3), and collecting sites for the original palaeontological samples (AS257–259), and the new samples reported here (ND1–6).

lithology, clearly indicates derivation from the underlying Pacoota Sandstone. Thus, the mixed derivation of these samples and the problem of reworked fossils (see below) render them unreliable for dating purposes. New samples (ND 1-3) collected in 1984 from the vicinity of the original fish samples contained conodonts indicating an Ordovician age, but no fish remains. Reference to the original aerial photographs indicates that these samples come from a horizon just below that of samples AS257-259.

On the published map (BMR, 1983), the N'Dahla Member on the northwestern limb of the Ross River Syncline is shown as overlain by another sandstone of the Pacoota, which extends as far east as the northwestern opening of N'Dhala Gorge (locality 2, Fig. 2). Here it is truncated by a low-angle unconformity at the base of the overlying Mereenie Sandstone. This interpretation was based on a study of aerial photographs, so this area was also examined in the 1984 field season, and further samples were collected for microfossils.

Field examination indicates that the sequence here is the same as at the southeastern end of N'Dhala Gorge. The sandstone previously interpreted as overlying the N'Dahla Member in fact underlies it and corresponds to the previously mentioned uppermost quartzitic strata of the Pacoota Sandstone, which crop out around the northeastern closure of the syncline. The underlying strata, which crop out on the southern slope of the valley immediately to the north of the gorge, were previously interpreted from aerial photographs as the recessive N'Dahla Member. However, this valley, which is formed by the creek that flows through N'Dhala Gorge, is in fact developed within a recessive shaly part of the Pacoota Sandstone. Looking west from the northwestern opening of the gorge, the upper part of the Pacoota can be seen to form a prominent strike ridge, overlain by the more recessive beds of the N'Dahla Member. The more resistant uppermost Pacoota Sandstone can be traced along strike across the opening of the gorge to the eastern side (locality 2, Fig. 2), where it can be seen to lie stratigraphically immediately beneath the N'Dahla Member. Lithology of the uppermost Pacoota Sandstone at this locality comprises interbeds 100-300 mm thick of sandstone and mudstone, with abundant vertical burrows and desiccation crack impressions, and some layers with numerous mud clast impressions. Poorly preserved gastropods (probably *Lecanospira* Butts 1926) are common in some beds.

The overlying N'Dahla Member at locality 2 is largely obscured by scree, and crops out poorly as a micaceous red siltstone, which may be very gritty, with small pebbles and pieces of limestone. Spot samples collected along strike to the east (ND4-6, Fig. 2) contained an abundant microvertebrate fauna (see below). The member was followed along strike around the closure of the syncline and back to the southeastern entrance of N'Dhala Gorge at the car park. Good exposures were only encountered in the gullies adjacent to the two northern openings of the gorge, and in small washouts on the eastern and southern scree slopes. The only locality where the sequence from the Pacoota Sandstone through the N'Dahla Member to the overlying sandstone is reasonably exposed is on the saddle between the two northern openings of the gorge. An approximate section measured through the N'Dahla Member at this locality (3, Fig. 2), is given in Fig. 3A. This is designated the type section for the N'Dahla Member.

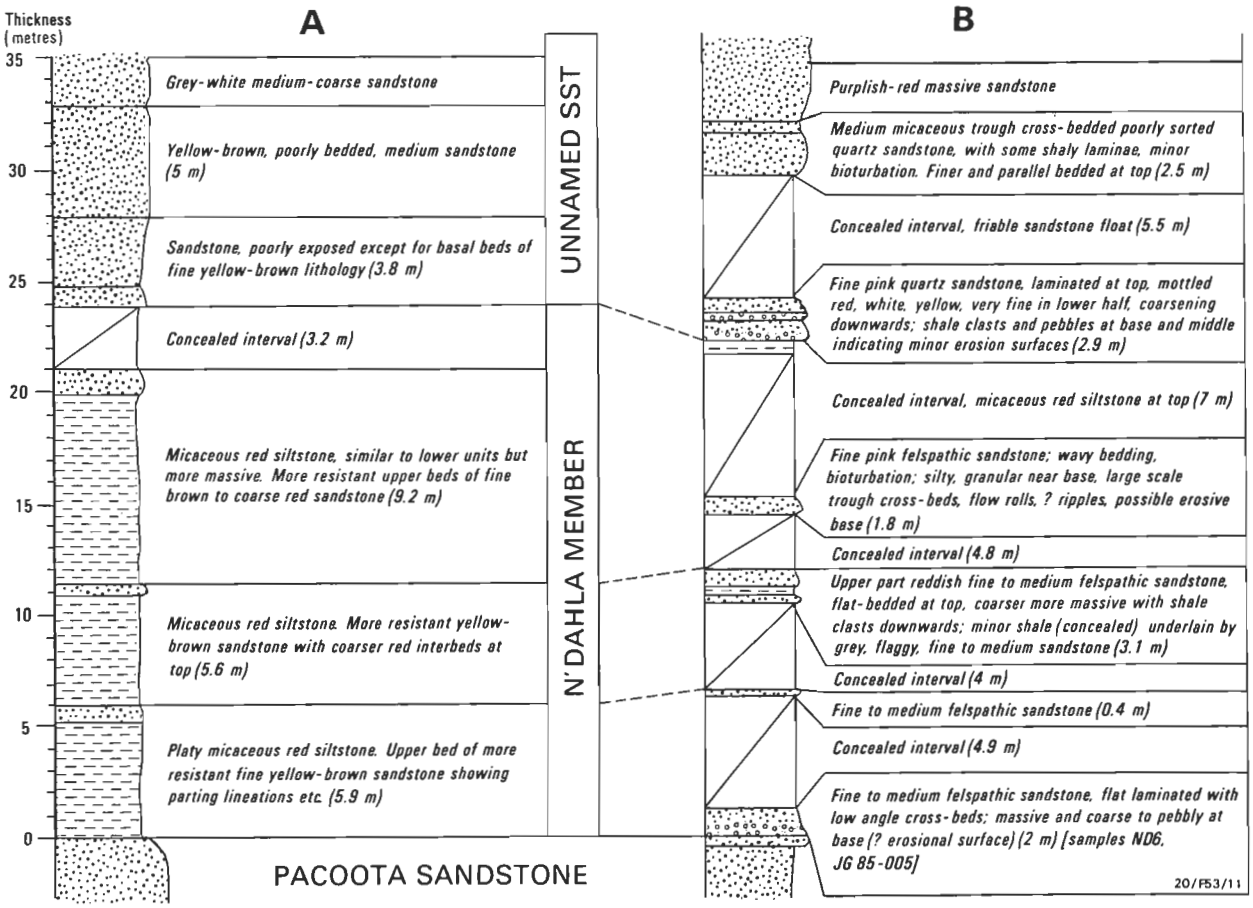

Figure 3. A — Proposed type section for the N'Dahla Member of the Pertnjara Group at N'Dhala Gorge (locality 3, Fig. 2). B — Section measured through the N'Dahla Member at the site of original palaeontological samples (locality 1, Fig. 2).
Suggested correlations between beds indicated by dashed lines.

The base of the N'Dahla Member is taken as the first red siltstone above the silicified fossiliferous sandstone of the Pacoota Sandstone. Interpretation of aerial photographs shows this contact to be a low-angle unconformity, as noted by Wells & others (1967, p. 48). The N'Dahla Member in the type section comprises four fining-upward cycles of interbedded micaceous red siltstone and yellow-brown fine lithic feldspathic quartz sandstone, the latter generally less than a metre thick. The red siltstone weathers recessively, and is poorly exposed. The top of the member is placed at the top of the highest red siltstone bed beneath the overlying sandstone. In the type section this is identified by its recessive exposure. The upper contact of the N'Dahla Member with the overlying sandstone may be unconformable, and is marked by a decrease in lithic and feldspathic content of the sandstone. The lower 10 m of section above the N'Dahla, and beneath the more massive bluff-forming sandstone unit previously identified as Mereenie Sandstone (Fig. 3A), comprises thin- bedded, poorly sorted quartz sandstone with local pebbly interbeds. Wells & others (1970) recorded a thickness of about 15 m for the N'Dahla Member, which is somewhat less than the measured type section of about 24 m (Fig. 3A).

In 1985 another section was measured at locality 1 (J.D.G. and B. Jakeman), to include the site of the first thelodont samples. Although the N'Dahla Member here is less well exposed, several fining-upward cycles can again be recognised. The basal beds are trough cross-bedded and conglomeratic quartz sandstones, a lithology not represented at the base of the type section. At locality 1 these represent an abrupt lithological change from the underlying white quartzite of the Pacoota Sandstone. Pebbles of quartzite, chert, and limestone up to 40 mm in size were seen, but no thin beds of limestone (cf. Wells & others, 1967). The conglomerate grades upwards into parallel-bedded fine-grained quartz sandstones, followed by a covered interval, assumed to be micaceous red siltstone. As in the type section, this cycle is repeated several times through the sequence (Fig. 3B).

Revised stratigraphy above the Pacoota Sandstone in the Ross River Syncline

According to previous interpretations, the Pacoota Sandstone in the Ross River Syncline was unconformably overlain by the Mereenie Sandstone (Silurian or Devonian), and this in turn was unconformably overlain by the Devonian Pertnjara Group.

A Middle to Late Devonian age for the Pertnjara Group elsewhere in the Amadeus Basin is given by placoderm fish remains (Gilbert-Tomlinson, 1968; Young, 1985) and spores (Hodgson, 1968; Playford & others, 1976). However, the age of the Mereenie Sandstone is less well constrained. As discussed by Young (1985), the precise stratigraphic horizon of some fish remains from Gosses Bluff, previously used to determine a Devonian age for the Mereenie Sandstone, is uncertain. Two alternative interpretations of Gosses Bluff stratigraphy were proposed (Young, 1985, fig. 2), with the Devonian fish fauna being derived either from near the Mereenie-Pertnjara contact or from an uppermost sandstone of the Larapinta Group underlying the Mereenie Sandstone.

The discovery of the new Devonian fish fauna reported here, apparently from beneath the Mereenie Sandstone in the Ross River Syncline, would appear to support the second alternative, thereby indicating a Devonian age for the Mereenie Sandstone. However, some samples collected (M.O.) in the 1985 field season from the Cleland Hills in the northwestern part of the Amadeus Basin (Fig. 1) suggest an alternative interpretation. These have yielded fragmentary thelodont scales and a single impression of a fish spine in sandstone. They come from calcareous sandstone beds that overlie the Mereenie Sandstone at Mount Winter (see Wells & others, 1965, p. 29). These were referred by Jones (1972, fig. 6) to the lowermost Deering Siltstone Member of the Parke Siltstone, the basal formation of the Pertnjara Group. This new Devonian vertebrate locality will be dealt with in more detail elsewhere, but there is little doubt that it is equivalent to the thelodont fauna from the N'Dahla Member, which must therefore represent a stratigraphic horizon approximately equivalent to the lowermost Pertnjara Group. This is consistent with recent field-work at Gosses Bluff (M.O.) suggesting that the fish fauna there comes from just above the top of the Mereenie Sandstone.

Thus, we suggest that the Mereenie Sandstone previously mapped in the Ross River Syncline was incorrectly identified, and instead represents an unnamed sandstone formation belonging to the Pertnjara Group. It is noteworthy that the occurrence of Mereenie Sandstone as previously mapped in this region is a small outlier of the main Mereenie outcrop in the Amadeus Basin (e.g. Wells & others, 1970, fig. 34). The difficulty of distinguishing the Mereenie Sandstone from overlying sandstones of the Pertnjara Group in areas to the south, where the Parke Siltstone is missing from the sequence, was noted by Wells & others (1967, p. 49). The new interpretation proposed here necessitates a revision of the stratigraphy of the overlying Pertnjara Group.

Jones (1972) identified three units in the Pertnjara Group in the Ross River Syncline: a lower member about 200 m thick identified as the basal Ooraminna Sandstone Member of the Hermannsburg Sandstone; an upper Ljiltera Member of the Hermannsburg Sandstone, about 300 m thick; and a thin sequence of Brewer Conglomerate at the top of the section (thicknesses after Jones, 1972, figs 7, 9, 10). The conglomerate occurs only as isolated outcrops (Jones, 1972, p. 243), which Wells & others (1967, p. 49) recorded as unconformable on underlying formations. Although an unconformity was also mapped between the Pertnjara and the underlying 'Mereenie' (BMR, 1983), this presumably was based on the apparent absence of lower formations of the Pertnjara Group. There is no clear evidence of an unconformity in the field, and both Wells & others (1970) and Jones (1972, p. 231) regarded the contact between the Parke Siltstone of the Pertnjara Group and Mereenie Sandstone throughout the Amadeus Basin as generally conformable. Jones also suggested (p. 240) that the distribution of the Ooraminna Sandstone Member coincided with the area where the Hermannsburg Sandstone lies directly on Mereenie Sandstone, but this generalisation no longer applies in the Ross River area.

Reconnaisance examination of the post-N'Dahla Member units in the Ross River Syncline by one of us (M.O.) has shown that both the Ljiltera Member of the Hermannsburg Sandstone and the Brewer Conglomerate can be recognised, but that the sandstone occurring above the type section between the N'Dahla Member and the Ljiltera Member cannot be directly correlated, on lithological grounds, with any existing Pertnjara Group formation. This unnamed sandstone unit is composed of dominantly fine quartz sandstone with minor feldspar, and appears to have been deposited mainly in an aeolian environment. Much more detailed work is necessary before the unit can be formally described.

On the faunal evidence presented below, we suggest that the N'Dahla Member is equivalent to the Deering Siltstone Member of the Parke Siltstone as defined in Jones (1972), and that the sandstone formation previously mapped as Mereenie Sandstone in the Ross River Syncline broadly

correlates with that part of the Pertnjara Group between the Harajica Sandstone of the Parke Siltstone and Ljiltera Member of the Hermannsburg Sandstone (Fig. 4).

Preliminary description of the new fauna

Vertebrates

Fish remains from the first sample (NDG from locality 1) are fragmentary and few in number, and the best material comes from samples ND4–6 on the northern limb of the syncline (Fig. 2B). The following forms have so far been identified in the N'Dahla fish fauna:

turiniid thelodont scales (abundant)
nikoliviid thelodont scales (rare)
acanthodian scales in two morphologies (very rare)
crossopterygian tooth (one specimen)
cosmoid bone pieces (uncommon)
indeterminate bone fragments (uncommon)
fragments ornamented with bifurcating ridges (very rare)

The turiniid scales are variable in size and shape (Fig. 5A–J), but generally show striations or grooves on the ridges of the crown (e.g. Fig. 5A, E, H, J), and lateral wings or lappets on these ridges (e.g. Fig. 5C, D). Both are features observed in *Turinia* scales from the Cravens Peak Beds in the Georgina Basin (e.g. Turner & others, 1981), in *Turinia hutkensis* and

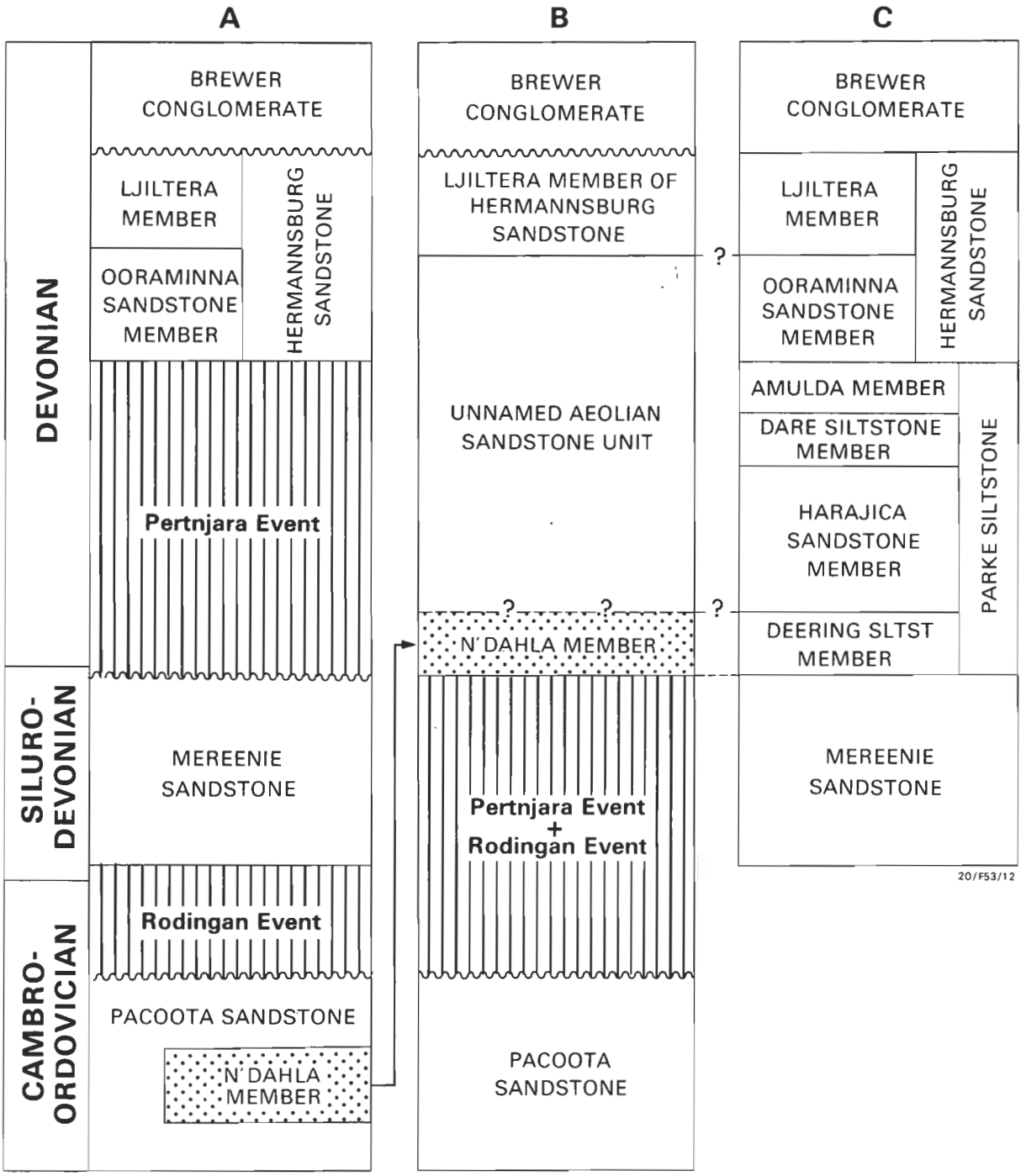

Figure 4. A — Original stratigraphic interpretation of the N'Dahla Member of the Pacoota Sandstone and overlying formations in the Ross River sequence (after Wells & others, 1970; Alice Springs Region, 1:100 000 Geological Special Sheet). B — revised stratigraphy based on the new Devonian vertebrate fauna described here. C — suggested broad correlation with subdivisions of the Pertnjara Group defined by Jones (1972).

T. cf. hutkensis from Iran and southeastern Australia (Blieck & Goujet, 1978; Young & Gorter, 1981), and in *Australolepis* from the Carnarvon basin (Turner & Dring, 1981). These forms are provisionally regarded as ranging in age from late Early Devonian (Emsian) to early Late Devonian (Frasnian). In the present sample, several scales show the elongate anterior basal process typical of *Turinia* body scales (Fig. 5A, E). The head scales closely resemble corresponding scales of *T. pagei* from Europe (e.g. Fig. 5G, H; cf. Ørvig, 1969) or *T. australiensis* from the Cravens Peak fauna (e.g. Fig. 5J; cf. Turner & others, 1981). Turiniid scales of post-Emsian age are not known from Europe, and appear to be a Gondwanan group. They have also recently been reported from South America (Goujet & others, 1984), China (Wang & others, 1986), and many localities in southeastern Australia (Pickett & others, 1985).

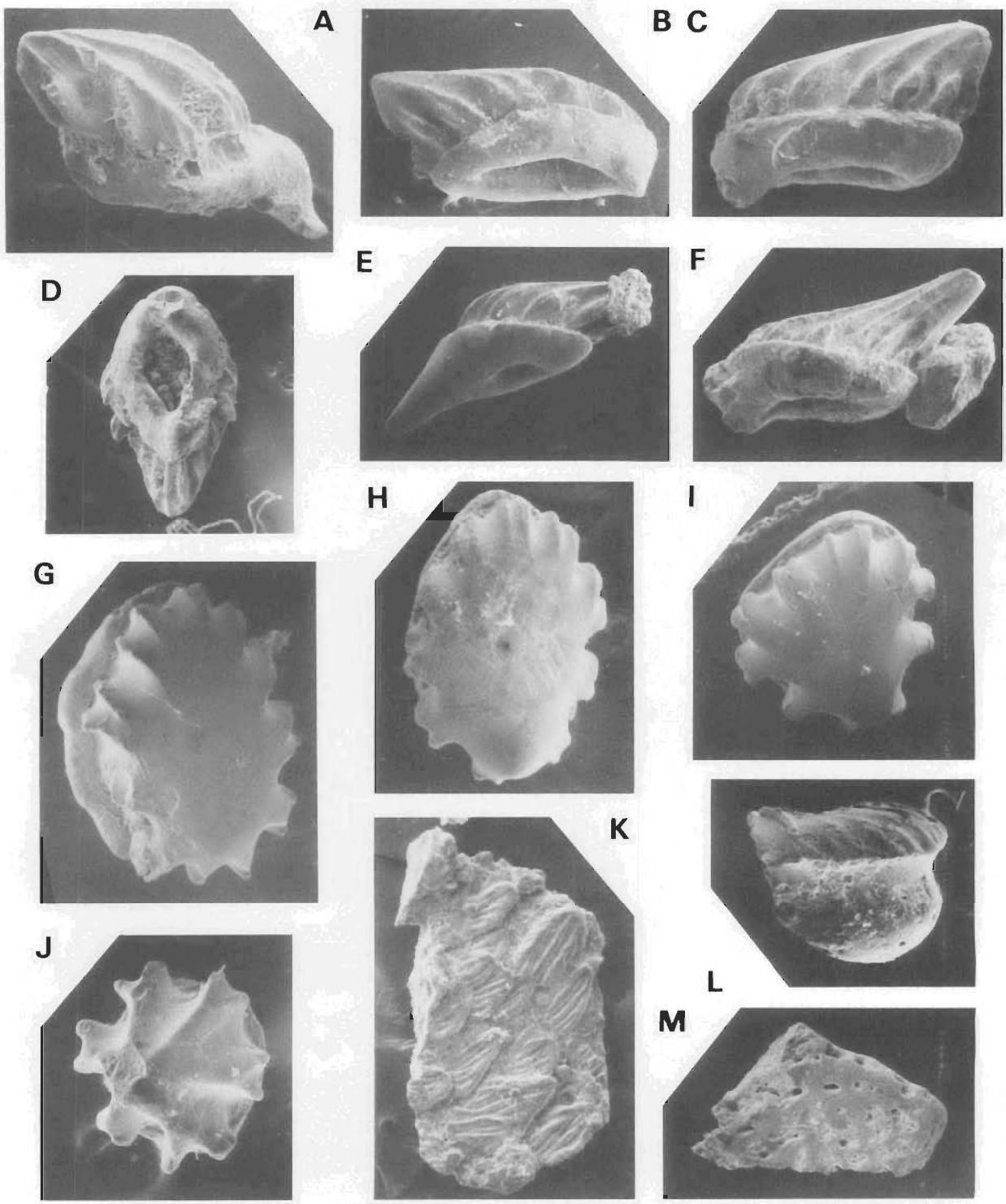

Figure 5. Devonian vertebrate fossils from the N'Dahla Member of the Pertnjara Group, Ross River Syncline, eastern Amadeus Basin. A–J, *Turinia* sp. (CPC 25768–25777 respectively), body scales in approximate lateral (A–C, E, F) and ventral (D) views, and head scales (G–J) in dorsal view (all ×50 except A, J, ×100, and E, F, ×35). K, ornamented bone fragment (CPC 25778), possibly acanthodian, in external view (×50). L, acanthodian scale (CPC 25779), cf. *Cheiracanthoides*, in anterolateral view (×75). M, cosmoid bone fragment (CPC 25780) in external view (×35). C, D, E, H, J, from sample ND4, others from sample ND6. (All specimens deposited in the Commonwealth Palaeontological Collection, Bureau of Mineral Resources, Canberra.)

The ornamented acanthodian scales have a flat crown with faint, widely spaced ridges converging posteriorly (Fig. 5L). There is a slightly constricted neck and a convex base. They resemble the form genera *Cheiracanthoides* (e.g. Gross, 1973, pl. 27, fig. 6) or *Homalacanthus* (e.g. Denison, 1979), which are similar in the rounded anterior and bluntly pointed posterior margins of the crown, and the widely spaced ridges. *Cheiracanthoides* scales were described from the Eifelian limestones of the eastern United States (Wells, 1944), and are abundant in Emsian limestones at Taemas (Giffin, 1980), and other eastern Australian localities. In Germany similar scales occur in faunas near the Emsian-Eifelian boundary (e.g. Vieth-Schreiner, 1983; Poltnig, 1984), but they are not associated with thelodontids. However, *Cheiracanthoides* scales and thelodont scales do occur together in the late Emsian-Eifelian Broken River Formation of Queensland (S.T., personal observation).

The only examples of ornamented bone in the sample may also belong to acanthodians. Only two fragments less than 1 mm across have been found. They are ornamented with curved ridges flanked by radiating striations (Fig. 5K), and show some resemblance to tesserae of the acanthodian *Nostolepis striata* (e.g. Gross, 1971a, pl. 3, figs. 15, 21, 25), but also the *Onychodus* remains illustrated by Wells (1944, pl. 3). Until better material becomes available these fragments are tentatively referred to the Acanthodii.

The crossopterygian tooth has a fluted base, and fine longitudinal striations. The distal end is missing. The preserved part is 7mm long and 2.5 × 3.5 mm in diameter at the narrow end. It could belong to a rhipidistian, onychodontid, or coelacanth fish. Histological sections show a very distinct enamel layer with fan-shaped radial striations, a feature typical of sarcopterygian fishes and higher vertebrate groups (M. M. Smith, personal communication). The absence of infolding of the dentine suggests that the tooth belongs either to an early osteolepid or an onychodontid fish. The latter group is associated with thelodontid scales in the Cravens Peak Beds of the Georgina Basin (Turner & others, 1981; Young, 1984).

Cosmoid bone fragments show the typical pores and shiny surface of the tissue cosmine (Fig. 5M). They could belong to rhipidistians or dipnoans.

A few bone fragments were sectioned to see if other groups could be identified, particularly placoderms, which are normally well represented in Devonian fish assemblages. However, in none of the thin sections was the bone well enough preserved to show diagnostic tissues.

Conodonts

Samples ND and JG85-005 (collected by J.D.G.), ND1-3 (collected by G.C.Y.), and 84-2011/1 (collected by R.S.N.) from locality 1 (Fig. 2) yielded conodonts indicating an Ordovician (Tremadocian) age, and presumably came from the uppermost beds of the Pacoota Sandstone. As noted above, these beds were previously mapped erroneously as part of the N'Dahla Member. Sample ND from this locality (collected by J.D.G.) also contained fragments of Devonian fish scales, suggesting reworking of the older faunal component. However, no conodonts were found in samples ND4-6 from the northern limb of the syncline, which are clearly within the N'Dahla Member (Fig. 2), and it is possible that the first samples from locality 1 were from several horizons near the Pacoota-N'Dahla contact and included pieces from both formations. Of earlier palaeontological samples collected from this locality, AS257 has yielded a rich conodont assemblage typical of the P2 horizon, the second highest of four subdivisions recognised in the Pacoota Sandstone.

Gastropods

Poorly preserved gastropods in sample AS230 mentioned above are indeterminable, so whether they are part of the Devonian fauna or of the reworked component is at present unknown. Sample ND6 produced two phosphatic steinkerns, probably belonging to the mollusc *Pelagiella deltoides*, a species first described by Runnegar & Jell (1976) from the post-Templetonian part of the Currant Bush Limestone in the Georgina Basin, western Queensland. Forms of similar morphology and preservation are also known from the Middle Cambrian Giles Creek Dolomite in the Amadeus Basin (J.R.L. unpublished) and from the lowermost carbonates in the Arthur Creek Formation of the western Georgina Basin, Northern Territory (Freeman, 1986). In the latter fauna they are associated with the mollusc *Protowenella* sp. and the trilobites *Xystridura* sp., *Pagetia* sp., and ?*Peronopsis* sp., which also indicate a Templetonian age.

The specimens in sample ND6 must have been reworked and, because of their excellent preservation (Fig. 6), they either underwent little water transport or, more probably, were transported within clasts, presumably derived from the Giles Creek Dolomite, since a different species of *Pelagiella* occurs in the Todd River Dolomite (Laurie, 1986).

Age and correlation of the N'Dahla fish fauna

The closest thelodont locality is that from the Toko Syncline in the Georgina Basin, where the Cravens Peak Beds contain turiniid scales similar to those from the N'Dahla Member. The Cravens Peak fauna also contains onychodontid and dipnoan remains (Young, 1984), which would account for the osteichthyan fragments occurring here. However, it is a more diverse fauna, and notable absences from the N'Dahla assemblage are *Machaeracanthus* spines and scales, smooth ischnacanthid scales, chondrichthyan scales and teeth (Turner & Young, in press), and placoderms (antiarchs).

Young (1985, p. 245) suggested that the fragmentary fish fauna from Gosses Bluff in the north central part of the Amadeus Basin was probably equivalent to the Cravens Peak fauna of the Georgina Basin. The same fauna occurs in the lower Dulcie Sandstone of the Georgina Basin and, as noted above, is also represented in basal beds of the Pertnjara Group in the Cleland Hills, about 140 km to the west of Gosses Bluff (Fig. 1). Gross (1971b) described turiniid scales from the Canning Basin of Western Australia, and similar scales have recently been recognised in the subsurface in the Officer Basin. Thus it seems that this fauna was widespread across the Australian craton during Early to Middle Devonian time. Much the same fauna also occurs in the Mulga Downs Group of western New South Wales, where a maximum age of Emsian is provided by a marine invertebrate fauna in the underlying Buckambool Sandstone (see Turner & others, 1981, p. 64; Young, 1984, p. 75). Although a lower biostratigraphic limit to turiniid occurrences in the Australian Devonian is not yet established, an age near the Early to Middle Devonian boundary is indicated for the N'Dahla fauna.

Environment and provenance

Both thelodont scales and bone fragments are excellently preserved, although the latter are badly broken. There is little evidence of significant transportation of the material. A

noteworthy feature is the variable colour of the thelodont scales, ranging from very dark grey, to pink, to translucent. This is an unusual feature, possibly indicating multiple provenance.

Marss & Einasto (1978) studied Siluro-Devonian microvertebrate assemblages in the Baltic region of the Russian Platform in relation to other palaeoenvironmental indicators. A high ratio of thelodonts to acanthodians characterised shallow lagoonal or littoral deposits. However, there is as yet no evidence that Australian assemblages show corresponding proportions. Turner & others (1981) interpreted the thelodont fauna from the Cravens Peak Beds in the Georgina Basin as a marine or marginal marine assemblage, on the evidence of the crustacean *Cryptophyllus*. Abundant glauconite in one N'Dahla sample (JG85-005; Amdel, 1985) was probably derived or reworked from the underlying Pacoota (cf. Wells & others, 1967), and other sedimentological evidence from the member suggests a fluvial depositional environment.

The occurrence of reworked limestone clasts of Cambrian age unconformably above Ordovician strata in the N'Dhala section implies an adjacent source which was tectonically active in post-Cambrian time and subject to erosion into both Larapinta and Pertaoorrta Groups during the Early to Middle Devonian. The inferred 'pre-Mereenie' erosional surface illustrated by Wells & others (1970, fig. 35) shows a boundary between the Pacoota Sandstone and the Pertaoorrta Group at least 25 km to the southeast of the N'Dhala Gorge locality.

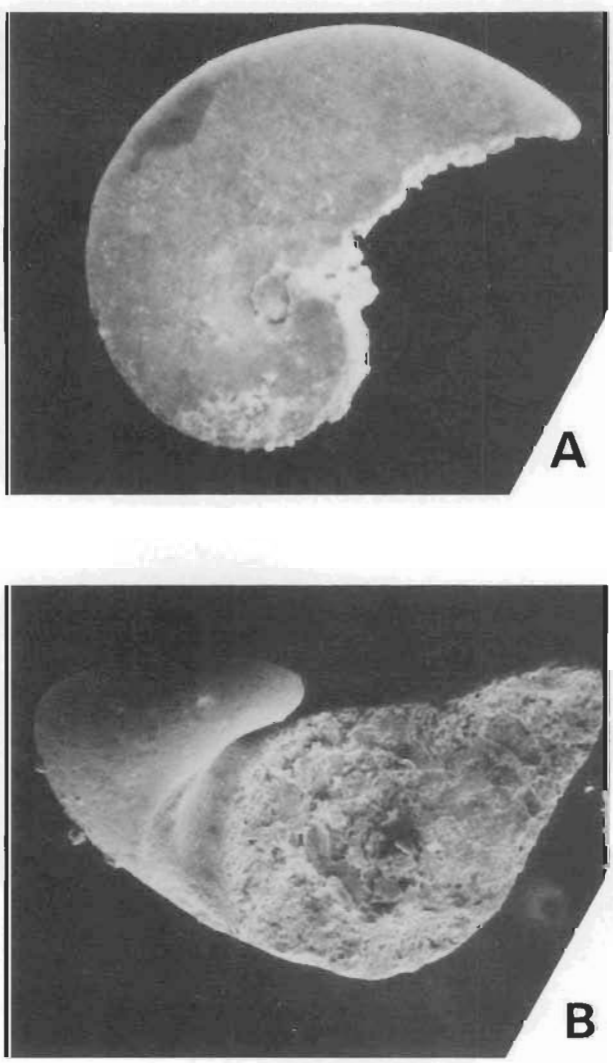

Figure 6. Reworked Cambrian molluscs (*Pelagiella deltoides* Runnegar & Jell 1976) from the N'Dahla Member of the Pertnjara Group, Ross River Syncline, eastern Amadeus Basin.
A — dorsal view (CPC 25781); B — apertural view (CPC 25782). (Both ×50, from sample ND6; specimens deposited in the Commonwealth Palaeontological Collection, Bureau of Mineral Resources, Canberra.)

Discussion

A reinterpretation of the post-Ordovician stratigraphy of the Ross River sequence based on this new Devonian fish fauna has important implications for the interpretation of the depositional history, tectonics, and hydrocarbon potential of the northeastern part of the Amadeus Basin. Many outcrops of Mereenie Sandstone have been mapped in the region, in spite of the difficulties in distinguishing field occurrences in the eastern part of the basin from sandstones of the overlying Pertnjara Group (Wells & others, 1967). The Mereenie has also been widely recognised in the subsurface in petroleum wells (e.g. Schroder & Gorter, 1984, fig. 12), but it now seems likely, at least in the northeastern area, that some correlations based on identification of Mereenie Sandstone may be erroneous, the sandstones so identified belonging instead to the Pertnjara Group. The thickness of the Pertnjara Group is thought to have played a major role in the timing of hydrocarbon generation in the Amadeus Basin (Gorter, 1984; Jackson & others, 1984), so documentation of thickness variation is important. Moreover, thermal maturation levels of Early Palaeozoic source rocks may have been influenced by the amount of sedimentary unloading and reduced depths of burial during the various phases of post-Ordovician tectonism (Gorter, 1984).

The new stratigraphic scheme proposed above excludes the possibility that the lithostratigraphic units recognised are largely diachronous. Thus, we consider it most unlikely that the Mereenie Sandstone, with a thickness in excess of 700 m, can be completely diachronous, such that the top of the formation in the west was deposited at the same time as the base of the formation in the Ross River area. An alternative interpretation is that the base of the Parke Siltstone is diachronous, with the relatively thin sequences of Parke Siltstone containing datable fossils in the west (Cleland Hills), and some 380 km to the east at N'Dhala Gorge, correlating not with the base of the formation in the central northern part of the basin, where it reaches maximum thickness, but somewhere near its top. Evidence against both hypotheses is provided by the fish fauna at Gosses Bluff, which lies approximately midway between the western and eastern fossil localities. According to the first hypothesis, the Gosses Bluff fish fauna should lie in the middle of the Mereenie Sandstone, and according to the second it should lie at the top of the Parke Siltstone or the base of the Hermannsburg Sandstone. Although the sequence at Gosses Bluff is highly disturbed and difficult to interpret, the fish fauna occurs in a red siltstone bed that is apparently resting on immediately underlying sandstones of Mereenie lithology (Young, 1985, p. 242). This lithological association has not been observed elsewhere either at a level within the Mereenie or at a level at the top of the Parke Siltstone or the base of the Hermannsburg Sandstone. We suggest that the Gosses Bluff occurrence is entirely consistent with the interpretation that the basal part of the Parke Siltstone containing the fish fauna in the west and the east is essentially synchronous.

It follows that either the Mereenie Sandstone was never deposited in the Ross River area or, if it was, it was completely eroded before deposition of the N'Dahla Member. Jones (1972) discussed tectonic events identified by earlier workers

that were manifested in the depositional history of the Pertnjara Group. Two separate orogenic events were proposed by Wells & others (1970), before and after deposition of the Mereenie Sandstone. They regarded the Early Palaeozoic Rodingan Movement as an epeirogenic pre-Mereenie uplift of a large part of the Amadeus Basin, including the northeastern portion. The Middle to Late Devonian Pertnjara Movement was defined (Wells & others, 1970, p. 133) as the event that produced unconformity between the Mereenie Sandstone and the Pertnjara Group in the central-northern and northeastern parts of the basin. It was noted that this movement apparently had little effect in the central to southwestern Amadeus Basin, where the Parke Siltstone appears conformable on the Mereenie Sandstone. They suggested the possibility that the unconformity lay above and not beneath the Parke Siltstone.

According to Jones (1972, p. 246), the Pertnjara Movement produced a disconformity between the Mereenie Sandstone and the Pertnjara Group in the northeast, but the stratigraphy as revised above (Fig. 4B) now places the unconformity in the Ross River sequence between the Ordovician Pacoota Sandstone and the Devonian Pertnjara Group. Elsewhere in the basin the Mereenie is clearly seen to thin towards the east along the MacDonnell Ranges, as the erosional surface representing the Pertnjara Movement cuts down through older formations. East of Ellery Creek the Mereenie Sandstone has been completely removed, with Pertnjara Group sediments progressively lying uncomformably on older sediments of the Larapinta and Pertaoorrta Groups. In the Waterhouse Range, the James Ranges, and the Ooraminna Anticline and Camel Flat Syncline to the south and east, the Hermannsburg Sandstone of the Pertnjara Group directly overlies the Mereenie Sandstone.

However, as noted above, where the basal Parke Siltstone of the Pertnjara Group is developed, it is generally conformable on the Mereenie Sandstone (Wells & others, 1970; Jones, 1972). Exceptions to this recorded in the literature are in the Illamurta Springs–Seymour Range area (Ranford & others, 1965, p. 31) and in the Deering Hills (Wells & others, 1965, p.29; Jones, 1972, p.234), but the former may be a local feature and the latter is probably an onlap of basal Parke Siltstone on a Mereenie palaeoslope. Thus, it seems that, if the Mereenie Sandstone was deposited in the Ross River sequence, and was subsequently eroded, the latter erosional event may have been somewhat older than the erosional events that produced the unconformity between the Pertnjara Group and Mereenie Sandstone as recorded elsewhere in the basin. Alternatively, the Mereenie Sandstone may never have been deposited in the Ross River sequence.

A similar depositional and erosional history is recorded in the Georgina Basin sequence, over 200 km to the north, where the basal part of the Dulcie Sandstone in the northwestern Dulcie Syncline, which contains an equivalent fish fauna to that of the N'Dahla Member, lies unconformably on the Tomahawk Beds, which are comparable in fauna, lithology, and age to the Pacoota Sandstone (J. H. Shergold, personal communication). It is therefore of interest that the Ross River sequence is interpreted as part of an allochthonous sheet (the N'Dhala Nappe), with a displacement from the north, recently estimated at between 30 and 60 km (Stewart & Oakes, in press).

To summarise, there is evidence of at least one depositional break in the Palaeozoic sequence of the Ross River syncline (Fig. 4B): an Early Palaeozoic event corresponding to the Rodingan Movement. If the Mereenie Sandstone was ever deposited in the Ross River area, it was removed by another erosional event (Pertnjara Event) older than Parke Siltstone time, and probably not of basin-wide significance. The N'Dahla sequence resembles that of the Georgina Basin to the north, where the same fish fauna occurs unconformably above Early Palaeozoic sediments equivalent to the underlying Pacoota Sandstone of the Ross River sequence.

From the Ross River sequence a palaeomagnetic reading of presumed Devonian age has recently been cited for the Australian craton (e.g. Goleby, 1980; Livermore & others, 1985). This is the 'Ross River overprint', to which an age of 374 Ma has been ascribed, based on Kirschvink's (1978) analysis of palaeomagnetic directions in Late Precambrian to Early Cambrian sediments from the Amadeus Basin. A secondary component in samples from the Ross River area, when corrected for structure, was found to lie between results for the Mereenie Sandstone (Embleton, 1973a) and the Paterson Toscanite (Carboniferous), according to the apparent polar wander curve of Embleton (1973b). Uncertainties about the age of the Mereenie Sandstone magnetisation (interpreted as Silurian or Devonian) have been discussed previously (Young, 1985). In view of the various alternative interpretations placed on palaeomagnetic data for the Middle Palaeozoic of Gondwana (e.g. Schmidt & Morris, 1977; Goleby, 1980; Livermore & others, 1985), a Devonian age for the Ross River overprint is at present unsupported. The status of these data should be clarified when new palaeomagnetic investigations of Devonian strata in the Ross River area are completed (C. Klootwijk, personal communication).

Acknowledgements

We thank J.H. Shergold, A.J. Stewart, and A.T. Wells for reading and commenting on the manuscript, M.M. Smith for commenting on histological sections, and M. Idnurm and C. Klootwijk for advice on palaeomagnetism. C. Steward provided assistance in the field, and R.W. Brown and A.T. Wilson processed samples and photographed the material. The figures were drafted by Janet Kovacs.

References

Blieck, A., & Goujet, D., 1978—A propos de nouveau matériel de Thélodontes (Vertébrés Agnathes) d'Iran et de Thailande: apercu sur la répartition géographique et stratigraphique des Agnathes des 'regions gondwaniennes' au Paléozoique moyen. *Annales de la Société Géologique du Nord*, 97, 363-72.

BMR, 1983—Geology of the Alice Springs Region. 1:100 000 Geological Special Sheet. *Bureau of Mineral Resources, Canberra.*

Cook, P.J., 1971—Illamurta diapiric complex and its position on an important central Australian structural zone. *Bulletin of the American Association of Petroleum Geologists*, 55, 64-79.

Denison, R.H., 1979—Acanthodii. Handbook of Paleoichthyology, Volume 5. H-P. Schultze (Editor) *Gustav Fischer Verlag. Stuttgart, New York.*

Embleton, B.J.J., 1973a—The palaeomagnetism of some Palaeozoic sediments from central Australia. *Journal and Proceedings of the Royal Society of New South Wales*, 105, 86-93.

Embleton, B.J.J., 1973b—The palaeolatitude of Australia through Phanerozoic time. *Journal of the Geological Society of Australia*, 19, 475-482.

Freeman, M.J., 1986—Huckitta, *1:250 000 Geological Map Series, Explanatory Notes, Northern Territory Geological Survey.*

Giffin, E.B., 1980—Devonian vertebrates from Australia. *Postilla*, 180, 1-15.

Gilbert-Tomlinson, J., 1968—A new record of *Bothriolepis* in the Northern Territory of Australia. *Bureau of Mineral Resources, Australia, Bulletin* 80, 191-224.

Goleby, B.R., 1980—Early Palaeozoic palaeomagnetism in southeast Australia. *Journal of Geomagnetism and Geoelectricity*, 32, supplement 3, 11-21.

Goujet, D., Janvier, P., and Suares-Riglos, M., 1984—Devonian vertebrates from South America, *Nature*, 312: 311.

Gorter, J.D., 1984—Source potential of the Horn Valley Siltstone, Amadeus Basin. *APEA Journal*, 24, 66-90.

Gross, W., 1971a—Downtonische und Dittonische acanthodier-reste des ostseegebeites. *Palaeontographica* (A), 136, 1-82.

Gross, W., 1971b—Unter devonische Thelodontier- und Acanthodier-Schuppen aus Westaustralien. *Palaontologischen Zeitschrift*, 45, 97-106.

Gross, W., 1973—Kleinschuppen, Flossenstacheln und Zahne von fischen aus europaischen und Nordamerikanischen Bonebeds des devons. *Palaeontographica* (A), 142, 51-155.

Hodgson, E.A., 1968—Devonian spores from the Pertnjara Formation, Northern Territory. *Bureau of Mineral Resources, Australia, Bulletin* 80, 65-82.

Jackson, K.S., McKirdy, D.M., & Deckelman, J.A., 1984—Hydrocarbon generation in the Amadeus Basin, central Australia. *APEA Journal*, 24, 42-65.

Jones, B.G., 1972—Upper Devonian to Lower Carboniferous stratigraphy of the Pertnjara Group, Amadeus Basin, central Australia. *Journal of the Geological Society of Australia*, 19, 229-249.

Kirschvink, J.L., 1978—The Precambrian-Cambrian boundary problem: paleomagnetic directions from the Amadeus Basin, central Australia. *Earth and Planetary Science Letters*, 40, 91-100.

Laurie, J.R., 1986—Phosphatic fauna of the Early Cambrian Todd River Dolomite, central Australia. *Alcheringa*, 10, 431-454.

Livermore, R.A., Smith, A.G., & Briden, J.C. 1985—Palaeomagnetic constraints on the distribution of continents in the Late Silurian and Early Devonian. *Philosophical Transactions of the Royal Society of London* B309, 29-56.

Marss, T., & Einasto, R. 1978—Distributions of the vertebrates in the sediments of the various facies of the Silurian in northern Baltic countries. *Eesti N.S.V. Teaduste Akadeemia Tounetised Geology* 27, 16-22 (Russian with English abstract).

Ørvig, T. 1969a—The vertebrate fauna of the *primaeva* Beds of the Fraenkelryggen Formation of Vestspitsbergen and its biostratigraphic significance. *Lethaia* 2, 219-39.

Pickett, J., Turner, S., & Myers, B., 1985—The age of oolitic sediments from Tumblong, New South Wales. *Quarterly Notes of the Geological Survey of N.S.W.*, 12-14.

Playford, G., Jones, B.G., & Kemp, E.M., 1976—Palynological evidence for the age of the synorogenic Brewer Conglomerate, Amadeus Basin, central Australia. *Alcheringa*, 1, 235-243.

Poltnig, W., 1984—Fischreste aus dem Unterdevon von Graz (Steiermark). *Mitteilungen naturwissenschaften verein Steiermark*, 114, 107-131.

Ranford, L.C., Cook, P.J., & Wells, A.T. 1965—The geology of the central part of the Amadeus Basin, Northern Territory. *Bureau of Mineral Resources, Australia, Report* 86.

Ritchie, A., & Gilbert-Tomlinson, J., 1977—First Ordovician vertebrates from the Southern Hemisphere. *Alcheringa, 1*, 351-368.

Runnegar, B., & Jell, P.A., 1976—Australian Middle Cambrian molluscs and their bearing on early molluscan evolution. *Alcheringa*, 1, 109-138.

Schmidt, P.W., & Morris, W.A., 1977—An alternative view of the Gondwana Palaeozoic apparent polar wander path. *Canadian Journal of Earth Sciences*, 14, 2674-2678.

Schroder, R.J., & Gorter, J.D., 1984—A review of recent exploration and hydrocarbon potential of the Amadeus Basin, Northern Territory. *APEA Journal* 24, 19-41.

Shergold, J.H., Gorter, J.D., Nicoll, R.S., & Haines, P.W., in prep.—The Pacoota Sandstone, Amadeus Basin, Northern Territory.

Stewart, A.J., & Oakes, R.Q., in press—Nappes in the northeastern Amadeus Basin, Northern Territory. *International conference on deformation of crustal rocks, 2-6 February 1987, Mt Buffalo, Victoria, Abstracts.*

Turner, S., & Dring, R.S., 1981—Late Devonian thelodonts (Agnatha) from the Gneudna Formation, Carnarvon Basin, Western Australia. *Alcheringa*, 5, 39-48.

Turner, S., Jones, P.J., & Draper, J.J., 1981—Early Devonian thelodonts (Agnatha) from the Toko Syncline, western Queensland, and a review of other Australian discoveries. *BMR Journal of Australian Geology & Geophysics*, 6, 51-69.

Turner, S., & Young, G.C. in press—Shark teeth from the Early-Middle Devonian Cravens Peak Beds, Georgina Basin, Queensland. *Alcheringa*.

Vieth-Schreiner, J., 1983—Fisch-schuppen und-Zahne aus der Eifeler Kalkmulden-Zone (Emsium, Eifelium). *Senckenbergiana lethaea*, 64, 129-177.

Wang, S.-T., Dong, Z-Z, & Turner, S., 1986—Discovery of Middle Devonian Turiniidae (Thelodonti:Agnatha) from west Yunnan, China. *Alcheringa*.

Wells, A.T., Forman, D.J., & Ranford, L.C., 1965—The geology of the northwestern part of the Amadeus Basin, Northern Territory. *Bureau of Mineral Resources, Australia, Report* 85.

Wells, A.T., Ranford, L.C., Stewart, A.J., Cook, P.J., & Shaw, R.D., 1967—Geology of the northeastern part of the Amadeus Basin, Northern Territory. *Bureau of Mineral Resources, Australia, Report* 113.

Wells, A.T., Forman, D.J., Ranford, L.C., & Cook, P.J., 1970—Geology of the Amadeus Basin, central Australia. *Bureau of Mineral Resources, Australia, Bulletin* 100.

Wells, J.W., 1944—Fish remains from the Middle Devonian bone beds of the Cincinatti arch region. *Palaeontographica Americana* 3, 99-160.

Young, G.C., 1984—An asterolepidoid antiarch (placoderm fish) from the Early Devonian of the Georgina Basin, central Australia. *Alcheringa*, 8, 65-80.

Young, G.C., 1985—New discoveries of Devonian vertebrates from the Amadeus Basin, central Australia. *BMR Journal of Australian Geology & Geophysics*, 9, 239-254.

Young, G.C., & Gorter, J.D., 1981—A new fish fauna of Middle Devonian age from the Taemas/Wee Jasper region of New South Wales. *Bureau of Mineral Resources, Australia, Bulletin* 209, 83-147.

BMR Journal of Australian Geology & Geophysics, 10, 243-251

McArthur Basin, Northern Territory: mapping of deep troughs using gravity and magnetic anomalies

K.A. Plumb[1] & P. Wellman[2]

Published models for the Proterozoic McArthur Basin show up to 4 km of sedimentary cover over widespread shelves, and a 50–80 km wide by 600 km long, central meridional half-graben, the Batten Trough, in which up to 10 km of cover is preserved. This model is supported and extended herein by basin-wide interpretation of gravity and magnetic anomalies. The margins of the area of thick cover correlate with steep gravity and/or magnetic anomaly gradients. The dominant rock types in this cover are identified from their combined gravity and magnetic signatures. Estimates of depth to magnetic basement are combined with geological constraints to map the basement configuration throughout the basin. The predicted form of the Batten Trough is essentially confirmed, and concealed extensions outlined beneath the Gulf of Carpentaria. However, it is now shown that this trough is separated into two distinct structures by the Urapunga Tectonic Ridge, and it is now redefined as the Batten Trough (south only) and Walker Trough (north). The concealed Beetaloo Sub-basin of thick Roper Group, in the southwest, and possible adjacent troughs of 'McArthur Group' carbonates, represent the subsurface link between the McArthur Basin and Tomkinson Creek beds. An east-west extension model, related to block rotation and accommodation by northwest transfer faults, is invoked to explain the evolution of the several rifts in the basin. Later deformation has modified these structures and reversed many of the earlier displacements.

Introduction

The present geological model of the Proterozoic McArthur Basin of northern Australia proposes the existence of a north-trending synsedimentary half-graben, the 'Batten Trough', bounded by thinner sedimentary sections on stable shelves on either side (Plumb & others, 1980). This model is critical to conceptual models for exploration for McArthur-type mineral deposits. The large McArthur River lead-zinc deposit and minor deposits of other base metals are located next to (Figs. 2, 9), and are genetically related to, bounding faults of this graben (Plumb & Derrick, 1975; Walker & others, 1977; Williams, 1978). The basin is also prospective for oil, despite its great age, with the recent discovery of live oil in BMR Urapunga 4 (BMR, 1985; Jackson & others, 1986).

The deep structures can only be inferred with confidence from surface geology in limited areas of good exposure, where the stratigraphic section is exposed by suitable structure. Elsewhere, the deep structure is obscured by Palaeozoic and Mesozoic cover or because the exposed formations are extensive and flat-lying. Deep structures have been determined by geophysics only along adjacent seismic-refraction, magnetotelluric, and gravity traverses across the southern part of the basin, and these essentially confirmed the geological model of Plumb & others (1980) along the line of section.

This study interprets regional gravity and magnetic anomalies together, to provide information on the regional structure, sediment thickness, and rock types throughout most of the McArthur Basin. The study utilises a different approach, in the resolution of a somewhat different problem, to the earlier studies of the adjacent Georgina Basin (Tucker & others, 1979) and Pine Creek Geosyncline (Tucker & others, 1980).

Previous studies

Geology

The McArthur Basin is a large (170 000 km^2) basin of mild to moderately deformed mid-Proterozoic (Carpentarian; 1700–1400 Ma) sediments in the northeast of the Northern Territory (Fig. 1). Its geology has been summarised by Plumb & Derrick (1975), Plumb (1977), Plumb & others (1980), and Jackson & others (1987). The basin sediments were deposited in predominantly shallow water environments — shallow-marine to supratidal, lacustrine, and fluviatile. Therefore, for a long period, sediment supply exceeded or kept pace with subsidence. Formations are uniform over large areas. The maximum accumulative sediment thickness is about 12 km.

The sequence is now divided into four main intervals separated by regional unconformities (Jackson & others, 1987), and regional correlations have been significantly revised by Plumb (1985, Fig. 7; cf. Plumb & Derrick, 1975, Fig. 6; Plumb & others, 1980, Fig. 8). Starting with the oldest, the intervals are: (1) the Tawallah and Parsons Range Groups and their equivalents — quartz-rich arenites and subordinate basic volcanics, carbonates, and lutites, locally up to 6 km thick, but more generally about 3–4 km; (2) the McArthur Group, comprising mainly carbonates up to about 3 km thick, and now correlated with the quartz-rich arenites, basalts, and carbonates of the Katherine River Group in western Arnhem Land; (3) the overlying carbonates of the Nathan and Mount Rigg Groups, which are up to 1.7 km thick and were previously included within the McArthur Group; (4) the Roper Group and its equivalents, which are mainly quartz sandstones and micaceous lutites, and range up to 5 km thick.

In the following geophysical discussion the McArthur and Nathan Groups will generally be described together as 'McArthur Group', because they are not distinguishable geophysically.

The geological syntheses outlined a central north-trending syndepositional graben, 50–80 km wide and 600 km long, the 'Batten Trough', in which about 10 km and, locally, up to 12 km of sediments accumulated. Only about 3 km accumulated over most of the stable shelves to either side.

In the better known southern part of the basin the Tawallah Group maintains a similar 3–4.5 km thickness in both the Batten Trough and on the adjoining shelves. Here, the Batten Trough is seen only from the local deposition of up to 5 km of McArthur and Nathan Groups and very thin equivalents on the shelves to either side. In the north the history was different. There, the Parsons Range Group (4–6 km) was deposited only in the central trough. Differential thickening continued with deposition of 5 km of 'McArthur Group' in the trough, compared with less than 3 km of the equivalent Katherine River and Mount Rigg Groups on the Arnhem Shelf. Later in this paper, this northern part of the trough will be redefined on the basis of new geophysical interpretations as the Walker Trough, and the Batten Trough retained for the southern 'type' area only (Fig. 2).

Post-depositional uplift along the various major faults then uplifted much of the central part of the graben into a 'horst'. A totally different depositional pattern was then shown by

[1]Division of Continental Geology, Bureau of Mineral Resources, GPO Box 378, Canberra, ACT 2601
[2]Division of Geophysics, BMR.

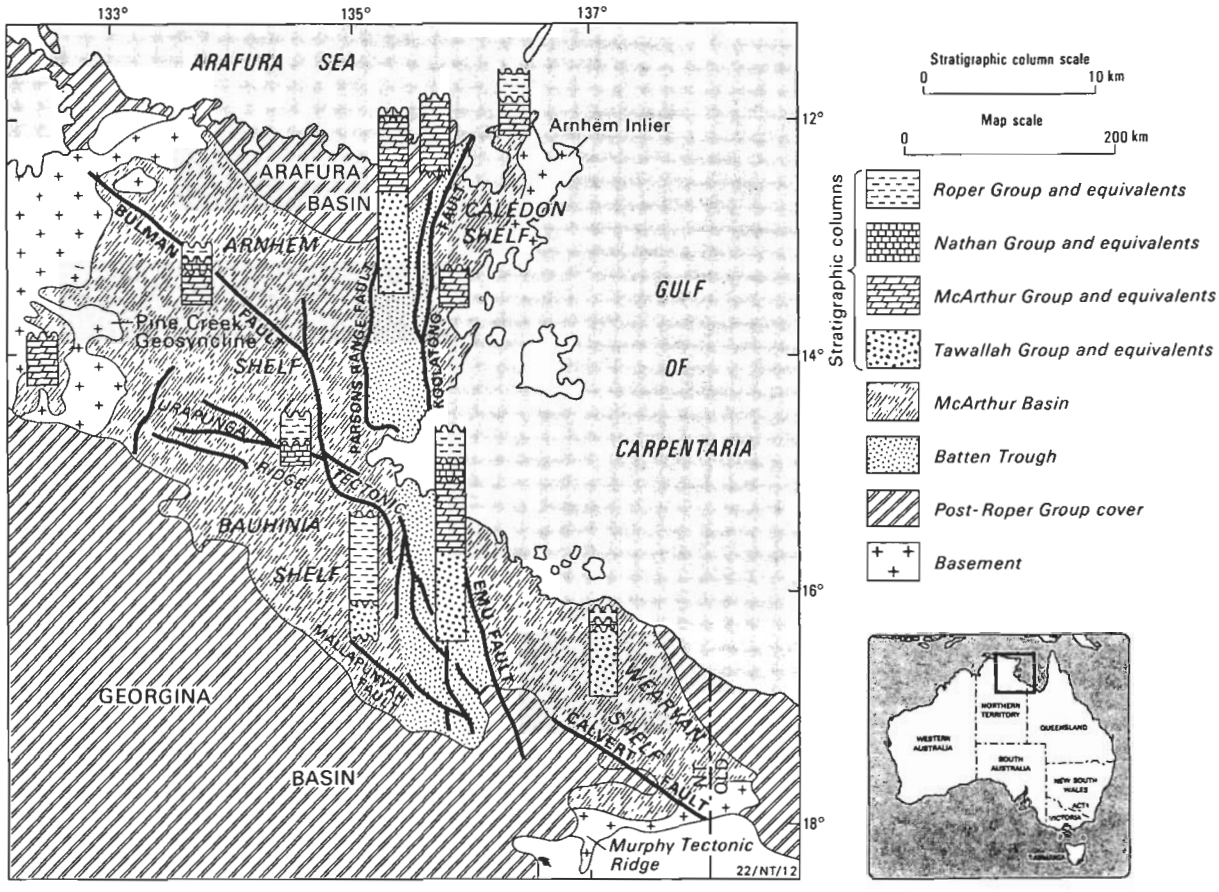

Figure 1. Major tectonic elements of the McArthur Basin, and sediment thickness variation from geological mapping. From Plumb & Derrick, 1975.

the Roper Group. This group thickens gradually to the southwest, from less than 1 km in Arnhem Land to about 5 km to the southwest of the Bauhinia Shelf; this thick sequence of Roper Group now occupies the Beetaloo Sub-basin (Fig. 2).

Basic volcanics are ubiquitous in the Tawallah Group throughout the southern part of the McArthur Basin, but they are thickest on the Wearyan Shelf rather than in the Batten Trough. They are also widespread in the Katherine River Group on the Arnhem Shelf, and occur locally in the Nathan Group at Roper River. However, basic lavas are totally unknown from the sequence in the Walker Trough, in either the Parsons Range or McArthur Groups. Abundant dolerite sills intrude the Roper and Mount Rigg Groups on the Arnhem and Bauhinia Shelves, and also their equivalents on the northern Caledon Shelf. Tucker & Boyd (in press), using aeromagnetic anomalies, show that elongate widely spaced dykes extend over much of the McArthur Basin, but none of these have been identified in outcrop.

Seismic refraction and magnetotelluric profiles

During 1978 and 1979, seismic refraction and magnetotelluric observations were recorded along two adjacent, but only partly coincidental, traverses across the southern part of the basin; approximately along 16°15'S. Figure 3 shows that the structure inferred from the seismic refraction and gravity (Fig. 3a, b) (Collins, 1983) is generally consistent with the interpretation of the magnetotelluric measurements (Cull, 1982) (Fig. 3c).

A major gravity low over the southwestern Bauhinia Shelf was shown by both seismic and magnetotelluric results to overlie the Beetaloo Sub-basin: 4 km of Roper Group overlying Tawallah Group, according to seismic refraction; 5 km of Roper Group overlying 5 km of Tawallah Group, according to the magnetotelluric modelling. This is consistent with the nearest available outcrops to the east, which show that the Roper Group thickens to its maximum of about 5 km in this area; the 'McArthur Group' wedges out westwards, and the Tawallah Group apparently maintains its normal thickness. Gravity modelling shows that the whole of the gravity anomaly can be modelled in terms of the density contrast between the low-density Roper Group and the underlying Tawallah Group, and this agrees with the apparent low density contrast shown between Tawallah Group and basement on the Wearyan Shelf farther east.

At the eastern edge of the Batten Trough, the magnetotelluric modelling indicated about 5 km of 'McArthur Group' carbonates overlying about 5 km of Tawallah Group, in agreement with the geological expectation from stratigraphy. Seismic refraction did not penetrate the thick carbonates of the Batten Trough, and so was unable to yield data on the deep structure beneath this important zone.

Beneath the Wearyan Shelf, seismic refraction indicates 3.5 km of sediment, mainly Tawallah Group. Magnetotelluric modelling gives a total thickness of 4–5 km; mainly of Tawallah Group, but with a wedge at the western margin of 0.5 km of Roper Group and, locally, up to 2 km of 'McArthur Group'. These thicknesses are again in agreement with geological expectations of around 3–4 km of section on the

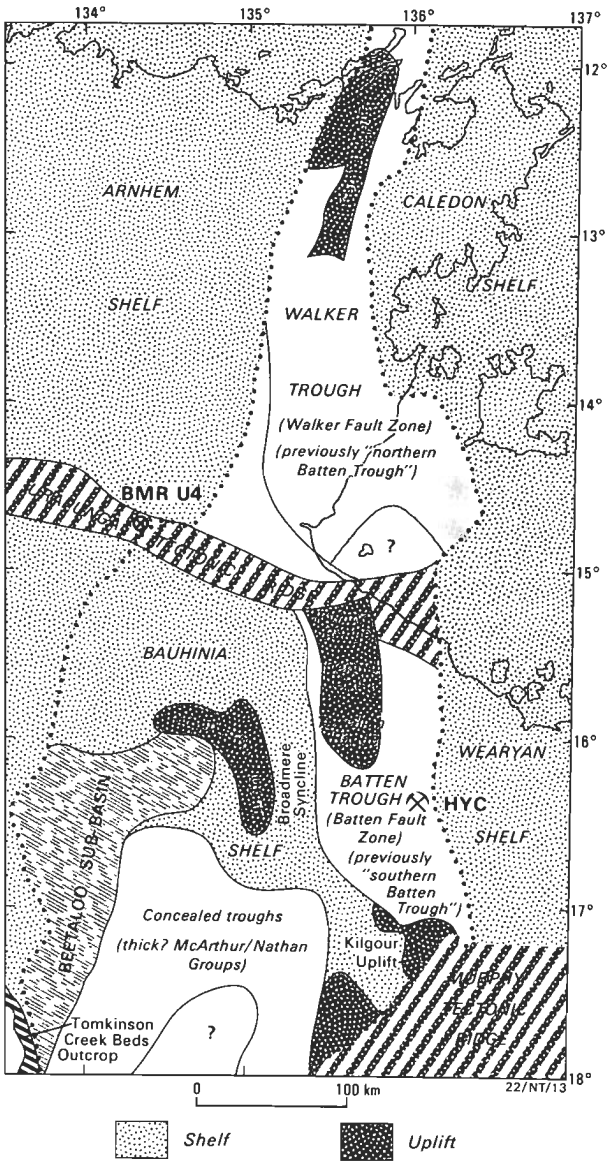

Figure 2. Principal tectonic elements of McArthur Basin as outlined by this study.

shelf, and the magnetotelluric model confirms the expectation of a sudden decrease in thickness of 'McArthur Group' carbonates across the eastern margin (Emu Fault) of the Batten Trough.

This study

Magnetic survey

An aeromagnetic survey of the whole McArthur Basin, by the Bureau of Mineral Resources during 1977 and 1978, recorded total magnetic intensity at 3 km line spacing from an altitude 150 m above ground level. Flight lines were oriented east-west, to intersect the north-trending structures of the Batten Trough, for all the area except Calvert Hills 1:250 000 Sheet area, within which flight lines were north-south. Figure 4 gives the magnetic anomalies with a contour interval of 25 nT, so that the minor anomalies are suppressed.

Major trends are west-northwest and north-northeast. This agrees with the dominance of northwest structural trends throughout the North Australian Craton (Plumb, 1979). Many of the major anomalies have a wavelength of about 100 km.

Gravity anomalies

Over most of the McArthur Basin the gravity anomalies are known only from an 11 km grid of helicopter gravity stations (Flavelle, 1965; Whitworth, 1970). In the south some semi-detailed traverses were observed; mainly along the traverses used for the seismic refraction and magnetotelluric surveys (Anfiloff, 1981).

The Bouguer anomaly map (Fig. 5) has low amplitude anomalies, and there is a regional gravity gradient with more positive anomalies on the northern half of the map. Most of the geologically important aspects of the Bouguer anomaly map have been emphasised by preparing a map of the second vertical derivative of the Bouguer anomaly (Fig. 6), using the method of Henderson (1960). This gives the sum of the second vertical derivatives of the two horizontal directions, and is essentially a residual map. It eliminates regional gradients, and emphasises local gradients.

Boundary of thick sedimentation

Where there is an abrupt change in the thickness of cover rocks, there is a major horizontal difference in rock type at depth that should be accompanied by a horizontal change in density or magnetic properties. These changes should produce steep gradients on the gravity and/or magnetic maps, and the position of the gradients should allow the extent of the deeper cover to be mapped. Figure 7 shows the boundary around the area of thick preserved sediments, inferred from the gravity gradient (Fig. 6), the gradient and trends of the magnetics (Fig. 4), and the pattern of sediment thickness determined later. The method used to determine the local position of the boundary is indicated by letters next to the boundary.

In general, the margins of the Batten-Walker Troughs are best located using gravity gradients (Fig. 6). The western extent of thick sediments across the Bauhinia Shelf is located by a combination of the termination of the east-west magnetic anomalies (Fig. 4) and gravity gradients (Fig. 6). These areas of thick sediment represent the accumulative thickness of several distinct intervals of sedimentation, and so additional geological constraints are required to define the position of the actual syndepositional grabens or troughs as such.

Geographic extent of rock types

The gravity and magnetic anomalies reflect changes in the sum of physical properties of all the thick rock-bodies that underlie them, but are most influenced by near-surface bodies. Figure 7 divides the area into blocks of distinctive combinations of high or low gravity residuals with high or low magnetic anomalies, and interprets them in terms of the dominant rock types causing these anomalies. Continuous patterns show areas where the outcropping rock association is known to be thick and corresponds to an area of uniform gravity and/or magnetic anomaly; discontinuous patterns show the inferred extension of these associations beneath younger cover. The types of anomalies associated with the association are as follows (less important features are bracketed).

a) Roper Group: gravity residual low, (magnetic anomaly low near base of section, and high near top of sections with abundant dolerite).

b) 'McArthur Group': gravity residual high, (magnetic anomaly generally low).

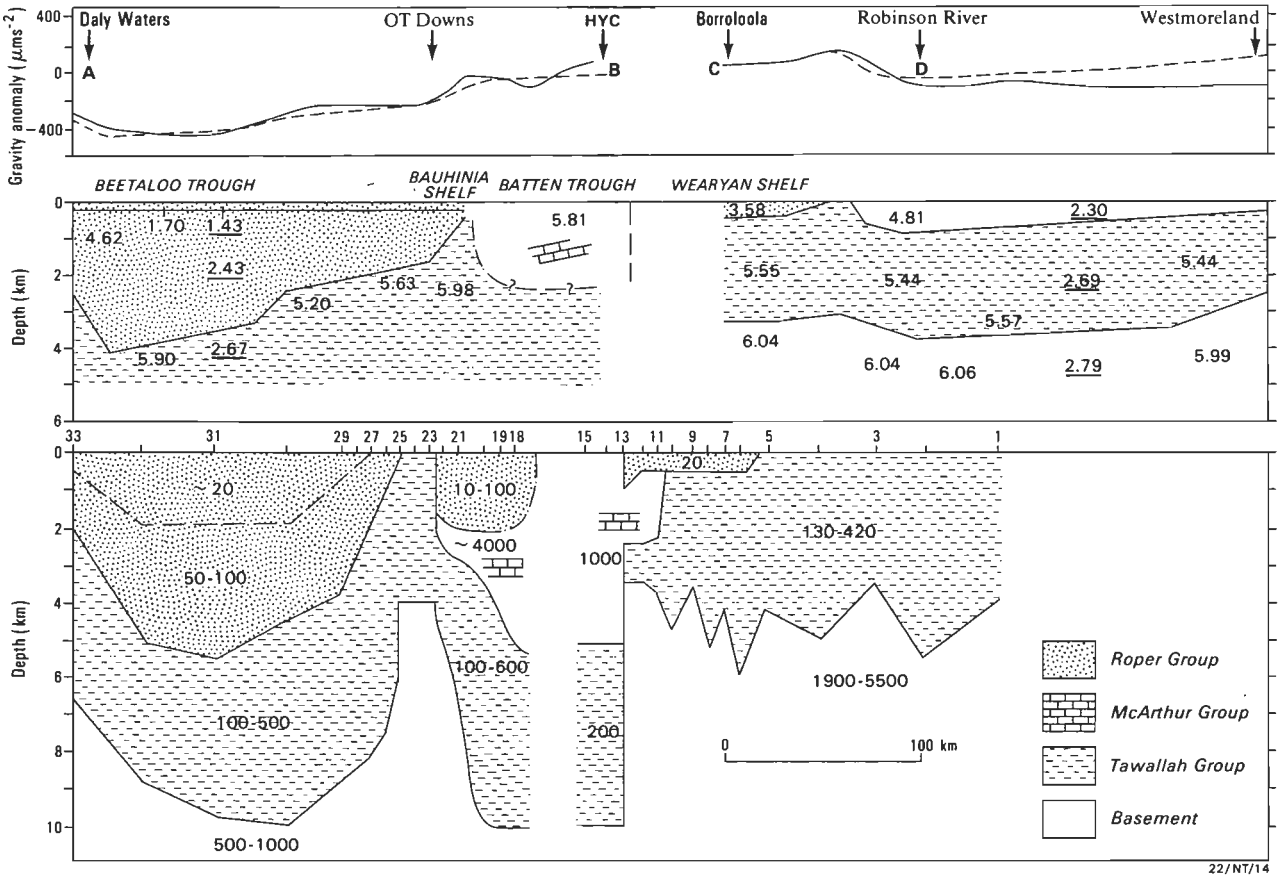

Figure 3. Interpretation of seismic refraction and magnetotelluric traverses along 16.5°S.
(a — upper diagram) observed and calculated Bouguer gravity anomalies, (b — middle diagram) seismic refraction model and geological interpretation. Values not underlined give apparent seismic velocity, values underlined give the density used in the calculated gravity anomaly profile (c — lower diagram) magnetotelluric interpretation with resistivity values in ohm.m. Location of sections a and b shown in Figure 5, a & b after Collins, 1983; c after Cull, 1982.

c) Tawallah Group: gravity residual low, (magnetic anomaly high because of volcanics, except Parsons Range Group with no volcanics is low).

d) Basement beneath the Batten Trough: gravity residual high in north, inferred to be high in south.

e) Arnhem Shelf high-level granites: gravity residual low.

f) Caledon Shelf granites, inferred to be similar to Arnhem Shelf granites.

These gravity anomaly relations are consistent with the expected density of the rocks, relative to average basement: the dolomites of the 'McArthur Group' are of relatively high density; the Roper Group rocks and high level granites are of relatively low density; and the more lithified Tawallah Group is only slightly lower density than the basement.

In Figure 7 the areas of most rock associations are known outcrops and their immediately adjoining extensions; e.g. the gravity highs over thick 'McArthur Group' in the Batten-Walker Troughs. Unidentified lows within the Batten-Walker Troughs overlie major fault zones, with only dense carbonates evident at the surface. The unpatterned area of the southeastern Walker Trough lacks gravity coverage to determine rock type. The unpatterned area of the northwest Bauhinia Shelf overlies northwest-trending magnetic ridges and complex near-zero gravity. Minor gravity lows can be correlated with synclines in thin (mostly less than 2 km) Roper Group cover; the over-all slightly positive gravity and thick sequence (up to 7 km; Fig. 8) suggest a moderate 'McArthur Group' overlying Tawallah Group beneath this cover.

The principal new data in Figure 7 come from the concealed areas in the southwest. Thick Roper Group (5 km) in the Beetaloo Sub-Basin is clearly outlined by the Bouguer anomaly (Fig. 5) forming the Dunmara Regional Gravity Low. Northeast linear gravity ridges over the poorly defined thick sequence to the southeast of the Beetaloo Sub-basin suggest thick 'McArthur Group' equivalents. Gravity lows in this area could be either Tawallah or Roper Group, except along the southeast margin, where combined gravity lows/magnetic highs indicate Tawallah Group uplifts at the western end of the Murphy Tectonic Ridge.

Sediment thickness from magnetic anomalies

One of the main objects of this study was to independently map the variation in thickness of the preserved McArthur Basin sediments, by estimating depths to magnetic basement. However, lavas, sills and dykes occur both within the sedimentary section over most of the McArthur Basin, and in the basement. Therefore, calculated depths to the source of the magnetic anomalies can give depths that reflect 1) levels of the land surface; 2) the top of magnetic bodies within the sedimentary column; 3) the top of the basement; or 4) the top of magnetic bodies totally enclosed within basement. Consequently, for much of the area, short-wavelength magnetic anomalies that reflect near-surface bodies within the basin sequence have been ignored, and simple and 'robust' methods of depth estimation have been used to obtain depth

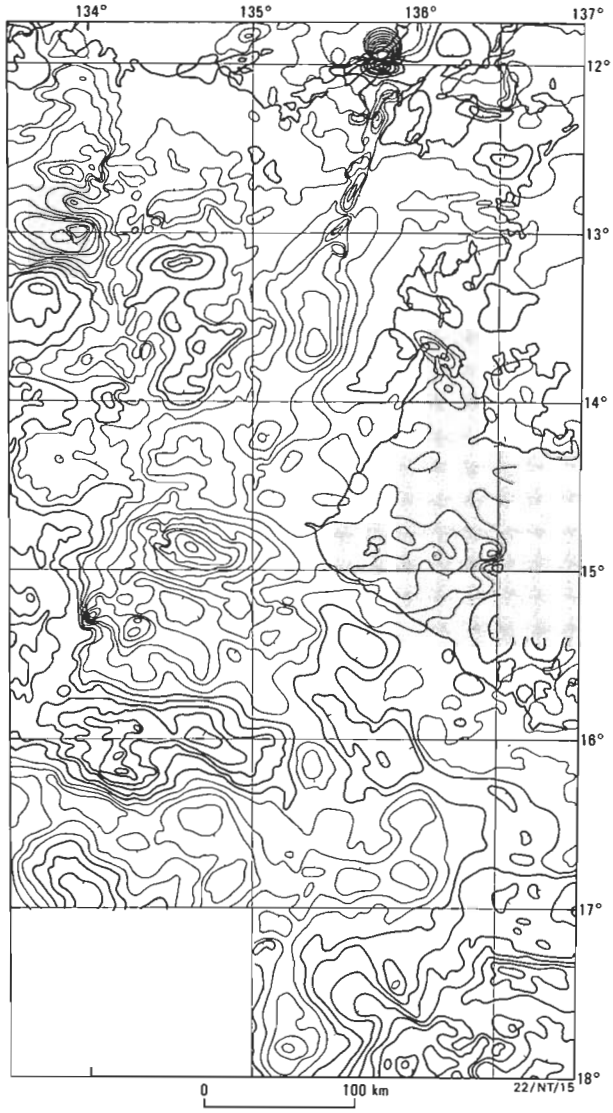

Figure 4. Aeromagnetic total magnetic intensity contour map.
Contour interval 25 nT. Negative contour lines are thick; zero and positive contour lines are thin.

estimates of the deeper bodies. These estimates have been further filtered by the use of all available geological constraints from adjacent outcrop data.

Four sets of estimates of the depth to the top of magnetic bodies have been used:

1) Depth equals 0.8 times the horizontal extent of the maximum anomaly slope, using the steepest of the linear gradients on the magnetic anomaly map (Vacquier & others, 1951);
2) Depth equals 0.7 times the width at one-half maximum amplitude, using isolated anomalies on the magnetic anomaly map (Henderson & Zeitz, 1948);
3) In areas of no short wavelength anomaly, the east-west flight line profiles are like sine waves, and the depth is taken to be one-quarter the wavelength. This is a modification of the one-half maximum width method of Henderson & Zeitz (1948);
4) Depth estimates were also used from an unpublished 1981 magnetic interpretation by I. Zadoroznyj (BMR plan 22/NT/3), which uses an iterative magnetic inversion program to fit models to the observed east-west profiles.

In areas where shallow magnetic sources dominate, the depth estimates were based on the estimates of Methods 1, 2, and 4. In areas of no shallow magnetic sources and no isolated anomalies the estimates were based on Method 3.

Figure 8 shows selected estimates of the thickness of sediments now preserved in the McArthur Basin after uplift and erosion, as inferred from depth to magnetic basement and geology. Depths were selected on the basis of consistency between magnetic anomalies, consistency between magnetic anomalies and geological constraints, or from geology alone. The depths so determined are in general agreement with those anticipated from the geological model, and with the seismic refraction and magnetotelluric models (Fig. 3).

For example, widespread shallow anomalies can be correlated with geologically constrained volcanics in the Tawallah Group; in these areas either only the deeper sources derived using Method 3 are used or the depths of shallow sources are corrected by adding appropriate stratigraphic thicknesses to the depths. Most of the direct magnetic depth estimates used in Figure 8 are based on Method 3, but these estimates

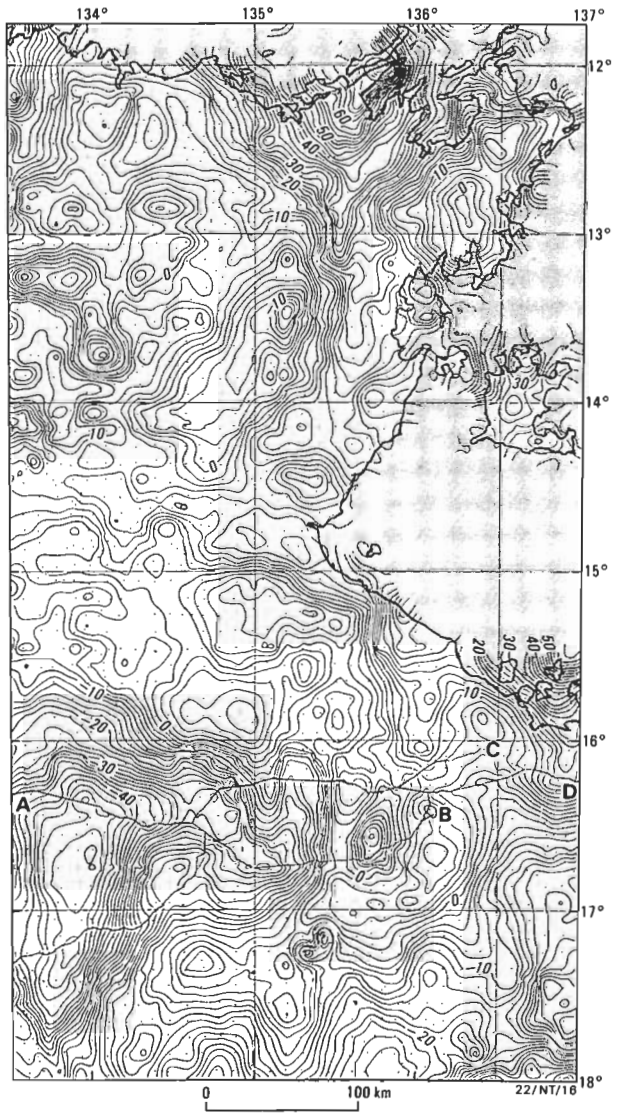

Figure 5. Bouguer gravity anomalies.
Contour interval 20 μm.s^{-2} for thin lines, 100 μm.s^{-2} for thick lines, grid 1.5 minutes, gravity station positions shown as dots. A-B, C-D shows location of sections in Figure 3 a, b.

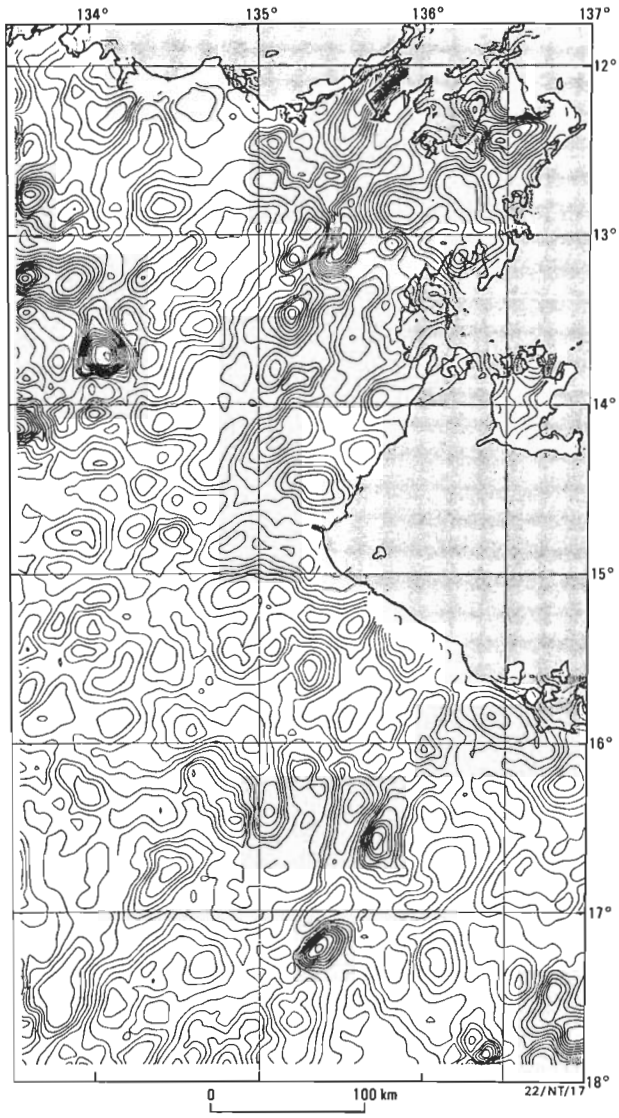

Figure 6. Second vertical derivative gravity anomaly map.
Contour interval 50 $\mu m.s^{-2}$. $(11\ km)^{-2}$, negative contours are thick, zero and positive contours are thin. Grid 3 minutes, unit grid interval for averaging circle is 11 km.

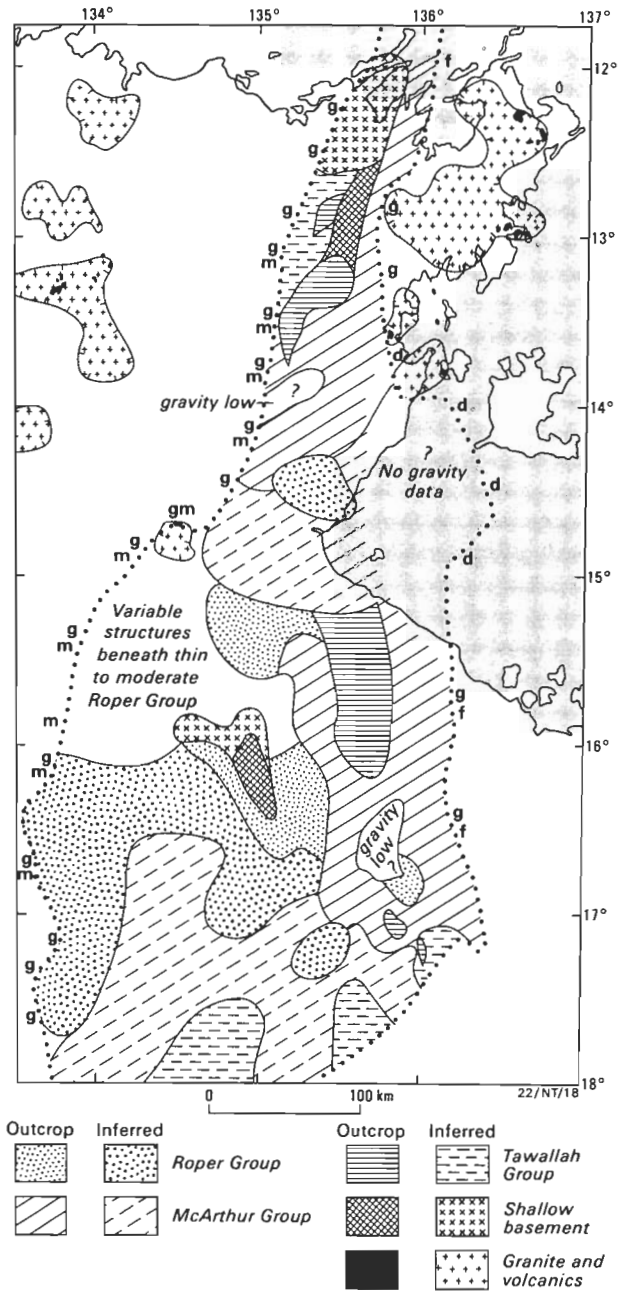

Figure 7. Areas of thick preserved sediment in the McArthur Basin and their geophysically dominant rock associations.
Thick line is the outer boundary of thick sediments. Letters at boundary give the method of locating the boundary — g, gravity gradient; m, magnetic gradient; d, inferred sediment thickness of Figure 4; f, geologically mapped fault. Pattern gives dominant rock association for areas, a continuous pattern if based on outcrop, and a discontinuous pattern if inferred from gravity and magnetics.

have been used with caution where the half wavelength of the anomaly approaches the width of known fault blocks (30–40 km).

Shallow sources predominate on the Arnhem, Caledon, and Wearyan Shelves, and a sedimentary thickness of less than 3 km is inferred, in general agreement with geology. On the Wearyan Shelf this thickness of 3 km or less agrees better with the 3.5 km average thickness inferred from the seismic refraction and geology than with the 4–5 km inferred from magnetotellurics.

A scatter of shallow magnetic sources, generally less than 5 km and commonly less than the basement depth inferred from well-constrained geological structure, dominates the structurally complex southern (Batten) trough. Locally, these can be directly attributed to Tawallah Group volcanics, but the pattern is too complex to contour over much of the area. Contours are, therefore, derived from magnetics and geology combined or from geology alone.

Volcanics do not occur in the basin sequence of the northern (Walker) trough. Here, inferred depths to magnetic sources in areas of good control agree with the geologically inferred depth to basement; for example the maximum depth to magnetic basement (> 10 km) corresponds to the area where structure and stratigraphy together indicate a similar depth. The southern extension of deep magnetic basement defines a new, totally geophysically controlled area of thick sediment (up to about 9 km thick), and now covered almost entirely by sea and coastal deposits of the Gulf of Carpentaria.

The northern (Walker) trough is sharply terminated to the south and separated from southern (Batten) trough by a narrow ridge — the concealed extension of the Urapunga Tectonic Ridge. This extension has a somewhat more

southeasterly trend than predicted by Plumb & Derrick (1975) and passes through the Central Uplift in the Yiyintyi Range area.

It had previously been shown from stratigraphy (Plumb & others, 1980) that these troughs to the north and south of the Urapunga Tectonic Ridge, now demonstrated herein to be structurally separate features, also have distinctive subsidence histories. They are, therefore, now given separate names: the northern trough is here named the Walker Trough (from the Walker River of eastern Arnhem Land), and the old name, Batten Trough, (from Batten Creek in the McArthur region) is restricted to the originally identified trough to the south (Fig. 2).

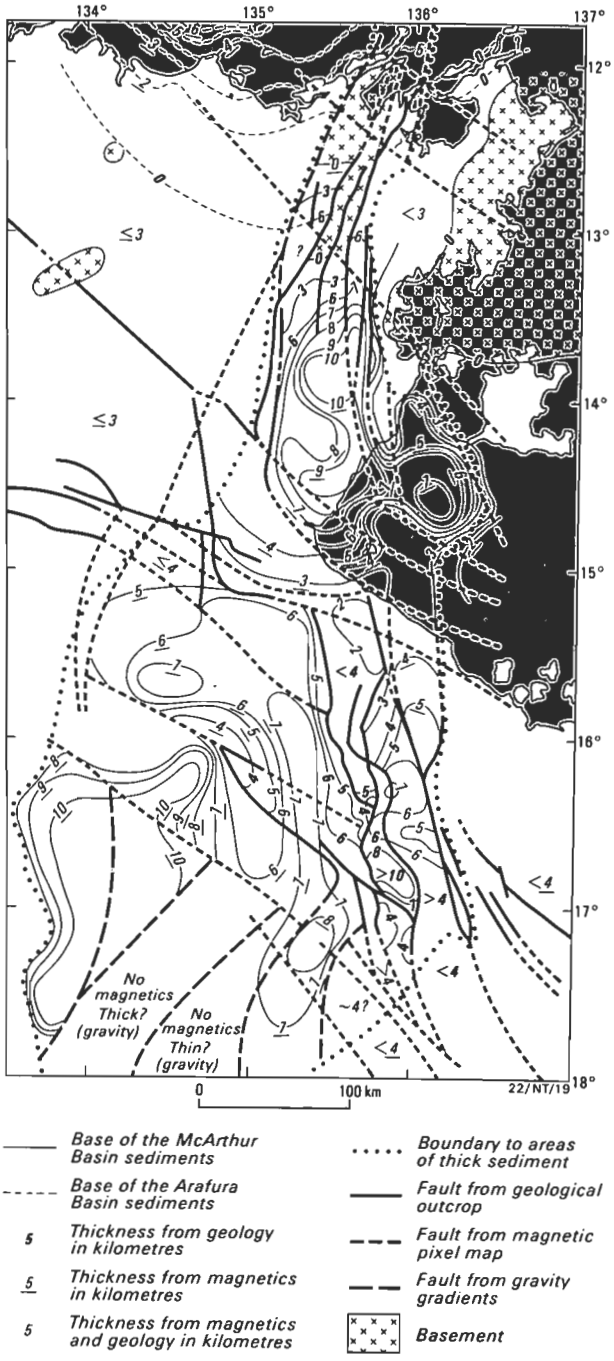

Figure 8. Inferred thickness of sediment in the McArthur Basin from magnetic anomalies and geology.

Inferred depths to magnetic sources beneath the eastern Bauhinia Shelf are consistent with the geological and magnetotelluric expression of the Broadmere Syncline. Thick, concealed pre-Roper Group sediments are inferred geologically for the first time to the northwest of the Tanumbirini Uplift, but cannot be characterised by their gravity/magnetic signatures (Figs. 4, 6). Inferred depths to magnetic sources to the southwest outline the concealed Beetaloo Sub-basin, in good agreement with the original magnetotelluric and seismic refraction expression. Further deep magnetic sources to the southeast of this sub-basin, also totally concealed beneath the Cambrian Georgina Basin, represent a link between the McArthur Basin and the sub-surface extension of Tomkinson Creek beds outlined by Tucker & others (1979) (Fig. 2). However, the sparse data and ill-defined pattern, and the probability of fault-controlled anomalies, preclude effective contouring over most of this area.

Principal structural trends change sharply across the Mallapunyah Fault, between the Tanumbirini and Kilgour Uplifts (Figs. 2, 7). Stratigraphic evidence shows that this zone was a depositional high, during at least part of the depositional history of the basin. This line is, therefore, interpreted as a ridge defining the southern boundary of the Batten Trough (c.f. Plumb & Derrick, 1975), and marks its boundary with the new concealed northeast-trending troughs to the southwest (Fig. 2).

In the north of the area, the post-McArthur Basin Arafura Basin is inferred to be up to 6 km deep offshore, in agreement with previous maps of depth to magnetic basement (Shell Development, 1965).

Tectonic evolution

A major problem in understanding the origin of the McArthur Basin is determining the cause of the greater than 10 km local subsidence and 3 km of regional subsidence. The presence of fault-bounded troughs of thick sediments and adjacent shelves of thin sediments makes it very unlikely that the subsidence was caused by overthrusting. Thermal cooling without rifting is also unlikely, because it would give a 'saucer'-shaped basin with no central linear trough. The cause is more likely to be crustal extension causing rifting, followed by a thermal recovery phase.

Plumb & others (1980) postulated a pattern of strike-slip displacements and accompanying block uplifts, along pre-existing basement fractures, to explain the structural evolution of the basin. From the data then available, it was not possible to differentiate whether the primary strike-slip movements occurred along the northerly trending faults that bound the grabens, or along the northwesterly trending faults now identified as related to the transverse ridges, or equally along both.

The zone of rifts in the McArthur Basin (Figs. 8, 9) shows an irregular widening southwards from 50 km wide at the northern end of the Walker Trough, at 12°N, to about 270 km wide in the south, at about 17°N. Within this broad zone, several distinct northerly trending troughs and rifts are truncated and separated by northwesterly trending transverse ridges and major fault zones (Fig. 9). The boundaries to this zone of rifts, and of the constituent rifts themselves, are all

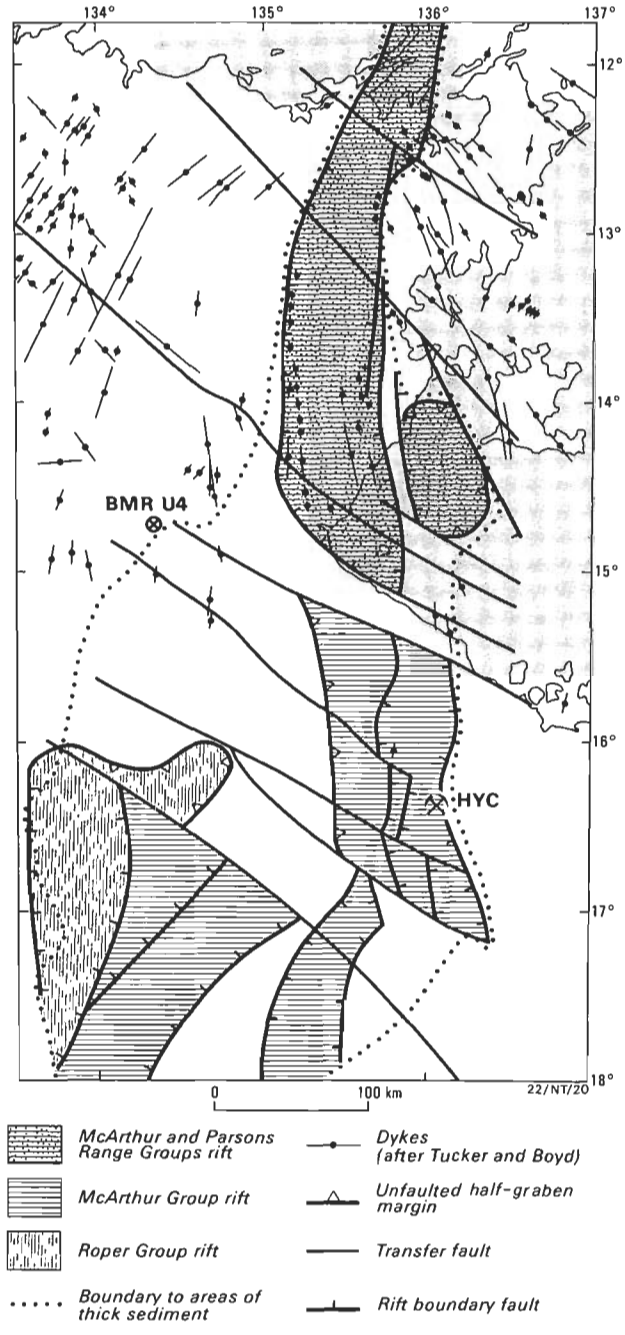

Figure 9. McArthur Basin tectonic model.

approximately radial about a pole near 11°N and 137°E. Dykes mapped by Tucker & Boyd (in press), using aeromagnetic anomalies, are radial about the same pole (Fig. 9). These dykes are probably mostly of Roper Group age or immediately afterwards, but it is not known which dykes are cogenetic. This radial pattern may be explained if the subsidence and dyke emplacement were all related to extension during a net relative counter-clockwise rotation of the block forming the Caledon and Wearyan Shelves away from the Arnhem and Bauhinia Shelves, about a pole of rotation near 11°N and 137°E.

Implicit in this model is accommodation of the differences in position and movement between the different rifts by strike-slip transfer faults (Gibbs, 1984), defined by the transverse ridges and fault zones just described. The fundamental role of these faults (cf. Plumb & others, 1980) reflects the dominance of northwest-trending faults throughout north Australia (Plumb, 1979).

The various rifts and troughs were initiated at different times and have subsided at different rates, and so this somewhat simple model requires the intermittent operation of rotational extension over a period of more than 200 Ma (Plumb, 1985); however, most rifts subsided during the relatively brief interval of 'McArthur Group' deposition, about 1600 Ma ago (Fig. 7). The pattern of strike slip displacements that Plumb & others (1980) observed on both the northwest and the northerly trending faults reflects only the latest movements; in fact, it is mostly post-Roper Group in age. These later displacements may well reverse those of the earlier extensional regime, because a subsequent compressive or shortening component is indicated by reverse faulting and folding and by the geometry of the interrelated strike-slip faults, and this has probably steepened the original tensional faults.

A prominent feature now of the Batten-Walker Troughs is elongate areas of uplifted basement and Tawallah–Parsons Range Groups near the trough axes. Similar uplifts are also inferred in the newly discovered troughs to the southwest. It can be shown by stratigraphy that, during Tawallah Group time, these axial uplifted areas had subsided at the same rate as the adjacent parts of the Batten-Walker Trough; indeed it is only in uplifts that the older section is exposed. Most of the uplift must post-date deposition of the Roper Group, but there are some indications that local positive areas were rising during 'McArthur Group' time as well. These uplifts could reflect isostatic release of stresses required to maintain wide grabens. A simpler and preferred alternative involves their initiation as tilt blocks during extension (e.g. Etheridge & others, 1984) and their accentuation during the subsequent compressive/shortening phase.

Within the present McArthur Basin we envisage around 6 km of preserved sediment overlying crust that was thinned during the rifting process and, on the adjacent shelves, sediment with an average thickness of about 3 km on crust that was not thinned by rifting. The present crust has similar sediment loading throughout, so, if the mean crustal densities are similar, because of isostasy the present crustal thicknesses should be similar. Collins (1983) presented deep crustal reflection and refraction results for both the rifted area (from Beetaloo Sub-basin to Batten Trough) and the adjacent unrifted Wearyan Shelf, which show similar relatively thick crust (43–53 km) throughout and no obvious features attributable to rifting.

Conclusions

1) In spite of 'noise' from magnetic sources within the basin sequence, simple and 'robust' techniques of analysis of regional magnetic and gravity data, combined with geological, seismic refraction, and magnetotelluric constraints, have yielded a new model of the regional structure, basement configuration, and origin of the McArthur Basin. Identification of new rifts and troughs define new prospective areas for hydrocarbon and base-metal deposits.

2) The form and boundaries predicted by the previous geological model for the central meridional rift ('Batten Trough') and adjoining shelves are essentially confirmed. However, a southeasterly extension of the Urapunga Tectonic

Ridge now separates two geologically distinct rifts, defined herein as the Batten Trough (in the south only) and Walker Trough (north).

3) The thickest preserved section (10 km) lies within the Walker Trough, and new extensions are concealed beneath the Gulf of Carpentaria and adjoining coastal plain. A southern limit to the Batten Trough is now identified — the Tanumbirini-Kilgour Ridge — but the Walker Trough extends northwards beneath the Arafura Sea beyond the present data coverage.

4) A newly identified trough in the southwest, comprising thick Roper Group (Beetaloo Sub-basin), and possible adjacent troughs of thick carbonate rocks ('McArthur Group' or equivalents to its southeast), are subsurface continuations beneath the Cambrian Georgina Basin of the McArthur Basin into the Tomkinson Creek beds, north of Tennant Creek.

5) A model involving intermittent block rotation and east-west crustal extension over a period of 200 Ma, and accompanying northwest transfer faults, is proposed to explain the distribution of the several northerly trending rifts, separated by northwesterly transverse ridges.

6) The present structure is the product of later deformation and erosion. The result is steepening of extensional faults, folding, and reversal of earlier syndepositional displacements.

Acknowledgements

We are grateful to I. Zadoroznyj who carried out earlier interpretation work. Figures were drafted by J. Convine.

References

Anfiloff, W., 1981—*In* Plumb, K.A. (Co-ordinator), McArthur Basin research, July-December 1980. *Bureau of Mineral Resources Australia, Record* 1981/20.

BMR, 1985—BMR strikes the World's oldest oil. *BMR Research Newsletter*, 3, 1-2.

Collins, C.D.N., 1983—Crustal structure of the southern McArthur Basin, northern Australia, from deep seismic sounding. *BMR Journal of Australian Geology & Geophysics*, 8, 19-34.

Cull, J.P., 1982—Magnetotelluric profiles in the McArthur Basin of Northern Australia. *BMR Journal of Australian Geology & Geophysics*, 7, 275-286.

Etheridge, M.A., Branson, J.C., Falvey, D.A., Lockwood, K.L., Stuart-Smith, P.G., & Scherl, A.S., 1984—Basin-forming structures and their relevance to hydrocarbon exploration in Bass Basin, southeastern Australia. *BMR Journal of Australian Geology & Geophysics*, 9, 197-206.

Flavelle, A.J., 1965—Helicopter gravity survey by contract, NT and Qld 1965. *Bureau of Mineral Resources, Australia, Record* 1965/212.

Gibbs, A.D., 1984—Structural evolution of extensional basin margins. *Journal of the Geological Society, London*, 141, 609-620.

Henderson, R.G., 1960—A comprehensive system of automatic computation in magnetic and gravity interpretation. *Geophysics*, 25, 569-585.

Henderson, R.G., & Zeitz, I., 1948—Analysis of total magnetic intensity anomalies produced by point and line sources. *Geophysics*, 13, 428-436.

Jackson, M.J., Powell, T.G., Summons, R.E., & Sweet, I.P., 1986—Hydrocarbon carbon shows and petroleum source rocks in sediments as old as 1.7 × 10^9 years. *Nature*, 322, 727-729.

Jackson, M.J., Muir, M.D., & Plumb, K.A., 1987—Geology of the southern McArthur Basin, Northern Territory. *Bureau of Mineral Resources, Australia, Bulletin* 200.

Plumb, K.A., 1977—McArthur Basin project. *Bureau of Mineral Resources, Australia, Record* 1977/33.

Plumb, K.A., 1979—Structure and tectonic style of the Precambrian shields of northern Australia. *Tectonophysics*, 58, 291-325.

Plumb, K.A., 1985—Subdivision and correlation of late Precambrian sequences in Australia. *Precambrian Research*, 29, 303-329.

Plumb, K.A., & Derrick, G.M., 1975—Geology of the Proterozoic rocks of the Kimberley to Mount Isa Region. *In* Knight, C.L. (editor), Economic geology of Australia and Papua New Guinea. 1. Metals. *Australasian Institute of Mining and Metallurgy, Monograph* 5, 217-252.

Plumb, K.A., Derrick, G.M., & Wilson, I.H., 1980—Precambrian geology of the McArthur-Mount Isa Region, northern Australia. *In* Henderson, R.A., & Stephenson, P.J. (editors), Geology and geophysics of northeastern Australia. *Geological Society of Australia, Queensland Division, Brisbane*, 71-83.

Shell Development Australia Pty Ltd., 1965—Arafura Sea aeromagnetic survey, OP's 86, 96, 127, 128, NT. *Bureau of Mineral Resources, Australia, Petroleum Search Subsidy Acts File* 65/4616 (unpublished).

Tucker, D.H., & Boyd, D.M., in press—Dykes of Australia detected by airborne magnetic surveys. *Geological Association of Canada, Special Paper on Mafic Dyke Swarms.*

Tucker, D.H., Wyatt, B.W., Druce, E.C., Mathur, S.P., & Harrison, P.L., 1979—The upper crustal geology of the Georgina Basin region. *BMR Journal of Australian Geology & Geophysics*, 4, 209-226.

Tucker, D.H., Stuart, D.C., Hone, I.G., & Sampath, N., 1980—The characteristics and interpretation of regional gravity, magnetic and radiometric surveys in the Pine Creek Geosyncline. *In* Ferguson,J., & Goleby, A.B. (editors) Uranium in the Pine Creek Geosyncline. *International Atomic Energy Agency, Vienna*, pp. 101-140.

Vacquier, V., Steenland, N.C., Henderson, R.G., & Zeitz, I., 1951—Interpretation of aeromagnetic maps. *Geological Society of America, Memoir* 47.

Walker, R.N., Logan, R.G., & Binnekamp, J.G., 1977—Recent geological advances concerning the H.Y.C. and associated deposits, McArthur River, N.T. *Journal of the Geological Society of Australia*, 24, 365-380.

Whitworth, R., 1970—Reconnaissance gravity survey of parts of Northern Territory and Western Australia, 1967. *Bureau of Mineral Resources, Australia, Record* 1970/15.

Williams, N., 1978—Studies of the base metal sulphide deposits at McArthur River, Northern Territory, Australia: 1. The Cooley and Ridge Deposits. *Economic Geology*, 73, 1005-1035.

Young, G.A., 1965—McArthur River area, aeromagnetic survey, Northern Territory 1963-64. *Bureau of Mineral Resources, Australia, Record* 1965/173.

BMR Journal of Australian Geology & Geophysics, 10, 253-259

Surface-wave magnitudes of some early Australian earthquakes

I.B. Everingham[1], D. Denham[2], & S.A. Greenhalgh[3]

Surface-wave magnitudes (M_S) of 35 of the larger Australian earthquakes that occurred before 1960 have been determined from seismograms written at Riverview (Sydney), Melbourne, Adelaide, and Perth. Magnitudes were computed by the methods of Nuttli (1973) and Marshall & Basham (1973) and found to be consistent. Empirical corrections were applied to the horizontal component recordings to bring them into agreement with vertical component amplitudes, implicit in the definition of the M_S scale. Richter magnitudes (M_L) were plotted against the adopted (average) surface-wave magnitudes for 19 earthquakes for which M_L values were available. However, the scatter of the data precludes the adoption of a definitive relation for M_S on M_L for the Australian continent.

Introduction

Instrumental recordings of earthquakes are a basic necessity for meaningful magnitude determinations used in earthquake risk assessment. In Australia such recordings older than about 1960 are rare. Australian seismographs suitable for magnitude determination commenced operation at Riverview (Sydney) in 1909, with Wiechert and Mainka seismometers; and in Perth (1923), Adelaide (1924), Melbourne (1928), and Brisbane (1937), using Milne-Shaw seismometers (Doyle & Underwood, 1965). By 1960 the majority of these seismographs had been replaced by more modern instruments or had become unreliable, and magnitudes for routine regional seismicity listings were measured from seismograms from a very different network of stations. An outline of this development of the Australian network was given by Cleary (1977).

Before 1960 the Riverview Observatory seismograph station (code name RIV) was the most reliable and best equipped station in Australia, and Drake (1974, 1976) used the RIV seismograms to determine local 'Richter' magnitudes (M_L) for New South Wales earthquakes recorded since 1909. Similarly, Perth (PER) records were used by Everingham & Tilbury (1972) for M_L determinations for earthquakes that occurred in the south of Western Australia before the establishment of a modern seismograph station at Mundaring (MUN) in 1959. These sets of uniform magnitude determinations for earlier Australian earthquakes are the only ones published to date.

In a preliminary analysis of intensity/attenuation relations in southeastern Australia (McCue, 1980), it was found that magnitudes listed for earthquakes before 1960 were commonly determined from the macroseismic data, and instrumentally determined magnitudes are unavailable for some important earthquakes. The instrumental magnitudes that are available are local magnitudes (M_L), determined from the maximum trace deflections on the seismograms, corrected for instrument characteristics. These magnitudes are assumed to be equivalent to the magnitudes (M_L) defined by Richter (1935) for Californian earthquakes.

However, as, for example, White (1968) has shown for South Australia, this assumption is not necessarily correct. Ideally, a local magnitude scale should be designed for each region (and the relation with Richter's M_L established) and magnitudes should also be determined by different methods to improve the assessment of the size of a given earthquake. See McGregor & Ripper (1976) for a discussion of magnitude determinations most commonly used.

To add to the limited amount of magnitude data, surface-wave magnitudes of larger Australian earthquakes have been determined from Riverview (RIV), Melbourne (MEL), Adelaide (ADE) and Perth (PER) seismograms for 37 events (Table 1). Although the interest is primarily in the seismicity of the eastern part of the continent, the magnitudes of all Australian earthquakes recorded by RIV, MEL, ADE, and PER were determined to give a complete set of surface-wave magnitude determinations from those seismograph stations. Included in Table 1 are the local magnitudes (M_L) and body-wave magnitudes (m_b) of these (and other) earthquakes, where available. For completeness, we have also included the 1906 earthquake (Abe & Noguchi, 1983), which was probably the largest to have occurred in the Australian region this century. Figure 1 shows the location of these earthquakes.

Surface-wave magnitude (M_S) determinations

Originally, surface-wave magnitudes (M_S) were used for recordings at epicentral distances greater than 20° (Gutenberg & Richter, 1956). However, in 1967 the International Association of Seismology and Physics of the Earth's Interior (IASPEI) recommended international usage of the following M_S formula (McGregor & Ripper, 1976) :

$$M_S = \log (A/T) + 1.66 \log \Delta + 3.3 \quad \text{.....(i)}$$

where T = the wave period (s) and $18 \leq T \leq 22$, Δ = epicentral distance (degrees) in the range $20 \leq 130$, and A = amplitude (mean-to-peak) of ground motion (μm). This is only slightly different to Gutenberg & Richter's 1956 relation.

Subsequently, Marshall & Basham (1973) and Nuttli (1973) devised extensions of the M_S magnitude relation for distances less than 20° and periods less than 20 s. Marshall & Basham's (1973) empirical relation, using Rayleigh waves with periods centred near 12 s, is:

$$M_S = \log A + B'(\Delta) + P(\Delta) \quad \text{.....(ii)}$$

where $B'(\Delta)$ = distance correction term, $P(\Delta)$ = path correction term, and A = maximum amplitude of Rayleigh wave train (nm).

Nuttli's (1973) empirical relation, using the vertical (Z) component of Rayleigh waves with period 3-12 s, is:

$$M_S = 2.60 + 1.66 \log \Delta + \log (A/T) \text{ max for } 2° < \Delta < 20° \quad \text{.....(iii)}$$

where A/T is the maximum value of A/T in $\mu m.s^{-1}$. Nuttli indicated that this formula is equivalent to the standard 20 s formula over the magnitude range $4.1 \leq M_S \leq 5.2$, and that there was no theoretical reason for having these magnitude cut-offs.

[1]Department of Mineral Resources, Private Mail Bag, Suva, Fiji.
[2]Australian Seismological Centre, Bureau of Mineral Resources, GPO Box 378, Canberra, ACT, 2601.
[3]School of Earth Sciences, Flinders University of South Australia, Bedford Park, S.A. 5042.

Table 1. Australian earthquake epicentres, 1906-1960

	Year	Date d	m	Origin time (UT) h	m	s	Area	Lat °S	Long °E	M_S	M_L	m_b
1	1906	19	Nov	07	18	54	Off NW Aust.	19.1	111.80	7.2**		
2	1913	18	Dec	13	54		Ravenswood	20.00	147.00	4.8		5.8
3	1918	6	Jun	18	14	29	Bundaberg	23.50	152.50	5.7	6.2 (RIV)	
4	1919	15	Aug	10	21	21	Kurrajong	33.50	150.70		4.6 (RIV)	
5	1920	8	Feb	05	24	30	Off SW Aust.	35.00	111.00	6.0		
6	1921	30	May	14	51	59	Hay	35.00	145.00		5.5 (RIV)	
7	1922	10	Apr	10	47	39	E of Bass St.	40.00	147.50	5.2		
8	1925	18	Dec	10	47	10	Sydney	33.00	152.00		5.2 (RIV)	
9	1929	16	Aug	21	28	22	Off NW Aust.	16.99	120.66	6.8		
10	1929	28	Dec	01	22	53	E of Bass St.	39.69	149.45	5.2		
11	1930	27	Oct	02	03	51	Boorowa	34.50	149.00	3.1	5.0 (RIV)	
12	1932	2	Sep	18	22	32	Mornington	38.25	145.00	4.4	4.5 (MEL)	
13	1933	11	Jan	20	10	51	Gunning	34.80	149.50	4.1	4.8 (RIV)	
14	1934	30	Jan	20	27	54	Gunning	34.80	149.50	3.9	4.7 (RIV)	
15	1934	12	Jul	14	24	27	Indian Ocean	14.80	112.30	5.5		
16	1934	10	Nov	23	47	40	Gunning	34.90	150.00	4.2	4.8 (RIV)	
17	1934	18	Nov	21	58	41	Gunning	34.50	149.50	5.0	5.6 (RIV)	
18	1934	21	Nov	06	32	06	Gunning	34.50	149.20	4.5		
19	1935	12	Apr	01	32	24	Gayndah	26.00	151.10	5.4	6.1 (RIV)	
20	1937	28	Oct	09	34	43	Simpson Des.	26.10	136.50	5.1		5.9*
21	1937	20	Dec	22	35	02	Simpson Des.	25.50	137.20	5.3	4.7 (RIV)	6.3*
22	1938	24	Mar	20	03	33	Riverina	35.50	146.00	4.5		
23	1938	17	Apr	08	56	22	Simpson Des.	25.50	137.20	5.5		6.3*
24	1938	27	Jun	22	38	47	Armidale	30.40	151.80		4.7 (RIV)	
25	1939	26	Mar	03	56	05	L Torrens	32.00	138.00	5.7	5.8 (ADE)	6.2*
26	1939	1	May	19	07	29	L Torrens	31.40	138.00	4.2		
27	1939	5	Jun	12	20	43	Motpena	31.50	138.50	4.2		
28	1941	29	Apr	01	35	41	Meeberrie	26.80	116.10	6.5	7.2 (MUN)	7.3
29	1941	4	May	22	07	30	Simpson Des.	26.30	136.90	5.8		
30	1941	4	May	22	31	50	Simpson Des.	26.30	136.90	4.9		
31	1941	4	May	23	23	57	Simpson Des.	26.30	136.90	5.5		
32	1941	27	Jun	07	55	51	Simpson Des.	25.95	137.34	6.5		
33	1942	14	Feb	20	50	43	L Torrens	29.50	136.00	4.5	5.6 (ADE)	5.3*
34	1946	14	Sep	19	48	42	E of Bass St.	40.20	149.00	5.4		
35	1948	6	Aug	03	29	23	Robe	37.36	139.68	5.3	5.6 (ADE)	
36	1949	10	Mar	22	30	30	Gunning	34.80	149.20	4.7	5.5 (RIV)	
37	1952	24	Jun	01	46	00	Maryborough	25.50	152.80	4.2	5.0 (RIV)	
38	1952	7	Sep	05	41	14	Gunning	34.80	149.30	3.9	4.7 (RIV)	
39	1952	19	Nov	01	59	16	Gunning	34.80	149.30	3.6	4.9 (RIV)	
40	1954	28	Feb	18	09	52	Adelaide	34.93	138.67	4.9	5.3 (ADE)	
41	1954	19	Sep	10	37	13	St George	28.50	148.60	4.0	5.3 (RIV)	4.8
42	1958	1	Jan	00	07	00	Queenstown	42.20	146.10		5.3 (RIV)	
43	1958	1	Sep	11	28	02	Rock Flat	36.40	149.30		4.0 (CAN)	
44	1959	18	May	11	28	46	Berridale	36.22	148.64	3.8	5.3 (RIV)	
45	1959	12	Oct	21	23	40	Uralla	31.00	151.50		4.7	

* Nuttli (1973) m_b (L_g) formula.
** Abe & Noguchi (1983).

The parameters for determining magnitudes by the two methods are shown in Table 2. The distance corrections for amplitude measurements in micrometres are given for both methods, although different units of measurement were used in the published descriptions of the magnitude determinations.

Neither method for M_S determination is necessarily accurate for the Australian continent as a whole, because the nature and attenuation of Rayleigh waves is related to upper and lower crustal and upper mantle structure, which varies throughout the continent (Dooley, 1972; Cleary, 1973). For example, Nuttli (1973) pointed out that the 12 s surface waves (R_g) used in Marshall & Basham's (1973) study of earthquakes in the central United States are poorly recorded at eastern stations. The effect of the variations in continental structure is illustrated in the right-hand part of Table 2, where Marshall & Basham's (P(Δ)) terms for Eurasian and North American paths give a 0.45 magnitude difference for waves with a 10 s period.

For this study it is assumed that Nuttli's (1973) method is suitable for eastern Australia, because crustal and upper mantle properties for this region (e.g. Finlayson & others, 1979) are similar to those found for the central United States (Herrin & others, 1968), and that the Marshall & Basham (1973) parameters determined for North America could be similar in the Australian continent, because of its general similarity to North America. Magnitudes were calculated by each method wherever possible. For periods less than 10 s Nuttli's (1973) method is the only one available.

Table 2. Parameters for surface-wave magnitudes

Distance-correction						Path-correction term P (Δ) (totally continental)		
Δ°	B(Δ)	N(Δ)	Δ°	B(Δ)	N(Δ)	T(secs)	North America	Eurasia
1	3.17	—	11	4.05	4.33	10	-.75	-.30
2	3.35	3.10	12	4.08	4.39	11	-.67	-.27
3	3.57	3.39	13	4.11	4.45	12	-.61	-.24
4	3.67	3.60	14	4.13	4.50	13	-.53	-.21
5	3.78	3.76	15	4.15	4.55	14	-.46	-.18
6	3.84	3.89	16	4.17	4.60	15	-.38	-.15
7	3.90	4.00	17	4.19	4.64	16	-.30	-.13
8	3.95	4.10	18	4.21	4.68	17	-.24	-.10
9	3.98	4.18	19	4.23	4.72	18	-.16	-.07
10	4.02	4.26	20	4.25	4.76	19	-.08	-.04
						20	.00	.00

M_S (Marshall & Basham, 1973) = $\log A + B(\Delta) + P(\Delta) + 0.2$
M_S (Nuttli, 1973) = $\log A + N(\Delta) - \log T + 0.2$
A = maximum horizontal component amplitude in micrometers
= $\frac{\text{½ (peak-to-peak) trace amplitude in millimetres}}{\text{instrument magnification at period T}} \times 10^3$
NB. Where A is measured on the vertical component, subtract 0.2 from M_S determined by the above relations.

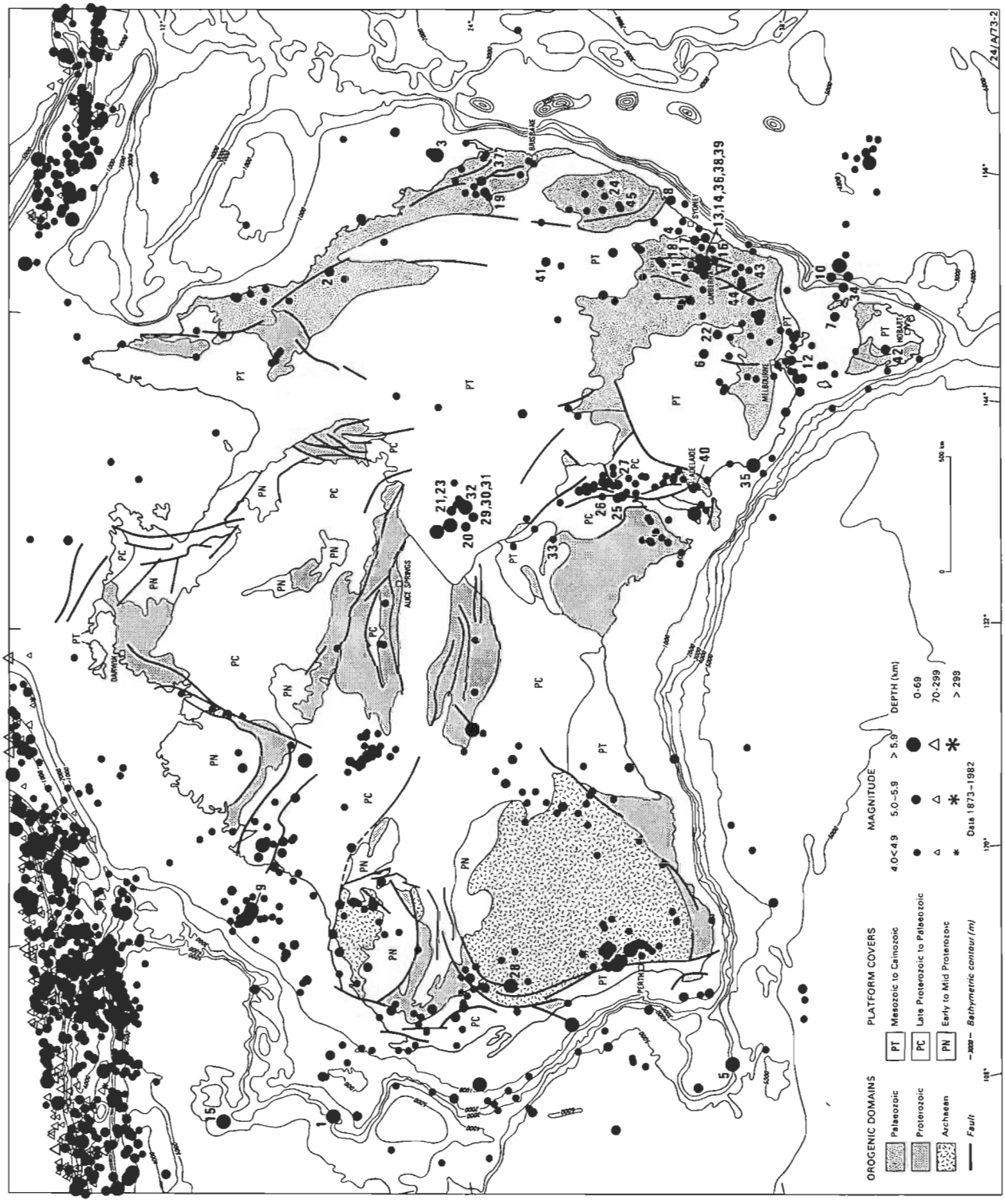

Figure 1. Location of earthquakes examined in this paper.
The numbers on the diagram correspond to those in Table 1. The data set plotted is for earthquakes having $M_L \geq 4.0$ in the period 1873–1983.

Seismograph details

The peak vertical-component amplitudes of Rayleigh waves were used by Nuttli (1973) and Marshall & Basham (1973) for their magnitude determinations, because these are more easily recognised on vertical-component seismograms, than on the horizontal-component seismograms and the amplitude of the vertical component of ground motion is generally greater than the horizontal component for such waves. However, for this study it was necessary to work from horizontal-component seismograms, because during 1910–1960 only one horizontal Milne-Shaw seismograph operated at MEL, ADE, and PER, whilst at RIV the vertical Wiechert seismograph was too insensitive to obtain useful recordings of many of the earthquakes for which magnitudes were required.

The Wiechert N–S and E–W seismograms were used for the RIV magnitude determinations. The magnification curve given by Drake (1974) is reproduced in Figure 2 and illustrates the instrumental characteristics. The Wiechert calibration figures used in the determinations were taken from the RIV monthly bulletins and differ slightly from the curve in Figure 2. It is to be noted that the Wiechert magnification is approximately uniform for seismic wave periods in the range

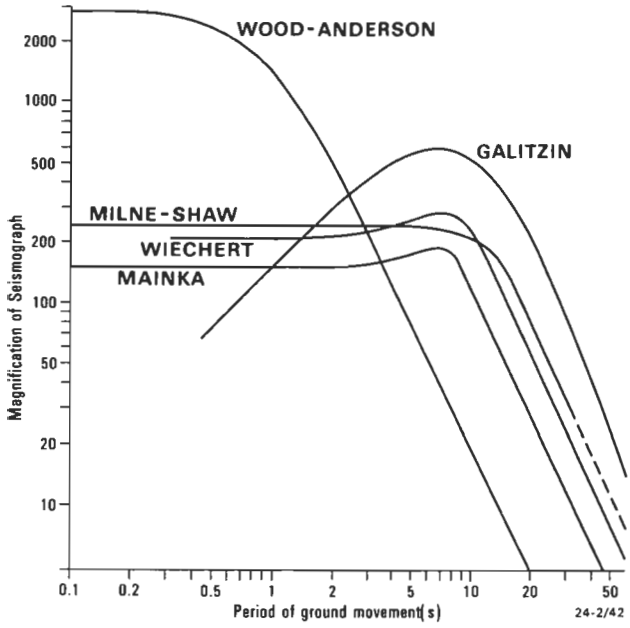

Figure 2. Displacement magnification curves for the Riverview seismographs (after Drake, 1974) and the Wood-Anderson and Milne-Shaw seismographs.

1-15 s. A sample seismogram, which shows the RIV recording of the 1954 Adelaide earthquake ($M_L \sim 5.5$), is shown in Figure 3.

Milne seismograph recordings were made in PER for the period 1901-1923, but most of these have been lost. A N-S-component Milne-Shaw instrument was put into operation at the start of 1924 and dismantled in 1963. At ADE a Milne horizontal pendulum operated from 1909 to 1948. It was of low sensitivity and not well suited to the study of local earthquakes. A higher gain Milne-Shaw instrument provided improved capability from 1924 to 1955.

The Milne seismograph characteristics are those of a simple undamped pendulum. Inspection of the MEL Milne records revealed that the instrument free period was about 20 s and the only waves recorded from earthquakes appeared to have a period of about 20 s. The magnification at this period was taken as 50.

To improve the M_S estimate, a correction of 0.2 was added to the magnitude determined from the parameters and formulae given in Table 2, for the following reasons:

(1) Magnitudes were determined from maximum amplitudes measured on one horizontal component, whereas surface-wave magnitudes should be taken from the resultant amplitude measured on two horizontal components, namely $A = (A_N^2 + A_E^2)^{1/2}$, where A = resultant amplitude, A_N = mean-to-peak amplitude from N-S seismogram, and A_E = mean-to-peak amplitude from E-W seismogram. Thus, if the trace amplitudes (A) on two components are equal, the resultant is $A\sqrt{2}$ and the magnitude may be greater by up to 0.15 than that measured on a single component.

(2) The formulae for magnitude determinations (Table 2) are based on amplitudes of the vertical component of Rayleigh waves, which are approximately 1.5 times as great as the horizontal component (i.e. giving about 0.18 higher magnitude; Båth, 1981).

Charters Towers (CTA) long-period seismograms of a 1981 earthquake in Bass Strait (Fig. 3) illustrate features of Rayleigh waves very clearly. The epicentre was almost due south of CTA, so that the Rayleigh waves are recorded on the longitudinal N-S seismogram and are not noticeable on the transverse E-W seismogram. Largest-trace amplitudes are recorded on the vertical component at a time corresponding to a group velocity of the waves of about 2.9 $km.s^{-1}$.

The computed surface-wave magnitudes for the earthquakes listed in Table 1 are given in Table 3. The individual station magnitudes are tabulated for both the Nuttli (1973) and Marshall & Basham (1973) formulations, where available.

The M_S determinations for the Bass Strait earthquake (1981) are shown in Figure 4. It is noteworthy that the M_S values for both formulations appear to increase with distance and indicate the need for special studies of the Australian region to establish appropriate attenuation factors.

M_S (Nuttli) versus M_S (Marshall & Basham)

Magnitudes considered reliably determined (averaged over two or more stations) by both methods (see Table 3) are plotted in Figure 5.

With either method, they differ by about 0.4 in extreme examples, but the standard least squares linear regression for M_S (Nuttli) on M_S (Marshall & Basham) passes very close to the line for M_S (Nuttli) = M_S (Marshall & Basham). For the 14 reliable data points represented, the average M & B magnitude is 5.35 ± 0.58. This is almost identical to the corresponding M_S (Nuttli) average of 5.33 ± 0.67.

The additional points plotted as open circles in Figure 5 represent magnitudes (from either method or both) based on only one station recording. Again, there is some scatter about the 45° line, but the data are consistent with the other group of reliable magnitude determinations. Combining all the data points with equal weight gives a mean value for M_S (Marshall & Basham) – M_S (Nuttli) of 0.03 ± 0.31, where the error term is the standard deviation. It is therefore concluded that there is no significant difference between the results for each method. The adopted surface-wave magnitudes listed in Table 3 were obtained from the arithmetic mean of all the available station magnitudes for each event (no weighting).

M_S versus M_L

The relation between M_S and M_L is important for comparison with relations found elsewhere, so that the magnitude data may be interpreted more meaningfully, particularly for Australian earthquake risk assessment. To ascertain the M_S-M_L relation, local magnitudes (M_L) given by Drake (1974), Singh (1985), and Rynn (personal communication, 1986) for several New South Wales, South Australian, and Queensland earthquakes are listed in Table 3 and plotted against adopted M_S values in Figure 6.

The plotted points (Fig. 6) are too scattered to permit an accurate M_S-M_L formula to be derived: this was to be expected in view of the paucity of data. However, it is interesting to compare Australian results with those from other sources, and the latter are also plotted in Figure 6.

The first formulae relating magnitude scales were reviewed by Gutenburg & Richter (1956) for North American earthquakes.

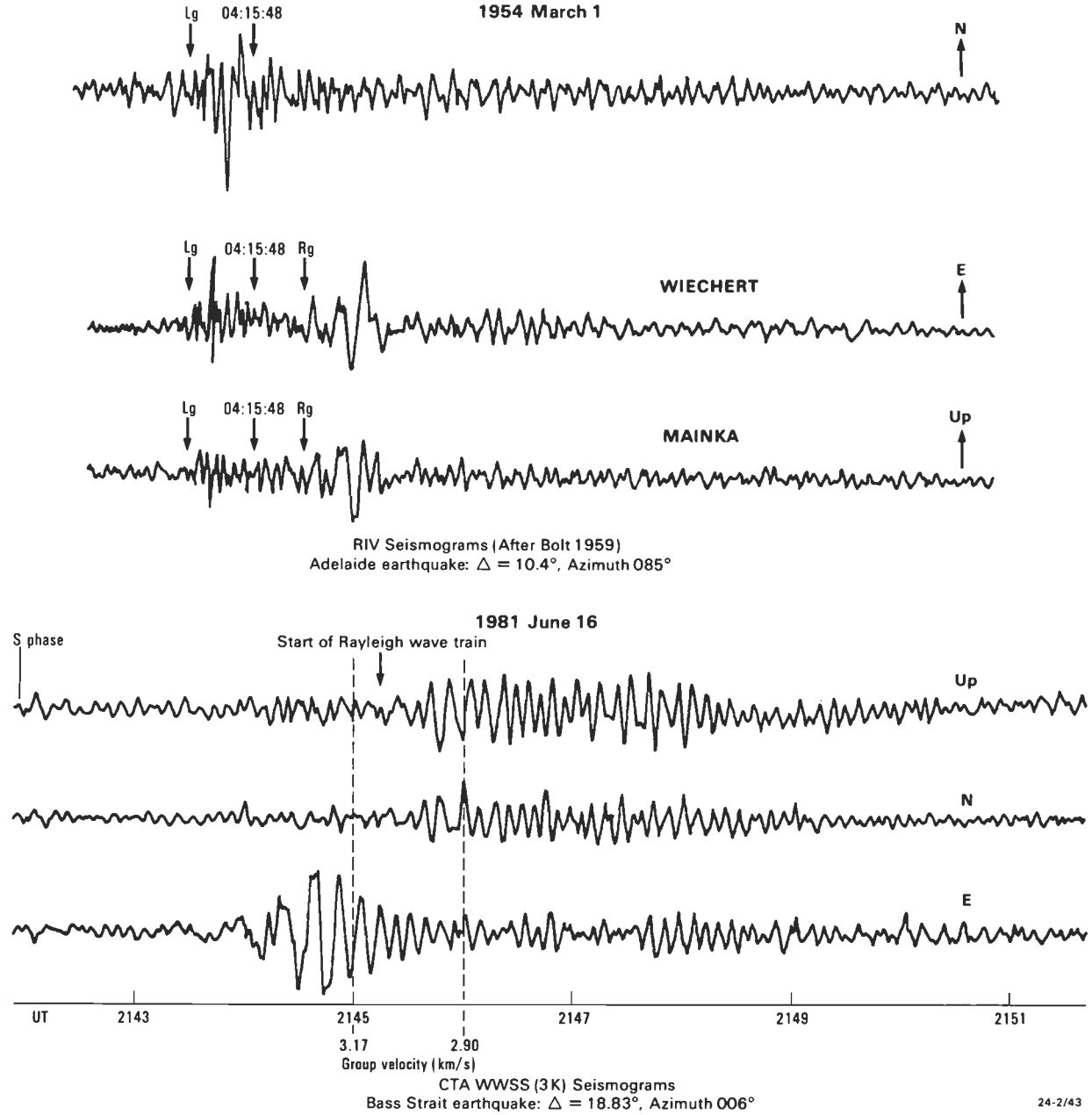

Figure 3. Three-component seismograms of the 1954 (Adelaide) and 1981 (Bass Strait) earthquakes, showing Rayleigh waves R_g.

The basic relations given were :

$m_b = 0.63\ M_S\ (G\ \&\ R) + 2.5$ .....(iv)
$m_b = 1.7 + 0.8\ M_L - 0.01\ (M_L)^2$ .....(v)
$M_S\ (G\ \&\ R) = 1.27\ (M_L - 1) - 0.016\ (M_L)^2$.....(vi)

where m_b, and M_S (G & R) are the magnitudes determined from body wave and surface waves respectively, using Gutenberg & Richter's (1956) formula, and M_L is Richter's (1935) local magnitude.

In 1967 IASPEI endorsed Gutenberg & Richter's (1956) formula for m_b, but amended the M_S formula to that given in equation (i).

This latter formula gave magnitudes about 0.2 greater than those given by Gutenberg & Richter's (1956) original formula (see McGregor & Ripper, 1976) and the recommended m_b/M_S relation became:

$m_b = 0.56\ M_S + 2.9$.....(vii)

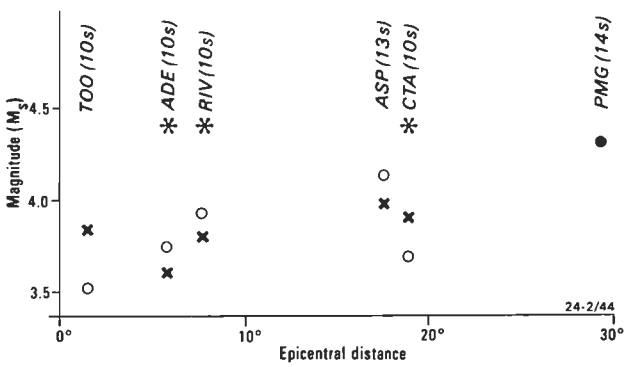

Figure 4. M_S determinations for the Bass Strait earthquake (16 June 1981) from long-period vertical seismograms.

The three-letter code and bracketed period (in seconds) represent the seismograph station and period of the Rayleigh wave with maximum amplitude. The magnitude symbols are: cross, Nuttli (1973); open circle, Marshall & Basham (1973); solid circle, IASPEI. The stations with asterisks are WWSSN stations.

Table 3. Surface-wave magnitudes (M_S) from RIV, MEL, ADE, and PER seismograms, 1913–1960

Event no.	Year	Date d	Date m	Origin time (UT) h	Origin time (UT) m	Origin time (UT) s	Area	M_S Marshall & Basham RIV	M_S Marshall & Basham MEL	M_S Marshall & Basham ADE	M_S Marshall & Basham PER	M_S Nuttli/IASPEI* RIV	M_S Nuttli/IASPEI* MEL	M_S Nuttli/IASPEI* ADE	M_S Nuttli/IASPEI* PER	M_S (Adopted)	M_L
1	1913	18	Dec	13	54		Ravenswood	4.7				4.8				4.8	5.5 (G-R)
2	1918	6	Jun	18	14		Bundaberg	5.8	5.9			6.1	5.1			5.7	6.2 (RIV)
3	1920	8	Feb	05	24	30	Off SW Aust.					6.2*	5.9*			6.0	
4	1922	10	Apr	10	47	39	E of Bass St.	5.1	5.6	5.9		5.1	4.3	5.0		5.2	
5	1929	16	Aug	21	28	22	Off NW Aust.					7.1*	6.7*	6.6*		6.8	
6	1929	28	Dec	01	22	53	E of Bass Str.	5.3				5.1				5.2	
7	1930	27	Oct	02	03	51	Boorowa		3.1				3.1			3.1	5.0 (RIV)
8	1932	2	Sep	18	22	32	Mornington					4.4				4.4	4.5 (RIV)
9	1933	11	Jan	20	10	51	Gunning		4.1				4.1			4.1	4.8 (RIV)
10	1934	30	Jan	20	27	54	Gunning		3.9				3.9			3.9	4.7 (RIV)
11	1934	12	Jul	14	24	27	Indian Ocean	4.9				5.9*	6.0*	5.3*		5.5	
12	1934	10	Nov	23	47	40	Gunning		4.2				4.2			4.2	4.8 (RIV)
13	1934	18	Nov	21	58	41	Gunning		5.2				5.2	4.5		5.0	5.6 (RIV)
13b	1934	21	Nov	01	32	06	Gunning					4.5		3.7		4.1	
14	1935	12	Apr	01	32	24	Gayndah	5.6	5.2			5.5	5.3			5.4	6.1 (RIV)
15	1937	28	Oct	09	34	43	Simpson Des.	5.0	5.1			5.4	5.2	5.0		5.1	
16	1937	20	Dec	22	35	02	Simpson Des.	5.2	5.3	5.0		5.7	5.5	5.1		5.3	
17	1938	24	Mar	20	03	33	Riverina	4.9				4.5	4.4	4.2		4.5	4.7 (RIV)
18	1938	17	Apr	08	56	22	Simpson Des.	5.8	5.5	5.0		5.9	5.7	5.3		5.5	
19	1939	29	Mar	03	56	05	Lake Torrens	5.6	5.6			6.1	5.8	5.5		5.7	5.8 (RIV)
20	1939	1	May	19	07	29	Lake Torrens					4.2		4.3		4.2	
21	1939	5	Jun	12	20	43	Motpena					4.2		4.3		4.2	
22	1941	29	Apr	01	35	41	Meeberrie			6.5		6.8*		6.2		6.5	
23	1941	4	May	22	07	30	Simpson Des.	5.7			5.9	5.7		5.4	6.2	5.8	
24	1941	4	May	22	31	50	Simpson Des.	5.0				4.9		4.9		4.9	
25	1941	4	May	23	23	57	Simpson Des.	5.3			5.7	5.2			5.9	5.5	
26	1941	27	Jun	07	55	51	Simpson Des.	6.5			6.3	6.5		6.4	6.7	6.5	
27	1942	14	Feb	22	50	43	Lake Torrens	4.8		4.5		4.6		4.2		4.5	5.6 (ADE)
28	1946	14	Sep	19	48	42	E. of Bass Str.	5.2	5.6			5.2	5.6			5.4	5.6 (ADE)
29	1948	6	Aug	03	29	23	Robe	5.3	5.1			5.7	5.2			5.3	5.6 (ADE)
30	1949	10	Mar	22	30	33	Gunning					4.6		4.8		4.7	5.5 (RIV)
31	1952	24	Jun	01	46	00	Maryborough	4.0				4.4				4.2	5.0 (RIV)
32	1952	7	Sep	05	41	14	Gunning		4.1			3.6	4.1			3.9	4.7 (RIV)
33	1952	19	Nov	01	59	16	Gunning		3.8			3.3	3.8			3.6	4.9 (RIV)
34	1954	28	Feb	18	09	52	Adelaide	4.6				5.2				4.9	5.3 (ADE)
35	1954	19	Sep	10	37	13	St George					4.2	3.7			4.0	5.3 (RIV)
36	1959	18	May	11	28	46	Berridale	4.1	3.7			3.8	3.6			3.8	5.3 (RIV)

Using (v) and (vii) we obtain the approximate formula:

$$M_S \text{ (IASPEI)} = 1.3\ M_L - 2.0 \quad \text{.....(viii)}$$

Because magnitudes determined by a given method may differ from region to region as a result of variations in seismic attenuation, it is necessary to undertake special studies for each region. Everingham & Ripper (1974) studied magnitude relations for earthquakes in Papua New Guinea, using several hundred earthquakes and local magnitudes M_L (PMG) determined from standard Wood-Anderson seismographs recording in the network of Papua New Guinea. They found that

$$M_S\text{(IASPEI)} = 1.2\ M_L \text{ (PMG)} - 1.36 \quad \text{.....(ix)}$$

Also Hattori (1979), using US Geological Survey catalogues of world earthquakes, found:

$$M_S \text{ (IASPEI)} = 1.48\ M_L - 2.69 \quad \text{.....(x)}$$

Equations (viii) (IASPEI), (ix) (Everingham & Ripper, 1974), and (x) (Hattori, 1979) are plotted in Figure 6 to indicate the range of M_S-M_L relations that can be expected from studies using different data sets. The Gutenberg & Richter (1956) equation (vi) is very close to that determined by Everingham & Ripper (1974) and has not been plotted, because it could not be clearly separated on the diagram. The data do not lie close to a straight line and there appears to be no simple linear relation between M_S and M_L, particularly at the lower values of M_S. However, for most earthquakes for which M_S is greater than 4.0, the published relations are reasonable approximations.

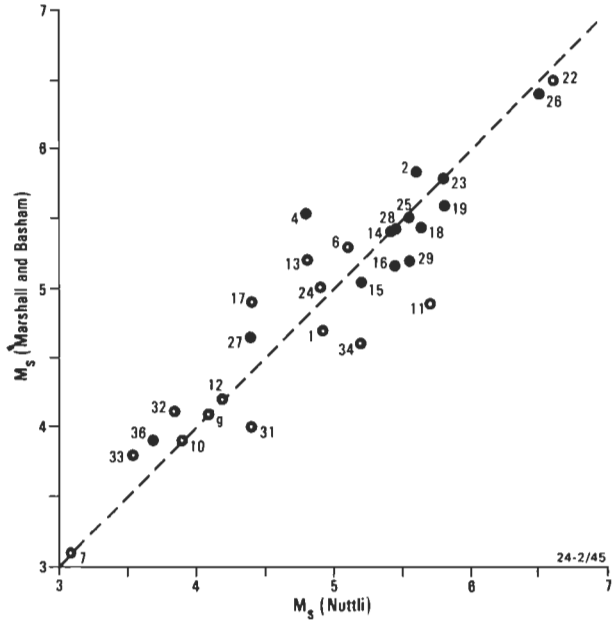

Figure 5. M_S (Marshall & Basham) versus M_S (Nuttli) for Australian earthquakes, 1913–1960.

The closed circles denote magnitudes averaged for two or more stations for each of the Nuttli and Marshall & Basham determinations. The open circles are magnitudes based on only one station recording for either determination or both. The numbers are the event numbers in Table 3.

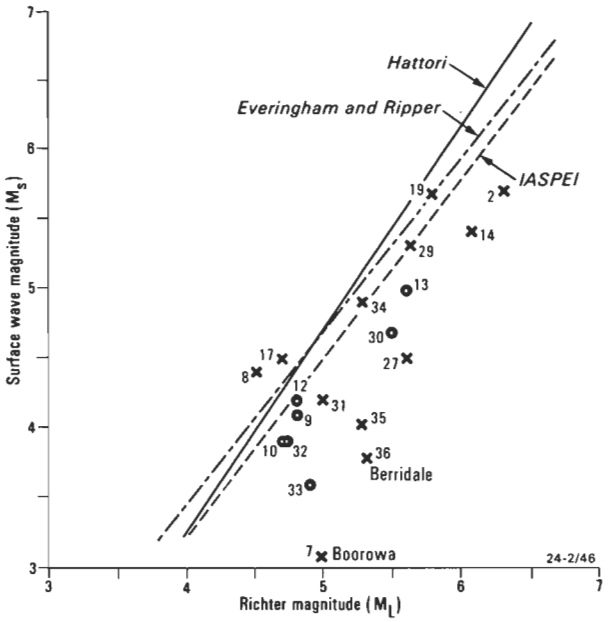

Figure 6. $M_S - M_L$ relation for eastern Australia.
The numbers are the event numbers in Table 3. The open circles represent Gunning zone earthquakes.

Acknowledgements

We thank Jack Rynn and Laurence Drake for critically reviewing the manuscript, John Convine for preparing the figures, and Pat Burrell and Helen Tozer for typing the text.

References

Abe, K. & Noguchi, S., 1983—Revision of magnitudes of large shallow earthquake 1897-1912. *Physics of the Earth and Planetary Interiors*, 33, 1-11.

Båth, M., 1981—Earthquake magnitude — recent research and current trends. *Earth-Science Reviews*, 17, 315-398.

Bolt, B.A., 1959—Seismic travel times in Australia. *Journal and Proceedings of the Royal Society of New South Wales*, 91, 64-72.

Cleary, J., 1973—Australian crustal structure. *Tectonophysics*, 20, 241-48.

Cleary, J., 1977—Australian seismicity studies: a historical survey. *Earthquake Information Bulletin*, 9, 4-8.

Dooley, J.C., 1972—Seismological studies of the upper mantle in the Australian region. *Geophysical Research Board of the National Geophysical Research Institute, Hyderabad, Proceedings of the Second Symposium on the Upper Mantle Project December 1970, Hyderabad*, 113-46.

Doyle, H.A. & Underwood, R., 1965—Seismological stations in Australia. *The Australian Journal of Science*, 28 40-43.

Drake, L., 1974—The seismicity of New South Wales. *Journal and Proceedings of the Royal Society of New South Wales*, 107, 35-40.

Drake, L., 1976—Seismic risk in Australia. *Journal and Proceedings of the Royal Society of New South Wales*, 109, 115-21.

Everingham, I.B., & Ripper, I.D., 1974—Comparison of earthquake magnitudes, Papua New Guinea. *Port Moresby Geophysical Observatory Report*, 54, (unpublished).

Everingham, I.B., & Tilbury, L., 1972—Information on Western Australian earthquakes 1849-1960. *Journal of the Royal Society of Western Australia, 55, 90-96.*

Finlayson, D.M., Prodehl, C. & Collins, C.D.N., 1979—Explosion seismic profiles, and implications for crustal evolution in southeastern Australia. *BMR Journal of Australian Geology & Geophysics*, 4, 243-52.

Gutenberg, B. & Richter, C.F., 1956—Magnitude and energy of earthquakes. *Annali di Geofisica*, 9, 1-c2-15.

Hattori, S., 1979—Seismic risk maps in the World (maximum acceleration and maximum particle velocity) (II)—Balkau, Middle East, Southeast Asia, Central America, South America and others. *Bulletin of the International Institute of Seismology and Earthquake Engineering*, 17, 33-96.

Marshall, P.D. & Basham, P.W., 1973—Rayleigh wave magnitude scale M_S. *Pure and Applied Geophysics*, 103, 406-14.

McCue, K., 1980—Magnitudes of some early earthquakes in southeastern Australia. *Search*, 11, 78-80.

McGregor, P.M. & Ripper, I.D., 1976—Notes on earthquake magnitude scales. *Bureau of Mineral Resources, Australia, Record* 1976/56.

Nuttli, O.W., 1973 973—Seismic wave attenuation and magnitude relations for eastern North America. *Journal of Geophysical Research*, 78, 896-85.

Richter, C.F., 1935—An instrumental earthquake magnitude scale. *Bulletin of the Seismological Society of America*. 25, 1-32.

Singh, R., 1985—Seismicity and crustal structure of South Australia. *M.Sc. thesis, Flinders University* (unpublished).

White, R.E., 1968—A local magnitude scale for South Australian earthquakes. *Bulletin of the Seismological Society of America*, 58, 1041-57.

BMR Journal of Australian Geology & Geophysics, 10, 261-265

The musculature and vascular systems of two species of Cambrian Paterinide (Brachiopoda)

John Laurie[1]

Two species of Paterinide brachiopod preserving details of the musculature and vascular systems have been studied. Their dorsal valves are shown to have a large quadripartite muscle field not unlike that of the articulates with further scars located on the inner face of the apex of the homeochilidium. The dorsal vascular system is possibly saccate (apocopate). The ventral muscle field has two short subtriangular scars divided from one another by the proximal portions of main vascular canals. The location of other scars is uncertain. The ventral vascular system is probably saccate.

Introduction

The paterinides are an enigmatic group of brachiopods that have customarily been assigned to the Inarticulata because they lack tooth and socket articulation and possess phosphatic shells. Their relationship to other brachiopod groups has long been problematical, a dilemma partly caused by the paucity of knowledge of their musculature and vascular systems.

During a study of Early and Middle Cambrian faunas from central Australia two species of paterinide exhibiting relatively well-preserved interiors were recovered from acid residues. Their internal structures are described herein.

Acknowledgements

The author wishes to thank Mr M.J. Freeman for his encouragement during the author's tenure as an officer of the Northern Territory Geological Survey and Dr J.H. Shergold for his encouragement during the preparation of this paper. The specimens figured in this work have been deposited in the Commonwealth Palaeontological Collection (CPC prefix) of the Bureau of Mineral Resources, Canberra.

Localities

Two groups of specimens are studied herein. The first is referable to *Paterina* sp. and comes from locality H583 in the Middle Cambrian Arthur Creek Formation of the southwest Georgina Basin (136°07'00"E, 22°35'45"S, Huckitta 1:250 000 Sheet SF53-11). The second belongs to a new genus and species, here referred to aff. *Dictyonina* sp., and was found at locality NT600 in the late Atdabanian (Laurie & Shergold, 1985) Todd River Dolomite of the northeast Amadeus Basin (134°18'40"E, 24°2'00"S, Rodinga 1:250 000 Sheet SG53-2).

Previous work

Walcott (1912, p. 333) noted meagre details of the interiors of several species of paterinide, with the dorsal valve of one species (*Micromitra (Iphidella) pannula ophirensis*) exhibiting 'a median ridge, the base of the main vascular sinuses and two central muscle scars.'

Bell (1941, p. 211), in discussing the species *Iphidella hexagona*, noted that the pattern of internal callosities in the species 'remotely resembled the distribution of muscle attachment sites in the most primitive calcareous "articulates". He suggested that, in the ventral valve, the median callosity may have been the site of 'adductor' attachment with the pair of callosities anterior to it bearing the 'diductors'.

Williams & Rowell (1965, p. H127) and Rowell (1965, p. H294) reviewed knowledge of the internal structure of members of the group. They concluded that all the scars were narrowly triangular and radiated from the apices of their respective valves. In the ventral valve, two narrow slightly divergent tracks extended from the beak to near the valve mid-length, whereas in the dorsal valve two pairs of tracks radiated from the beak, a longer pair extending to near the valve mid-length, forming a single median depression, and a shorter pair diverging anterolaterally.

More recently, Rowell (1980, p. 18), in studying etched material of *Dictyonina pannula* (White), generally reiterated the view that the ventral muscle field is elongate triangular, but noted that it was divided into three sectors by long, slightly divergent troughs, which he suspected were mantle canals.

Descriptions and interpretations

***Paterina* sp.** (Plate 1, figs 1-14, Plate 2, figs 1-11)

The ventral interior has a low broad median ridge that bifurcates anteriorly and a pair of very low indistinct submedian ridges that, a short distance anterior to the umbo, curve abruptly to become subparallel to the median ridge or ridges. These ridges are interpreted as bounding a pair of broad subparallel vascular canals, as advocated by Rowell (1980, p.18). Anteriorly, these canals appear to curve laterally, becoming concentric (see Plate 1, figs 12, 13; Plate 2, figs. 2, 9), subsequently giving rise to many radially disposed terminal branches (see Plate 1, figs. 13, 14; Plate 2, figs. 1, 6-9).

Lateral to the submedian ridges in the posterior fifth (or less) of the valve are two short, triangular areas, which, in some specimens, are thickened (Plate 1, fig. 13; Plate 2, fig. 2), and, in others, have a well-developed concentric growth lineation (Plate, 1, fig. 12; Plate 2, figs. 2, 3, 8) or are bounded anterolaterally by low ridges (Plate 2, figs. 4, 6, 7, 11). These triangular areas are interpreted as the major ventral muscle scars, possibly homologous with the diductors of the articulates.

Indications of other scars are less clear. Possible candidates are found as depressions inserted between the branches of the median ridge (Plate 1, fig. 13; Plate 2, fig. 2) or as thickenings in the same area (Plate 2, fig. 5). It is also conceivable that the area between the major muscle scars in the apex of the valve was occupied by muscle attachment sites. In some specimens, this area is quite deeply impressed (Plate 1, figs. 12, 13; Plate 2, figs; 2, 3, 7, 8) and occasionally appears to be separated from the proximal parts of the main vascular canals by low transverse ridges (Plate 1, figs. 12, 13; Plate 2, figs. 3, 6, 7).

[1] Division of Continental Geology,
Bureau of Minerals Resources
GPO Box 378, Canberra, ACT 2601

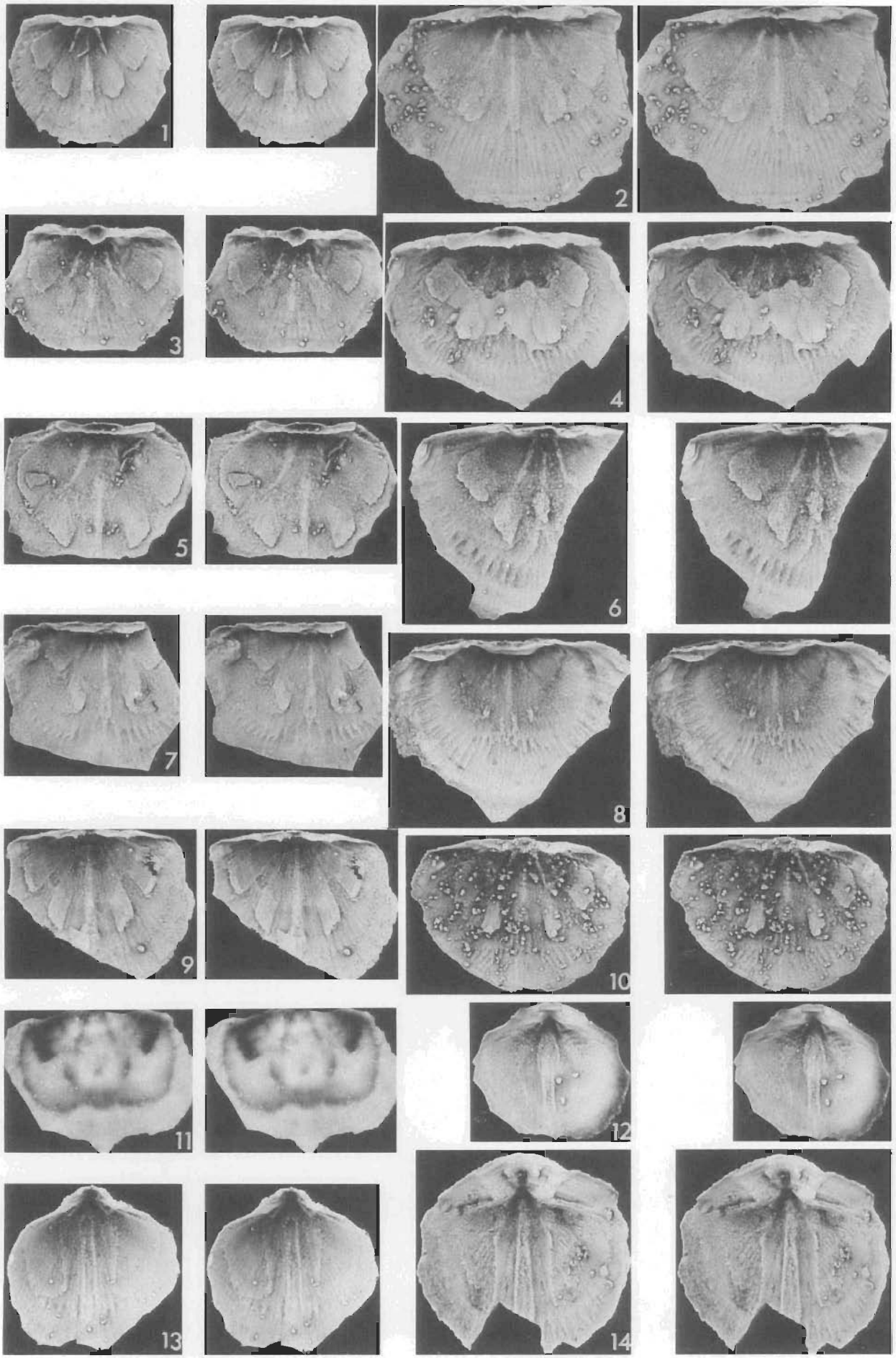

Plate 1. ***Paterina*** **sp.**
All stereo pairs; all ×10; all coated with ammonium chloride except where noted. Figs. 1–11, Dorsal valve interiors: 1, CPC25016; 2, CPC25024; 3, CPC25017; 4, CPC25014; 5, CPC25015; 6, CPC25011; 7, CPC25010; 8, CPC25022; 9, CPC25013; 10, CPC25012; 11, CPC25023, uncoated. Figs. 12–14, Ventral valve interiors. 12, CPC24990; 13, CPC25000; 14, CPC24989.

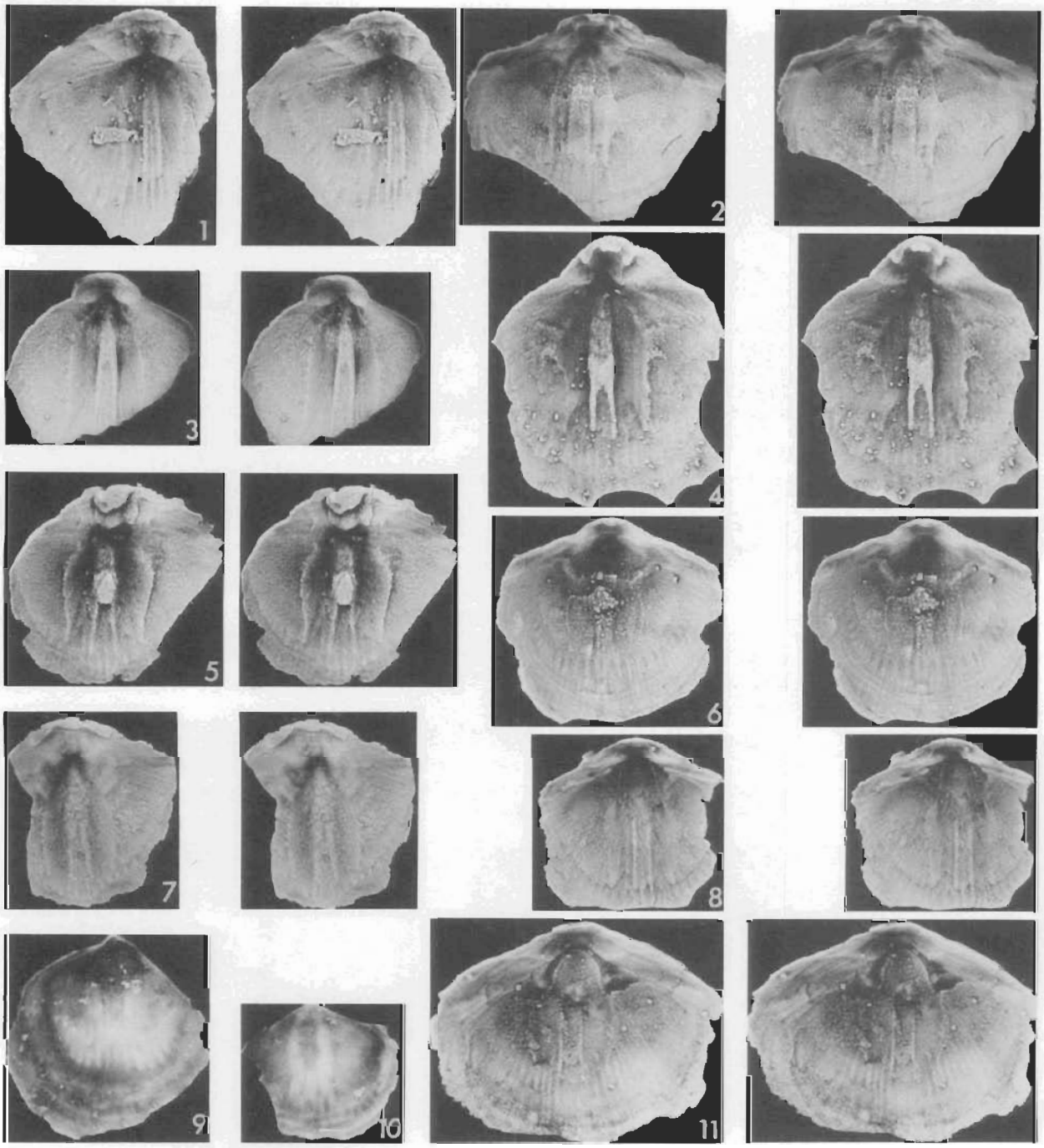

Plate 2. *Paterina* sp.

All stereo pairs except where noted; all ×10; all coated with ammonium chloride except where noted; all ventral valve interiors: 1, CPC24992; 2, CPC25004; 3, CPC24999; 4, CPC24988; 5, CPC24996; 6, CPC24997; 7, CPC25006; 8, CPC25007; 9, CPC25001, not stereo pair, uncoated; 10, CPC25002, not stereo pair, uncoated; 11, CPC25003.

Also present in several ventral valves are large reniform areas located laterally to the main vascular canals (Plate 1, figs. 12, 13, 14; Plate 2, figs. 1, 3, 5, 8). These have, in some cases, a pustulose ornamentation, and resemble the saccate vascula genitalia of some orthides.

The interior of the homeodeltidium is quite variable in its structure, but generally seems to consist of a median trough bounded by variably developed ridges (Plate 1, figs. 12, 13, 14; Plate 2, figs. 1, 2, 4, 5) with occasional thickening of the distal margin (Plate 2, figs. 2, 4, 5, 6).

The dorsal interior has a low median ridge, commonly extending to or beyond the valve mid-length, and two submedian ridges, which rarely extend very far from the umbonal region. Two pairs of muscle scars are located on the floor of the valve: one pair being located at about valve mid-length, a short distance laterally to the median ridge; the other pair being located about midway between the anterior scars and the posterolateral extremities of the valve, a short distance laterally to the anterior extremities of the submedian ridges (Plate 1, figs. 1-11).

Passing between the median ridge and the anterior pair of muscle scars is a pair of large vascular canals, whose anterior ends curve abruptly laterally to become concentric (Plate 1, figs. 4, 6, 7), subsequently giving rise to many radially disposed terminal branches (Plate 1, figs. 2, 4, 6, 7). The

posterolateral extent of these main canals is uncertain, but they appear to extend at least one third of the distance from the midline to the posterolateral margin. Other markings on the valve floor are unclear or ambiguous.

The interior of the homeochilidium has a variably developed transverse pit, which in some specimens is weakly bilobate (Plate 1, figs. 4, 8). It is very tempting to suggest that this is a muscle attachment site homologous with the dorsal diductor attachment sites of the articulates.

Aff. *Dictyonina* sp. nov.

The ventral interior has two well-developed broad submedian ridges diverging anteriorly at about 10–15 degrees, commonly with a low narrow ridge between them. One further pair of ridges (lateral ridges), found in several specimens, extends anterolaterally from the lateral margins of the pedicle callist(?) (see Plate 3, fig. 3). The lateral and submedian ridges bound a pair of subtriangular to semicircular muscle scars (Plate 3, figs. 1–4). No other attachment areas are apparent. Anterior to the muscle scars, the submedian ridges become lower and less regular, and appear to laterally bound a pair of principal vascular canals. These canals apparently branch at about two-thirds valve length, then become obscure (Plate 3, fig. 1). A further series of vascular markings arises from the anterolateral margins of the muscle scars, trends anterolaterally for a short distance, then curves abruptly but not very strongly towards the anterior, whereupon they disappear (Plate 3, fig. 1). These may be impressions of the radial structure of the vascula genitalia.

The dorsal interior has a transversely ovate to subquadrate, slightly depressed posteromedial area that is divided into roughly equal quarters by a low narrow median ridge and two oblique ridges or groups of ridges diverging anteriorly from the median ridge at about 45 degrees (Plate 3, figs. 5–7). In one specimen, faint impressions of muscle scars can be seen (Plate 3, fig. 7). One pair of scars (anterior pair) are rounded triangular to longitudinally ovate and bounded laterally by the oblique ridges, and the two scars are separated from one another by the median ridge. The other pair (posterior pair) are posterolateral to the oblique ridges and are narrow, rounded triangular in shape. As in *Paterina* sp., some specimens have a small pit on the inner surface of the apex of the homeochilidium. No traces of the vascular system have been observed.

Comparisons

Each of the above species has a short ventral muscle field with the scars lateral to the submedian ridges, which in turn laterally bound major mantle canals, proximally separated from one another by the usually low median ridge. It is these mantle canals and their bounding ridges that Rowell (1980) assumed to be the ventral muscle field. In aff. *Dictyonina* sp. nov. these mantle canals are obscure distally, but in *Paterina* sp., at about two-thirds valve length, they curve abruptly laterally to become concentric. In so doing they apparently encircle, at least in part, somewhat reniform fields, herein interpreted as impressions of saccate vascula genitalia. Laterally disposed radial markings in the ventral valve of aff. *Dictyonina* sp. nov. are interpreted similarly.

Both species have a large quadripartite dorsal muscle field with the slightly smaller anterior pair of scars located a short distance laterally to the median ridge and the posterior pair located posterolaterally to the anterior pair. Only *Paterina* sp. shows any trace of the vascular system. In this species one median pair of canals passes between the median ridge

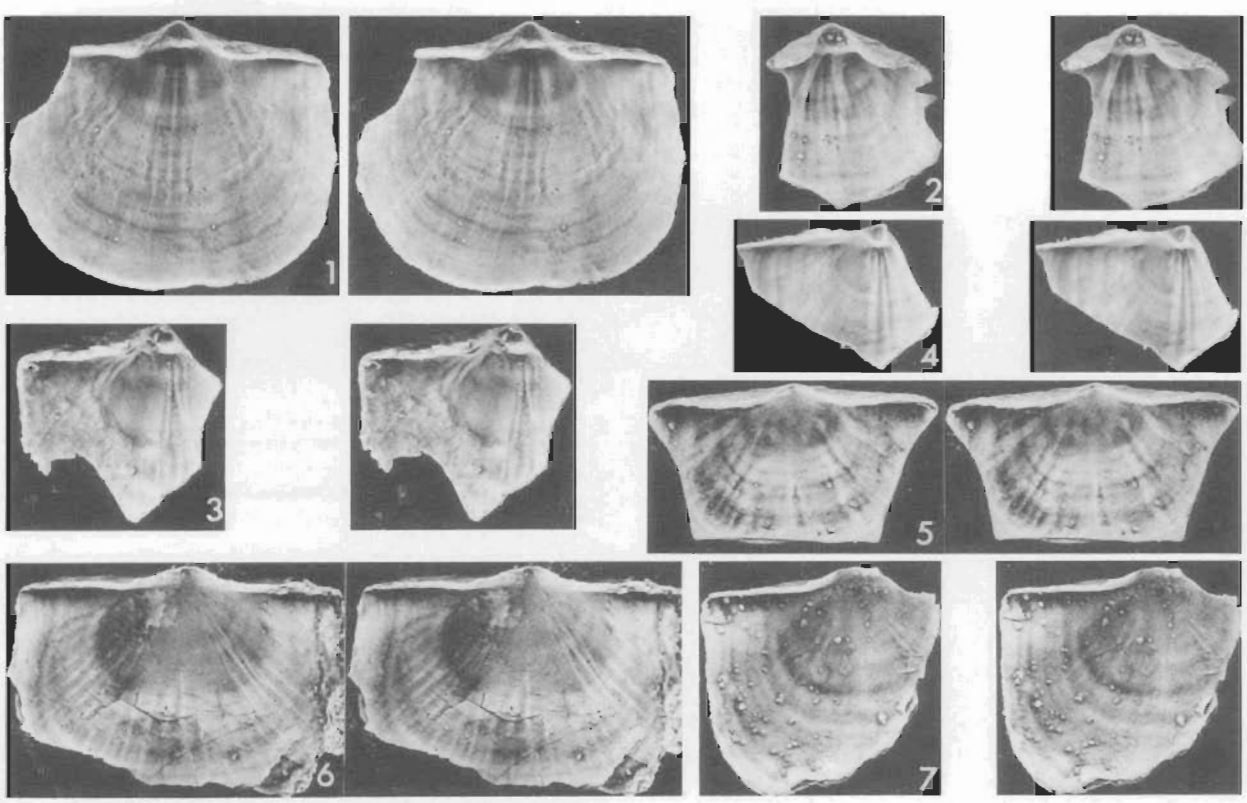

Plate 3. aff. *Dictyonina* sp. nov.
All stereo pairs, all ×7; all coated with ammonium chloride. Figs. 1–4, Ventral valve interiors: 1, CPC23642; 2, CPC23648; 3, CPC23644; 4, CPC23649; Figs 5–7, Dorsal valve interiors: 5, CPC23655; 6, CPC23654; 7, CPC23656.

and the anterior muscle scars, then curves laterally to become concentric. Their extent towards the posterolateral margins is unclear, but the pattern has similarities with the saccate (apocopate) condition.

Both species commonly have a small pit or depression on the inner face of the apex of the homeochilidium. It is suggested that this too is a site of muscle attachment.

Concluding remarks

The striking feature of the internal structure of the species studied herein is its similarity to that of articulate brachiopods, particularly the orthides. Although it is not clear how the valves of paterinides opened and closed, the general similarity in musculature to representatives of the Articulata suggests a similar system operated. For the paterinides to use such a lever action, a suitable axis of rotation and a line of action for one set of muscles posterior to this axis must exist. The broken nature of the specimens of *Paterina* sp. prevent the examination of such geometric considerations, but the specimens of aff. *Dictyonina* sp. nov. exhibit a wide, straight hingeline, a feature that suggests coincidence with the rotational axis. If this is the case, then one set of muscles necessarily occurs posterior to this hinge. For this to occur in a species with an apsacline (nearly catacline) ventral pseudointerarea and an anacline (nearly catacline) dorsal pseudointerarea, the muscles must be close to the posterior margin of either or both valves. For such a muscle arrangement to occur in a species with a procline ventral interarea (e.g. *Dictyonites perforata* Cooper 1956), the dorsal valve must extend posteriorly to the hinge axis, with the dorsal and ventral attachment sites of the 'diductors' tending to be more posterior than in an apsacline-anacline species. Such is the case when comparing the ?procline-?anacline species discussed above as *Paterina* sp. with the apsacline-anacline aff. *Dictyonina* sp. nov. A more detailed geometric analysis of these functional possibilities must await the availability of more specimens of a less fragmented nature that I have at my disposal.

References

Bell, W.C., 1941—Cambrian Brachiopoda from Montana. *Journal of Paleontology*, 15(3), 193-255.

Cooper, G.A., 1956—Chazyan and related brachiopods. *Smithsonian Miscellaneous Collections*, 127; pt. I, 1-1024; pt II, 1025-1245, pls. 1-269.

Laurie, J.R. & Shergold, J.H., 1985—Phosphatic organisms and the correlation of Early Cambrian carbonate formations in central Australia. *BMR Journal of Australian Geology & Geophysics*, 9, 83-89.

Rowell, A.J., 1965—Inarticulata. *In* Moore, R.C., (editor), Treatise of invertebrate paleontology. Part H, Brachiopoda, H260-H296, *Geological Society of America and University of Kansas Press.*

Rowell, A.J., 1980—Inarticulate brachiopods of the Lower and Middle Cambrian Pioche Shale of the Pioche district, Nevada. *University of Kansas, Paleontological Contributions, Paper* 98, 1-26, pls. 1-8.

Walcott, C.D., 1912—Cambrian Brachiopoda. *Monographs of the United States Geological Survey*, 51; pt. I, 1-872, pt. II, 1-363, pls. 1-104.

Williams, A. & Rowell, A.J., 1965—Morphology. *In* Moore, R.C., (editor), Treatise of invertebrate paleontology. Part H, Brachiopoda, H57-H155, *Geological Society of America and University of Kansas Press.*

BMR Journal of Australian Geology & Geophysics, 10, 267-275

Cainozoic geology and geomorphology of the Wahgi Valley, central highlands of Papua New Guinea

C.F. Pain[1], C.J. Pigram[2], R.J. Blong[3] & G.O. Arnold[4]

The Wahgi Valley is a structural depression, between the Bismarck Fault Zone to the north and the Kubor Anticline to the south, which has been enlarged by erosional removal of northward-dipping sedimentary rocks on the northern flank of the Kubor Anticline. The geomorphic history of the area began when it became land about 35 Ma ago. The Wahgi Valley contains volcanic debris avalanche and lahar deposits in the west and fluviatile/lacustrine deposits elsewhere. The latter are dominated by undissected swamp and lake deposits in the west, and dissected fan and terrace deposits in the east. There is clear evidence of knickpoint retreat up the Wahgi River from the east, causing the fans to trench progressively from the east. Earlier interpretations of the evolution of the Wahgi Valley stressed drainage reorganisation, with reversal of a westerly flowing Wahgi River caused by damming by volcanics in the west, and capture in the east. Evidence from sediments, tephra, and landforms now suggests that reversal was probably restricted to the westernmost drainage, and any reversal of drainage occurred earlier than previously thought, perhaps 400 000 years ago.

Introduction

The highland valleys of Papua New Guinea originated in the Late Cainozoic with rapid uplift, extensive detachment tectonics, and Pleistocene volcanism (Dow, 1977). Many of the major rivers lie between high mountain ranges and traverse gently sloping infilled basin floors, as well as steeper gradients (Bik, 1967; Blong & Pain, 1976).

The Wahgi Valley has all the attributes of a typical highland basin. The upper reaches of the Wahgi River flow eastward for more than 50 km through an intermontane basin, between the Kubor and Bismarck Ranges, before entering the Wahgi Gorge southwest of Mingende (Fig. 1).

In this highlands environment, where tectonism and volcanism have played such an important role in landform development, drainage reorganisation has been relatively common. The often postulated reversal of flow in the Wahgi Valley is of particular interest because it involves a major highland river switching from the north-coast drainage of the Sepik catchment to the south-coast drainage of the Purari catchment.

Drainage reorganisation in the Wahgi Valley has been a topic of discussion since European man penetrated the area in the early 1930s. Michael Leahy, one of the first Europeans to enter the valley, was also the first to speculate on the prior existence of a lake in the area (Leahy, 1936). Rickwood (1955) went into more detail, suggesting that the late or post-Pliocene drainage was dictated by the main fold axes in the area. This drainage pattern, he suggested, was disrupted by vigorous Pleistocene volcanism, which led to capture of the eastern drainage of the Baiyer and Nebilyer Rivers by the Wahgi River. This resulted in deposition and swamp development in the upper Wahgi and Gumants basins. Rickwood contrasted the low gradient and broad, alluvium-filled valley of the Wahgi with the high gradient and narrow alluvium-free valleys of the Lai and Nebilyer Rivers. He also noted the rejuvenation of the Wahgi River as far upstream as Mingende (Fig. 1).

More recent work has added little to this basic story. Haantjens (1970) postulated a river flowing from the Wahgi valley into the Baiyer River, and suggested that the reversal took place in two steps — capture of the then upper Wahgi River in the east, followed by volcanic blocking in the west. However, it is equally possible that these events occurred either together or in the reverse order. Bain & others (1975) reiterated Haantjens, while Löffler (1977) and Pain (1978) reintroduced the idea first suggested by Rickwood (1955) that the Wahgi River may have flowed into either the Baiyer or Nebilyer Rivers, or both.

In this paper we present first an account of the late Cainozoic geology and the landforms of the Wahgi Valley area, and then return to the general question of drainage reorganisation in the context of over-all landform history and drainage pattern development.

Geology

The Wahgi Valley lies between two major structural units in the Papua New Guinea highlands, the Bismarck Fault Zone to the north, and the Kubor Anticline to the south. The Kubor Range is a Mesozoic horst (Pigram & Panggabean, 1984), which has been reactivated and uplifted perhaps as much as 5000 m since the Miocene to form the south side of the valley. Uplift along the Bismarck Fault Zone (Bain & others, 1975) on the north side of the valley produced the Bismarck Ranges. There is little geological evidence for the age of these movements within the Wahgi Valley. However, further east the major movements on the Bismarck Fault Zone postdate rocks of middle Miocene age.

Basement rocks

The Kubor Anticline is cored with Palaeozoic metamorphics and Triassic granodiorite (Bain & others, 1975), and is flanked by Upper Triassic, Upper Jurassic, and Cretaceous sediments. These sediments also occur on the north side of the Wahgi Valley, where they are deformed by the Bismarck Fault Zone, and intruded by Miocene intrusive rocks. Inliers of basement sedimentary rocks occur within the areas of the areas of both the Quaternary volcanic rocks and sediments (Fig. 1).

Quaternary volcanics

The Hagen Range, which rises to more than 3800 m a.s.l., at the western end of the Wahgi Valley, is a large pile of volcanic lavas, pyroclastics, and associated foot-slope deposits. This basaltic stratovolcano (with later andesitic flows) is made up of three coalesced cones aligned north-northeast (Mackenzie & Johnson, 1984). Volcanic breccia and lahar deposits also extend down the Nebilyer River, almost to the junction with the Kaugel River. The foot- slopes, which extend into the upper Wahgi Valley (Fig. 1), are composed of volcanic breccias, a massive volcanic debris avalanche (Blong, 1986), lahar deposits, and airfall tephras.

The whole of the Wahgi Valley has been covered with volcanic ash (airfall tephras) from a number of different sources. Most

[1]School of Geography, University of NSW.
[2]Division of Marine Geosciences & Petroleum Geology, Bureau of Mineral Resources, Canberra.
[3]School of Earth Sciences, Macquarie University.
[4]Gold Fields Exploration Pty Ltd, Canberra.

of the tephra units were apparently erupted from the Mount Hagen volcanoes, but some have come from the east, while others have come from the west (Pain & Blong, 1979). At many sites the tephras are well bedded, and mantle the underlying landscape, thus providing an important means of relative age control on the different geomorphic surfaces, which are discussed below (Table 1).

Lavas from the Hagen Volcanics have radiometric ages between 420 000 and 220 000 years (Loffler & others, 1980; Mackenzie & Johnson, 1984). The massive Mount Hagen debris avalanche occurred at least 80 000–100 000 years ago and probably more than 400 000 years ago (Blong, 1986). The uppermost tephra unit (Tomba Tephra) is older than 50 000 years, the limit of radiocarbon dating (Pain & Blong, 1979). The oldest lahar deposits are older than the lowermost tephra units, while others directly underlie Tomba Tephra. These age relationships are discussed further in the section on geomorphic history.

Quaternary fluviatile and lacustrine sediments

A wide range of Quaternary fluviatile sediments lies on the floor of the Wahgi Valley, extending up the larger tributaries of the Wahgi River (Figs 1, 2). The sediments consist of fanglomerates, lake deposits, flood-plain and terrace deposits, and swamp deposits, and have been named the Minj Group. The nature of the sediments in the valley allows them to be divided into four informal units, Qm_2–Qm_4.

Qm_1 consists of coarse polymictic conglomerate, pebbly sandstone, sandstone and siltstone, and laminated siltstone and mudstone with peat horizons. Coarser clastics, generally massive or poorly bedded, lie near the edges of the valley, while beds of finely laminated carbonaceous mudstone and siltstone are common towards the centre of the valley. This distribution is consistent with Qm_1 deposits being formed on alluvial fans that debouched into and periodically filled a transient lake and swamp environment. The intercalation of coarser sediments with beds of laminated siltstone, mudstone and peat suggests that alluvial fans periodically coalesced across the valley. In most exposures, Qm_1 deposits are strongly weathered, suggesting considerable antiquity.

Qm_2 deposits are similar, although perhaps slightly less weathered than Qm_1 deposits. The basis for the distinction between Qm_1 and Qm_2 deposits lies in the morphology of the fans they underlie (Fig. 3) (see below).

Qm_3 materials occur in terraces in the Wahgi Valley, cut into Qm_1 and Qm_2 deposits (Fig. 3). They typically consist of polymictic conglomerate and sandstone, generally present as a veneer on erosional surfaces cut into the older Quaternary

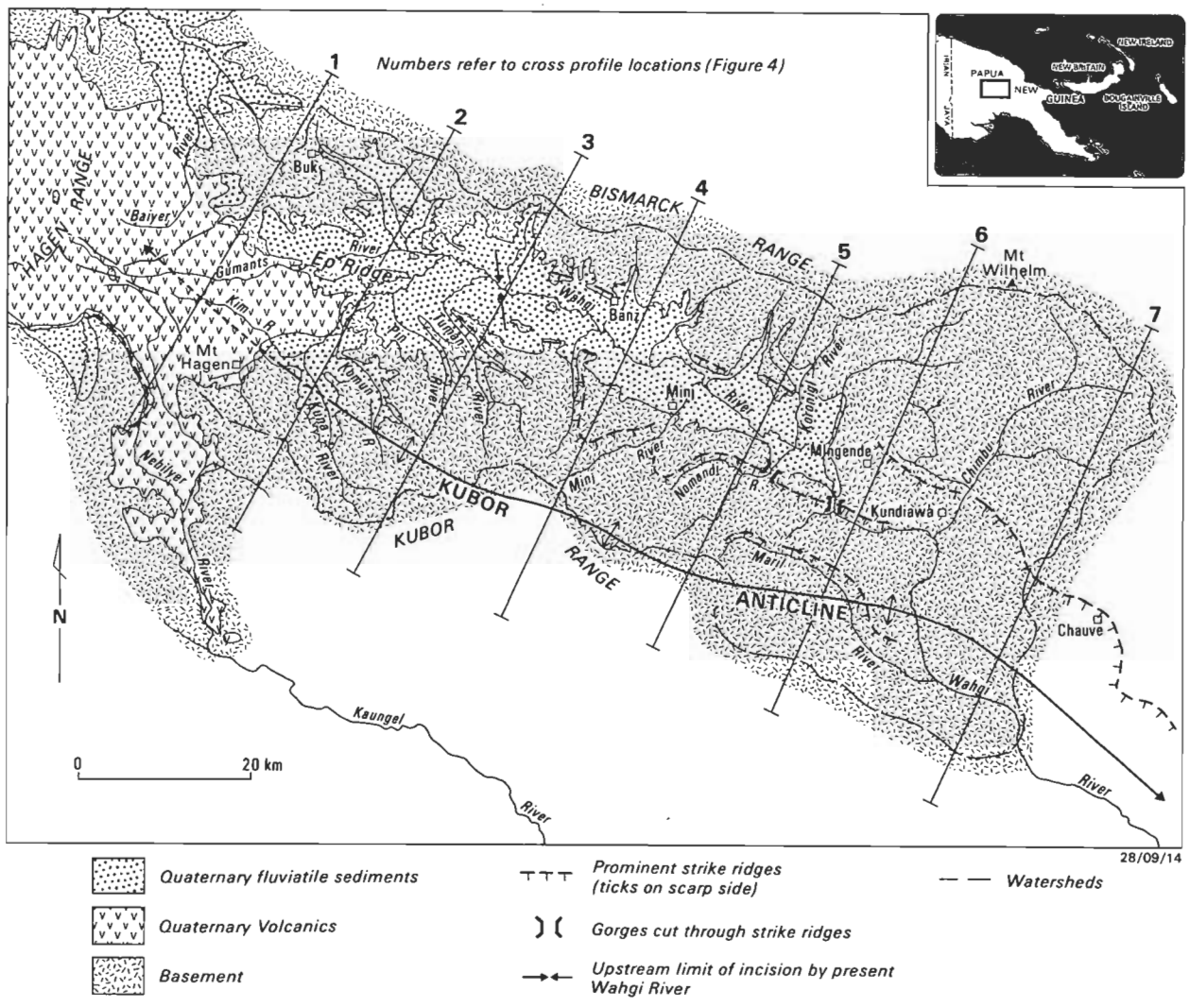

Figure 1. The Wahgi Valley, showing its location between the Bismarck Range and the Kubor Range, and some geomorphic features. Cross-section locations refer to Figure 4. For topographic details refer to Figures 4, 5, 7.

deposits. They are distinctly less weathered than the older deposits, and are a result of alluviation and subsequent downcutting in the Wahgi River meander trench.

Qm_4 deposits consist of gravel, sand, silt, mud, and peat. In the eastern part of the Wahgi Valley they form typical flood-plain deposits, while in the west they underlie extensive swamps such as the North Wahgi Swamp (Fig. 2). Qm_4 deposits are currently being laid down in a variety of environments ranging from distributary fans, flood plains, and active meander belts to alluvial back swamps and organic-rich lakes. However, in some places Qm_4 deposits range back into the late Pleistocene. A sample of wood collected from a layer of silt, clay, and peat below 2.5 m of alluvial gravel and sand near the confluence of the Komun and Wahgi Rivers gave a radiocarbon age of $40\,800^{+3100}_{-2200}$ years (SUA-1278). Similarly, late Pleistocene ages have been obtained from materials in the Kuk Swamp, and in the North Wahgi Swamp (Blong, 1972).

Landforms

Pigram and coworkers (personal communication), following Löffler (1977), divide the eastern part of the Wahgi Valley into six physiographic units. In this paper, their division is modified slightly to take into account the swamps and valley-fill areas in the western part of the valley. Moreover, landforms on basement rocks are not subdivided on our maps (Figs 1, 2).

Landforms on basement rocks

Landforms on basement rocks in the Wahgi Valley all fall into the general category of ridge and V-valley forms (Löffler, 1977). These landforms are generally of high relief, and have dense drainage patterns. Narrow ridges are separated from V-shaped valley floors by long straight or irregular valley side slopes. A distinctive feature of these landforms in some areas is the presence of prominent strike ridges (Figs 1, 4), formed on the sedimentary rocks that dip to the north, away from the Kubor Anticline. Where they occur south of the Wahgi River, these strike ridges have a marked effect on the direction of drainage, good examples being the Nomandi and Maril Rivers (Figs 1, 4). In most places where rivers cross these strike ridges, they do so through characteristic V-shaped gorges such as that on the Chimbu River near Kundiawa (Fig.). The Wahgi River itself leaves the Wahgi Valley and begins its gorge section by cutting through a strike ridge in Wahgi Group

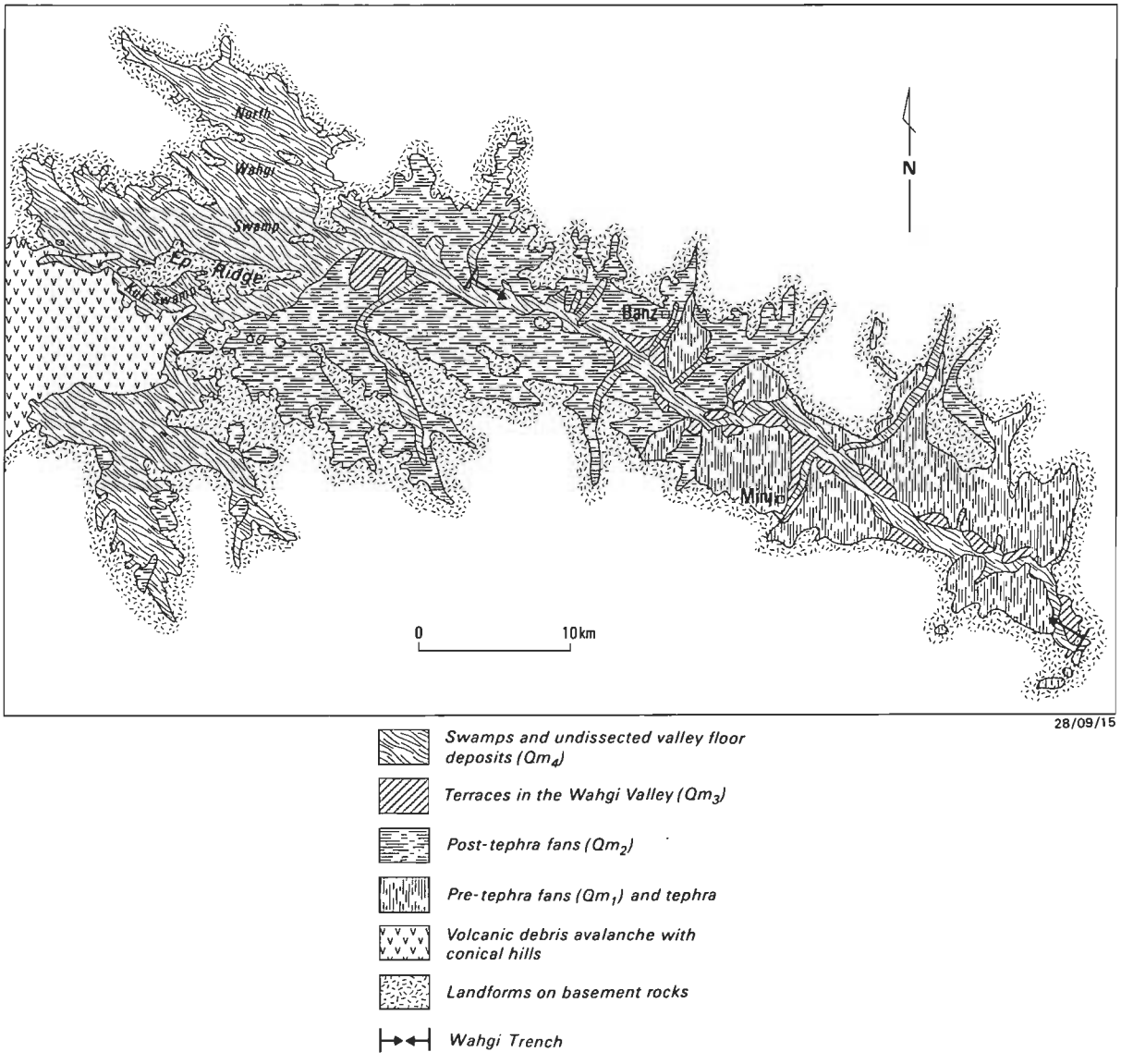

Figure 2. Landforms of the Wahgi Valley, showing the distribution of the major Quaternary landform units and their associated bodies of sediment.

rocks. In the absence of control by strike ridges, drainage patterns are generally dendritic.

Volcanic landforms

A description of the landforms of the Hagen volcanic complex can be found in Mackenzie & Johnson (1984). The upper part of the complex, which lies within the catchment of the Gumants River, a major tributary of the Wahgi River, consists of segments of smooth constructional surfaces separated by relatively shallow, steep-sided stream valleys. These surfaces fall towards a broad area of volcanic foot-slopes, which includes both the northern and southern divides of the Wahgi Valley (Figs 1, 5). The foot-slope area northwest of Mount Hagen town consists of gently sloping, generally smooth foot-slopes with streams incised only a few tens of metres. However, the eastern part of the foot-slope area is underlain by a debris avalanche with numerous low conical hills ranging up to 60 m high (Fig. 2). These hills continue beneath the Quaternary swamp and alluvial sediments of the Kuk Swamp and, probably, western portion of the North Wahgi Swamp (Blong, 1986).

Fans

Fans in the Wahgi Valley fall into two broad groups, based on their degree of dissection, and on the presence or absence of a cover of tephras (Fig. 2). The pre-tephra fan surfaces are underlain by Qm_1 deposits, while the post-tephra fans are made up of Qm_2 deposits (Fig. 3).

Table 1. Tephra units of the Papua New Guinea Highlands, and selected deposits from the Wahgi Valley.

Western (Tari-Mendi)	Central (Mendi-Minj)	Eastern (Minj-Kainantu)
	Qm_2, Qm_3, Qm_4 deposits	
Tomba Tephra	Tomba/Bune Tephras	'upper' tephra
	Balk Tephra	Balk Tephra
	Kiripia Tephra	'middle' tephra
	Kebaga Tephra	
Ambulai Tephra	Ambulai Tephra	Ambulai Tephra
	'basal' tephra	'basal' tephra
	western Qm fans	
Wanabuga Tephra	Wanabuga Tephra	Wanabuga Tephra
		eastern Qm fans
w_1	Turuk Tephra	
w_2	Togoba Tephra	
w_3		
w_4	undifferentiated 'western' tephras	
w_5		
	Hagen debris avalanche	

Notes: 1. Formal tephra names, where 'tephra' is capitalised, are from Pain & Blong (1976). 'upper', 'middle' and 'basal' tephras are described in Pain & Wood (1976). Other tephra units are from unpublished work by C. Pain.
2. Column headings refer to geographical location, and not to the sources listed in Pain & Blong (1979).

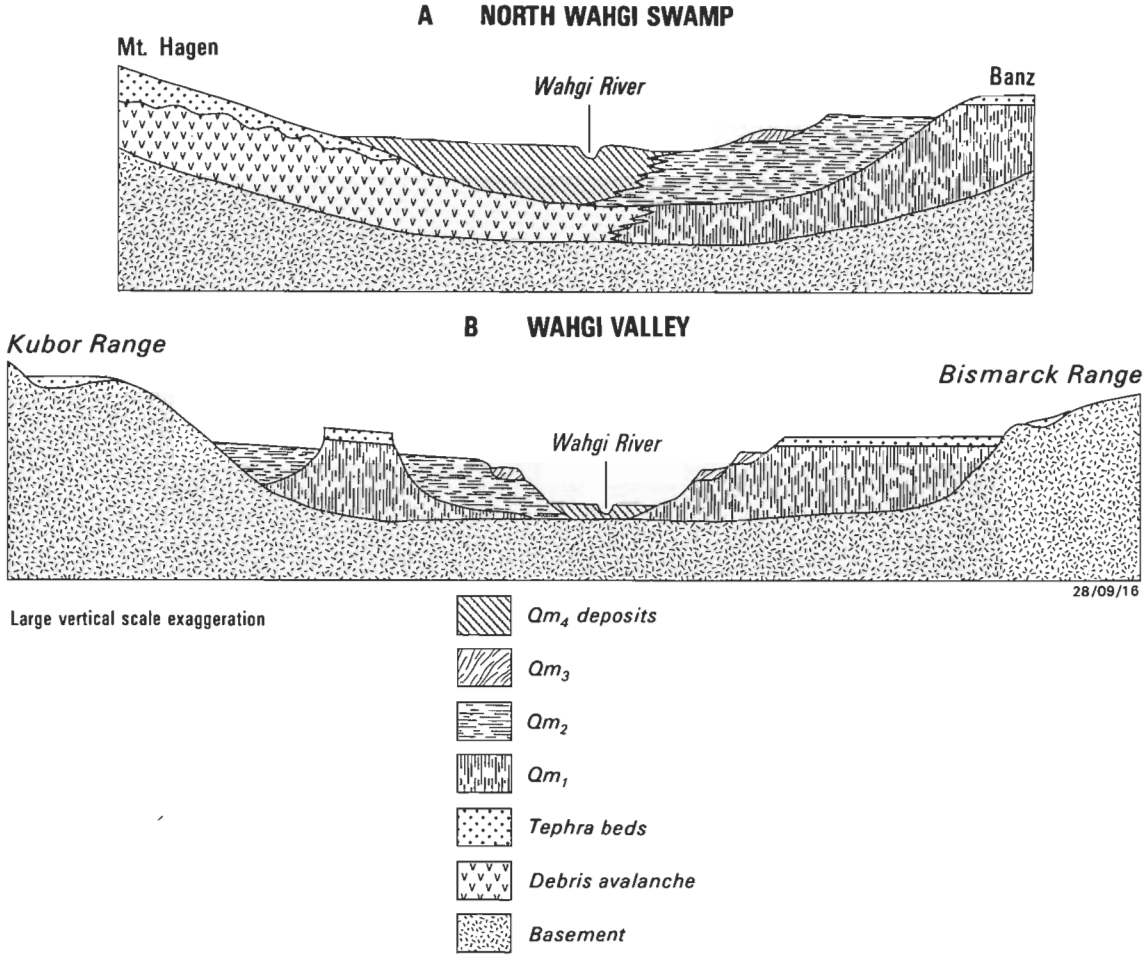

Figure 3. Schematic cross-sections across the Wahgi Valley, A—Western Wahgi Valley; B—Central Wahgi Valley.

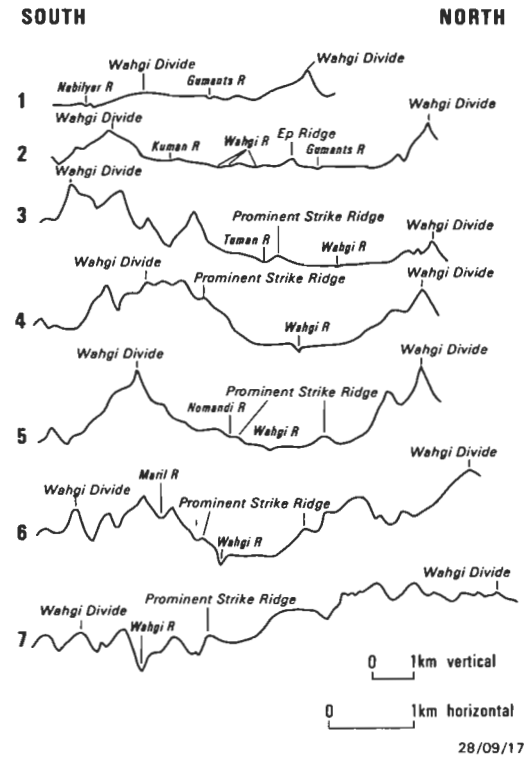

Figure 4. Cross-profiles of the Wahgi Valley, from the southern to northern divides.
See Figure 1 for cross-section locations.

The pre-tephra (Qm_1) fans are strongly dissected by closely spaced gullies and ravines. Original depositional surfaces, now covered with tephra beds, are preserved as long narrow interfluves, which coalesce towards the apices of the fans. These apices can be traced upstream into the ranges bordering the Wahgi Valley. A result of this dissection is that the original cover of tephra is preserved only on undissected parts of the fan surfaces, and is, therefore, often quite limited in extent. The oldest fans in the east are covered with Wanabuga Tephra, and, therefore, were formed before that unit was erupted (Table 1). Fans around Minj on the other hand are covered with 'basal' tephra, but not with Wanabuga Tephra, suggesting that they were formed somewhat later. This observation is supported by the degree of dissection, which increases towards the east.

The upper fan surfaces have elevations between 1560 and 1640 m, and slope gently towards the centre of the valley at angles between 1 and 3 degrees. The pre-tephra fans are the highest alluvial surfaces in the Wahgi Valley.

Post-tephra (Qm_2) fans occupy the central third of the Wahgi Valley Fig. 2). They have well-defined fan shapes, with apices high in the foothills and distal parts coalescing along the middle of the Wahgi Valley. In the west they pass beneath a thin veneer of flood-plain deposits in the meander trench. The upper surfaces of the post-tephra fans have elevations of 1520–1560 m, about 40 m lower than the surfaces of the pre-tephra fans. This difference is marked where the two sets of fans are juxtaposed, for example, west of Minj.

The absence of any tephra cover on these fans, despite the well-preserved nature of their upper surfaces, indicates that they were formed after the deposition of all the tephra units listed in Table 1. The presence of 6 tephra units and associated palaeosols emphasises the time interval between Qm_1 and Qm_2 deposits.

The Wahgi meander trench

The Wahgi Valley is incised into the toes of both pre-tephra and post-tephra fans from about 7 km downstream from the confluence of the Wahgi and Gumants Rivers (Figs 1, 2). From this point to Mingende, the trench increases in depth to 140 m. Within this incised trench, which is about 1.5 km wide, the Wahgi River flows on a flood plain that is characterised by shifting meanders and a number of meander cutoffs. Terraces are developed along the edges of the Wahgi meander trench and the lower parts of the major tributaries that join it (Fig. 2). Löffler (1977) reported two terrace levels, but, while there are usually only two or three levels, the maximum number in one place is five. Along the Wahgi River the terrace remnants are elongate to equant in shape, while along tributaries they tend to be triangular, widening downstream (Fig. 2). All terraces along the Wahgi River slope to the east, and they all postdate tephra deposition.

In some places small fans debouch from the higher fan remnants onto the floor of the meander trench, and in one place, near the eastern end of the valley, two fans constrict the Wahgi River so that there is no flood plain at all.

Swamps and undissected valley floors

The western end of the Wahgi Valley is dominated by swamps and undissected valley fills. In the southwest, the Komun and Kuna River valleys have more-or-less level valley floors, with only minor relief features resulting from flood-plain formation and shifts in the locations of the rivers that flow through them. These infilled valleys may be a result of the damming of their rivers by deposits associated with the Mount Hagen debris avalanche. The northwestern part of the Wahgi Valley consists of two major swamp basins, Kuk Swamp and North Wahgi Swamp (Fig. 2). The Gumants River drains the North Wahgi Swamp and the western part of Kuk Swamp. Undissected valley fill occupies the valleys that drain into the basins. A major bedrock ridge (Ep Ridge) forms an island between the two swamps. Deposition is continuing in the swamps and on the lower valley floors.

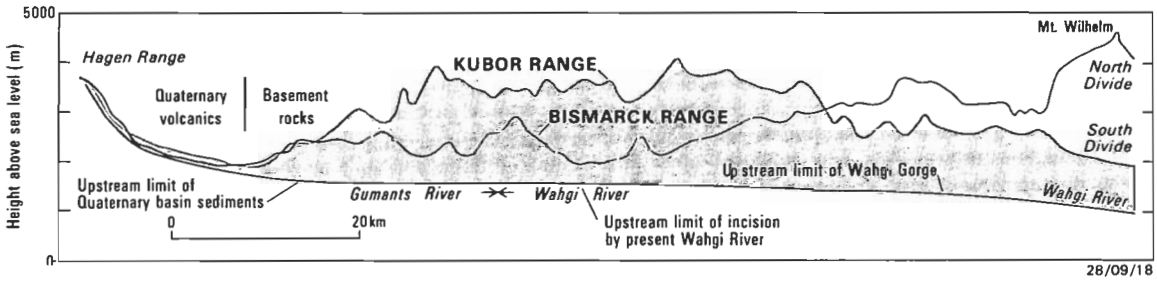

Figure 5. Projected profiles of the north and south Wahgi divides, and the Wahgi River, as seen from the south.
Note the distinct increase in the slope of the Wahgi River downstream from the beginning of the Wahgi gorge. Also note the decrease in elevation of the Bismarck Range, which is parallelled by the sub-Quaternary bedrock elevations on the Wahgi Valley floor.

Minor post-tephra fans (Qm_2, Qm_4) occupy re-entrants in the valley sides.

Geomorphic history of the Wahgi Valley

Earlier attempts to outline the history of the Wahgi Valley have centred on the theme of drainage reversal. We also concentrate on the development of drainage in the area, and consider the other aspects of the geomorphic history of the area in this context.

Various arguments have been used to support the idea of drainage reversal in the Wahgi Valley. The following points come from either Haantjens (1970) or Löffler (1977), and cover those made by other authors:

1. Bedrock elevations below the Quaternary sediments in the valley generally decrease to the west.
2. Valley width increases westwards.
3. Degree and depth of entrenchment and incision decrease westwards.
4. There is a significant westwards decrease in the relative height of fans above the Wahgi River.
5. The deep gorge in Tertiary rocks through which the Wahgi River flows in the east contrasts with the west, where no such obstacle existed in pre-volcanic times.

Two features, the nature of the pre-volcanic landsurface and the Quaternary deposits filling the Wahgi Valley, and their relative ages, provide evidence relating to the theme of drainage reversal.

The pre-volcanic landsurface

A reconstruction of the distribution of land and sea at various times during the Tertiary, such as that carried out by Dow (1977), shows that the Kubor Range became land in the Eocene, and the area that is now the Wahgi Valley has been land since at least the early Oligocene (Fig. 6). Thus, the landscape and drainage system go back at least 35 Ma.

The Wahgi Valley had its origin in the uplift of the northern flank of the Kubor Anticline — for the most part it is a strike-aligned structural depression between the anticline and the Bismarck Fault Zone.

This structural trench is widest in the west, extending eastwards as far as Chuave (Fig. 1), where it becomes narrower. However, serial cross-sections (Fig. 7) show that the valley has been enlarged by erosional removal of northward-dipping sedimentary rocks on the northern flank of the Kubor Anticline. While Wahgi Group rocks crop out throughout (Fig. 8), Cretaceous upper Wahgi Group rocks, the most erodible rocks in the area (Blong & Pain, 1978), are confined to the eastern part of the catchment. In the west, for the most part, basement rocks are more resistant. Thus, river incision could be more easily achieved in the east than in the west (cf. point 5 above). Bedrock slopes (Fig. 5) and westward widening of the Wahgi Valley are suggestive, but not definitive, evidence of a pre-volcanic, westerly flowing Wahgi River.

At least part of the area now covered by the Hagen Volcanics was a topographic high in pre-volcanic times (cf. point 5 above). Inliers of the Cretaceous upper Wahgi Group occur within the area of volcanics; one of these is located high on the Hagen Range, at an altitude of 2700 m (Fig. 1). Hagen Volcanics overlie Upper Jurassic Maril Shale in the Baiyer River gorge above the Baiyer River basin at about 1600 m altitude. The Nebilyer River, to the south, flows on Hagen Volcanics all the way to its confluence with the Kaugel River at 1000 m (Fig. 1). Due west of Mount Hagen town the bed level of the Nebilyer is about 1640 m.

These observations indicate that deep pre-volcanic valleys were connected to both the Baiyer and Nebilyer Rivers, but they do not demonstrate that the Wahgi Valley drained into either.

North of a line joining Ep Ridge and the strike ridge north-east of the Tuman River (Fig. 1) the plan shape of the Wahgi River and its tributaries (and the angles at which they join) is consistent with an easterly flowing drainage network. South of this line, the tributary rivers, including the Tuman, all flow westwards before turning to join the Wahgi, and are thus more consistent with a westerly flowing drainage system. As these differences seem to be unrelated to structural or lithological controls, they perhaps suggest an early drainage divide, as indicated on Figure 8.

Quaternary deposits and landforms

The pre-tephra fans originated from both sides of the valley and coalesced across it. Despite Löffler's (1977) observation that their relative height decreases to the west (point 4 above), the fans do not provide evidence for direction of river flow. The problem here is twofold. First, since the fans slope towards the river, where should elevations be measured?

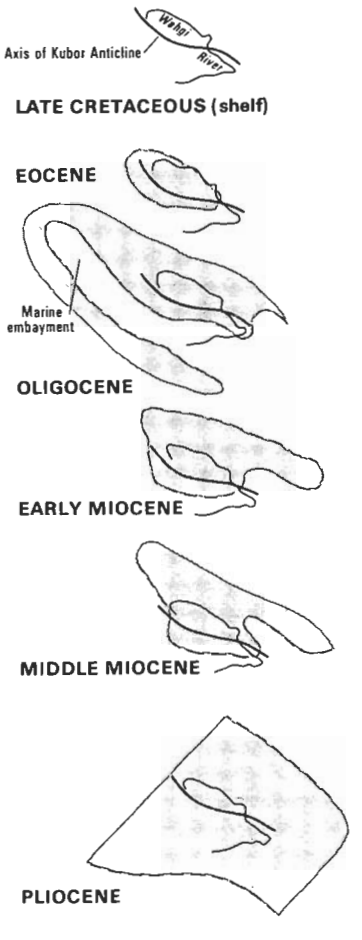

Figure 6. Reconstructions of the distribution of land and sea during the Tertiary in the Kubor Anticline/Wahgi Valley area (after Dow, 1977).

Note that the Kubor Anticline was emergent in the Eocene, and that by the Oligocene the Wahgi Valley area was also land.

Second, active fan deposition is controlled at the apex, not the toe, and therefore is not related to the altitude of the river (cf. point 4 above). If the fan toes did not reach the river, the river would have been unaffected. If the fan toes did reach the river, they would have blocked it, causing lakes to form, perhaps temporarily.

The relative ages of the Quaternary volcanic and sedimentary landforms provide some information about the sequence of events that occurred in the Wahgi Valley in the late Cainozoic. The volcanic footslopes and lahar surfaces range considerably in age. Lavas lying below lahar deposits at Togoba have a K/Ar age of about 200 000 years (Löffler & others, 1980). On the other hand, a shallow trench near the modern course of the Kim River (Fig. 1) contains lahar deposits that are directly overlain by Tomba Tephra, and are thus much younger. However, palaeosol on the main debris avalanche deposit is covered with at least some of the 'western' tephras, which indicates that the avalanche was emplaced at least as early as the early part of the tephra deposition (Table 1). Blong (1986) argues that the absence of an evident source area on Mount Hagen for the avalanche deposit, which has a minimum volume of 3.2 km^3, suggests that the avalanche occurred before the late cone-building phase. This indicates an age of at least 210 000 years and, possibly, as much as 400 000 years. The avalanche and lahar deposits would, by virtue of their volume and location, have been capable of blocking and reversing drainage directions in the western Wahgi Valley. However, there is no direct evidence that drainage ever flowed westwards.

The above consideration of the ages of avalanche and lahar deposits from Mount Hagen shows clearly that any blockage of the western end of the Wahgi Valley must have occurred before (perhaps considerably before) the pre-tephra fans finished forming in the eastern part of the valley (Table 1).

Quaternary lake deposits occur in several parts of the Wahgi Valley. In the west, lake and swamp sediments lie at various levels below the North Wahgi Swamp (Blong, 1972), but the presence of a large continuous lake cannot be demonstrated. However, boreholes have been drilled to a maximum depth of only 35 m; the total thickness of sediments in the basin is unknown, but is probably the order of several hundred metres.

Qm_1 lake beds are exposed in road cuttings at the eastern end of the valley up to 40 m above the present Wahgi River, whereas fan sediments occur at least 160 m higher. The sequence indicates a history of fan deposition into a lake followed by further fan building after the lake was completely filled. The presence of peats in the sequence suggests that swamps may have occupied low-lying areas at some time. Thus, the eastern end of the Wahgi Valley has a modern analog in the western end, where lake, swamp, and fan sediments are interbedded and the area is still occupied by extensive swamps.

The systematic decrease in fan dissection and age towards the west suggests that the Wahgi River began trenching the fans from the east, beginning in pre-Wanabuga Tephra times. As the toe of each fan was trenched, deposition on the fan surface ceased, and fan dissection began, Thus, while trenching and dissection were taking place in the east, fan building was continuing in the middle part of the valley, leading to the formation of the pre-'basal' tephra fans, which were then in turn trenched by the Wahgi River. Major fan building in the west did not cease until after the Tomba Tephra was deposited. The trenching represents the retreat of a knickpoint from the upper end of the Wahgi gorge to the upstream limit of the meander trench during this time.

Unfortunately, there are no direct dates on the tephras or the fan deposits. Löffler (1977) considered that the fans are considerably older than the age of the youngest Hagen lavas, dated about 200 000 years. However, it can now be demonstrated that the tephras are younger than this, because they overlie both volcanic breccias and lahar deposits, which in turn overlie the dated lavas. Wanabuga Tephra, the oldest tephra found on Qm_1 fan surfaces, could be quite a lot younger than 200 000 years, because it lies in about the middle of the sequence of tephras that overlies the dated lavas. As already pointed out, Tomba Tephra is older than 50 000 years. Given these ages, it is clear that the Qm_1 fans in the middle and eastern Wahgi Valley fall in the age range 200 000–50 000 years, while the Qm_4 fans are younger than 50 000 years. Qm_2 fans are still being formed, mainly in the western part of the valley.

Drainage reorganisation

The evidence for drainage reorganisation in the Wahgi Valley is equivocal on several points, and provides support for at least two hypotheses. The two hypotheses differ mainly in the location of the drainage divide before reversal of flow took place.

The generally accepted view has been that the gorge through the strike ridge southwest of Mingende is the location of river capture from the east, and that the previous divide would have been between the Chimbu and Maril Rivers, and the Wahgi River (Figs 1, 8). The Wahgi Valley was dammed in the west by Hagen volcanics, causing a lake to flood the entire

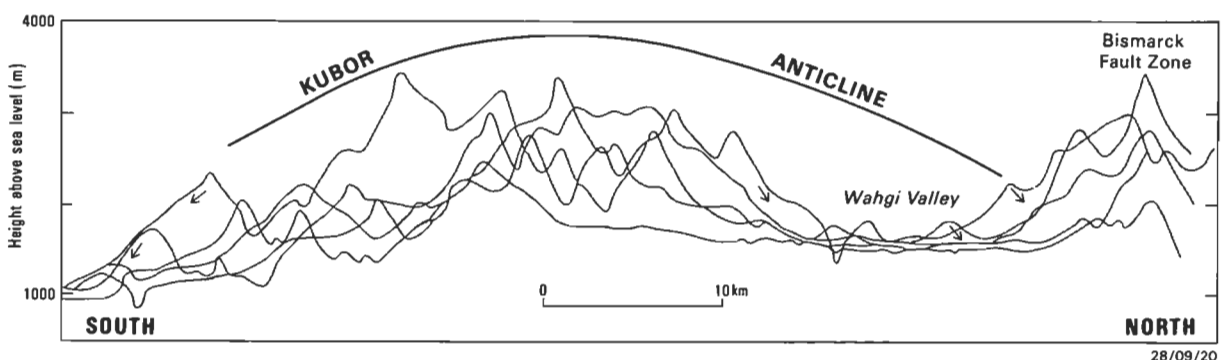

Figure 7. Serial cross-profiles of the Kubor Anticline and Wahgi Valley, as seen from the east.
The outline of the Kubor Anticline is only approximate. Although the valley originated as a structural depression, owing to uplift of the northern flank of the Kubor Anticline by the Bismarck Fault Zone, dip slopes (arrowed) on the north side of the valley show that the Wahgi Valley has been enlarged by erosion of the northern limb of the anticline.

valley and then overtop in the east, leading to river capture (Bain & others, 1975). Haantjens (1970) suggested that river capture may have taken place before blocking in the west, as a result of active knickpoint retreat related to the rejuvenation of the gorge downstream from the present-day Wahgi-Chimbu confluence. Whichever the case, the development of the fans and the deposition of lake and swamp beds must all have taken place either in a lake-filled valley or in a valley with an easterly flowing river.

An alternative, and in some ways simpler, hypothesis is that most of the Wahgi Valley always drained to the east. The previous divide in this case would have passed through Ep Ridge (Fig. 8). Inliers of basement north and east of Ep Ridge suggest that basement is not far below Quaternary sediments in this part of the valley. The debris avalanche from the Hagen volcano diverted the Kuna, Komun, Pin, and Tuman Rivers into the Wahgi River. The Kuna and Komun Rivers may have been completely blocked for some time before the present upper Wahgi River cut a channel between the deposit and basement rocks (Fig. 1). The plan form of these four rivers, structural trends, and the distribution of basement rocks west and south of Mount Hagen town are all consistent with former drainage into the Baiyer River rather than the Nebilyer River.

Following these events, fan formation began in the east, in the process damming the Wahgi River for sufficient periods to allow the the deposition of lake beds and swamp deposits. The location of this depositional activity appears to have shifted westward with time, but this may be an artefact of the trenching pattern, which has occurred from the east.

Extrapolating the slopes of the Koronigl and Nomandi fans to the centre of the valley at its eastern end (Fig. 1) suggests that they met at an altitude of about 1550 m. This altitude places an upper limit on the level of any lake, or lakes, that may have occupied the valley. Perhaps, coincidentally, this is about the level of the lower parts of the North Wahgi Swamp at the present time, and may explain the presence of the swamp. This contrasts with the first hypothesis, which implies a much higher lake level, perhaps shortlived, before overtopping occurred at the eastern end.

Largely for reasons of simplicity, then, the second hypothesis seems more likely. However, whichever hypothesis is preferred, a necessary implication is that much of the activity took place at a time when the valley was adjusted to a higher base level than at present. This is not to say that the area has been uplifted in the last 200 000 years. All that is required is that a knickpoint, or knickpoints, reached the area slightly earlier than the deposition of Wanabuga Tephra, thus initiating the

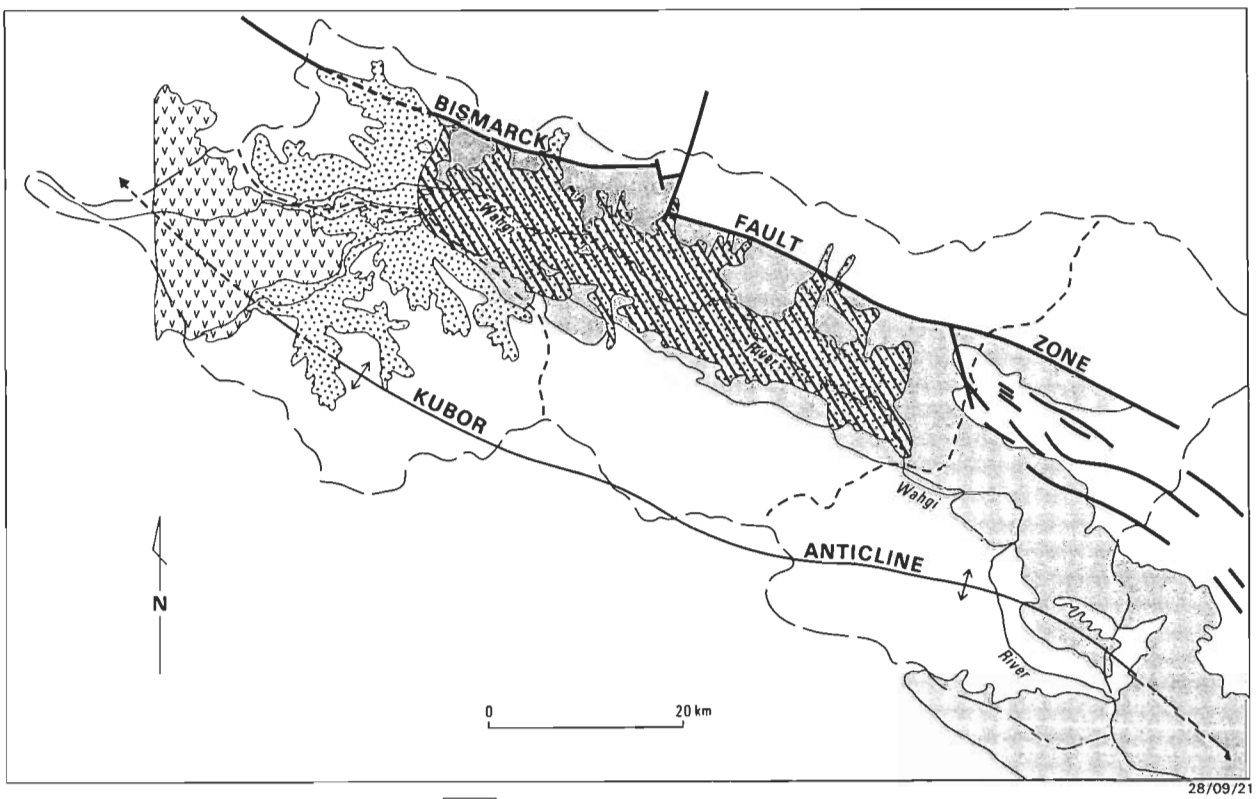

Outcrop of upper Wahgi Group

Subcrop of upper Wahgi Group beneath Quaternary sediments of the Wahgi Valley

Debris avalanche

Boundary of Quaternary sediments

Alternative early drainage divides

Watersheds

Figure 8. The Wahgi Valley, showing the area of outcrop of Cretaceous upper Wahgi Group rocks within the valley, and the two alternative divides between easterly and westerly flowing drainage before the western end of the valley was blocked by lahars and agglomerates from the Hagen volcanoes.

See the section on **Drainage reorganisation** for further explanation of the divides. The distribution of the upper Wahgi Group is taken from Bain & others (1975).

cutting of the Wahgi meander trench. Once this had happened, trenching led to the cessation of fan deposition from the east, as outlined above.

Summary

The relevant points about landform and drainage changes in the Wahgi Valley may be summarised as follows:

1. The Wahgi Valley has its origins as a tectonic depression between the Kubor Anticline and the Bismarck Fault Zone, and results from uplift of the northern limb of the anticline on the Bismarck Fault Zone. However, part of its present form is a result of erosion of sedimentary rocks dipping northward from the Kubor Anticline.

2. Drainage patterns and directions on basement rocks may have originated as long ago as 35 Ma.

3. The eruptions from the Mount Hagen volcano, and any associated blocking of the western end of the Wahgi Valley, took place well before the deposition of most of the Quaternary sediments in the valley. The massive debris avalanche that may have created the blockage occurred at least 80 000–100 000 years ago and, possibly, 400 000 years ago.

4. The formation of fans at the eastern end of the Wahgi Valley took place over a considerable time, during which any drainage of the valley must have been to the east.

5. Trenching of the fans took place from the east as the Wahgi River began to incise its bed. This probably happened as a result of up-valley migration of a knickpoint from outside the study area.

6. The location of the divide between easterly and westerly flowing rivers, before blocking took place in the west, is not clear from the available evidence. It may have been in the east, in which case the entire Wahgi River above Mingende has been reversed. Alternatively, Ep Ridge may mark the previous divide, and only the upper, or southwest, part of the Wahgi Valley has undergone a drainage reversal. This second alternative seems more likely.

Acknowledgements

Funding for fieldwork by CFP was provided initially by the Australian National University, and then the University of Papua New Guinea. Fieldwork by CJP and GOA was carried out while they were employed by the Geological Survey of Papua New Guinea. Fieldwork by RJB was supported by the Wahgi Project (Prof. J. Golson, Australian National University), The Myer Foundation, and Macquarie University. Borehole information has been kindly provided by Wilton & Bell, Dobbie & Partners, and Vallentine, Laurie & Davies, engineering consultants of Sydney. Figures were drafted by Kathy Ambrose.

References

Bain, J.H.C., Mackenzie, D.E. & Ryburn, R.J., 1975—Geology of the Kubor Anticline, central highlands of Papua New Guinea. *Bureau of Mineral Resources, Australia, Bulletin*, 155.

Bik, M.J.J., 1967—Structural geomorphology and morphoclimatic zonation in the central highlands, Australian New Guinea. *In* Jennings, J.N., & Mabbutt, J.A., (editors), Landform studies from Australia and New Guinea, *Australian National University Press, Canberra*, 26-47.

Blong, R.J., 1972—A report on the geomorphology and Quaternary history of the Gumants Basin and surrounding areas, Western Highlands District, Territory of Papua New Guinea. *Geological Survey of Papua New Guinea Data File* 20 DU.

Blong, R.J., 1986—Pleistocene volcanic debris avalanche from Mount Hagen, Papua New Guinea. *Australian Journal of Earth Sciences*, 33, 287-294.

Blong, R.J. & Pain, C.F., 1976—The nature of highlands valleys, central Papua New Guinea. *Erdkunde*, 30, 212-217.

Blong, R.J., & Pain, C.F., 1978—Slope stability and tephra mantles in the Papua New Guinea highlands. *Geotechnique*, 28(2), 206-210.

Dow, D.B., 1977—A geological synthesis of Papua New Guinea. *Bureau of Mineral Resources Australia, Bulletin*, 201.

Haantjens, H.A., 1970—Outline of the geologic and geomorphic history of the Goroka-Mount Hagen area. *In* Lands of the Goroka-Mount area, Territory of Papua New Guinea. *CSIRO Land Research Series*, 27, 19-23.

Leahy, M., 1936—The Central Highlands of New Guinea. *Geographical Journal* 87, 229-262.

Löffler, E., 1977—Geomorphology of Papua New Guinea. *Australian National University Press, Canberra.*

Löffler, E., Mackenzie, D.E. & Webb, A.W., 1980—Potassium-argon ages from some of the Papua New Guinea highlands volcanoes, and this relevance to Pleistocene geomorphic history. *Journal of the Geological Society of Australia*, 26, 387-397.

Mackenzie, D.E. & Johnson, R.W., 1984—Pleistocene volcanoes of the western Papua New Guinea highlands: morphology, geology, petrography, modal and chemical analyses. *Bureau of Mineral Resources, Australia, Report*, 246.

Pain, C.F. & Wood, A.W., 1976—Tephra beds and soils in the Nordugl-Chuave area, Western Highlands and Chimbu Provinces, Papua New Guinea. *Science in New Guinea*, 4, 153-164.

Pain, C.F., 1978—Landform inheritance in the central highlands of Papua New Guinea. *In* Davies, J.C., & Williams, M.A.J., (editor), Landform evolution in Australasia. *Australian National University Press, Canberra.* 48-69.

Pain, C.F. & Blong, R.J., 1976—Late Quaternary tephras around Mount Hagen and Mount Giluwe, Papua New Guinea. *In* Johnson, R.W.,(editor), Volcanism in Australasia. *Elsevier, Amsterdam.* 239-251.

Pigram, C.J. & Panggabean, H., 1984—Rifting of the northern margin of the Australian continent and the origin of some microcontinents in eastern Indonesia. *Tectonophysics*, 107, 331-353.

Rickwood, F.K., 1955—The geology of the western highlands of New Guinea. *Journal of the Geological Society of Australia*, 2, 64-82.

BMR Journal of Australian Geology & Geophysics, 10, 277-286

Eastern Highlands of Australia; their uplift and erosion

Peter Wellman[1]

The Eastern Highlands form a broad arch, with similar cross sections along its length, and varying altitude of its axis. At least on the western margin in Queensland and near Sydney, most of the uplift was by warping. Mesozoic sediments preserved on the summit and flanks of the highlands prove that most of the uplift was after the Early Cretaceous in Queensland, after the mid Triassic near Sydney, and after the Triassic in Tasmania. Uplift of the highlands was most likely initiated at the time of change of the sedimentation pattern and tectonics, 95 Ma ago, as suggested by Jones & Veevers, except that uplift is thought to have started in the Jurassic in Tasmania. Denudation rates vary with local relief. The Cainozoic average rate for Queensland and New South Wales is near 3 m.Ma^{-1}, and for Victoria and Tasmania 5-7 m.Ma^{-1}. Gravity studies show that the Eastern Highlands are on relatively weak lithosphere, so the denudation would have resulted in denudation isostatic rebound of the local area, and the total amount of tectonic uplift is given approximately by the smoothed altitude of the present highlands. In general, the amount of denudation is smaller than the total amount of tectonic uplift. The timing of the tectonic uplift is not well determined, but most is earlier than mid Cainozoic, and there is evidence that possibly one third of it was during the late Cainozoic. The early tectonic uplift is thought to be due to removal of the lower lithosphere from beneath the highlands at the time of rifting to form the Tasman and Coral Seas, leading to uplift both by crustal underplating, and by the short and long-term effects of crustal heating. Later tectonic uplift is thought to be caused by crustal underplating associated with Cainozoic basaltic volcanism.

Introduction

Papers given at a symposium on 'The evolution of the Eastern Highlands' on 9 August 1985 by the Commonwealth Territories Division of the Geological Society of Australia showed a wide range of views on the uplift history of the highlands. There were major differences in opinion on all major issues:

a) The amount of local relief of the highlands in the mid Cretaceous.
b) The timing of the tectonic uplift forming the highlands.
c) Whether tectonic uplift was by underplating, tectonic shortening, or thermal expansion.
d) The average denudation rate.
e) Whether late Cainozoic downcutting of major rivers is a measure of the late Cainozoic uplift rate.

This paper tries to integrate gravity studies of crustal strength, the results of studies of Mesozoic geological mapping, geomorphic studies of river downcutting and denudation, and petrological and other studies bearing on underplating and heating models of tectonic uplift. These subjects are introduced in the above order. The first section of the paper deals with the time of the Mesozoic initial uplift and the shape of the resultant total uplift, the middle section is on Cainozoic denudation and uplift, and the last is on highland uplift mechanisms.

General description of the Eastern Highlands

The Eastern Highlands extend along the length of the eastern margin of Australia, roughly following the coastline (Fig. 1). They are a major watershed, 0.3-1.6 km high and about 400 km wide, separating the interior lowlands, generally of 0.1-0.2 km altitude, from the Pacific Ocean. The distance of the highland crest from the coast is mostly 100-150 km, but up to 400 km in central eastern Queensland. Its altitude varies irregularly along its length. There seems a tendency for higher parts of the crest to be spaced 300-400 km apart, with intervening saddles (geocols) about one third the altitude of the adjacent higher parts. The highlands are of two types — asymmetrical highlands with a steep eastern margin occurring close to the coast north of 18°S and south of 26°S, and inland symmetrical highlands between 18° and 26°S. It is not clear from the shape of the highlands whether the asymmetrical parts result from greater erosion on the eastern margin or asymmetrical uplift.

[1]Division of Geophysics, Bureau of Mineral Resources, GPO Box 378, Canberra, ACT 2601

Isostatic equilibrium

The numerous studies of isostasy in the area of the Eastern Highlands (Wellman, 1976, 1979b; Karner & Weisell, 1984; Stephenson & Lambeck, 1985) show that the crust is close to being in local isostatic equilibrium. Hence, models of tectonic uplift and denudation should incorporate the effect of isostatic equilibrium. (Denudation is used in the sense of general erosion of an area at least 0.5° × 0.5°.)

The precise pattern and amount of isostatic rebound in an area of denudation depends on the pattern and timing of denudation, on lithospheric and asthenospheric physical properties, such as strength and viscosity, on pre- uplift stresses in the lithosphere, and on present-day external stresses acting on the lithosphere (Stephenson & Lambeck, 1985). However, these quantities are poorly known, so this complicated modelling is not recommended. Where the rate of denudation changes only gradually with position, the amount of isostatic rebound can be determined approximately from the local isostatic response to the average denudation over a 0.5° × 0.5° or 1.0° × 1.0° area. For denudation of amount H, the resulting highland after local isostatic rebound will be only slightly lower, how much (h) being given by $h = H.(sm-sc)/sm = 0.12\ H$, where sc is mean crustal density (about 2.9 t.m^{-3}) and sm is mantle density (about 3.3 t.m^{-3}).

On the time scale of 5-10 Ma, isostatic rebound would be simultaneous with denudation. Wellman (1979) showed that for 0.5° × 0.5° areas the variance of gravity anomalies from isostatic equilibrium was 15 600 (μm.s^{-2})^2 in eastern Queensland, and 7200 (μm.s^{-2})^2 in eastern New South Wales and Tasmania, which, because there is some geological variation in crustal density, is equivalent to the present topography being, respectively, better than 62 m and 42 m from isostatic equilibrium.

Time of Mesozoic initial uplift, and shape of total uplift

Pre-erosion shape of the highlands from Mesozoic structural contours

Mesozoic sediments cover about one quarter of the highlands. The altitude and extent of these provide important constraints on the starting time of the uplift that formed the highlands, and also the type of surface deformation resulting from the uplift. Figure 2 shows structural contours on Mesozoic formations, and Figure 3 shows selected cross sections — mainly for Queensland. Which are the best structural

Figure 1. Eastern Highlands of Australia, altitudes.
Continuous contours, 200 m interval; dashed, 100m. From an 11 km × 11 km grid derived from gravity station altitudes, contours smoothed. Bathymetric contours at 1 km intervals.

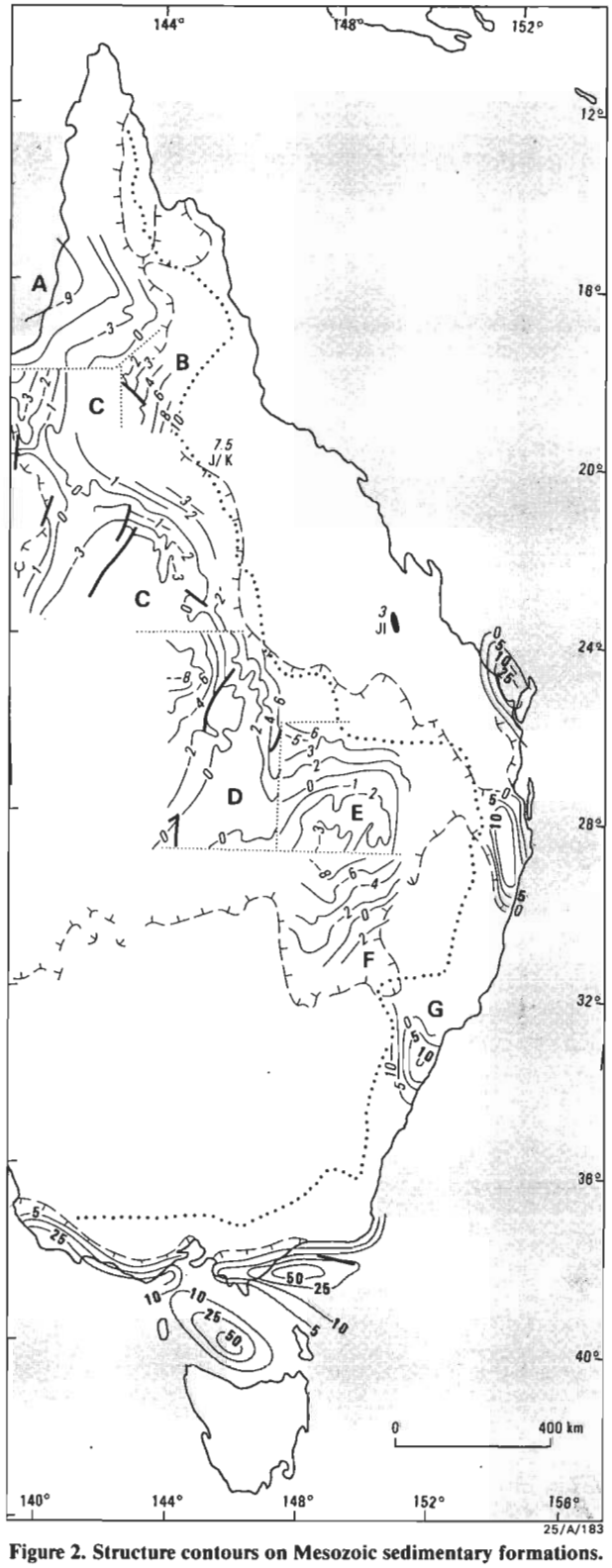

Figure 2. Structure contours on Mesozoic sedimentary formations.
Contours in 100 m units, bold numbers are negative. A, late Albian (from Doutch & others, 1972); B, base of Mesozoic (from J.H.C. Bain, personal communication); C & D, base Albian (from Senior & others, 1978); E, late Aptian (from Exon, 1976); F, late Jurassic (from Hawke & Bourke, 1984); G, base Triassic (from Mayne & others, 1974); other areas from Wilford & others (1981). Faults shown as thick lines. Boundaries of areas shown as lines of small dots. Boundary of continuous Cretaceous and Jurassic sediment shown with dip symbols. Axis of Eastern Highlands shown as line of large dots. The black area is a mid Cainozoic deep fault-bounded trough.

contours to show is problematic, because, although the oldest formations have the widest extent on the highlands, they are relatively more faulted and folded. The contours given in Figure 2 are of the youngest horizon of wide extent for which contours have been published. There is no reason to infer that the regions where Mesozoic sediments occur differ significantly in origin or structure from most of the remaining areas. With the exceptions of Tasmania and central eastern Queensland, mentioned below, the Mesozoic structural information shows that (1) faulting displacements are minor

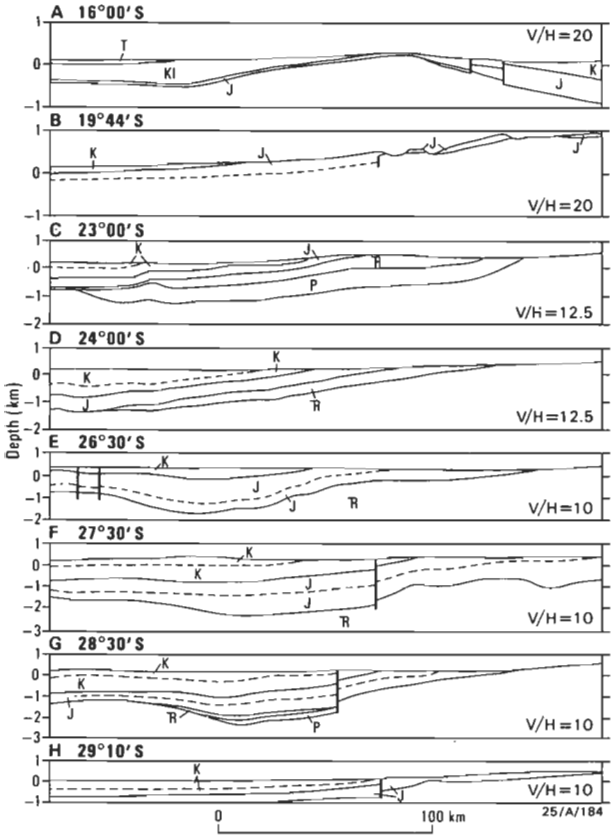

Figure 3. Cross sections showing Jurassic and Cretaceous sediments on the western flanks of the Eastern Highlands.
A & B from Smart & others, 1980; C & D from Senior & others, 1978; E from Exon, 1976; F redrawn from Hawke & Bourke, 1984.

compared with warping displacements; and (2) the highland was formed with gently sloping flanks merging with a wide near-horizontal crest.

Along the central coast of Queensland there are deep, narrow, elongate basins filled with early Cainozoic sediments (Robertson, 1961; Swarbrick, 1974). These basins are up to 1.3 km deep, and fault bounded on the western side. In Tasmania, the Triassic sediments are block faulted and intruded by Jurassic dolerites (Tas. Dept. Mines, 1976).

Uplift in Queensland since the early Cretaceous

During the later part of the Early Cretaceous several periods of high sea level and consequent marine transgression resulted in extensive marine and low-altitude flood-plain sedimentation. The amount of uplift since the marine sediments were laid down is given by the present height of the Cretaceous sediments, plus the early Cretaceous water depth, and minus the drop in sea level since the early Cretaceous. The drop in sea level since the early Albian transgression is estimated here to be 100–150 m, using Figure 2 of Hallam (1981) to calibrate the relative sea-level changes of Vail & others (1977) for the Jurassic. The water depth would be minor (less than 50 m). Sediments of early Cretaceous age cross the crest of the highlands (or are within 50 m height of the crest) at 200 m altitude, west of Laura, at about 15.6°S (Smart & others, 1980); at about 700 m near Georgetown, at 19°S (Bain & others, 1985); at 350 m, east of Hughenden, at about 21°S (Senior & others, 1978); and at 350 m, near Miles, at about 26.5°S (Exon, 1976). The presence of the early Cretaceous sediments shows that the crest of the highlands north of 26.5°S was near sea level in the early Cretaceous, and has since been substantially uplifted to its present altitude.

Cross sections (Fig. 3) show that the thickness of Jurassic and Cretaceous sediments in the basins is less than 2 km, and generally less than 1 km. The original sediments are likely to have thinned towards the axis of the present highlands, but the amount of thinning is variable. The original total thickness was as little as 80 m 40 km southeast of Forsayth (from Bain & others, 1985), while there is no apparent thinning of Jurassic between the Surat and Clarence- Moreton Basins (Fig. 3F). Using the formula given above, the highlands' altitude in Queensland before erosion and isostatic rebound was less than 0.2 km higher than the present highlands (Fig. 1).

An independent argument for the area of the present highlands of Queensland being below sea level in the mid Cretaceous is given by the large volume of sand-size andesitic volcanic material in the Rolling Downs Group of the Eromanga Basin. Eromanga and Surat Basin sediments are of two types (Exon & Senior, 1976): Neocomian and Aptian sediments are largely quartz and resistant rock fragments, and were probably derived from basement surrounding the basins; Albian and Cenomanian sediments are quartz-poor, being dominated by plagioclase and volcanic fragments, and were probably derived from unweathered contemporaneous intermediate and basic volcanics. There is no known volcanism of this age within the basins. The closest is terrestrial (Clarke & others, 1971) andesitic and acidic volcanism, about 111 ± 5 Ma old (Aptian), associated with granites, and occurring mainly offshore along the east coast of Queensland. The amount of material transported is large, and for this to have been a source of Eromanga and Surat Basin sediments there would have to have been no mountain ranges between the present coastline and the basins.

Uplift south of Queensland

In the Sydney Basin, Permian to late mid Triassic sediments extend to the higher parts of the highlands at 1.2 km altitude, proving that all the uplift of this part of the highlands is post mid Triassic. Early Jurassic sediments are preserved in diatremes in the lowland part of the Sydney Basin (Helby & Morgan, 1979), but these sediments may not have extended west. The total amount of eroded sediment is estimated to be 1 km or less (Branagan, 1983), so if the tectonic uplift was completed before erosion, those highlands would have been only 0.1 km higher than the present highlands. The Triassic sediments have few major faults, and the Blue Mountains formed mainly by warping.

In Tasmania, the extensive lower and upper Triassic sediments (Hale, 1962), prove that the uplift was post Triassic. The amount of denudation was inferred by Sutherland (1977) to be 1.5–2 km. The amount of tectonic uplift is given by the present mean altitude, plus 0.2 km for erosion correction, plus a correction for sea-level change and altitude of sediment deposition; a total tectonic uplift of about 0.7 km.

Elsewhere, there is much poorer control on the time of initiation of the uplift forming the highlands, and on the faulting and warping causing the uplift. The Mesozoic sediments of the Maryborough, Clarence-Morton, and Lorne Basins are largely unfaulted, consistent with the eastern margin of the highlands being largely uplifted by warping. However, the sediments do not extend sufficiently high up

the highlands to prove that uplift is post sedimentation. There seems no positive proof that the New England or Victorian highlands were below sea level after the Permian.

The above observations show that the Eastern Highlands did not exist north of Brisbane before the mid Cretaceous, and that they did not exist in central New South Wales in the mid Triassic, and in Tasmania in the Late Triassic. The amount of tectonic uplift since the highlands were formed is likely to be the present mean altitude plus less than 0.2 km.

Pre-Cainozoic surfaces of low local relief

Many geomorphological studies have been made of sub-basaltic land surfaces on the highlands to investigate the local relief during the early to mid Cainozoic. The studies have generally found several hundred metres of former relief in the early and mid Cainozoic, and have disproved the idea that the highlands were a surface of very low relief in the mid Cainozic (Woolnough, 1927).

In some areas, the apparent high local relief in the early Cainozoic landscape is due to warping by Cainozoic intrusions. Studies of the sub-basaltic surface under major Cainozoic volcanoes generally show a dissected dome under the volcanoes; this is 0.5 km high under the Barrington Volcano (Galloway, 1967). Wellman (1986) has shown that each of these volcanoes has an underlying associated intrusive complex, which has domed up the basement under the volcano, the dome being 0.3 to 0.7 km high, with a diameter of about 30 km. Hence, is likely that the pre-volcanic surface in the area of these volcanoes had a low relief.

There are many highland areas, such as near Georgetown, near Armidale, near Crookwell, and in the Victorian High Plains, where steeply dipping basement rocks at high altitude are truncated to low relief. In places where they are overlain by mid Cainozoic lavas the post mid Cainozic erosion has increased the relief by more deeply dissecting the softer rocks and areas around thicker lavas. It seems likely that these surfaces of low relief were formed by denudation of the landscape close to a base level that was stable over a long time, as suggested for the Crookwell area by Young (1981). The surfaces of low relief probably formed at various times in the Palaeozoic and Mesozoic. Many were unconformities overlain by soft rock, which was subsequently eroded (e.g. parts of the western margin of the highlands in Queensland). It seems likely that the highlands had their lowest relief in the late Mesozoic, and that major uplifts were younger, as stated earlier by Craft (1933).

Initiation of the Eastern Highlands 95 Ma ago

Jones & Veevers (1983) summarised the considerable evidence for a change in sedimentation pattern and tectonics at 95 Ma ago, and they suggested initiation of the highlands then. 95 Ma ago (Cenomanian) was the end of andesitic volcanogenic sedimentation in Queensland and Bass Strait areas. In all the active basins — Carpentaria, Eromanga, Surat, Maryborough, Clarence-Moreton, Otway, Gippsland, and Murray Basins — it was either the end of basin subsidence and sedimentation and the begining of deep weathering or it was a major unconformity. In terms of plate tectonics, 95 Ma ago is thought to have been a time of change, from the margin of Australia being a convergent boundary north of Brisbane and an oblique-slip boundary south of Brisbane, to the later crustal extension and 80-60 Ma seafloor spreading.

The conclusion of Jones & Veevers (1983) that the initiation of the highlands was 95 Ma ago is consistent with the stratigraphic evidence of the previous section, except in Tasmania, where some uplift is thought to have been caused by the Tasmanian dolerites (M.R. Banks, personal communication).

Cainozoic denudation and uplift

Highlands denudation rates

The following section summarises the available information on highlands denudation. The strong evidence for low denudation rates is critical in showing that tectonic uplift is much greater than denudation rebound uplift (c.f. Stephenson & Lambeck, 1985). Denudation rates are quoted as $m.Ma^{-1}$. ($1\ m.Ma^{-1} = 1$ mm/1000 yr = 1 Bubnoff unit (B)). Note that the denudation rate is the average erosion rate over an area, as distinct from the downcutting rate of a river, which may only reflect local erosion of the river bed.

Highlands denudation rates from adjacent basins. Bishop (1985) has calculated rates of denudation for the western margin of the southeastern highlands. The volume of post Oligocene sediment in the Lachlan fan portion of the Murray Basin and in the Lachlan's upland valley is equivalent to a denudation of 100 m over the last 25 Ma for the highland part of the catchment, giving an average rate of $4\ m.Ma^{-1}$; this is a minimum estimate because of sediment and dissolved material not preserved in this area. Similarly, Tertiary sediment in the Murray Basin (corrected for limestone) gives a minimum denudation of 200 m over 65 Ma (an average rate of $3\ m.Ma^{-1}$), assuming that there was no significant contribution from the Darling River to the Murray Basin.

Similar minimum estimates of the highlands erosion rate can be made using isopach maps of three cycles of erosion of onshore Cainozoic sediments of the Karumba Basin (Smart & others, 1980) together with estimates of the area of the eroding highland. Because these are very shallow sloping basins it is expected that much sediment and all dissolved material has passed through the onshore basin and is offshore, so the denudation estimates are minimum values, and the true rates may be 2-3 times higher. The minimum denudation calculated is 30 m for the Bulimba Formation, 10 m for the Wyaaba Beds (both northwest of the Georgetown Inlier), and 50 m for the Claraville and Wondoola Beds (southwest of the Georgetown Inlier). Adding these together, the minimum estimate of total highlands denudation is 90 m over 65 Ma, or $1.4\ m.Ma^{-1}$.

P.J. Davies (personal communication) calculated the sediment volume on the continental shelf between Eden and Newcastle as 3400 km^3. The density of these sediments is about $2.0\ t.m^{-3}$, compared with $2.7\ t.m^{-3}$ for the highlands rocks. Finer sediment and dissolved matter bypass the shelf. Therefore, as the shelf was formed 80 Ma ago, this gives a minimum denudation rate of about $0.9\ m.Ma^{-1}$

Denudation of highlands crest. In the Georgetown area of northeast Queensland (Bain & others, 1985, Bain, personal communication) the denudation since the mid Cretaceous has been roughly 80 m of Jurassic and early Cretaceous cover and 50 m of basement, a total of 130 m over 130 Ma, or an average rate of $1.0\ m.Ma^{-1}$. On the western flank of the southeast Queensland highlands, Galloway (1987) found that erosion to expose granite indicated denudation at $10\ m.Ma^{-1}$ over the last 100 Ma, that resistant Mesozoic rocks give a rate of more than $3\ m.Ma^{-1}$, and that erosion of three weathered profiles gave rates of 2, 1, and less than $1\ m.Ma^{-1}$ since 20 Ma ago.

For the Armidale area of northern New South Wales, Ollier (1982a) calculated a denudation rate since 33 Ma ago of between 1.5 and 10 m.Ma^{-1}. More recently, Schmidt & Ollier (1987) have shown that deeply weathered volcanics capping hills were weathered in the mid Cretaceous. These volcanics are in an area of 80 m relief, giving a denudation rate of less than 1 m.Ma^{-1}. Speight (1985) estimated denudation rates for the tablelands near Nowra as 0.5 m.Ma^{-1} for the two periods Permian-Eocene and Eocene-present. For this tableland Young (1983) found a denudation rate between 0.66 and 1.8 m.Ma^{-1} since the Eocene, and Ruxton & Taylor (1987) gave a denudation of 200 m in 44 Ma, or 4.5 m.Ma^{-1}. To the west, near Crookwell, the hills are flat topped and partly covered with lavas approximately 40 Ma old, while the Lachlan River has cut down 80 m in 20 Ma (Wellman & McDougall, 1974; Bishop & others, 1985). As the interfluves in this area have not been downwasted significantly, the denudation rate for the whole area must be less than the river downcutting rate of 4 m.Ma^{-1}.

In the southeastern highlands, several studies on the highlands axis of relatively low relief have shown that Eocene basalt flows are preserved, and post Eocene denudation has been small (?50 m) (Young, 1977, 1981; Ruxton & Taylor, 1982; Taylor & others, 1985). However, Jurassic shallow intrusive rocks (plugs, dykes, laccoliths, and sills) are common in the same general area (McDougall & Wellman, 1976; Dulhunty, 1976; Carr & Facer, 1980; Embleton & others, 1985). The volcanic rocks that must have accompanied these shallow intrusives are nowhere preserved, and, therefore, denudation since the mid Jurassic (170 Ma ago) must have been at least equal to the present-day relief in these areas.

Denudation of the highlands margin. The eastern margin of the highlands in northeast Queensland and south of Brisbane is generally very abrupt, and it is separated from the coastline by low hills (Fig. 1). In no area is there good evidence that the scarp is a fault line scarp, and it is probably an erosional feature (Ollier, 1982b). Where the amount of erosion changes abruptly from a high to a low rate, the land surface will be upturned on the low erosion side of the scarp by isostatic rebound. This is likely to be the explanation for the relatively high peaks at the eastern margin of the highlands, where high-altitude highlands are adjacent to wide low-altitude lowland.

Erosion of the eastern margin of the highlands was by deep dissection (e.g. Blue Mountains, 33°S 150°E) or rapid scarp retreat reducing the altitude of large areas (e.g. Bega Valley, 37°S 149.5°E). The minimum amount of material eroded is given approximately by ignoring isostatic rebound and assuming that the previous highlands surface extended down linearly to the coastline from the present escarpment, and that one half of this volume has been removed by erosion. Between Eden and Newcastle this gives a minimum denudation rate of 0.12 km over 80 Ma or $>$ 1.6 m.Ma^{-1} (Ollier, personal communication).

Speight (1985) has estimated a denudation rate of 5 m.Ma^{-1} for the margin of the highlands east of the escarpment near Nowra. Sutherland (1977), using zeolites in the Prospect intrusion near Sydney, inferred a burial of 0.8-1.0 km since 168 Ma ago, giving a denudation rate of 5-6 m.Ma^{-1} for the Sydney Basin. For the deeply dissected Hunter Valley in central New South Wales, Galloway (1967) calculated a denudation rate of 5-10 m.Ma^{-1}, depending on the depth of the original basalt cover. Basalt is unlikely to have completely covered the valley, and a value near 5 m.Ma^{-1} seems more probable.

There is good evidence that the coastal strip along the eastern margin of the highlands differed from the rest of the highlands, in that it had a period of thermal uplift with deep erosion in the mid Cretaceous, at the time of initiation of seafloor spreading. Moore & others (1986) studied basement apatites between Woolongong and Melbourne. They showed that along the coastal strip there was a thermal event 80-100 Ma ago that resulted in considerable erosion. The erosion is estimated to be 2-2.5 km near Batemans Bay, and 1.5-2 km between Batemans Bay and Bairnsdale. Evidence for similar thermal uplift and erosion along the coastal part of the Sydney Basin at this time is given by a mid Cretaceous, palaeomagnetic, thermal overprint on Sydney Basin sediments (Schmidt & Embleton, 1981), petrological studies of sediment diagenesis (Raam, 1968), zeolites in a Jurassic intrusion (Sutherland, 1977), and studies of coal maturation (Middleton & Schmidt, 1982).

In Tasmania, rates have been calculated by Sutherland (1977), using zeolites in Jurassic intrusions as depth of burial indicators. He calculated a burial of 1.6-2.2 km since 165 Ma ago, giving a denudation rate of 10-15 m.Ma^{-1}. In the valleys of the Ringaroom and Jordan Rivers, dated Cainozoic lavas (Sutherland & Wellman, 1986) are consistent with river downcutting at an average rate of 6 m.Ma^{-1} since the mid Cainozoic. The denudation rate here would be lower. Deep dissection in Victoria suggests a fast denudation rate there.

Mean denudation rates. The denudation rates given above for Tasmania are 6-15 m.Ma^{-1}, and for Queensland to southeastern New South Wales generally 0.5-6 m.Ma^{-1}. All values of denudation rate are very uncertain, but a mean value of about 5-7 m.Ma^{-1} for Tasmania and eastern Victoria, and about 3 m.Ma^{-1} for New South Wales and Queensland seems most likely.

The Appalachian Mountains have a similar mean denudation rate of 3 m.Ma^{-1} for the Mesozoic and Cainozoic (Chorley & others, 1984, p. 56).

Episodic uplift and denudation

In the Karumba and Murray Basins 3-4 cycles of sedimentation are recognised. These cycles were interpreted by Smart & others (1980) and Jones & Veevers (1982) as being due to several periods of uplift and consequent fast erosion, the uplift being associated or caused by igneous activity. However, geomorphological studies (Young, 1977; Bishop & others, 1985) have shown that the erosion rate of the west part of the highlands is relatively low and insensitive to uplift, and Brown (1983) showed that the cycles of deposition in the Murray Basin are better explained as being caused by eustatic changes in sea level. In the land part of the Karumba Basin the sedimentary cycles may be due to these eustatic sea-level changes or climatic changes or both, as mentioned by Smart & others (1980), and also in part to episodic lowland warping in an area of continuous sediment passage. In neither the Karumba nor Murray Basin is there proof of episodic uplift.

Distribution of uplift with time and rate of river downcutting

In studying uplift it is desirable to separate it into its two components:

1) tectonic uplift, which increases the average elevation of the highlands, and

2) denudation rebound uplift, which results in a slightly lower average elevation of the highlands, although rock bodies are uplifted.

In Queensland and New South Wales the present altitude of the axis of the highlands varies from 300 m to over 1000 m

(Fig. 1); the total amount of tectonic uplift will be only slightly greater than this. The denudation rate averages about 3 m.Ma^{-1} and, therefore, as the denudation rebound uplift over the last 100 Ma would be about 300 m in the highlands, the denudation rebound uplift would generally have been less than tectonic uplift.

Uplift can be studied by measurement of the absolute altitude of the highland axis. Preliminary measurements of altitude using oxygen isotopes in clays were reported by Bird & Chivas (1985), and this method may provide useful results in the future. Uplift is usually inferred from the relative movement of rocks on the highlands margin, from river downcutting. However, there is disagreement as to the interpretation of the river downcutting observations, because the two likely geomorphic models lead to similar histories of late Cainozoic river downcutting. The geomorphic models relate to the possible maximum rate of river downcutting, and the timing of the tectonic uplift. Downcutting rates will not be constant, because of temporary barriers to river downcutting, and climate and vegetation changes. These changes in downcutting rate will lead to variation in downstream sedimentation rate.

The two extreme models for downcutting of major rivers in the outer part of the highlands (downstream of discontinuities in river bed profile caused by rock that is exceptionally hard to erode) are: 1) fast river downcutting — the river bed in the outer part of the highlands cuts down sufficiently fast to maintain a constant profile and altitude relative to the base-level outside the highlands, while the surrounding highlands rocks are relatively raised by tectonic uplift and denudation rebound uplift; 2) slow river downcutting — the river bed on the outer part of the highlands cannot cut down fast enough to maintain a constant profile during fast tectonic or denudation rebound uplift of the highlands.

(In this paper the amount of river downcutting is taken to be the height difference between the top of the Cainozoic river gravels and the top of the present gravels. The river downcutting is not taken as from the top of the Cainozoic lava flows to the top of the present day river gravel (Bishop, 1985a), because what we are really interested in is the downcutting that would have taken place if the lava flow had not occurred.)

There are many hypotheses concerning the timing of the tectonic uplift of parts of the highlands.

1) Pre-Mesozoic for the southeastern highlands (Stephenson & Lambeck, 1985; Lambeck & Stephenson, 1985; Bishop & others, 1985). This is impossible on geological grounds, Triassic sediments forming the highest parts of these highlands.
2) Pre-Cainozic.
3) Pre-mid Cainozic (Craft, 1933; Young, 1977; Young & McDougall, 1982).
4) Mainly late Cainozoic (Andrews, 1911; Browne, 1969; Doutch & others, 1970).
5) Throughout the late Cretaceous and Cainozoic (semi-continuous) (Hills, 1940; Wellman & McDougall, 1974b; Wellman, 1974, 1979a; Ollier, 1978; Smart & others, 1980).

There is now general agreement that the presence of mid-Cainozic basaltic flows deep within valleys in the southeastern highlands makes it impossible for the tectonic uplift to be mainly late Cainozoic in this area.

The two presently favoured models are: a) Pre-mid Cainozoic tectonic uplift and slow river downcutting of major rivers (Craft, 1933; Young, 1977; Young & McDougall, 1982; Bishop & others, 1985); b) semi-continuous tectonic uplift and fast river downcutting of major rivers (Hills, 1940; Wellman & McDougall, 1974b; Wellman, 1974, 1979a; Ollier, 1978).

It is difficult to separate these models on the rate of river downcutting or the past profiles of major rivers, because, when the uncertainty in the amount of denudation and denudation rebound uplift is allowed for, the erosion delay in the early-uplift slow-downcutting model has similar effects to semi-continuous-uplift and fast-downcutting.

I outline below four arguments in favour of the model with semi-continuous tectonic uplift and fast river downcutting.

1) There are several places with Miocene basalts overlying gravels just upstream of where the rivers change from downcutting to aggrading (Fig. 4). Here there is a large height difference between the Late Cainozoic and present river bed levels. If all tectonic uplift is earlier than mid Cainozoic, then even at low downcutting rates the rivers just within the margin of the highlands would now have a level close to the base level outside the highlands, because the downstream parts of a river bed adjust level first. As the amount of downcutting is greater than the expected rate of denudation, these localities support the model with some late Cainzoic uplift and fast downcutting.

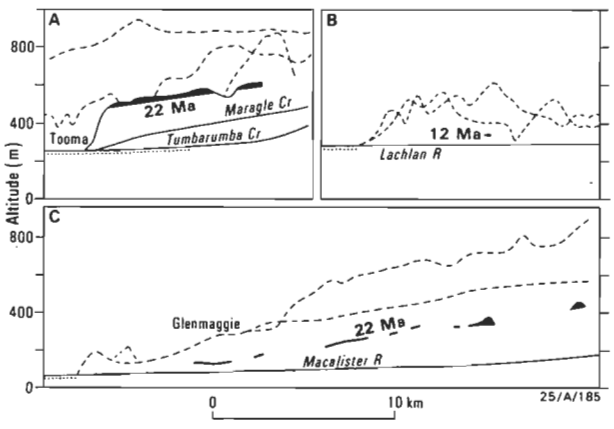

Figure 4. Profiles along river beds.
Showing present river bed (solid line, dots where alluviated), level and age of mid Cainozoic lava flows overlying river gravels (black, ages in Ma), and levels of the valley margin (dashed lines). Ages from Wellman & McDougall (1974b), Wellman (1974), and McKenzie & others (1984).

2) The lower Snowy River near Gelantipy has a low, uniform gradient, consistent with it being able to achieve fast river downcutting. The river has a high late Cainozic downcutting rate of 10 m.Ma^{-1} (Wellman, 1974), which is much greater than any likely denudation, as the area to the west is relatively flat and covered by early Cainozoic lava flows. This area is likely to have had late Cainozoic tectonic uplift and fast river downcutting.

3) Much of the area of the (Mesozoic) Clarence-Moreton Basin is covered by remnants of mid Cainozoic (mainly 24–20 Ma) basaltic lava flows. Figure 5 is a contour map of the altitude of the base of these lava flows. The high sub-basaltic altitude on parts of the basement north, east, and southwest of the basin is attributed to basement generally being more difficult to erode than the basin sediments. Sub-basaltic highs at A, B, & C in Figure 5 are interpreted as being due to Cainozoic upper-crustal mafic intrusions (Wellman, 1986). The other major feature on the map (Fig. 5) is an abrupt step in the sub-basaltic altitude along 152.8°-152.9°E,

which coincides with a series of faults and anticlines in the Clarence-Moreton Basin sediments. The step in sub-basaltic level is trangressive across the boundaries of the basin sedimentary formations, so it is not likely to be due to differences in formation erodability. It is thought that at the time of the 24–20 Ma volcanism, or up to 20 Ma earlier, the surface of the basin varied gradually in level, and that the 200–300 m step in level is due to mid to late Cainozoic uplift of the southwestern part of the basin. This interpretation is consistent with a mid to late Cainozoic uplift of the New England highlands of at least 300 m and, hence, consistent with semi-continuous uplift and fast downcutting of rivers.

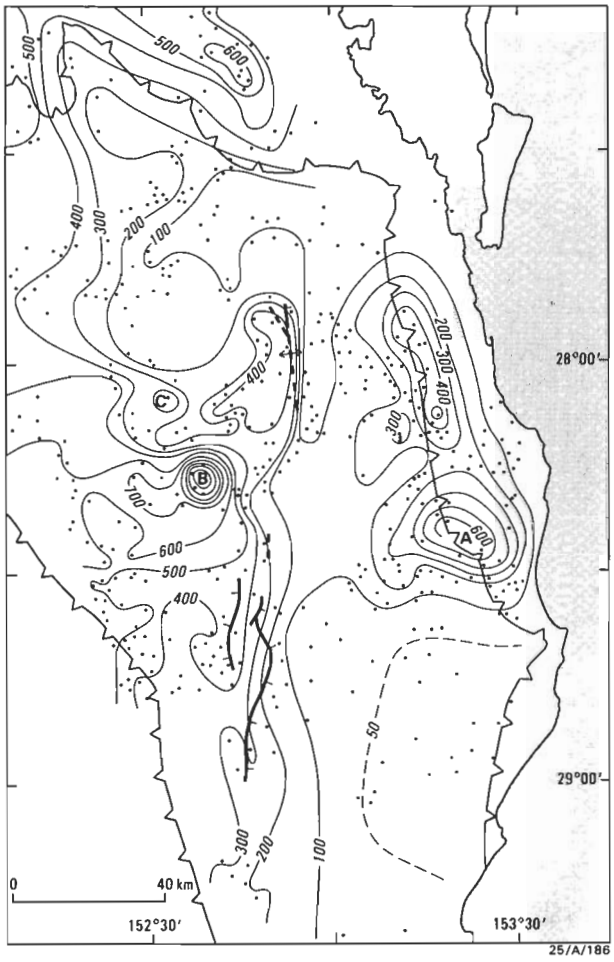

Figure 5. Altitude of the sub-basaltic surface in the Clarence-Moreton Basin.
Contour interval mainly 100 m; dots show location of data points. Symbols show faults and anticlines in the basin sediments and the generalised basin margin. A, B, and C are associated with Cainozoic central volcanoes.

4) In northeast Queensland there are three broad areas of uplift of the highlands, corresponding to three vent areas of volcanism in the last 5 Ma — Atherton Province, McBride Province, and the combination of Chudleigh, Nulla, and Sturgeon Provinces (Stephenson, 1987). The uplift was thought by Stephenson to pre-date the volcanism, at least in the southern area. The three uplifts are about 400 m high and 100 km across, superimposed on a 500 m high, 400 km wide main highlands. It seems very likely that they and the volcanism are related both in space and time, the magma causing uplift in passing through the lithosphere on its way to the surface in the late Cainozoic, both by its underplating the crust and by its heating of the lithosphere. Hence, in this area it is likely that there was approximately 400 m of late Cainozoic tectonic uplift.

The above four arguments support tectonic uplift continuing in the late Cainozic, and they therefore favour the model of semi-continuous tectonic uplift and fast river downcutting. In southeastern New South Wales, eastern Victoria, and Tasmania there is evidence for uplift before the Eocene in the occurrence of Eocene basaltic flows deep within river valleys. Except for the Georgetown region, there is little evidence for pre-Eocene uplift in Queensland. In the Georgetown region a late Jurassic-Early Cretaceous sedimentary sequence, 80 m thick, was laid down as a thin extensive sheet. Cut into the basement below this sheet in the valleys of the Langdon and Etheridge Rivers are river valley deposits of the Bulimba Formation (Mackenzie & others, 1979 a & b; D.E. Mackenzie, personal communication), 30 m below the level of surrounding basement hills. The Bulimba Formation was deposited between Albian and mid Cainozoic. In the period between deposition of these sequences (between the mid Cretaceous and mid Cainozoic), there must have been over 110 m of valley incision, and a greater amount of uplift. This is probably the best evidence that some of the uplift in north Queensland was pre-mid Cainozoic.

Mechanisms of highland uplift

There are several possible mechanisms of uplift of the present Eastern Highlands. All involve crustal thickening, because gravity studies show that the area is in isostatic equilibrium.

1) The highlands may have been thickened and uplifted in the Palaeozoic, and may be 'primarily an erosional residue of Paleozoic orogenies' (Lambeck & Stephenson, 1985). This timing is impossible for the whole of the present highlands, because of extensive Mesozoic sediments on the highest parts of the highlands axis in Queensland, the Sydney Basin, and Tasmania (Fig. 2). It is unlikely to apply to any of the highlands.

2) The highlands could have been uplifted by post-Palaeozoic thrust faulting or folding, causing crustal shortening and thickening, with consequent isostatic uplift. However, there is no evidence for this crustal thickening mechanism since the Palaeozoic. Similarly, there is no evidence that the uplift is the result of continental collision and accretion, as suggested for the world's major mountain ranges by Ben-Avraham & others (1981).

3) Karner & Weissel (1984) proposed that uplift was caused by crustal and lithospheric heating, owing to asymmetric lithosphere stretching, before and during rifting and seafloor spreading that formed the Tasman and Coral Seas, 80–60 Ma ago. The upper crustal heating, underplating, and replacement of the lower lithosphere would result in expansion and isostatic uplift, followed by erosion, cooling, and some sinking. The model gives a Late Cretaceous–early Cainozoic uplift, and is consistent with the location of the higher parts of the highlands, with the crustal heating 80–100 Ma ago, and with the westward apparent migration of the initiation of the Cainozoic volcanics (Wellman & McDougall, 1974a). However, there is no evidence for much late Cainzoic sinking. Lambeck & Stephenson (1985) rejected this model on the basis that 'the wavelength of the eastern half of the highland (up to 2000 m elevation change in 150 km) is inconsistent with the thermal uplift model'.

4) Lister & others (1986) have proposed that the lithosphere extension prior to formation of the Tasman and Coral Seas was by low angle detachment faults, which removed the lowermost crust and lower lithosphere from beneath the southeastern and northeastern highlands. This resulted in heating of the crust, crustal underplating, and replacement

of the lower lithosphere. In common with the Karner & Weissel model, the underplating and heating would result in mid Cretaceous uplift, with some later cooling and sinking.

5) Several independent studies have concluded that the highlands uplift could have been caused by Cainozoic underplating of the crust, with subsequent isostatic uplift. Wellman (1979b) inferred Cainozoic mafic underplating from the uplift of the highlands, inferred from river downcutting, the isostatic equilibrium determined from gravity studies, and the high seismic velocity lower part of the crust between 33 and 53 km. Ewart & others (1980) investigated the petrogenesis of Cainozoic mafic lavas in Queensland, using thermodynamic equilibration techniques. They found that the mafic magmas are best explained as the result of 'intrusion and magma fractionation within the crust-mantle interface region with consequent crustal underplating and thickening'. Wass & Hollis (1983) and Knutson & others (1984) showed from a study of xenoliths that the lower crust contains basaltic derived cumulates and intrusions, and they inferred that mafic underplating at the crust-mantle boundary has significantly thickened the crust. Rudnick (1985) interpreted the mafic xenoliths in late Cainozoic north Queensland basalts as basaltic accumulates, and interpreted their isotopic ratios as indicating an age less than 100 Ma. The underplating model sucessfully links the area of the highlands with the area of Cainozoic volcanism. The geographic coincidence of this 0–5 Ma volcanism in northeast Queensland with broad uplifts is consistent with a late Cainozoic underplating origin for the uplift, with perhaps some heating-induced uplift. Uplift due to underplating may have been continuous everywhere, owing to a constant over-all rate of volcanism (Wellman & McDougall, 1974a), or uplift may have been local and correspond in time with the local volcanism. If the volcanism and underplating are linked, then it is difficult to model tectonic uplift as all pre-mid Cainozoic. The linking of volcanism, associated underplating, and tectonic uplift leaves unexplained their relationship to seafloor spreading.

The models based on removal of the lower lithosphere just before 100 Ma ago, by asymmetrical stretching or low-angle detachment faulting, explain that much uplift is late Cretaceous, explain the geographic relationship of the southeastern and northeastern highlands to adjacent oceanic basins, and explain some of the uplift as caused by underplating, but they predict some Cainozoic sinking of the highlands, which is not observed. The model in which Cainozoic volcanism causes underplating of the crust explains the similar geographic distribution of volcanism and uplift and the evidence for late Cainozoic tectonic uplift. It is likely that uplift of the Eastern Highlands was by a combination of mechanisms — heating and underplating in the mid Cretaceous, and underplating, some heating, and erosion in the Cainozoic.

Conclusions

1. Mesozoic sediments found on the highlands' summit and flanks can be used to put a limit on the time of first uplift of the highlands from near sea level. Uplift must have been after the early Cretaceous sedimentation in Queensland, after the middle Triassic sedimentation near Sydney, and after the Triassic sedimentation in Tasmania. The change in sedimentation pattern and tectonics in the mid Cretaceous (95 Ma ago) documented by Jones & Veevers (1983) seems the most likely time for initiation of uplift, except in Tasmania, where Jurassic uplift seems likely.

2. Along the highlands axis are numerous areas where steeply dipping Palaeozoic rocks have been truncated to low relief and are now covered by thin, flat-lying Mesozoic or Cainozoic rocks. It is inferred that the area of the present highlands had its lowest relief in the mid to late Mesozoic, and that its altitude and local relief have increased since then.

3. Where sediment is preserved in the highlands, it generally shows that uplift has been mainly by warping with only minor faulting, giving gently sloping flanks and a wide crest. However, major faulting is found on the eastern margin of the highlands in Queensland, and in Tasmania.

4. Gravity studies show that the area is close to being in local isostatic equilibrium. Hence, denudation would cause isostatic rebound, tectonic uplift is likely to be a result of crustal thickening or heating, and the relatively high mountains near the Great Escarpment are likely to be caused by local isostatic rebound resulting from the greater denudation of the coastal lowlands.

5. Estimates of the highlands' Cainozoic denudation rate give a mean near 3 $m.Ma^{-1}$ for Queensland and New South Wales, and 5–7 $m.Ma^{-1}$ for eastern Victoria and Tasmania. The highlands axis is generally over 300 m in altitude; therefore, the amount of denudation rebound uplift over the last 100 Ma has been generally less than the total amount of tectonic uplift.

6. The timing of the tectonic uplift within the last 100 Ma is not well documented. In north Queensland, some early tectonic uplift is inferred from erosion prior to the deposition of the pre-mid Cainozoic Bulimba Formation, and 400 m of late tectonic uplift is inferred from late Cainozoic doming associated with, and prior to, the late Miocene-Recent volcanism. Of the 1.0 km of tectonic uplift of the northern New England highlands, 0.3 km is inferred to have taken place in the mid to late Cainozoic on a monoclinal flexure or fault in the Clarence-Moreton Basin. Within New South Wales and Victoria, the position of the basaltic lavas within the valleys shows that over half the uplift on the eastern and southern margin of the highlands occurred before 50 Ma ago. On the western and northern margin of these highlands the amount of late Cainozoic downcutting is greater than the amount of late Cainozoic denudation, so it is likely that some of the tectonic uplift occurred in the late Cainozoic. In summary, most of the tectonic uplift was earlier than mid Cainozoic, but there is some evidence that the remainder (possibly one third) was in the late Cainozoic.

7. The post-100 Ma uplift of the Eastern Highlands is thought to have four components. The two early components were due to rifting along the present eastern margin of the Australian continent to form the Tasman and Coral Seas by asymmetric lithosphere stretching or lithosphere extension, mainly along low-angle detachment faults. These removed the lower lithosphere under the highlands (except in southern Queensland) and caused uplift of the highlands by both crustal underplating replacing the removed lower lithosphere, and by upper lithosphere heating. The lithosphere heating caused thermal expansion and uplift. During the Cainozoic, additional uplift was caused by the isostatic rebound resulting from denudation of the highlands, and from isostatic uplift resulting from underplating (and possible heating of the crust) at the time of the Cainozoic highlands volcanism.

Acknowledgements

I am grateful for discussions with J.H.C. Bain, M.R. Banks, P. Bishop, H.F. Doutch, M.A. Etheridge, G.D. Karner, D.E. Mackenzie, and C.D. Ollier, and comments on the draft text by P. Bishop, K. Grimes, G.E. Wilford, N.C. Stevens, and R.W. Young. The figures were drafted by J. Convine.

References

Andrews, E.C., 1911—Geographical unity of eastern Australia in the late and post Tertiary time, with applications to biological problems. *Journal and Proceedings of the Royal Society of New South Wales*, 44, 420-480.

Bain, J.H.C., Withnall, I.W., Oversby, B.S. & Mackenzie, D.E., 1985—Geology of the Georgetown region, Queensland, 1:250 000 map. *Bureau of Mineral Resources, Canberra.*

Ben-Avraham, Z., Nur, A., Jones, D., & Cox, A., 1981—Continental accretion: from oceanic plateaus to allochthonous terranes. *Science*, 213, 47-54.

Bird, M.I. & Chivas, A.R., 1985—Oxygen-18 in kaolinite and uplift of the Eastern Highlands. *Abstract of talk presented at Commonwealth Territories Division, Geological Society of Australia, Canberra, 9 August 1985* (unpublished).

Bishop, P., 1985—Southeast Australian late Mesozoic and Cenozoic denudation rates: a test for late Tertiary increases in continental denudation. *Geology*, 13, 479-482.

Bishop, P., Young, R.W. & McDougall, I., 1985—Stream profile change and longterm landscape evolution: early Miocene and modern rivers of the east Australian highland crest, central New South Wales, Australia. *Journal of Geology*, 93, 455-474.

Branagan, D.F., 1983—The Sydney Basin and its vanished sequence. *Journal of the Geological Society of Australia*, 30, 75-84.

Brown, C.M., 1983—Discussion: a Cainozoic history of Australia's southeast highlands. *Journal of the Geological Society of Australia*, 30, 483-486.

Browne, W.R., 1969—Geomorphology of New South Wales. *Journal of the Geological Society of Australia*, 16, 559-569.

Carr, P.F & Facer, P.A., 1980—Radiometric ages of some igneous rocks from the southern and southwestern coalfields of New South Wales. *Search*, 11, 382-383.

Chorley, R.J., Schumm, S.A., & Sugden, D.E., 1984—Geomorphology. *Methuen, London.*

Clarke, D.E., Paine, A.G.L., & Jensen, A.R., 1971—Geology of the Proserpine 1:250 000 sheet area, Queensland. *Bureau of Mineral Resources, Australia, Report* 144.

Craft, F.A., 1933—The coastal tablelands and streams of New South Wales. *Proceedings of the Linaean Society of New South Wales*, 58, 437-460.

Doutch, H.F., Ingram, J.A., Smart,J., & Grimes, K.G., 1970—Progress report on the geology of the southern Carpentaria Basin. *Bureau of Mineral Resources, Australia, Record* 1970/39.

Doutch, H.F., Smart, J., Grimes, K., Needham, S. & Simpson, C.J., 1972—Progress report on the geology of the central Carpentaria Basin. *Bureau of Mineral Resources, Australia, Record* 1972/64.

Dulhunty, J.A., 1976—Potassium-argon ages of igneous rocks in the Wollar-Rylstone region, New South Wales. *Journal and Proceedings of the Royal Society of New South Wales*, 109, 35-39.

Embleton, B.J.J., Schmidt, P.W., Hamilton, L.H., & Riley, G.H., 1985—Dating volcanism in the Sydney Basin: evidence from K-Ar ages and palaeomagnetism. *In* Sutherland, F.L., Franklin, B.J., & Waltho, A.E., (editors), Volcanism in eastern Australia: with case histories from New South Wales. *Geological Society of Australia, New South Wales Division, Publication*, 1, 59-72.

Ewart, A., Baxter, K., & Ross, J.A., 1980—The petrology and petrogenesis of the Tertiary anorogenic mafic lavas of southern and central Queensland, Australia — possible implications for crustal thickening. *Contributions to Mineralogy and Petrology*, 75, 129-152.

Exon, N.F., 1976—Geology of the Surat Basin in Queensland. *Bureau of Mineral Resources, Australia, Bulletin* 166.

Exon, N.F. & Senior, B.R., 1976—The Cretaceous of the Eromanga and Surat Basins. *BMR Journal of Australian Geology & Geophysics*, 1, 33-50.

Galloway, R.W., 1967—Pre-basalt, sub-basalt, and post-basalt surfaces of the Hunter Valley, New South Wales. *In* Jennings, J.N., & Mabbutt, J.A., Landform studies in Australia and New Guinea. *Australian National University Press, Canberra.* 293-314.

Galloway, R.W., 1987—The age of landforms in southeastern Queensland. *In* Galloway, R.W., (compiler), The age of landforms in eastern Australia : conference summary and field trip guide (7-12 September 1986). *Division of Water & Land Resources, CSIRO, Canberra, Technical Memorandum* 87/2, 38-46.

Hale, G.E., 1962—Triassic System. *In* Spry, A., & Banks, W.R., The geology of Tasmania. *Journal of the Geological Society of Australia*, 9, 217-231.

Hallam, A., 1981—A revised sea-level curve for the Jurassic. *Journal of the Geological Society, London*, 138, 735-743.

Hawke, J.M. & Bourke, D.J., 1984—Stratigraphy. *In* Hawke, J., & Cramsie, J.N., Contributions to the geology of the Great Australian Basin in New South Wales. *Geological Survey of New South Wales, Bulletin* 31, 23-124.

Helby, R & Morgan, R., 1979—Palynomorphs in Mesozoic volcanoes of the Sydney Basin. *Quarterly Notes of the Geological Survey of New South Wales*, 35, 1-15.

Hills, E.S., 1940—The physiography of Victoria. *Whitcombe & Tombs, Melbourne.*

Jones, J.G., & Veevers, J.J., 1982—A Cainozoic history of Australia's southeast highlands. *Journal of the Geological Society of Australia*, 29, 1-12.

Jones, J.G. & Veevers, J.J., 1983—Mesozoic origins and antecedents of Australia's Eastern Highlands. *Journal of the Geological Society of Australia*, 30, 305-322.

Karner, G.D. & Weissel, J.K., 1984—Thermally induced uplift and lithospheric flexural readjustment of the eastern Australian highland. *Geological Society of Australia, Abstracts*, 12, 293-294.

Knutson, J., O'Reilly, S.Y., Duggan, M.B., & Jaques, A.L., 1984—The nature of the lower crust and upper mantle beneath eastern Australia as inferred from xenolith studies. *Geological Society of Australia, Abstracts*, 12, 310-311.

Lambeck, K., & Stephenson, R., 1985—Post orogenic evolution of a mountain range: southeastern Australian highlands. *Geophysical Research Letters*, 12, 801-804.

Lister, G.S., Etheridge, M.A., & Symonds, P.A., 1986—Detachment faulting and the evolution of passive continental margins. *Geology*, 14, 246-250.

McDougall, I., & Wellman, P., 1976—Potassium-argon ages for some Australian Mesozoic igneous rocks. *Journal of the Geological Society of Australia*, 23, 1-9.

McKenzie, D.A., Nott, R.J., & Bolger, P.F., 1984—Radiometric age determinations. *Geological Survey of Victoria, Report* 74.

Mackenzie, D.E., Withnall, I.W., Blythe, P., O'Donnell, I.C., & Knight, C., 1979a—Geology of the North Head region. 1:100 000 geological map; preliminary edition. *Bureau of Mineral Resources, Canberra.*

Mackenzie, D.E., Withnall, I.W., Blythe, P., O'Donnell, I.C. & Knight, C., 1979b—Geology of the Forest Home region. 1:100 000 geological map; preliminary edition. *Bureau of Mineral Resources, Canberra.*

Mayne, S.J., Nicholas, E., Bigg-Wither, A.L., Rasidi, J.S., & Raine, M.J., 1974—Geology of the Sydney Basin — a review. *Bureau of Mineral Resources, Australia, Bulletin* 149.

Middleton, M.F., & Schmidt, P.W., 1982—Palaeothermometry of the Sydney Basin. *Journal of Geophysical Research*, 87, 5351-5359.

Moore, M.E., Gleadow, A.J.W., & Lovering, J.F., 1986—Thermal evolution of rifted continental margins: new evidence from fission tracks in basement apatites from southeastern Australia. *Earth and Planetary Science Letters*, 78, 255-270.

Ollier, C.D., 1978—Tectonics and geomorphology of the Eastern Highlands. *In* Davies, J.L., & Williams, M.A.J., Landform evolution in Australasia. *Australian National University Press, Canberra.* 5-47.

Ollier, C.D., 1982a—Geomorphology and tectonics of the Armidale region. *In* Flood, P.G. & Runnegar, B., (editors), New England geology. *Department of Geology, University of New England, Armidale*, 141-147.

Ollier, C.D., 1982b—The Great Escarpment of eastern Australia: tectonic and geomorphic significance. *Journal of the Geological Society of Australia*, 29, 13-23.

Raam, A., 1968—Petrology and diagenesis of Broughton Sandstone (Permian), Kiama district, New South Wales. *Journal of Sedimentary Petrology*, 38, 319-331.

Robertson, C.S., 1961—Emerald-Duaringa seismic survey. *Bureau of Mineral Resources, Australia, Record* 1961/150.

Rudnick, R., 1985—Xenolithic evidence for Cenozoic additions to eastern Australia's lower crust. *Abstract of talk presented at Commonwealth Territories Division, Geological Society of Australia, Canberra, 9 August 1985.* (unpublished).

Ruxton, B.P., & Taylor, G., 1982—The Cainozoic geology of the middle Shoalhaven Plain. *Journal of the Geological Society of Austalia*, 29, 239-246.

Ruxton, B.P., & Taylor, G., 1987—Burial and exhumation of landscapes in the Willello-Windellama area. *In* In Galloway, R.W., (compiler), The age of landforms in eastern Australia: conference summary and field trip guide (7-12 September 1986). *Division of*

Water & Land Resources, CSIRO, Canberra, Technical Memorandum 87/2, 66-75.

Schmidt, P.W., & Embleton, B.J.J., 1981—Magnetic overprinting in southeastern Australia, and the thermal history of its rifted margin. *Journal of Geophysical Research*, 86, 3998-4008.

Schmidt, P.W., & Ollier, C.D., 1987—Cretaceous weathering in New *England. In* Galloway, R.W., (compiler), The age of landforms in eastern Australia: conference summary and field trip guide (7-12 September 1986). *Division of Water & Land Resources, CSIRO, Canberra, Technical Memorandum* 87/2, 19-22.

Senior, B.R., Mond, A., & Harrison, P.L., 1978—Geology of the Eromanga Basin. *Bureau of Mineral Resources, Australia, Bulletin* 167.

Smart, J., Grimes, K.G., Doutch, H.F., & Pinchin, J., 1980—The Carpentaria and Karumba Basins, North Queensland. *Bureau of Mineral Resources, Australia, Bulletin* 202.

Speight, J.G., 1985—Post-orogenic rates of uplift and erosion at Tianjara, near Ulladulla. *Abstract of talk presented at Commonwealth Territories Division, Geological Society of Australia, Canberra, 9 August 1985.*

Stephenson, P.J., 1987—Landforms in north Queensland, aspects of their origin, age and evolution. *In* Galloway, R.W., (compiler), The age of landforms in eastern Australia: conference summary and field trip guide (7-12 September 1986). *Division of Water and Land Resources, CSIRO, Canberra, Technical Memorandum* 87/2, 32-37.

Stephenson, R., & Lambeck, K., 1985—Erosion-isostatic rebound models for uplift: an application to south-eastern Australia. *Geophysical Journal of the Royal Astronomical Society*, 82, 31-55.

Sutherland, F.L., 1977—Zeolite minerals in the Jurassic dolerites of Tasmania: their use as possible indicators of burial depth. *Journal of the Geological Society of Australia*, 24, 171-178.

Sutherland, F.L., & Wellman, P., 1986—Potassium-argon ages of Tertiary volcanic rocks and Cainozoic uplift of Tasmania. *Papers and Proceedings of the Royal Society of Tasmania*, 120, 77-86.

Swarbrick, C.F.J., 1974—Oil shale resources of Queensland. *Geological Survey of Queensland, Report 83.*

Tas. Dept. Mines, 1976—Geological map of Tasmania, 1:500 000. *Tasmania Department of Mines, Hobart.*

Taylor, G., Taylor, G.R., Bink, M., Foudoulis, C., Gordon, I., Hedstrom, J., Minello, J., & Whippy, F., 1985—Pre-basaltic topography of the northern Monaro and its implications. *Australian Journal of Earth Sciences*, 32, 65-71.

Vail, P.R., Mitchum, R.M., Thompson, S., Todd, R.G., Sangree, J.B., Widmier, J.M., Bubb, J.N., & Hatlelid, W.G., 1977—Seismic stratigraphy and global changes of sea level. *American Association of Petroleum Geologists Memoir*, 26, 49-212.

Wass, S.Y., & Hollis, J.D., 1983—Crustal growth in south-eastern Australia—evidence from lower crustal eclogitic and granulitic xenoliths. *Journal of Metamorphic Petrology*, 1, 25-45.

Wellman, P., 1974—Potassium-argon ages of the Cainozoic volcanic rocks of eastern Victoria, Australia. *Journal of the Geological Society of Australia*, 21, 359-376.

Wellman, P., 1976—Regional variation of gravity, and isostatic equilibrium of the Australian crust. *BMR Journal of Australian Geology & Geophysics*, 1, 297-302.

Wellman, P., 1979a—On the Cainozoic uplift of the southeastern Australian highlands. *Journal of the Geological Society of Australia*, 26, 1-9.

Wellman, P., 1979b—On the isostatic compensation of Australian topography. *BMR Journal of Australian Geology & Geophysics*, 4, 373-382.

Wellman, P., 1986—Intrusions beneath large alkaline intraplate volcanoes. *Exploration Geophysics*, 17, 135-139.

Wellman, P., & McDougall, I., 1974a—Cainzoic igneous activity in Eastern Australia. *Tectonophysics*, 23, 49-65.

Wellman, P., & McDougall, I., 1974b—Potassium-argon ages on the Cainozoic volcanic rocks of New South Wales. *Journal of the Geological Society of Australia*, 21, 247-272.

Wilford, G.E., Brown, C.M., & Bultitude, J., 1981—Sedimentary sequences, 1:10 000 000 map. *Bureau of Mineral Resources, Australia, Earth Science Atlas.*

Woolnough, W.G., 1927—Presidential Address, Part I Chemical criteria of pneplanation, Part II The duricrust in Australia. *Journal and Proceedings of the Royal Society of New South Wales*, 61, 17-53.

Young, R.W., 1977—Landscape development in the Shoalhaven River catchment of southern New South Wales. *Zeitschrift fur Geomorphologie*, 21, 262-283.

Young, R.W., 1981—Denudational history of the south-central uplands of New South Wales. *Australian Geographer*, 15, 77-88.

Young, R.W., 1983—The tempo of geomorphological change: evidence from southeastern Australia. *Journal of Geology*, 91, 221-230.

Young, R.W., & McDougall, I., 1982—Basalts and silcretes on the coast near Ulladulla, southern New South Wales. *Journal of the Geological Society of Australia*, 29, 425-430.

BMR Journal of Australian Geology & Geophysics, 10, 287-300

Rhytiobeyrichia, a new beyrichiacean ostracod from the late Devonian of Western Australia

P.J. Jones[1]

A palaeocope ostracod with a distinct lobation and crumina occurs in the late Devonian (Strunian) sequences of the Canning and Bonaparte Basins. It is assigned to the new genus *Rhytiobeyrichia*, and is interpreted, within Martinsson's scheme of beyrichiacean phylogeny, as an advanced beyrichiine. The interpretation of its ontogeny and sexual dimorphism, based on limited material, indicates that the genus is represented by a single rather than sympatric, species. The species, *Rhytiobeyrichia waruwa* sp.nov. (=type species of *Rhytiobeyrichia*), if interpreted correctly, is unique in representing a possible example of the phenomenon of preadult dimorphism in the Beyrichiacea. This tentative claim would be negated if later work, based on more material, shows that *R. waruwa* sp.nov. does in fact consist of more than one species. The occurrence of *Rhytiobeyrichia waruwa* sp. nov. in strata of comparable (Strunian) age in the Canning and Bonaparte Basins indicates its value for correlation. In the Canning Basin, the stratigraphy of the Fairfield Group, as identified by Druce & Radke (1979) in several well sections, is in need of revision. This interval, a good source potential for petroleum, is reinterpreted for the Napier No. 1 and No. 4 Wells.

Introduction

Published research on Australian late Devonian ostracods has been solely concentrated on assemblages from Western Australia, where 23 species, eridostracans excluded, have been described from the onshore Bonaparte Basin (Jones, 1968, 1985). Although some of these ostracod species have been recognised in the onshore Canning Basin, many more from the uppermost Devonian sequence of this basin await formal description (Jones, 1974). This material was obtained during biostratigraphic investigations between 1956 and 1971 (Jones, 1961; see citations of Jones *in* Druce & Radke, 1979) of surface and subsurface samples of upper Devonian–lower Carboniferous platform sediments that postdate the Famennian part of the Devonian reef complex (Playford & Lowry, 1966). Between the late 1950s and early 1970s, Devonian reef plays were the primary targets for petroleum exploration; today, plays in the post-reef sediments are regarded as targets of equal importance (Poll, 1983). Thus, the search for stratigraphic and structural traps in the uppermost Devonian and lowermost Carboniferous Fairfield Group has emphasised the need for more biostratigraphic research over this interval. As a contribution to this research the present paper describes, illustrates, and documents the stratigraphic distribution of *Rhytiobeyrichia waruwa* gen. et sp. nov, a new beyrichiid from the late Devonian (Strunian) of the onshore Canning and Bonaparte Basins.

Rhytiobeyrichia waruwa gen. et sp. nov. was first found by the writer in the northern Canning Basin (Fig. 1), in subsurface sections of the Luluigui Formation on the Jurgurra Terrace, the Napier Formation, and the overlying Gumhole Formation (the lowermost formation in the Fairfield Group) on the Lennard Shelf and Margaret Terrace. Further specimens were recovered from the onshore Bonaparte Basin (Fig. 2), after Dr Robert S. Nicoll and I sampled the type section of the Buttons beds in 1978.

All samples studied were subjected to conventional preparatory techniques (Sohn, Berdan & Peck *in* Kummel & Raup, 1965), most of which yielded rich concentrations of ostracods. Individuals of *Rhytiobeyrichia* are rare, and were examined under both light and scanning electron microscopes. The morphological terminology follows Kesling (1951), Jaanusson (1957), Martinsson (1962), and Siveter (1980). All type and figured specimens are deposited in the Commonwealth Palaeontological Collection (prefix CPC), Bureau of Mineral Resources, Canberra.

[1] Division of Continental Geology, Bureau of Mineral Resources, GPO Box 378, Canberra, ACT 2601

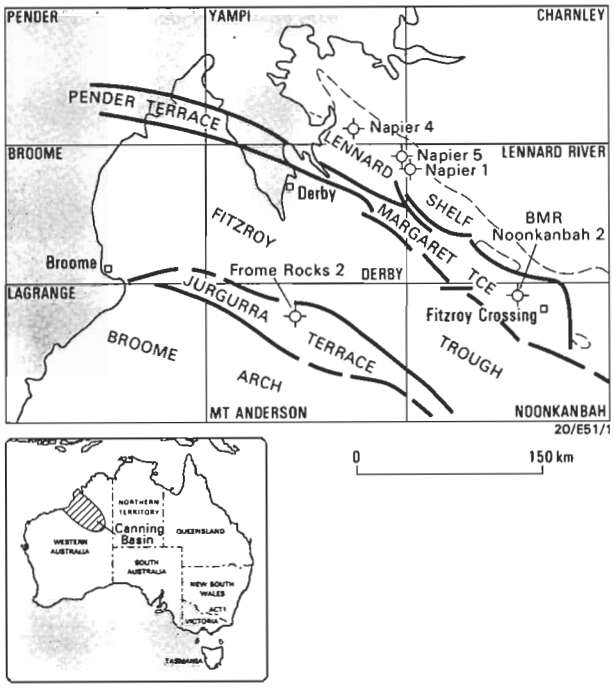

Figure 1. Locality map, northern Canning Basin, Western Australia, showing main structural divisions (after Forman & Wales, 1981), bore hole locations, and 1:250 000 map sheet areas.

Stratigraphy

Canning Basin

Summaries of previous investigations of the geology and structural subdivisions of the onshore Canning Basin have been published in recent reviews by Towner & Gibson (1983) and Yeates & others (1984). Detailed discussion of the geology and previous interpretations of the late Devonian to early Carboniferous Fairfield Group are given in Druce & Radke (1979).

The Fairfield Group consists of a sequence of interbedded limestone, shale, and sandstone with minor dolomite, that post-dates the Famennian reef complex (Nullara Cycle) on the Lennard Shelf. As defined by Druce & Radke (1979), it includes three formations, the Gumhole Formation, the Yellow Drum Sandstone, and the Laurel Formation (in ascending order), and closely approximates to the interval referred to the Fairfield Formation by Playford & Lowry (1966) and G. Playford (1976). The biostratigraphic evidence, based on conodonts (Nicoll & Druce, 1979), miospores

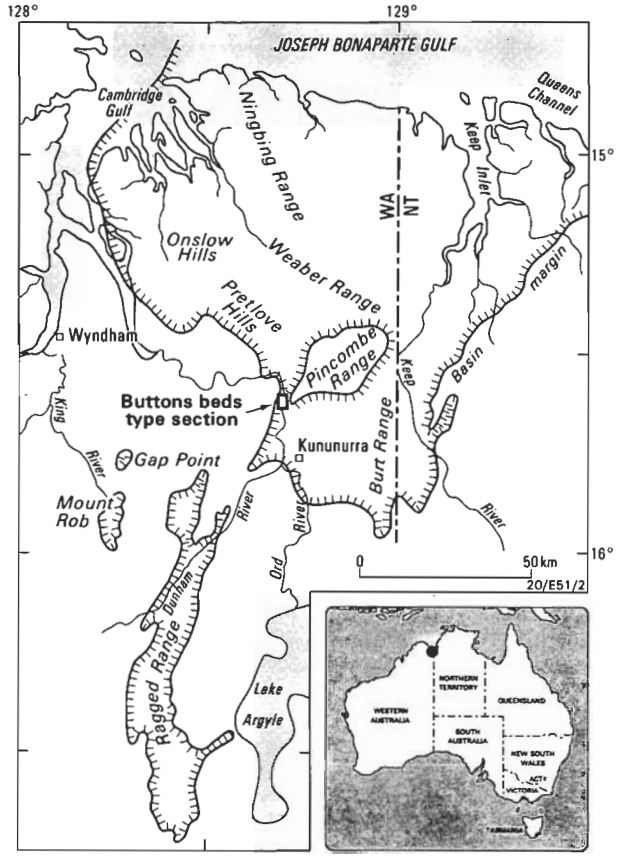

Figure 2. Locality map, Bonaparte Basin, Western Australia and Northern Territory.

(Playford, 1976), and ostracods (Jones, 1974), indicates that the Devonian/Carboniferous boundary (*sensu* Paproth, 1980) lies within the Yellow Drum Sandstone.

The Gumhole Formation (= Fairfield beds *sensu* Roberts & others, 1972) consists of limestone, siltstone, and shale with minor dolomite and sandstone, thought to have been deposited in shallow marine waters, less than 15 m deep, on an open platform with bioherms and a restricted platform with shoal and intershoal areas (Druce & Radke, 1979). It contains a relatively abundant and diverse biota, regarded by Druce & Radke (1979), on the basis of conodont (Nicoll & Druce, 1979) and miospore (Playford, 1976) evidence, to be latest Famennian (doV1; Tnla) in age. This biota marks the final Devonian transgression in the Canning Basin, after the cessation of reef growth on the Windjana-Nullara platforms (Druce & Radke, 1979). As the conodont evidence (Nicoll, 1980) indicates that the bank facies of the Nullara Limestone is early to middle *costatus* Zone in age, the Gumhole Formation, where it directly overlies the Nullara, is no older than middle *costatus* Zone. The Gumhole Formation, of course, may be slightly older than middle *costatus* Zone where it interfingers with the Nullara Limestone.

The Luluigui Formation, thin-bedded shale and siltstone with minor limestone, was defined in the subsurface on the Jurgurra Terrace (Willmott, 1966). Like the Gumhole Formation, it contained the *Retispora lepidophyta* microfloral assemblage (Balme & Hassell, 1962; Playford, 1976) of latest Famennian age. Druce & Radke (1979) suggested that the Gumhole Formation overlies the Luluigui Formation or its equivalent in several subsurface sections on the Lennard Shelf, in the area southwest of the Oscar and Napier Ranges. Alternatively, they suggested that the dominantly clastic sequence below the Gumhole Formation in these sections may be a basin facies of the Napier Formation. Because these well sections are close to outcrops of the Napier Formation, the second interpretation is accepted here.

Rhytiobeyrichia gen. nov. forms a minor, but distinctive, component of the benthic ostracod fauna of the Canning Basin, previously designated 'Assemblage A' (Jones, 1961, 1974). This informal biostratigraphic unit has been used to correlate subsurface sections of the Gumhole Formation, plus the upper part of the Napier Formation on the Lennard Shelf and the Margaret Terrace, with the upper part of the Napier Formation on the Jurgurra Terrace (Jones, 1961; see citations of Jones *in* Druce & Radke, 1979).

The upper limit of the stratigraphic range of Assemblage A approximately corresponds with those of the *Retispora lepidophyta* miospore Assemblage of Playford (1976) and the *Icriodus platys* conodont zone of Nicoll & Druce (1979). Both these horizons more or less coincide with the Devonian—Carboniferous boundary (*sensu* Paproth, 1980; i.e., at the base of the *Siphonodella sulcata* Zone). In BMR Noonkanbah No. 2 well the lower limit of Assemblage A falls within the stratigraphic range of the *Retispora lepidophyta* Assemblage (Playford, 1976), thus, by palynostratigraphic correlation with the Strunian of Belgium, Assemblage A is at least Tnla in age, and could be as old as Fa2d, i.e., the Lower *costatus* Zone. A Tnla age for Assemblage A is supported by the presence of an undescribed species of *Shishaella* Sohn, 1971 (= *Paraparchites nicklesi* sensu Jones, 1959). Authentic records of this genus appear to be absent below Tnla (Tschigova, 1977). *Rhytiobeyrichia* gen. nov. ranges between the depths of 856 m and 541 m in BMR Noonkanbah No. 2; that is for most of the interval represented in this well by Assemblage A (966-541 m).

Bonaparte Basin

The geology and structure of the Devonian and Carboniferous sequence of the onshore Bonaparte Basin have been described in some detail by Veevers & Roberts (1968), and useful summary accounts have been provided by Robert & Veevers (1973), Laws & Brown (1976), and Laws (1981). Detailed discussion of the stratigraphy and previous interpretations of the latest Devonian (Strunian) Buttons beds have been provided by Playford (1982) and Jones (1985).

The ostracod fauna of the Buttons beds was previously regarded as early Famennian (Jones 1968), but current palynological (Playford, 1982) and ostracod research (Jones, 1985) now indicates a (younger) Strunian age. Many of the ostracod species described from the Buttons beds are also present in the Gumhole and Luluigui Formations as part of Assemblage A (Jones, 1968, 1974), e.g. *Indivisia variolata* Zanina, 1960; *Marginia venula* Jones, 1968; *M. reticulata* Jones, 1968; *Coeloenellina* sp. cf. *C. fabiformis* Kesling & Kilgore, 1952; *Cavellina* sp. A Jones, 1968; and *Shishaella* sp. nov. (= *Paraparchites* sp. cf. *P. nicklesi sensu* Jones, 1968). Thus, it seems reasonable to regard both faunas as more or less coeval, rather than consisting of long-ranging forms of different ages.

The material from the Bonaparte Basin consists of two specimens of *Rhytiobeyrichia* gen. nov. from the lower part of the type section of the Button beds (Table 2), along the eastern bank of the Ord River, just north of Buttons Crossing (Fig. 2). The samples (02/08, 02/09), collected by Dr Robert S. Nicoll and me in 1978, were taken from thinly bedded silty limestones about 29 m (95 feet) below the lowest appearance of the *Retispora lepidophyta* Assemblage reported by

Playford (1982). It is unlikely that this part of the Buttons beds is older than Strunian *sensu* Conil, Groessens & Pirlet, 1976 (i.e., Fa2d, Tn1a, and the lower part of Tn1b), because it contains the paraparchitacean ostracod genus *Shishaella* Sohn, 1971, that elsewhere appears to be unknown in the Devonian (Tschigova, 1977). Further details on the latest Devonian age of the Buttons beds have been provided by Playford (1982) and Jones (1985). More documentation of this age will be provided on completion of my current studies of the entire ostracod fauna.

Stratigraphy of subsurface sections with *Rhytiobeyrichia* in the Canning Basin

Rhytiobeyrichia gen. nov. is present in the Canning Basin in subsurface sections of five wells (Fig. 3); three were drilled on the Lennard Shelf by Lennard Oil N.L. (LENNARD), one was drilled on the Margaret Terrace by the Bureau of Mineral Resources (BMR), and one was drilled on the Jurgurra Terrace by West Australian Petroleum Pty Limited (WAPET). The locations of the wells are shown in Figure 1, and the depth intervals of the core and cutting samples, the formations, and the specimens pertaining to them are listed in Table 1. The following summary of the drill hole sequences has been adopted from Druce & Radke (1979, Appendix 1), unless stated otherwise. The stratigraphy of the Fairfield Group in some of the well sections is in need of revision. For example, the Gumhole Formation is stated to reach a maximum thickness of 369 m in Meda No 1 Well in the interval 1649-2018 m (Druce & Radke, 1979, p. 9); however, Playford & Lowry (1966, p. 129) identified the interval below 1671 m (5483 ft) with the Famennian 'Pillara Limestone' (now the Nullara Limestone), which conversely reduces the thickness of the Gumhole Formation in this well to 22 m. The Fairfield Group is reinterpreted for Napier No. 1 and No. 4 wells; revision of this stratigraphic interval for other wells is beyond the scope of this paper.

BMR Noonkanbah No. 2

BMR Noonkanbah No. 2 Well, formerly known as BMR No. 2 (Laurel Downs), was drilled on the Margaret Terrace in 1955-56, and is the closest well to the type section of the Fairfield Group. It passed initially through Quaternary sand overlying a sandstone unit that probably belongs to the Permian—Carboniferous Grant Group. The Fairfield Group was intersected between 76.2 m (250 ft) and 567 m (1860 ft), and consists of the Laurel Formation (to 433 m; 1420 ft), Yellow Drum Sandstone (to 540 m; 1772 ft), and the Gumhole Formation.

The Gumhole Formation consists of 27 m of interbedded limestone, sandstone and shale, which conformably overlies the Napier Formation (basin facies) at 567 m, the latter extending to 1219.2 m (4000 ft; total depth). Jones (1961) recognised three ostracod assemblages in this well: these are (in ascending order) Assemblage A, occurring in the 966-541 m interval (upper part of the Napier Formation plus Gumhole Formation); Assemblage B, 462-369 m (upper part of the Yellow Drum Sandstone plus lower part of the Laurel Formation); and Assemblage C, 352-?76 m (Laurel Formation). Subsequent unpublished studies by the writer have shown that representative species of Assemblage B are present at 305 m (1000 ft), and hence the lower limit of Assemblage C must be above that point. Assemblage B is present in the Bonaparte Basin in the lower part of the Burt Range Formation, which is correlated on conodont evidence (Druce, 1969) with the cuI Zone of Germany and the Tn1b of the standard Belgian sequence (Jones, 1974). Thus, the

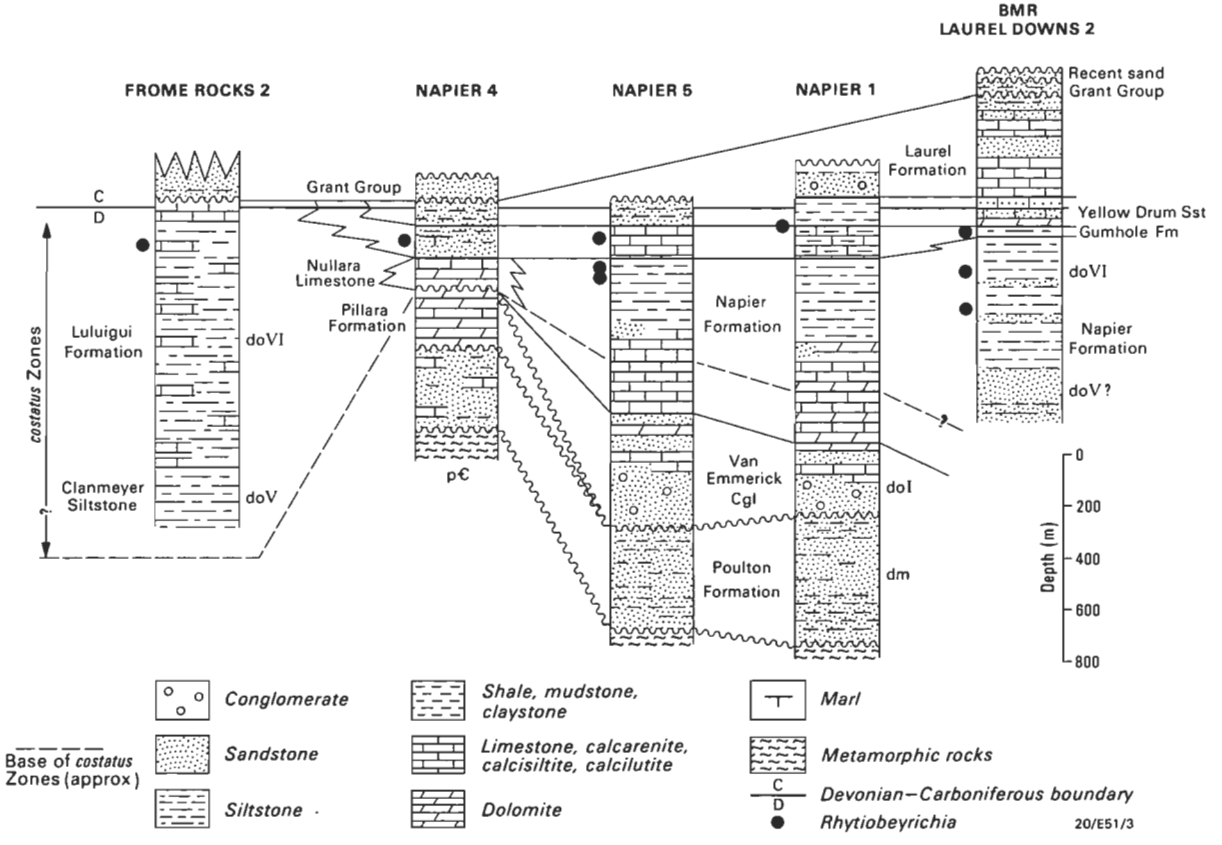

Figure 3. Subsurface distribution of *Rhytiobeyrichia waruwa* gen. et sp. nov., northern Canning Basin.
Lithologies after Forman & Wales (1981). Interpretation of sequence below the Fairfield Group in Napier No. 4 well, simplified after Lehmann (1984).

Table 1. Localities of *Rhytiobeyrichia waruwa* gen. et sp. nov. in the Gumhole, Napier, and Luluigui Formations of the northern Canning Basin.

Locality	1:250 000 Sheet & geographic coordinates	Sample type & depth (ft)	Formation	Specimen type & CPC number
BMR	Noonkanbah	core 18, 1775-1785	Gumhole	(A-1)ml, CPC25331
Noonkanbah 2	18°07'24"S	cuttings, 2390-2395	Napier	(A-1)fr, CPC25332
	125°19'58"E	core 30, 2800-2810	Napier	Af CPC25333
WAPET	Mt. Anderson	core 13, 4172-4180	Luluigui	(A-1)fc, CPC25321
Frome Rocks 2	18°15'15"S			
	123°39'35"E			
LENNARD	Lennard River	cuttings 660-665	Gumhole/Yellow	(A-1)fc, CPC25322
Napier 1	17°12'20"S		Drum Sandstone	Holotype
	124°31'36"E		boundary	
LENNARD	Yampi	core 1, 717-725	Gumhole	Amc CPC25323
Napier 4	16°15'00"S			Amc CPC25324
	124°05'35"E			(A-1)fc CPC25325
				(A-2)fc CPC25326
LENNARD	Derby	cuttings, 500-520	Gumhole	(A-1)mc CPC25327
Napier 5	17°06'30"S			(A-1)mc CPC25328
	124°28'06"E	cuttings, 750-760	Napier	(A-2)fc CPC25329
		cuttings, 800-900		(A-1)fc CPC25330

Table 2. Localities of *Rhytiobeyrichia waruwa* gen. et sp. nov. in the type section of the Buttons beds (Section 105 of Veevers & Roberts, 1968, p. 65 Figs 30, 35), Bonaparte Basin.

Samples & height above base of type section ft (m)	Specimen type & CPC number
02/09 300 (91)	Afc CPC25334
02/08 290 (88)	Afr CPC25335

Abbreviations as in Table 4.

Devonian-Carboniferous boundary, in terms of ostracod chronology, may be taken to lie in this well within the Yellow Drum Sandstone, between Assemblage A at 541 m and Assemblage B at 462 m. Playford (1976), on miospore evidence, placed this boundary between his *Retispora lepidophyta* Assemblage at 517. 2 m and his *Grandispora spiculifera* Assemblage at 460.2 m. Except for some preliminary work by Glenister (1960), no conodont investigations have been performed on this well.

LENNARD Napier No. 1

LENNARD Napier No. 1 Well was drilled in 1969, penetrating the Devonian sequence, and reaching basement in Precambrian granite gneiss at a depth of 1773 m (5816 ft). Druce & Radke (1979) proposed two interpretations of the stratigraphy of the Fairfield Group in this well, based on a compilation of the biostratigraphic information available in the well completion report (Newstead, 1969) from the preliminary palaeontological reports by Balme on miospores and Jones on ostracods. Subsequent unpublished work by the writer on the ostracods of this well has provided evidence disputing the interpretation preferred by Druce & Radke (1979); the alternative interpretation of these authors is closer to the one advocated here (Fig. 4).

The Fairfield Group was intersected between 4 and 332 m (13 and 1089 ft), and consists of the Laurel Formation (down to 94 m; 310 ft), the Yellow Drum Sandstone (down to 202 m; 664 ft), and the Gumhole Formation. The Laurel Formation consists of an upper claystone with Tournaisian ostracods and miospores, and a lower unfossiliferous coarse friable sandstone. The Yellow Drum Sandstone is 108 m (354 ft) thick and consists of a dominant siltstone (multicoloured and variegated) with interbedded shales and sandstones. Ostracods belonging to Assemblage A are first encountered in cuttings at 177-180 m (580-590 ft) in the lower

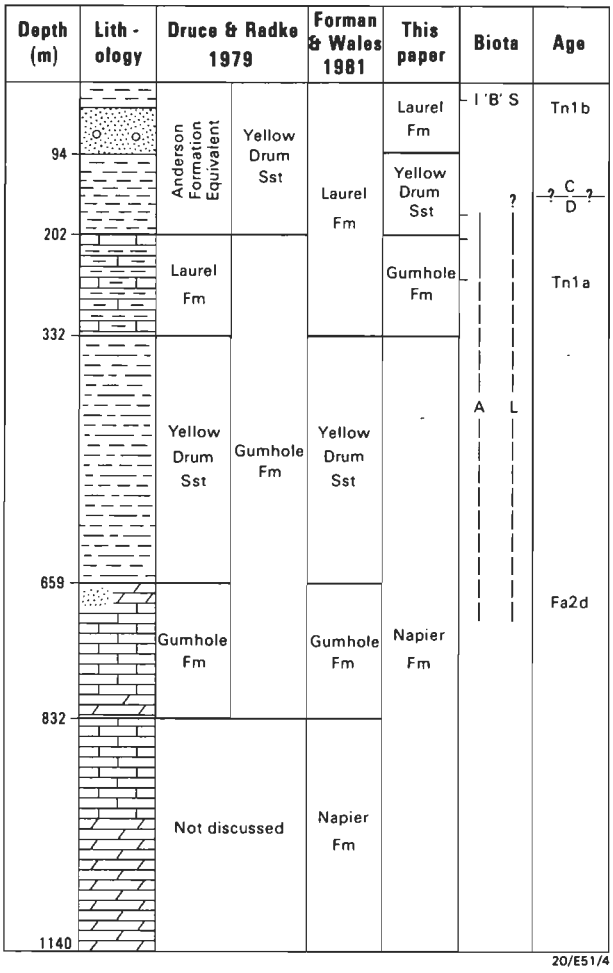

Figure 4. Interpretations of the Fairfield Group in Napier No. 1 well.
Abbreviations - Biota: A = ostracod Assemblage A; B = ostracod Assemblage B; Microfloral assemblages L = *Retispora lepidophyta*, S = *Grandispora spiculifera*, Age: D/C = Devonian-Carboniferous boundary.

part of the Yellow Drum Sandstone, some 22 m above the base, and continue to be found in the Gumhole Formation below. The Gumhole Formation is 130 m (425 ft) thick, and consists of a siltstone-limestone sequence that was interpreted by Druce & Radke (1979) as the Laurel Formation. However, ostracods are abundant in this sequence, and represent Assemblage A from the type area of the Gumhole Formation. Furthermore, Balme (*in* Newstead, 1969) reported an

uppermost Famennian microflora in core 1 (204 m; 670 ft) taken from near the top of the Gumhole Formation, which would now be assigned to the *Retispora lepidophyta* Assemblage of Playford (1976). Below the Gumhole Formation, the claystone, siltstone, and limestone sequence between 332 m (1089 ft) and 832 m (2733 ft) is here referred to the Napier Formation. Druce & Radke (1979) regarded this sequence as two formations, the Yellow Drum Sandstone, and (below 660 m; 2163 ft), the Gumhole Formation. Core 2 (717 m; 2352 ft), taken from the lower part of the Napier Formation in this well, contains ostracods that appear to belong to Assemblage A, and spores and conodonts that indicate a late Famennian age.

LENNARD Napier No. 5

LENNARD Napier No. 5 Well was drilled in 1970, 13 km north-northwest of Napier No. 1 well. It penetrated a Devonian sequence and reached basement in Precambrian granite gneiss at a depth of 1649 m (5412 ft). The well was spudded into 77 m (253 ft) of Yellow Drum Sandstone, and proceeded through the Gumhole Formation down to 204 m (670 ft; cf. Druce & Radke 1979, p. 52). The lower part of the Yellow Drum Sandstone between 49 m (160 ft) and 77 m (253 ft) contains a multicoloured and variegated siltstone similar to that of the Yellow Drum Sandstone in Napier No. 1 Well between 94 m (310 ft) and 202 m (664 ft). Ostracods of Assemblage A are first encountered in cuttings at 55 m (180 ft) in the lower part of the Yellow Drum Sandstone, some 22 m above the base, and continue to be found in the Gumhole Formation below. The Gumhole Formation is 127 m (417 ft) thick, with a base at 204 m (670 ft; 198 m *in* Druce & Radke, 1979). It consists of interbedded shale, limestone, siltstone, and rare sandstone. Ostracods are abundant throughout the unit and represent Assemblage A, the typical assemblage from the Gumhole Formation in the type area. They are also common below the Gumhole Formation, in the Napier Formation, and indicate a late Famennian age (Jones *in* Watts & Temple, 1971). Apparently no palynological investigations have been performed on this well.

LENNARD Napier No. 4

LENNARD Napier No. 4 Well was drilled in 1970, 45 km northwest of Napier No. 5 well, and 66 km northeast of Derby. It penetrated the Devonian sequence and reached basement in Precambrian quartzite at a depth of 943 m (3094 ft). The well was spudded into a thin sequence (10 m) of aeolian sand overlying a thick (58 m) friable sandstone unit that probably belongs to the Permian- Carboniferous Grant Group. The Fairfield Group was intersected between 68 m (223 ft) and 299 m (980 ft; 220 m cf. Druce & Radke 1979, p. 51).

The Gumhole Formation is 130 m (425 ft) thick and overlies the Nullara Limestone at 299 m (980 ft). The unit consists of sandstone, claystone, siltstone and shale, and contains much more sandstone in comparison with the Gumhole Formation of the type area. The sequence consists of three units (i) a lower sandstone (220-299 m; 723-980 ft), (ii) a thin calcareous claystone (216-220 m; 709-723 ft) and (iii) an upper argillaceous sandstone and claystone (169-216 m; 555-709 ft). The thin calcareous claystone (referred to as marl by Temple 1970) yielded ostracods (Jones *in* Temple, 1970) and spores (Balme *in* Temple, 1970) that indicate a late Famennian age. The microflora would now be assigned to the *Retispora lepidophyta* Assemblage of Playford (1976).

The remainder of the Fairfield Group consists of 101 m (332 ft) of Yellow Drum Sandstone in the interval 68-169 m (223-555 ft). The unit is predominantly sandstone, medium to very coarse, friable, and grading to pebbly conglomerate. The sandstone is interbedded with thin multicoloured variegated silty claystone. Balme (*in* Temple, 1970) recovered Tournaisian spores at 117 m (385 ft) and 120 m (394 ft) within the Yellow Drum Sandstone that would now be assigned to the *Grandispora spiculifera* Assemblage of Playford (1976).

The interpretation presented here (Fig. 5) differs slightly from those of Temple (1970) and Druce & Radke (1979). I refer the 'Laurel Formation' and the 'Fairfield Formation equivalent' of Temple (1970) to the Yellow Drum Sandstone and the Gumhole Formation, respectively. Contrary to the opinion of Druce & Radke (1979), I retain the dominantly sandstone part of Temple's (1970) 'Fairfield Formation equivalent' within the Gumhole Formation rather than place it in the Yellow Drum Sandstone, because this is more consistent with thickness data from other wells. Furthermore, the lower sandstone of the 'Fairfield Formation equivalent' is referred to the Gumhole Formation rather than to an equivalent of the Luluigui Formation. Thus, the concept of the Gumhole Formation envisaged here allows for a shift in the limestone-shale- sandstone ratio, so that limestone is reduced to a calcareous claystone representing 3 per cent of the section, and sandstone is greatly increased to at least 50 per cent of the total thickness. This exceeds the maximum amount of sandstone in the sections of the Gumhole Formation investigated by Druce & Radke (1979, p.9; 39 per cent at Red Bluffs). Such an increase in siliciclastic sedimentation over algal flat carbonates (Nullara Limestone) was probably due to increased run-off and river transport in the Yampi Embayment.

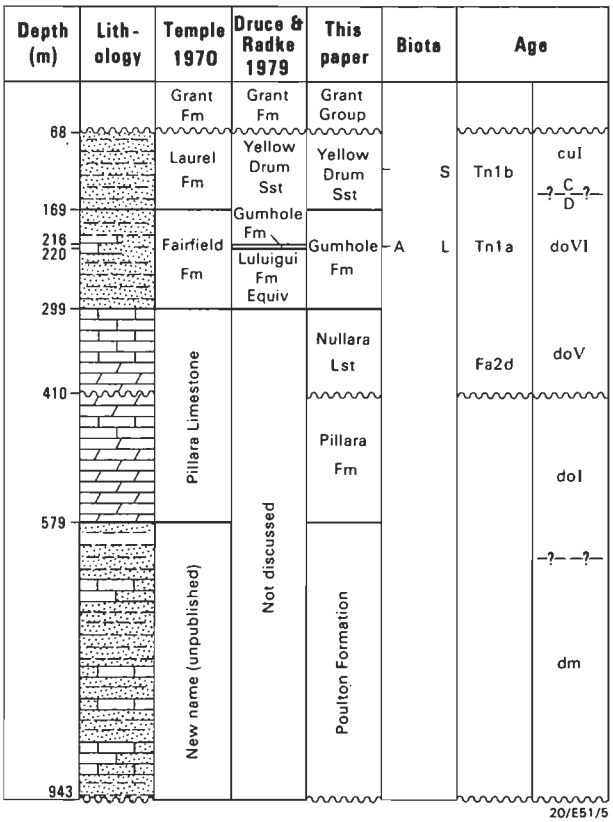

Figure 5. Interpretations of the Devonian sequence in Napier No. 4 well.

Section below the Fairfield Group, simplified after Lehmann (1984). Abbreviations of biota and age symbols, as in Fig. 4.

WAPET Frome Rocks No. 2

WAPET Frome Rocks No. 2 well was drilled in 1959 on the Jurgurra Terrace, south of the Fitzroy Trough, 150 km from the Napier Wells and 180 km from the type sections of the Fairfield Group on the Lennard Shelf. It penetrated a sequence of Jurassic, Permian, and Devonian sediments, and terminated within the Upper Devonian (Famennian; do V) Clanmeyer Siltstone at 2287 m (7504 ft). The well includes the type section of the Luluigui Formation, which extends from 1084 m (3557 ft) to 1909 m (6264 ft). Druce & Radke (1979) referred the upper 254 m (833 ft) of this sequence, in the interval 1084–1338 m (3557–4390 ft), to the Gumhole Formation, but this revision is not followed in this paper. The Luluigui Formation consists of interbedded siltstone, shale, limestone, and fine-grained sandstone, which conformably overlies the Clanmeyer Siltstone and is overlain with angular unconformity by the Grant Group (Willmott 1962, 1966). The shales are green-grey silty, fissile, slightly calcareous, and rich in ostracods. Assemblage A ostracods are present between 1109 m (3640 ft) and 1593 m (5227 ft; Jones 1961, 1962), which indicates a latest Devonian (Strunian; Tn1a–Fa2d) age. Balme (1962) and Balme & Hassell (1962) reported a latest Devonian microflora over this interval, which would now be regarded as the *Retispora lepidophyta* Assemblage.

Problems of taxonomic affinities and sexual dimorphism

Systematic position of *Rhytiobeyrichia*

The new genus and species described here was referred to the Beyrichiacea even though some morphological aspects suggest other possibilities for its superfamilial relationship. It exemplifies a problem that is commonly encountered in the description of new ostracod taxa, viz. the recognition of secondary sexual characteristics in the ostracod carapace. The specimens studied have an over-all similarity in carapace morphology in that they all possess the same type of dorsal lobation, velar structures, and ornamentation, but two subsets can be recognised — type A, carapaces with ventral lobes, and type B, carapaces without ventral lobes (Fig. 6).

In the Canning Basin, type A was reported (Jones, *in* Willmott, 1962) before type B was found. Subsequently, adult type A forms, with a cruminal swelling in the position of the anteroventral lobe, were recognised in the Bonaparte Basin. This sequence of events influenced the development of the taxonomic interpretation of the new genus, and its possible superfamilial affinities (i.e. ? Drepanellacea, Hollinacea, Beyrichiacea) are discussed below.

(i) Drepanellacea — Type A specimens, when first found, were referred to a separate species with drepanellacean affinities (Jones, *in* Willmott, 1962, p. 37). The pattern of dorsal (L4, L3, L1) spines is similar to that of *Neodrepanella* Zaspelova, 1952 (type species *Drepanella tricornis* Batalina, 1941), but type A is distinguished by the presence of a supersulcal tubercle, ventral lobes, and a velum that is confluent with the acroidal spines.

Zaspelova (1952) originally introduced the Neodrepanellinae as a subfamily of the Drepanellidae Swartz, 1936, to include the nominate genus, and the genera *Tetracornella* Zaspelova, 1952; *Limbatula* Zaspelova, 1952; and *Bicornellina* Zaspelova, 1952. These genera, which include species with small, apparently non-dimorphic carapaces were referred by Polenova & Zanina (*in* Chernysheva, 1960, p. 314) directly to the non-dimorphic family Drepanellidae, as did Scott (*in* Moore, 1961, p.Q 123), with the exception of *Bicornellina*, which he referred to the Eurychilinidae.

However, regarding the assumption that the Neodrepanellidae (*nom. transl.* Pokorny 1953) is non-dimorphic, it would be wise to heed the warning of Jaanusson (1957, p. 377), who commented that 'certain characters of *Neodrepanella* and allied genera (Neodrepanellinae Zaspelova, 1952), particularly the shape and position of the spurs, and the development of the dorsal part of L3, are so similar to those of hollinines that the presence in these genera of a hollinid type of dimorphism is strongly suspected. These species require a further study before they can be properly classified'. Today this statement is still valid.

(ii) Hollinacea — A second interpretation would be a hollinacean affinity. The well-developed, spinous ventral lobes

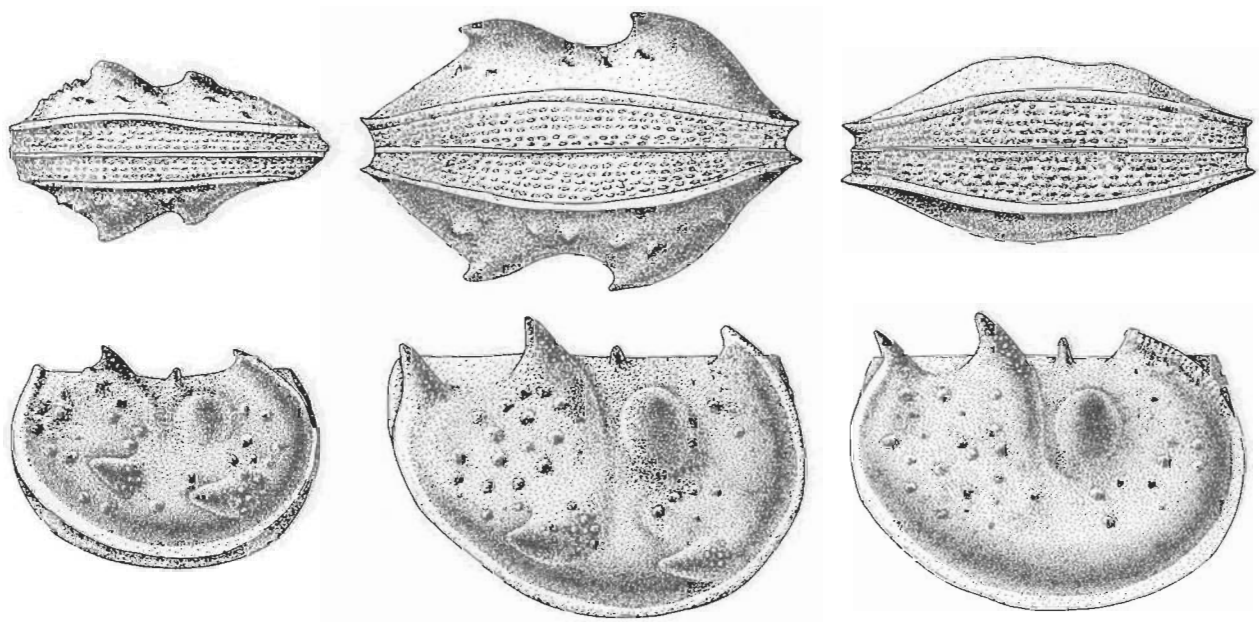

Figure 6. *Rhytiobeyrichia waruwa* gen. et sp. nov. Schematic drawings of carapaces in right lateral and ventral views.
(A) pre-adult female, 'type A', (B) adult female 'type A' and (C) adult male 'type B' (×40).

of type A specimens bear a superficial resemblance to the ventral spurs that are present in male specimens of species of the ctenoloculinid genus *Abditoloculina* Kesling, 1952 (e.g., Kesling & Peterson 1958, pl. 1, figs. 50–57; 60–69). They differ in having a posterior acroidal spine, a supersulcal tubercle, and a post-adductorial lobe (L3) that is extended to form a spinose conical cusp, rather than having the characteristic bulbous L3 of the hollinaceans. Also, the velum is continuous along the free border, without incorporating the anteroventral spur; the velar structures of hollinaceans differ in that they are absent along the posteroventral part of the free border. Finally, if type A forms are closely related to *Abditoloculina* or an allied genus, loculate forms (the female dimorphs) would also be expected. However, the apparent absence of loculate forms weakens the argument in support of a ctenoloculinid relationship, and of hollinacean affinities in general.

(iii) Beyrichiacea — The recognition of type B specimens in the Canning Basin gave the first clue that type A specimens may be dimorphs of the same species, and this was confirmed when large (adult) type A specimens with a cruminal swelling in the position of the anteroventral lobe were found in the Bonaparte Basin. Thus the recognition of the cruminate type A form (Pl. 2, figs. 2a, b) as the adult female dimorph, indicated that the dimorphism was a cruminal (beyrichiid) type, and that types A and B could be treated as one species, referable to the Beyrichiacea. Arguments for a hollinacean or a neodrepanellid relationship cannot be sustained.

Apart from the lack of ventral lobes, type B adult (L = 1.35 mm) and preadult specimens are morphologically similar to type A preadult specimens. Both types have a supersulcal spine, a beyrichiacean feature that is present in some Craspedobolbininae, Amphitoxotidinae, and Beyrichiinae (Siveter 1980, p. 15), and a spinous dorsal lobation that superficially resembles that of the Middle Devonian beyrichiaceans *Beyrichia ?tambovica* Egorova, 1967 (Eifelian, Moscow Basin), and *Kozlowskiella jurkowicensis* Olempska, 1974 (Givetian, Poland). These European species have a reticulate surface 'ornament', unlike *Rhytiobeyrichia waruwa* gen. et sp.nov., which has a granulose surface and superimposed tuberculation that is typical of the Beyrichiinae. The anteroventral spine of the pre-adult instars (type A) appears to have been inflated in the adult stage as a massive horn-shaped crumina. A few beyrichiaceans have a calcarine spur associated with the crumina; they include *Parasleia? grandicalcarata* Siveter, 1980, and species of *Aitilia* Martinsson, 1962 and *Hamulinavis* Martinsson, 1962 among the craspedobolbines and *Slependia armata* (Henningsmoen, 1954) among the zygobolbines (Beyrichiidae). In *Rhytiobeyrichia*, the cruminal swelling, of unknown genesis, has incorporated the horn-shaped anteroventral lobe.

Copulatory adaptations

Kesling (1969) has adroitly advocated that a study of carapace adaptations for copulation in extinct ostracods may be useful in taxonomy and reveal evolutionary trends. He noted that carapaces of palaeocope ostracods showing strong dimorphism seem adapted to favour some mating positions and to exclude others. Thus, one way of assessing the sexual significance of the dimorphic characters of the type A and type B carapaces that are described here is to attempt a reconstruction of the most plausible mating position. Not all dimorphic characters relate to copulation, some, e.g. the crumina, relate to brood care. The recognition of a crumina in type A specimens is *a priori* evidence of the adult female dimorph, because, as Martinsson (1962, p. 84) has pointed out, '—brood or egg care by male (ostracod) specimens is not known in nearer parts of the animal kingdom than the pantopods'.

Given that the cruminate form of type A is the adult female, with type B specimens as males of the same species then their secondary sexual characters would be recognisable in the carapace morphology of the pre-adult instars, i.e. the males (type B) lack the ventral lobes of the females (type A). On the other hand, if the type A and type B specimens were interpreted as different species, then the non-cruminate type A specimens would represent tecnomorphs (i.e. inferred males and unsexable juveniles of Guber, 1971). The decision as to which of these two hypotheses is the more reasonable is hindered by the paucity of specimens available, particularly from the same locality and horizon. In the Canning Basin, non-cruminate type A found in association with type B could be interpreted as evidence of sympatric species, especially as the only two cruminate type A specimens in the Bonaparte Basin lack the association of type B and non-cruminate type A forms.

In the absence of non-cruminate type A specimens of the same size as the cruminate (female) type A specimens (i.e. adults, L = 1.20–1.36 mm), I regard, on the basis of carapace morphology, the larger type B specimens (i.e., L = 1.13–1.35 mm) as male adults of the same species. One test of this idea is to determine whether the carapace morphologies of the cruminate type A and the adult type B forms permit a mating position that seems reasonable (Fig. 7).

The mating position that seems most feasible for the proposed dimorphs for *Rhytiobeyrichia waruwa* gen. et sp. nov. is posterodorsal, or perhaps more nearly posterior, as reported by Kesling & McGregor (1969) for the living freshwater ostracods *Cypria turneri* Hoff, 1942 and *Physocypria pustulosa* (Sharpe, 1897). The large syllobium, dorsally cusped, would seem to negate the dorsal position. Kesling (1969) has pointed out that a posterodorsal copulatory position would be difficult for ostracods with caudal or posterior acroidal spines, e.g. *Hexophthalmoides craterilobatus* Martinsson, 1962. However, posterior caudal spines may have assisted, rather than hindered, copulation in the posterodorsal position. They may have been used by female beyrichiids to keep the male valves apart, and locked into the optimum position for copulation. Those of the male may have enabled him to secure a firm hold in the substrate during copulation in the posterodorsal position (Fig. 7).

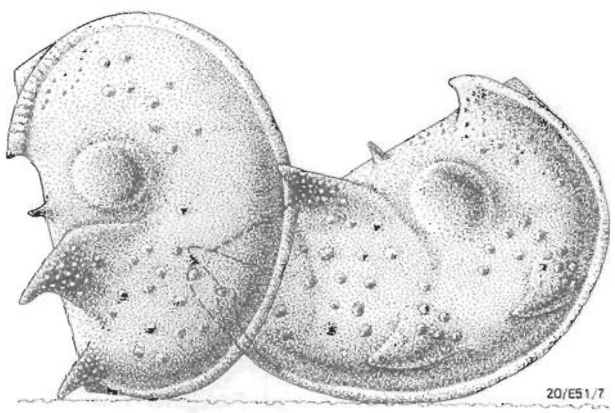

Figure 7. *Rhytiobeyichia waruwa* gen. et sp. nov. Adult female and male individuals in reconstructed mating position (×40).

Pre-adult dimorphism

Although it is generally the case that sexual dimorphy in the ostracod carapace is only manifested in the adult stage (e.g. van Morkhoven, 1962, p. 90, 94), several authors have demonstrated pre-adult dimorphism in the ontogeny of certain myodocopes (e.g., Kornicker, 1969, 1970, 1975), palaeocopes (Jaanusson, 1957; Guber, 1971; Schallreuter, 1976), and several podocope species from Jurassic (Whatley & Stephens, 1977), Tertiary and Recent (van Harten, 1975, 1980, 1983; Rohr, 1979) deposits. Pre-adult dimorphs have been described also in the ontogeny of some Cretaceous platycope species (Shaver, 1953; Herrig, 1963, 1966).

Whatley & Stephens (1977, p. 70) used Martinsson's (1956, p. 10–12) tentative assertion of the presence of pre-adult dimorphs in the Beyrichiidae in support of their argument for pre-adult ('precocious sexual') dimorphism in the Palaeocopida. They did not mention that Martinsson had revised his opinion when he wrote - 'there is at present, inspite of thorough investigation, no beyrichiid known with completely developed dimorphic characters in a preadult moult stage' (Martinsson 1962, p. 84). Martinsson's (1956, 1962) experience with *Beyrichia* (*Beyrichia*) *dactyloscopica* Martinsson, 1956, from the Mulde Marl of Gotland, is a salutary warning against the idea of proposing pre-adult dimorphs on the basis of limited material. After processing hundreds of kilograms of marl from the type locality of this species, Martinsson (1962, p. 285) recovered sufficient specimens to prove that its supposed pre-adult dimorphs belong to two species — *B. peponulifera* Martinsson, 1962 and *B. morifera* Martinsson, 1962. Martinsson (*fide* D.J. Siveter, personal communication) also rejected his earlier suggestion of pre-adult dimorphism in the primitiopsacean species *Clavofabella multidentata* Martinsson, 1955 (Martinsson 1956, p. 12), which he later considered to contain more than one species. Unfortunately, this study by Anders Martinsson was not published, because of his untimely death.

Thus, to date, the only palaeocopid examples that appear to contain pre-adult dimorphs are 6 hollinomorphs (Table 3). The fact that there are no proven cases of pre-adult dimorphism among the beyrichiomorphs means that the present example proposed in this paper must be regarded with caution. More material is needed for examination before a decision can be made as whether *Rhytiobeyrichia waruwa* gen. et sp. nov. is a genuine example of pre-adult dimorphism or whether the taxon consists of sympatric species.

Table 3. Palaeocope (Hollinomorph) species with pre-adult dimorphs (data from Jaanusson, 1957; Guber, 1971; and Schallreuter, 1976).

Eurychilinacea	
Euprimites suecicus (Thorsland, 1940)	A-1
Oepikella tvaerensis Thorsland, 1940	A-2
Hollinacea	
Tetrada memorabilis (Neckaja, 1953)	A-3
T. ventroconcava Schallreuter, 1976	A-1
Tetradella scotti Guber, 1971	A-3
T.quadrilirata (Hall & Whitfield, 1875)	A-3

Abbreviations as in Table 4.

Systematic palaeontology

Superfamily Beyrichiacea Matthew 1886
Family Beyrichiidae Matthew 1886
Subfamily Beyrichiinae Matthew 1886
Genus Rhytiobeyrichia gen. nov.

Derivation of name. Greek *rhytion*, a drinking horn, and the generic name *Beyrichia*: with reference to the shape of the crumina.

Type species. *Rhytiobeyrichia waruwa* sp. nov.

Diagnosis. Beyrichiinae with a weakly inflated, horn-shaped crumina in the anteroventral portion of the domicilium, separated from the preadductorial node and the ventral part of the syllobium by a ventral extension of the adductorial and pre-nodal sulcii. Anterior lobal cusp and posterior acroidal spine are confluent with a well-developed smooth velar ridge. A stout conical syllobial cusp, and distinct supersulcal tubercle. Velar ridge complete in both dimorphs; males lacking anteroventral and calcarine spines.

Remarks. On the basis of the lobation, ornament, and possibly the subcruminal field, *Rhytiobeyrichia* is allied to the subfamily Beyrichiinae. The subcruminal morphology of the sole cruminate carapace (CPC25334) of the type species is partially corroded, but it appears to have a transcruminal velar ridge, rather than the subcruminal finger-print striation of the normal beyrichiine field (Pl. 2, Fig. 2B). The genus is comparable with *Calcaribeyrichia* Martinson, 1962; *Gannibeyrichia* Martinsson, 1962; *Navibeyrichia* Martinsson, 1962; *Plicibeyrichia* Martinsson, 1962; and, possibly, *Innuitbeyrichia* Copeland, 1980 in lacking a zygal arch in both females and tecnomorphs, and the finger-print striation (cf. *Beyrichia* M'Coy 1846) on the ventral part of the crumina. It is distinguished from these genera particularly by the shape and extent of the anteroventral crumina, which is more a lateral than a ventral swelling. As with the treposellids recently described from the latest Devonian (Jones, 1985), *Rhytiobeyrichia* has a crumina that expands laterally into the carapace wall; the velum, apparently, is no longer used in its formation. The genus probably developed along the beyrichiine lineage, and the engagement of the velum in the formation of the crumina has apparently been lost in *Rhytiobeyrichia* in favour of space in the anteroventral lobal region of the carapace. In this respect, *Rhytiobeyrichia* may be near the end of the beyrichiine lineage, in the same way that *Copelandella* Bless & Jordan, 1971 is probably representative of the closing phase of the amphitoxotidine (Craspedobolbinidae Martinsson, 1962) lineage.

Rhytiobeyrichia waruwa sp.nov.

(Pl.1, Figs 1–3; Pl.2, Figs 1–3; Pl.3, Figs 1–5; Figs 6–8)

1962 undetermined drepanellacean genus C-Jones p. 37, 39 (*in* lists, unfigured).

Derivation of name. *Waruwa*, tribal name of the aboriginal inhabitants of the land between Derby and the King Leopold Ranges, Western Australia.

Material. 12 carapaces (1 adult female, 7 pre-adult female; 2 adult male; 2 pre-adult male); 1 left valve (adult female).

Holotype. Female carapace (A-1) CPC25322 (Pl.1, Figs 1A, B) from about the junction of the Gumhole Formation and the Yellow Drum Sandstone, Napier No. 1 well, 660–665 feet, Lennard Shelf, Canning Basin.

Paratypes. See Table 1.

Description. Adult male (Pl.1, Fig. 2; Pl.2, Fig. 3) — lateral outline preplete; hinge long, 90% of carapace length; cardinal angles obtuse; free margin evenly rounded, more broadly curved in posterior half. Bisulcate, with deep adductorial (S2) sulcus extending to mid-height, and curving anteriorly beneath the preadductorial node (L2) to join a shallow prenodal sulcus (S1); zygal arch absent. Anterior lobe (L1) flattened, with a stout cusp extending above the hinge-line and confluent with the anterodorsal part of the velum. Preadductorial node (L2) knob-like, outline subovate-

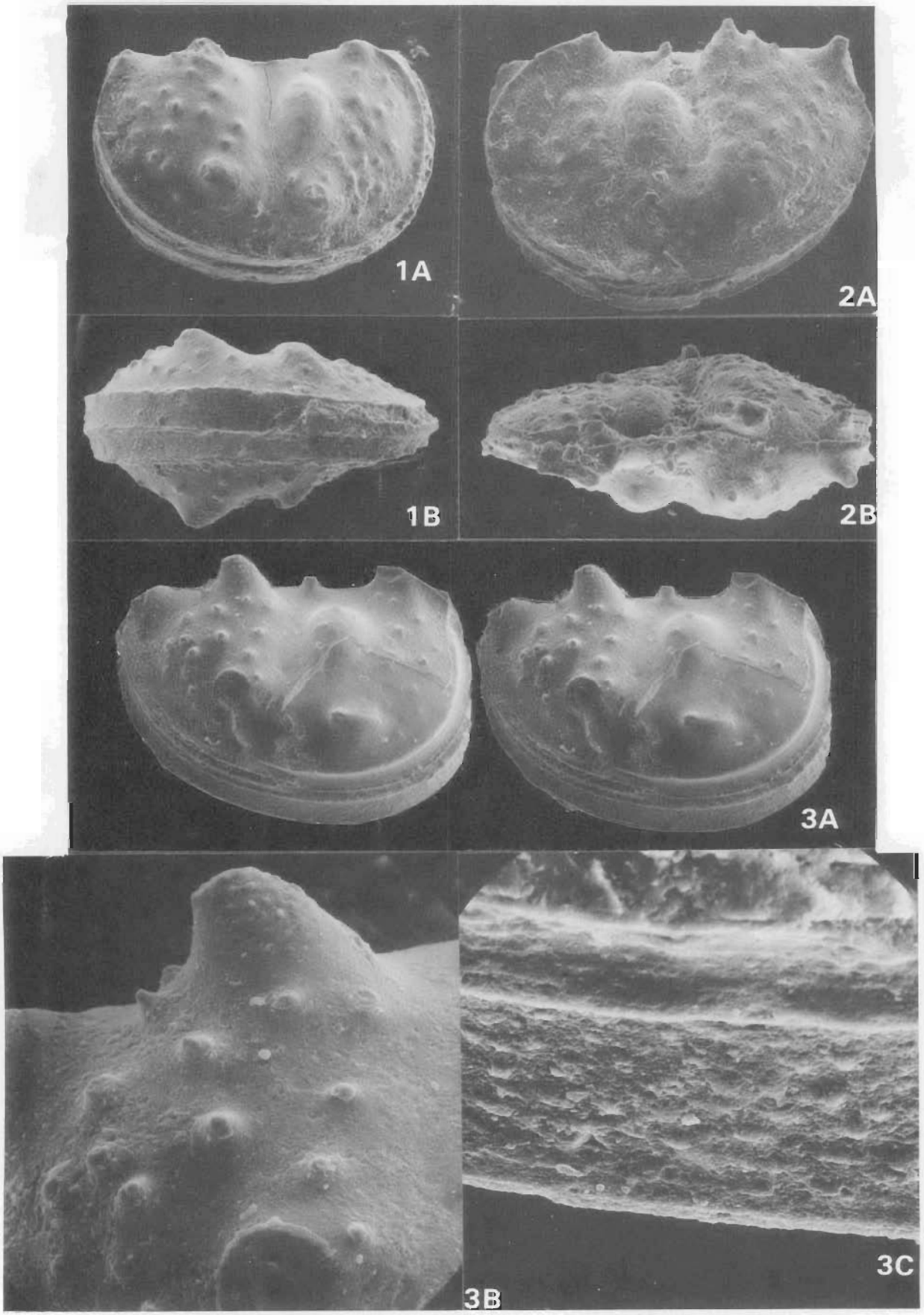

Plate 1. ***Rhytiobeyrichia waruwa*** **gen. et sp. nov.**

Figs 1A, B. Pre-adult (A-1) female carapace, holotype CPC25322, right lateral and ventral views, × 60; Gumhole Formation/Yellow Drum Sandstone boundary — Napier 1, 660–665 feet; Lennard Shelf, Canning Basin. Figs 2A, B. Adult male carapace, CPC25324, laterally compressed, left lateral view and dorsal views, × 60; Gumhole Formation — Napier 4, core 1, 717–725 feet; Lennard Shelf, Canning Basin. Figs 3A–C. Pre-adult (A-1) female carapace, CPC25321, anteroventral part of right valve exfoliated; right lateral view, × 60; syllobial ornament (× 200); ornament of subvelar field (× 600); Luluigui Formation — Frome Rocks 2, core 13, 4172–4180 feet; Jurgurra Terrace, Canning Basin.

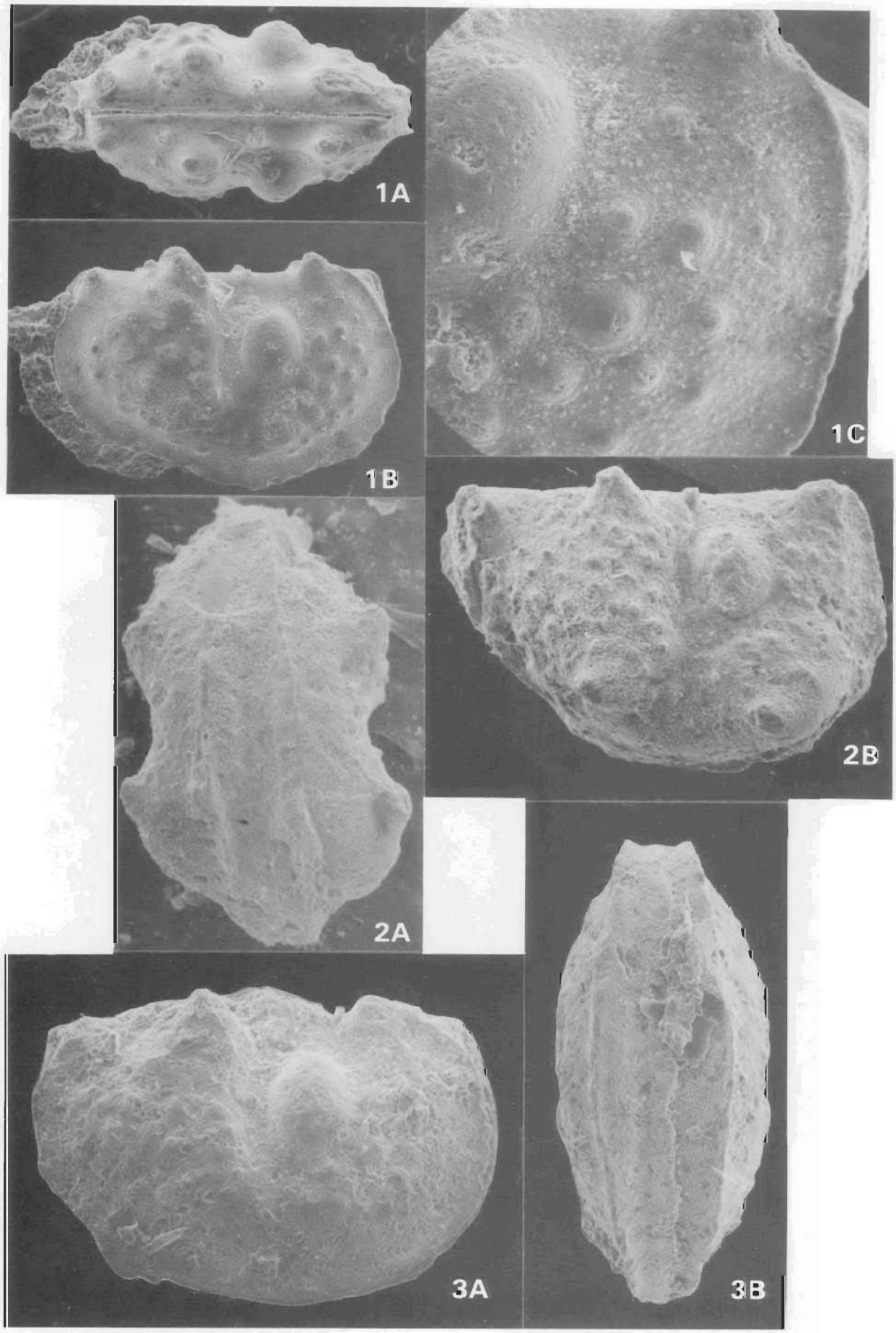
1A
1B
1C
2A
2B
3A
3B

subcircular. Syllobium (L3) undivided, with a stout conical cusp, extending above the hinge-line; ventral part of syllobium confluent with the anterior lobe. Posterior acroidal spine confluent with posterodorsal part of the velum, apex pointing posterodorsally; supersulcal tubercle short; both extending above the hinge-line. Lobal area with evenly distributed granulation, and a concentric pattern of tubercles.

Outline in ventral view broadly biconvex; velar ridge broad, flange-like, extending along entire free margin. Subvelar field with granulation aligned parallel to marginal and velar structures.

Adult female (Pl.2, Fig. 2) — domicilium as in the males, but with a crumina anteroventrally, and a stout calcarine spine at the base of the syllobium. The crumina is a horn-shaped inflation curving outwards and backwards; appears to be a lateral swelling of the spinose, anteroventral lobe of juvenile females; is confined to the anteroventral region; and is separated from the preadductorial node and the ventral part of the syllobium, by a ventral extension of the adductorial and prenodal sulci. The posterior acroidal spine is cone-like with a wide base, and situated slightly below the dorsal margin, with the apex pointing outwards and posterodorsally. Surface granulation and superimposed tuberculation, as in males.

Outline in ventral view with sulcule constriction at mid-length position; velar ridge complete, undeflected admarginally across the crumina. Subvelar field granulate as in the males.

Female (A-1) instars (Pl.1, Figs 1, 3; Pl.2, Fig. 1; Pl.3, Fig. 4) with a short calcarine and anteroventral spine on each valve; calcarine spine sited in the widest part of the carapace. Lobes granulose with superimposed tubercles.

Male (A-1) instars (Pl.3, Figs 1, 5) are without ventral spines and, apart from their smaller carapace size, are similar to adult males.

Dimensions. See Table 4 and Fig. 8.

Table 4. *Rhytiobeyrichia waruwa* gen. et sp. nov. — dimensions (microns) and form ratios of type material.

CPC No.		L	H	W	H/L	W/L	Plate & Fig. Number
25321	(A-1)fc	1037	625	575	0.60	0.55	1-3
25322	(A-1)fc	1025	600		0.59		1-1
25323	Amc	1350	900	650	0.67	0.48	2-3
25324	Amc*	1125	725	475	0.64	0.42	1-2
25325	(A-1)fc	1000	600	525	0.60	0.53	2-1
25326	(A-2)fc	825	537	475	0.65	0.58	3-3
25327	(A-1)mc	1000	625	500	0.63	0.50	3-5
25328	(A-1)mc	975	600	500	0.61	0.51	3-1
25329	(A-2)fc	762	450	350	0.59	0.46	3-2
25330	(A-1)fc	1025	687	460	0.67	0.45	3-4
25331	(A-1)ml	1025	612	—	0.60	—	unfigured
25332	(A-1)fr	925	587	475	0.63	—	unfigured
25333	Af	—	—	—	—	—	unfigured
25334	Afc	1362	825	875	0.61	0.64	2-2
25335	Afr	1200	750	—	0.63	—	unfigured

Abbreviations: L = length of carapace (or valve); H = height of carapace (or valve); W = width of carapace (or valve: excluding ventral lobes); H/L = height/length ratio; W/L = width/length ratio; f = female; m = male; c = carapace; l = left valve; r = right valve; A = presumed adult stage; A-1, A-2 = consecutive pre-adult instar stages; * = crushed specimen.

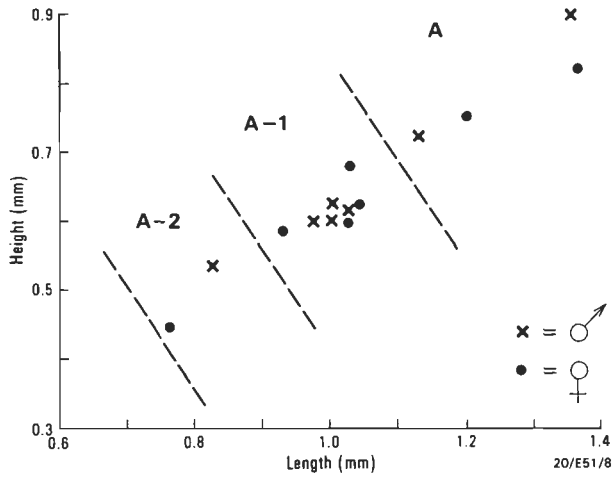

Figure 8. *Rhytiobeyrichia waruwa* gen. et sp. nov. Size dispersion diagram, based on a pooled sample (N=14) of the type material.

Age. Latest Devonian, Strunian (Fa2d-Tn1a).

Remarks. This species, if interpreted correctly, includes pre-adult dimorphs, and is unique in representing a possible example of the phenomenon of preadult dimorphism in the Beyrichiacea (cf. Martinsson, 1962 p. 84; Whatley & Stephens, 1977 p. 70).

Limbatula sp. A. Jones, 1968, from the late Frasnian Westwood Member of the Cockatoo Formation, Bonaparte Basin (Roberts & others, 1972) may belong to *Rhytiobeyrichia*. If correct, the genus would range into the late Frasnian.

Acknowledgements

This paper has benefited from the critical review of my colleagues Drs Robert S. Nicoll and G.C. Young, (Bureau of Mineral Resources), and Dr David J. Siveter (University of Leicester, England). The responsibility for the logic (or otherwise) on which the new palaeocope genus is established is mine. I am indebted to Messrs J. Mifsud and B. Pashley for the line illustrations, and A.T. Wilson for the photography.

References

Balme, B.E., 1962 — Palynological report on samples from Frome Rocks No. 2 well. *Bureau of Mineral Resources, Australia, Petroleum Search Subsidy Acts Publication* 8, 23-25.

Balme, B.E., & Hassell, C.W., 1962 — Upper Devonian spores from the Canning Basin, Western Australia. *Micropaleontology*, 8, 1-28, pls. 1-5.

Chernysheva, N.E., 1960 — Chlenistonogie, trilobitoobraznye i rakoobraznye (Arthropoda, Trilobitomorpha and Crustacea) — *in* Orlov, Y.A. (editor), Osnovy Paleontologii (Principles of Palaeontology), 7-515, text-Figs 1-1315, pls. 1-18, *Moskva*.

Conil, R., Groessens, E., & Pirlet, H., 1976 — Nouvelle charte stratigraphique du Dinantien type de la Belgique. *Annales de la Societe Geologique du Nord*, 96, 363-371.

Druce, E.C., 1969 — Devonian and Carboniferous conodonts from the Bonaparte Gulf Basin, Northern Australia, and their use in international correlation. *Bureau of Mineral Resources, Australia, Bulletin* 98, 1-157, pls. 1-43, 33 text-figs.

Plate 2. *Rhytiobeyrichia waruwa* gen. et sp. nov.

Figs 1A-C. Pre-adult (A-1) female carapace, CPC25325; dorsal and right lateral views, × 60; ornament of anterodorsal area, × 200; Gumhole Formation — Napier 4, core 1, 717-725 feet; Lennard Shelf, Canning Basin. Figs 2A,B. Adult female carapace, CPC25334; ventral and right lateral views, × 50; 02/09 Buttons beds, type section 91 m above the base; Bonaparte Basin. Figs 3A, B. Adult male carapace, CPC25323; right lateral and ventral views, × 60; Gumhole Formation — Napier 4, core 1, 717-725 feet; Lennard Shelf, Canning Basin.

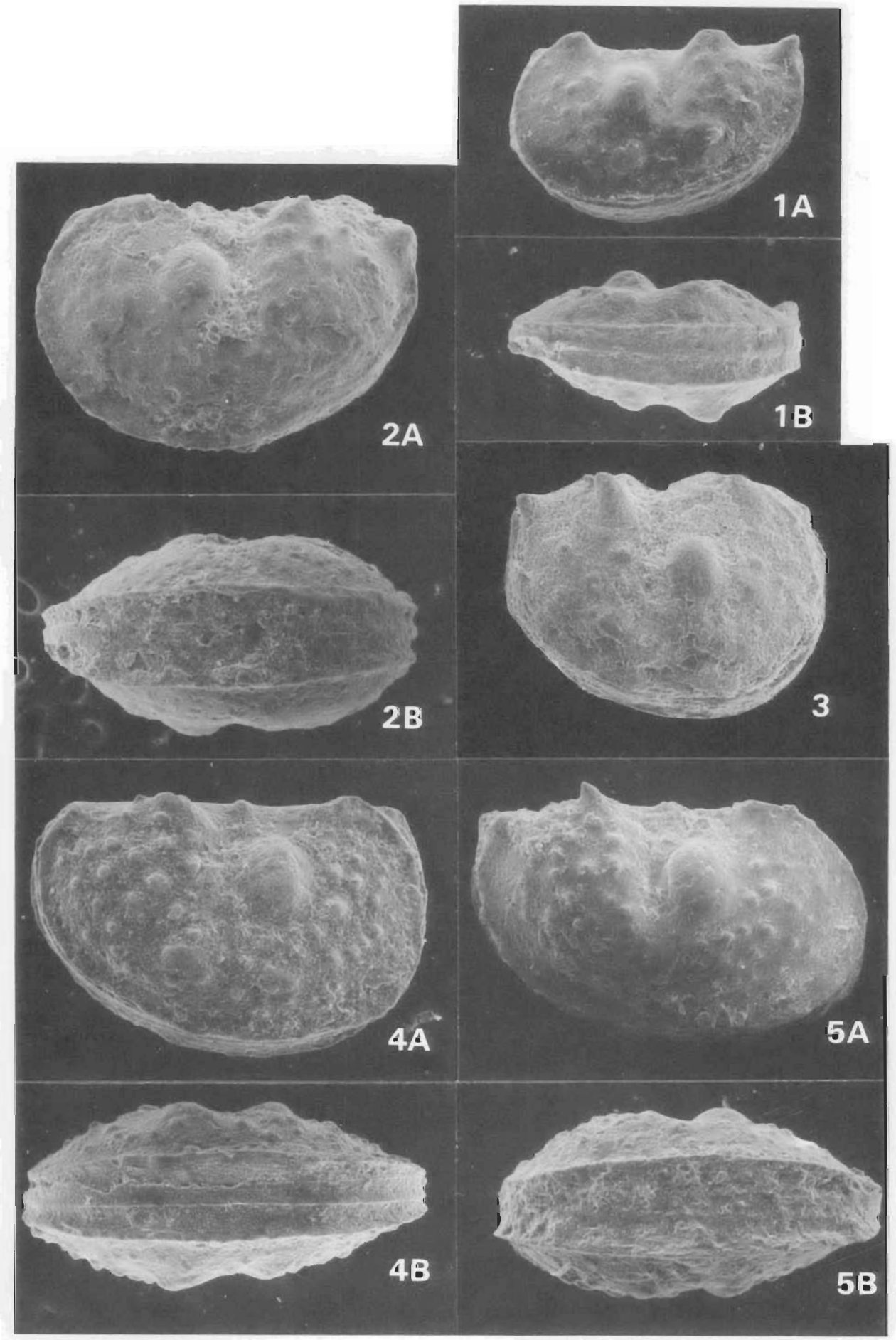
1A
1B
2A
2B
3
4A
4B
5A
5B

Druce, E.C., & Radke, B.M., 1979 — The geology of the Fairfield Group, Canning Basin, Western Australia. *Bureau of Mineral Resources, Australia, Bulletin* 200, 1-62.

Forman, D.J., & Wales, D.W. (Compilers), 1981 — Geological evolution of the Canning Basin, Western Australia. *Bureau of Mineral Resources, Australia, Bulletin* 210.

Glenister, B.F., 1960 — Carboniferous conodonts and ammonoids from Western Australia. *Compte Rendu 4-ieme Congres International de Stratigraphie et de Geologie du Carbonifere, Heerlen, (1958)*, 1, 213-217.

Guber, A.L., 1971 — Problems of sexual dimorphism, population structure and taxonomy of the Ordovician genus *Tetradella* (Ostracoda). *Journal of Paleontology* 45(1), 6-22, pls. 1-4, 8 text-figs.

Herrig, E., 1963 — Neue Ostracoden - arten aus der Weissen Schreibkreide der Insel Rugen (Unter-Maastricht). *Wissenschaftliche Zeitschrift der Ernst-Moritz-Arndt-Universitat Greifswald*, Jahrgang 12 (1963), Mathematisch-naturwissenschaftliche Reihe Nr. 3/4, 289-325, pls. 1-6.

Herrig, E., 1966 — Ostracoden aus der Weissen Schreibkreide (Unter-Maastricht) der Insel Rugen. *Palaontologische Abhandlungen (Geologische Gesellschaft DDR)*, Abteilung A, 2-4 693-1024, pls. 1-45, 144 text-figs. Berlin.

Jaanusson, V., 1957 — Middle Ordovician ostracodes of central and southern Sweden. *Bulletin of the Geological Institutions of the University of Uppsala*, 37, 173-442, pls. 1-15, 46 text-figs.

Jones, P.J., 1959 — Preliminary report on Ostracoda from Bore BMR No. 2, Laurel Downs, Fitzroy Basin, Western Australia. *Bureau of Mineral Resources, Australia, Report* 38, 37-52, 2 Figs.

Jones, P.J., 1961 — Ostracod assemblages near the Upper Devonian — Lower Carboniferous boundary in the Fitzroy and Bonaparte Gulf Basins. *In* Veevers, J.J., Wells, A.T., 1961. The geology of the Canning Basin, Western Australia. *Bureau of Mineral Resources, Australia, Bulletin* 60, 277-281, 1 Fig.

Jones, P.J., 1962 — Preliminary notes on Upper Devonian Ostracoda from Frome Rocks No. 2 Well. *Bureau of Mineral Resources, Australia, Petroleum Search Subsidy Acts Publication* 8, 35-39.

Jones, P.J., 1968 — Upper Devonian Ostracoda and Eridostraca from the Bonaparte Gulf, northwestern Australia. *Bureau of Mineral Resources, Australia, Bulletin* 99, 1-93, pls. 1-7, 21 text-figs.

Jones, P.J., 1974 — Australian Devonian and Carboniferous (Emsian-Visean) ostracod faunas: a review. *In* Bouckaert, J., & Streel, M., (Editors), *International Symposium on Belgian micropaleontological limits from Emsian to Visean, Namur, 1974. Publication* 6, 1-19.

Jones, P.J., 1985 — Treposellidae (Beyrichiacea: Ostracoda) from the latest Devonian (Strunian) of the Bonaparte Basin. *BMR Journal of Australian Geology & Geophysics*, 9(2), 149-162.

Kesling, R.V., 1951 — Terminology of ostracod carapaces. *Contributions from the Museum of Paleontology, University of Michigan*, 9(4), 93-171.

Kesling, R.V., 1969 — Copulatory adaptations in ostracods Part III. Adaptations in some extinct ostracods. *Contributions from the Museum of Paleontology, University of Michigan*, 22(21), 273-312, 23 text-figs.

Kesling, R.V., & Peterson, R.M., 1958—Middle Devonian hollinid ostracods from the Falls of the Ohio. *Micropaleontology*, 4(2), 129-148, pls. 1, 2.

Kornicker, L.S., 1969—Morphology, ontogeny and intraspecfic variation of *Spinacopia*, a new genus of myodocopid ostracod (Sarsiellidae). *Smithsonian Contributions to Zoology*, 8, 1-50.

Kornicker, L.S., 1970—Myodocopid Ostracoda (Cypridinacea) from the Philippine Islands. *Smithsonian Contributions to Zoology* 39, 1-32.

Kornicker, L.S., 1975—Antarctic Ostracoda (Myodocopina) pts I and II. *Smithsonian Contributions to Zoology*, 163, 1-720, pls 1-9, 432 text-figs.

Laws, R.A., 1981—The petroleum geology of the onshore Bonaparte Basin. *APEA Journal*, 21(1), 5-15.

Laws, R.A., & Brown, R.S., 1976—Bonaparte Gulf Basin - southeastern part. *In* Leslie, R.B., Evans, H.J., & Knight, C.L., (Editors) Economic geology of Australia and Papua New Guinea. Vol. 3. Petroleum. *Australasian Institute of Mining and Metallurgy, Monograph* 7, 200-208.

Lehmann, P.R., 1984—The stratigraphy, palaeogeography and petroleum potential of the Lower to lower Upper Devonian sequence in the Canning Basin. *In* Purcell, P.G., (Editor), The Canning Basin, W.A. *Proceedings of the Geological Society of Australia/Petroleum Exploration Society of Australia Symposium, Perth 1984*, 253-275.

McGregor, D.L., & Kesling, R.V., 1969—Copulatory adaptations in ostracods Part II. Adaptations in living ostracods. *Contributions from the Museum of Paleontology, University of Michigan*, 22(17), 221-239, 17 text-figs.

Martinsson, A., 1956—Ontogeny and development of dimorphism in some Silurian ostracodes. A study on the Mulde marl fauna of Gotland. *Publications from the Palaeontological Institution of the University of Uppsala* 14 (also issued as *Bulletin of the Geological Institutions of the University of Uppsala* 37), 1-42, pls. 1-5, 10 text-figs.

Martinsson, A., 1962—Ostracodes of the family Beyrichiidae from the Silurian of Gotland. *Publications from the Palaeontological Institution of the University of Uppsala, 41* (also issued as *Bulletin of the Geological Institutions of the University of Uppsala*, 41), 1-369.

Moore, R.C. (Editor) 1961—Arthropoda 3, Crustacea, Ostracoda — Treatise on invertebrate paleontology. Part Q, 1-442, text-figs. 1-334, *Geological Society of America and University of Kansas Press, Lawrence, Kansas.*

Newstead, P.G., 1969—Napier No. 1 well completion report (Lennard Oil NL). *Bureau of Mineral Resources, Australia, Petroleum Search Subsidy Acts File* 69/2015 (unpublished).

Nicoll, R.S., 1980—The multielement genus *Apatognathus* from the Late Devonian of the Canning Basin, Western Australia. *Alcheringa* 4(2), 133-152.

Nicoll, R.S., & Druce, E.C., 1979—Conodonts from the Fairfield Group, Canning Basin, Western Australia. *Bureau of Mineral Resources, Australia, Bulletin* 190, 1-134, pls. 1-28.

Paproth, E., 1980—The Devonian-Carboniferous boundary. *Lethaia* 13 (4), 287.

Playford, G., 1976—Plant microfossils from the Upper Devonian and Lower Carboniferous of the Canning Basin, Western Australia. *Palaeontographica* (B), 158, 1-71.

Playford, G., 1982—A latest Devonian palynoflora from the Buttons beds, Bonaparte Gulf Basin, Western Australia. *BMR Journal of Australian Geology & Geophysics*, 7, 149-157.

Playford, P.E., & Lowry, D.C., 1966—Devonian reef complexes of the Canning Basin, Western Australia. *Geological Survey of Western Australia, Bulletin* 118, 1-150, 47 text-figs.

Poll, J., 1983—Onshore Canning Basin: an historical perspective. *Journal of the Petroleum Exploration Society of Australia,* 3, 11-20.

Roberts, J., Jones, P.J., & Druce, E.C., 1967—Palaeontology and correlations of the Upper Devonian of the Bonaparte Gulf Basin, Western Australia and Northern Territory. *In* Oswald, D.H., (Editor), International symposium on the Devonian System. *Alberta Society of Petroleum Geologists, Calgary*, 2, 565-577.

Roberts, J., Jones, P.J., Jell, J.S., Jenkins, T.B.H., Marsden, M.A.H., McKellar, R.G., McKelvey, B.C., & Seddon, G., 1972—Correlation of the Upper Devonian rocks of Australia. *Journal of the Geological Society of Australia*, 18, 467-490.

Roberts, J., & Veevers, J.J., 1973—Summary of BMR studies of the onshore Bonaparte Gulf Basin 1963-71. *Bureau of Mineral Resources, Australia, Bulletin* 139, 29-58.

Rohr, W.-M., 1979—Nachweise von praadultem sexualdimorphismus bei den Podocopa (Ostracoda) und grossen-variabilitat brackischer ostracoden. (Evidence of preadult sexual dimorphism in the Podocopa (Ostracoda) and variability of sizes in brackish

Plate 3. *Rhytiobeyrichia waruwa* gen. et sp. nov.

Figs 1A,B. Pre-adult (A-1) male carapace, CPC25328, left lateral and ventral views, × 60; Gumhole Formation — Napier 5, 500-520 feet; Lennard Shelf, Canning Basin. Figs 2A, B. Pre-adult (A-2) female carapace, CPC25329, left lateral and ventral views, × 60; Napier Formation — Napier 5, 750-760 feet; Lennard Shelf, Canning Basin. Fig. 3. Pre-adult (A-2) female carapace, CPC25326, right lateral view, × 60; Gumhole Formation — Napier 4 core 1, 717-725 feet; Lennard Shelf, Canning Basin. Figs 4A, B. Pre-adult (A-1) female carapace, CPC25330, right lateral and ventral views, × 60; Napier Formation — Napier 5, 800-900 feet; Lennard Shelf, Canning Basin. Figs 5A, B. Pre-adult (A-1) male carapace, CPC25327, right lateral and ventral views, × 60; Gumhole Formation — Napier 5, 500-520 feet; Lennard Shelf, Canning Basin.

ostracods). *Neues Jahrbuch fur Geologie und Palaontologie*, Band 158(3), 346-380.

Schallreuter, R., 1976—Ctenonotellidae (Ostracoda, Palaeocopina) aus Backsteinkalk-geschieben (Mittelordoviz) Norddeutschlands. *Palaeontographica* Abteilung A, 153(4/6), 161-215.

Shaver, R.H., 1953—Ontogeny and sexual dimorphism in *Cytherella bullata*. *Journal of Paleontology*, 27(3), 471-480.

Siveter, D.J., 1980—British Silurian Beyrichiacea (Ostraccoda) Part 1. *Palaeontographical Society Monographs, London*, 1-76.

Sohn, I.G., Berdan, J.M., & Peck, R.E., 1965—Ostracods, 75-88. *In* Kummel, B., & Raup, D., (Editors). Handbook of paleontological techniques. *W.H. Freeman & Co., San Francisco & London*, 1-852.

Temple, P.R., 1970—Napier No. 4 well completion report (Lennard Oil NL). *Bureau of Mineral Resources, Australia, Petroleum Search Subsidy Acts File* 70/589 (unpublished).

Towner, R.R., & Gibson, D.L., 1983—Geology of the onshore Canning Basin, Western Australia. *Bureau of Mineral Resources, Australia, Bulletin* 215, 1-51.

Tschigova, V.A., 1977—Stratigrafiya i korrelyatsiya neftegazonosnykh otlozhenii Devona i Karbona Evropeiskoi chasti SSSR i zarubezhnykh stran (Stratigraphy and correlation of oil and gas-bearing deposits in the Devonian and Carboniferous from the European part of the USSR and neighbouring regions): Izdatel'stvo 'Nedra', *Moscow*, 194 pp., 47 pls.

van Harten, D., 1975—*Cyprideis baetica* n.sp. (Ostracoda, Cytheridae) from the Miocene of southeastern Spain. *Scripta Geologica*, 32, 1-17, 4 pls., 3 figs.

van Harten, D., 1980—On *Cyprideis exuberans* van Harten sp. nov., *A Stereo-Atlas of Ostracod Shells*, 7(16), 89-10.

van Harten, D., 1983—Resource competition as a possible cause of sex-ratio in benthic ostracodes. *In* Maddocks, R.F., (editor) Applications of Ostracoda. *Proceedings of the 8th International Symposium on Ostracoda, July 26-29, 1982, Houston, Texas, Department of Geosciences, University of Houston, Texas*, 568-580.

van Morkhoven, F.P.C.M., 1962—Post-Palaeozoic Ostracoda. Their morphology, taxonomy and economic use. Vol. 1, General. *Elsevier*, 1-204, 79 figs.

Veevers, J.J., & Roberts, J., 1968—Upper Palaeozoic rocks, Bonaparte Gulf Basin of northwestern Australia. *Bureau of Mineral Resources, Australia, Bulletin* 97, 1-155.

Watt, J.D., & Temple, P.R., 1971—Napier No. 5 well completion report (Lennard Oil NL). *Bureau of Mineral Resources, Australia, Petroleum Search Subsidy Acts File* 70/750 (unpublished).

Whatley, R.C., & Stephens, J.M., 1977—Precocious sexual dimorphism in fossil and recent Ostracoda. *In* Loffler, H., & Danielopol, D., (Editors) Aspects of ecology and zoogeography of Recent and fossil Ostracoda. *Proceedings of the 6th International Symposium on Ostracoda (Saalfelden, Salzburg), 1976*, 69-91. *Junk, The Hague.*

Willmott, S.P., 1962—Geological report on Frome Rocks No. 2 well. *Bureau of Mineral Resources, Australia, Petroleum Search Subsidy Acts Publication* 8, 15-20.

Wilmott, S.P., 1966—Definitions of new formations names. *Bureau of Mineral Resources, Australia, Petroleum Search Subsidy Acts Publication* 48, 6-8.

Yeates, A.N., Gibson, D.L., Towner, R.R., & Crowe, R.W.A., 1984—Regional geology of the onshore Canning Basin, W.A. *In* Purcell, P.G., (Editor), The Canning Basin, W.A. *Proceedings of the Geological Society of Australia/Petroleum Exploration Society of Australia symposium, Perth, 1984*, 23-55.

Zaspelova, V.S., 1952—Ostrakody semeistva Drepanellidae iz otlozhenii verkhnego devona Russkoi platformy (Ostracods of the family Drepanellidae from Upper Devonian deposits of the Russian platform), *Trudy vsesoyuznogo neftyanogo nauchno-issledovatel'skogo geologorazvedochnogo Instituta (VNIGRI)* 157-216, 11 pls. *Leningrad-Moskva.*

CONTENTS

R85/902 (2) Cat. No. 86 214 63